WEB CRIPPLING BEHAVIOUR OF COLD-FORMED STEEL MEMBER WITH WEB OPENINGS

A thesis submitted to the University of Strathclyde
for the degree of Doctor of Philosophy

by

MD. ASRAF UZZAMAN

Department of Mechanical & Aerospace Engineering
University of Strathclyde
Glasgow, UK

2012

ABSTRACT

Cold-formed steel sections are often used as wall studs or floor joists; such sections often include web holes for ease of installation of the services. Web crippling at points of concentrated, or localised, load or reaction in thin walled beams is well known to be a significant problem. Cold-formed steel design codes, however, do not consider the effect of such web holes. In this thesis, a combination of experimental tests and non-linear elasto-plastic finite element analyses is used to investigate the effect of such holes on web crippling under two loading conditions interior-two-flange (ITF) and end-two-flange (ETF). The cases of both flange fastened and flange unfastened are considered. A good agreement between the experimental tests and finite element analyses is obtained in terms of both strength and failure modes. The finite element model is then used for the purpose of a parametric study on the effect of different sizes and position of holes in the web. It is demonstrated that the main factors influencing the web crippling strength are the ratio of the hole depth to the depth of the web, and the ratio of the distance from the edge of the bearing to the flat depth of web and the ratio of the length of bearing plates to the flat depth of the web. The web crippling strength without holes predicted from test and finite element analysis results are compared with the web crippling strength obtained from design codes. An extensive statistical analysis is carried out on web crippling strength of cold-formed steel sections with web holes. Design recommendations in the form of web crippling strength reduction factors are proposed, that are conservative to both the experimental and finite element results.

ACKNOWLEDGEMENTS

I would like to express my sincerest thanks to my supervisor, Dr. David Nash for his supervision, guidance, encouragement and friendship throughout my studies at the University of Strathclyde, Glasgow. His invaluable experience helped me to guide my effort towards the successful completion of this research.

I would also like to thank Dr James Lim of the Queen's University Belfast for his support on my studies. Without his assistance, this study would not have been what it is. I am sincerely grateful to Professor Jim Rhodes at the University of Strathclyde for his valuable advice and support during my studies. Special thanks to Professor Ben Young at the University of Hong Kong for his advice in numerous ways towards my research.

The author gratefully acknowledges the help given by the Metsec Plc, UK, and Capital Steel Building Ltd. The author also wish to thank Mr Chris Cameron, Mr Andrew Crockett and Mr. Tom Farmer for their assistance in preparing the specimens and carrying out the experimental testing. It has been a pleasure to work with them.

I am very much grateful to my mother and father, for giving me lots of love and encouragement throughout my life. They always let me know that they are very proud of me which encouraged me in finishing this PhD. My deep love and appreciation goes to my fiancé, my brother, Rasel, sister, Lisa and her husband Babul. Finally, special thanks go to my friends Saikat, Hasib, Shahed and Imtiaz for their support to this research.

DECLARATION

I hereby declare that this thesis represents my own work conducted under the guidance of my supervisors, except where due acknowledgement is made, and that it has not been previously included in a thesis, dissertation or report submitted to this University or to any other institution for a degree, diploma or other qualifications.

Signed.....

MD.ASRAF UZZAMAN

PUBLICATION

Uzzaman A., Lim J.B.P., Nash D., Rhodes J. And Young B. (2012). "Web crippling behaviour of cold-formed steel channel sections with offset web holes subjected to interior-two-flange loading". *Thin-walled Structures* 50 (1), 76-86.

Uzzaman A., Lim J.B.P., Nash D., Rhodes J. And Young B. "Cold-formed steel sections with web openings subjected to web crippling under two-flange loading conditions-Part I: Tests and Finite element analysis". *Thin-walled Structures* (vol in press).

Uzzaman A., Lim J.B.P., Nash D., Rhodes J. And Young B. "Cold-formed steel sections with web openings subjected to web crippling under two-flange loading conditions-Part II: Parametric study and proposed design equations". *Thin-walled Structures* (vol in press).

CONTENTS

LIST OF FIGURES

LIST OF TABLES

NOTATION

The following symbols are used in this Thesis:

A	Web holes ratio;
a	Diameter of circular web holes;
b_f	Overall flange width of section;
b_l	Overall lip width of section;
COV	Coefficient of variation;
DL	Dead load;
D	Overall web depth of section;
E	Young's modulus of elasticity;
FEA	Finite element analysis;
F_m	Mean value of fabrication factor;
f_y	Material yield strength;
h	Depth of the flat portion of web;
L	Length of the specimen;
LL	Live load;
M_m	Mean value of material factor;
N	Length of the bearing plate;
P	Experimental and finite element ultimate web crippling load per web;
P_{EXP}	Experimental ultimate web crippling load per web;
P_{FEA}	Web crippling strength per web predicted from finite element (FEA);
P_m	Mean value of tested-to-predicted load ratio;
R	Reduction factor;
R_P	Proposed reduction factor;
r_i	Inside corner radius of section;

t	Thickness of section;
V_F	Coefficient of variation of fabrication factor;
V_M	Coefficient of variation of material factor;
V_P	Coefficient of variation of tested-to-predicted load ratio;
x	Horizontal clear distance of the web holes to the near edge of the bearing plate;
X	Web holes distance ratio;
β	Reliability index;
ε_f	Elongation (tensile strain) at fracture;
ϕ	Resistance factor;
$\sigma_{0.2}$	Static 0.2% proof stress;

CHAPTER 1. INTRODUCTION

1.1 Background

Cold-formed steel sections are increasingly used in residential and commercial construction. Since the 1940s, cold-formed steel members have used for cladding and decking materials for roofs, floors and walls. Currently, cold-formed steel members are used for primary and secondary framing components.

Cold-formed steel sections are fabricated from flats strips or welded from thin plates. Amongst these various sections, C-sections are widely used in construction industry as wall studs, floor joists, rafters, purlins, rails and trusses. Although the thickness of cold-formed steels typically varies between 0.5mm to 7mm, recent developments allow thicker steel sheets to be cold-formed. The steel used for these sections may have a yield stress ranging from 250 MPa to 550 MPa (Young and Hancock (2001)).

1.2 Statement of the problems

Cold-formed steel sections are often used as wall studs or floor joists; such sections often include web holes for ease of installation of the electrical or plumbing services. These holes are usually pre-punched in the factory.

Figure 1.1 Cold-formed steel with web holes

Web crushing or crippling at points of concentrated, or localised, load or reaction in thin walled beams is well known to be a significant problem, particularly in the case of beams with slender webs, and is of high importance in the field of cold-formed steel members, as such members are generally not stiffened against this type of loading. At points of concentrated loading and supports, severe lateral loading can result in a local buckling in the web (Rhodes and Nash (1998)). For the sections with holes, such web crippling needs to be taken into account.

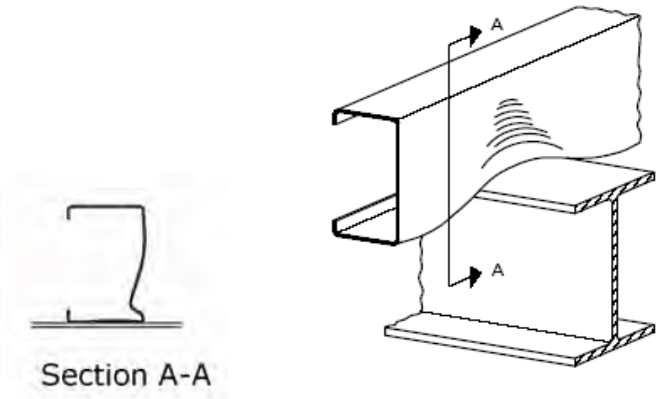

Figure 1.2 Web crippling at the support point (Rhodes and Nash (1998))

Web crippling may occur under various loading conditions, where these loading conditions are defined based on the position of the loading and the number of loads involved. If the loading is applied within the span of the beam, the loading condition is termed as interior loading, and if the loading is applied closer to the end of the beam, the loading condition is termed as end loading. Furthermore, if two loads are applied onto the opposite flanges within a distance of one-and-half of the web height, then this loading condition is termed as two flanged loading, and otherwise it is termed as one flange loading. Based on the above definitions, four distinct loading conditions, namely, End-One-Flange (EOF), End-Two-Flange (ETF), Interior-One-Flange (IOF), and Interior-Two-Flange (ITF) were defined by the North American Specification for cold-formed steel sections (NAS (2001)). These four loading conditions are illustrated in Figure 1.3. Two different support restraint conditions were considered. Firstly, a

section not fastened to support restraint condition with the flanges is not fastened to a support or to a bearing plates. The web crippling strength may be less than if the section fastened to the support. Secondly in the case of section fastened to support, bolts are used to fasten the section to the bearing plates.

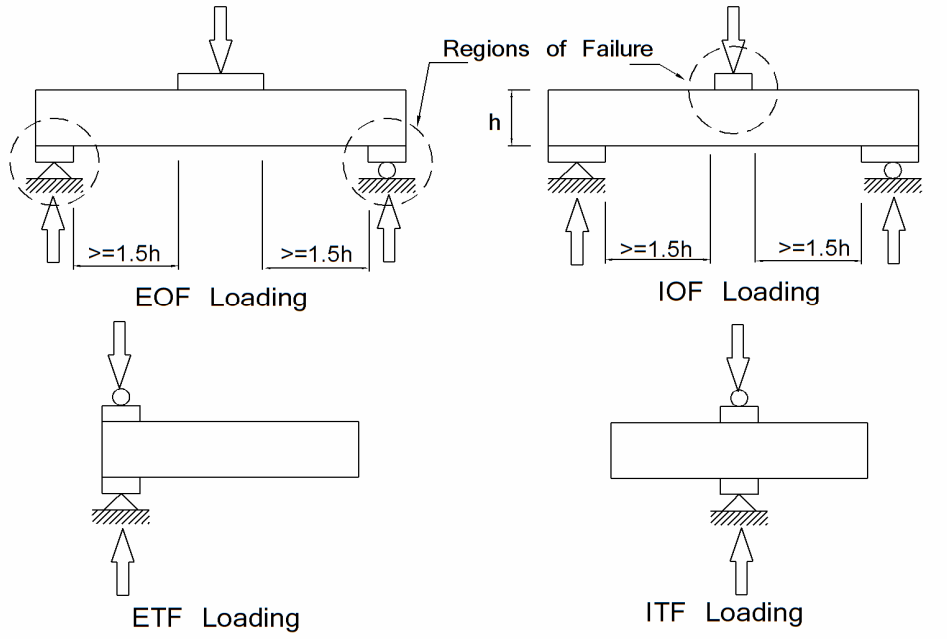

Figure 1.3 Four loading conditions defined by the North American Specification(NAS (2001))

Most design specifications for cold-formed steel structural members provide design rules for cold-formed steel channel sections without web holes; only in the case of the North American Specification for cold-formed steel sections (NAS (2001)) are reduction factors for web crippling with holes presented, covering the cases of interior-one-flange (IOF) and end-one-flange loading (EOF), and with the flanges of the sections unfastened to the support. The holes are assumed to be located at the mid-height of the specimen having a longitudinal clear offset distance between the edge of the bearing plates and the web holes. There is no design

recommendations available for the cases of the interior-two-flange (ITF) and end-two-flange (ETF) loading condition considering any web holes.

1.3 Aim and scope of this research

The aim of this research is to investigate the possible degradation in strength of the web crippling behaviour of the cold-formed steel due to the presence of web opening. Specific objectives of this research can be listed as follow:

1. To conduct experimental investigations to study the effect of web holes on the web crippling strength of cold formed steel section. The effect of both flanges fastened and unfastened to the support will be considered.
2. To develop nonlinear finite element analysis (FEA) models for all cases and validate them using experiment results.
3. To use the FEA models to undertake comprehensive parametric studies to investigate the possible parameters which are expected to affect the web crippling strength of cold-formed steel sections. The parameters includes web holes sizes and position into the web of the section, section geometry, section thickness and different lengths of bearing plate.
4. To compare the FEA and experimental without web holes results with the prediction from current design rules.
5. To examine web crippling strength reduction based on the results.
6. To propose design recommendation in the form of web crippling strength reduction factors for all the loading condition and cases.

1.4 Outline of the thesis

Thesis consists of seven chapters. This first chapter indicates the general objectives and presentation of the work.

Chapter 2 describes the literature review of related research.

Chapter 3 presents the experimental investigation of the lipped channel sections with and without web holes subjected to both interior-two-flange (ITF) and end-two-flange (ETF) loading conditions. In determining the web crippling strength of the sections, both support restraint conditions are considered: (1) Specimens not fastened to the support (2) Specimen fastened to the support.

Chapter 4 presents the details of the finite element analyses and parametric studies of the cold-formed steel sections.

Chapter 5 provides the comparisons of the FEA and experimental without web holes results with the design strength calculated using the current specifications.

Chapter 6 examines the web crippling strength reduction based on experiment and FEA results and proposes design recommendation in the form of web crippling strength reduction factors for all the loading condition and cases.

Chapter 7 summarises the thesis and provides conclusions and suggestion for future research.

CHAPTER 2. LITERATURE REVIEW

2.1 Introductory remarks

A literature review on the web crippling behaviour of cold-formed sections is presented in this Chapter. It should be noted that there has been little research on the web crippling of cold-formed steel sections with web holes.

2.2 Research on web crippling behaviour without web opening

Research on the web crippling of cold-formed steel sections began in 1939 at Cornell University under the supervision of Winter. Winter and Pian (1946) investigated the web crippling problem with cold-formed steel sections and considered four different load cases. They carried out 136 tests on I-sections and developed design recommendations. In these test, the specimen flanges were not fastened to the bearing plates. Later, Cornell (1953) reported 128 tests on hat sections and 26 tests on U-sections. Baehre (1975) tested single unreinforced multi-web sections subjected to interior-one-flange loading. Hetrakul and Yu (1978) developed new expressions for all loading condition based on 140 test results of single unreinforced webs for both stiffened and unstiffened flanges. Experimental studies on web crippling and the interaction of bending and web crippling of multi-web cold-formed steel sections were performed by Wing (1981) at the University of Waterloo. He also considered the specimens fastened to the support. In 1986, Santaputra et al. (1989) at the University of Missouri-Rolla, tested high strength steel I-sections and hat sections with material yield strength up to 1310 MPa were considered to investigate the web crippling strength. The finite element analysis package ADINA was used by Sivakumaran (1989) to find out the web crippling behaviour of cold-formed steel lipped section. Using the available experiment data found in the literature, Parabakaran and Schuster (1993) completed an extensive statistical analysis of web crippling capacity of cold-formed steel sections and developed a simplified expression. Setiyono (1994)

presented theoretical and experimental results on web crippling behaviour of plain sections. A total of 42 tests on web crippling test on Z-section subjected to end-one-flange loading and I-sections subjected to interior-one-flange loading performed by Cain *et al*. (1995). Flanges fastened and unfastened cases were considered and recommended a modification expression for fastened Z-section subjected to EOF loading. Rhodes and Nash (1998) carried out theoretical investigation on web crippling behaviour of channel section under interior-one-flange and interior-two-flange loading conditions. The above authors performed finite element and finite strip analysis and compared results with different design specifications. Based on 72 tests on C-section fastened to the support, Gerges and Schuster (1998) proposed new parameter coefficients using Parabakaran and Schuster (1993) expression. Beshara and Schuster (2000a) reported all the web crippling tests data found in literature and performed an extensive statistical analysis. The new improved coefficients were proposed. Young and Hancock (2001) reported that the AISI specification were unconservative for the unlipped channel section for the dimensions considered and proposed simple design equations using a plastic mechanic model. Later, Ren *et al*. (2006) developed finite element models for interior-one-flange (IOF) and end-one-flange (EOF) loading condition and validated these against Young (2001) test results. Zhou (2006) studied the structural behaviour of cold-formed stainless steel square and rectangular hollow sections subjected to web crippling. Heiyantuduwa (2008) investigated the web crippling behaviour of cold-formed steel lipped channel beams employing experimental, numerical and theoretical techniques and proposed new parameter coefficients for web crippling loading conditions.

2.3 Research on web crippling behaviour with web opening

2.3.1 Yu and Davis (1973)

Yu and Davis (1973) described 20 tests investigating the web crippling strength of back-to-back channel sections with an interior-one-flange loading condition. The tests were conducted on sections with an overall depth-to thickness ratios ranged from 66.7 to 101, web hole depth ratio ranged from 0 to 0.641, yield stress of 411 MPa to 487 MPa and the bearing length was 89 mm for all the tests.

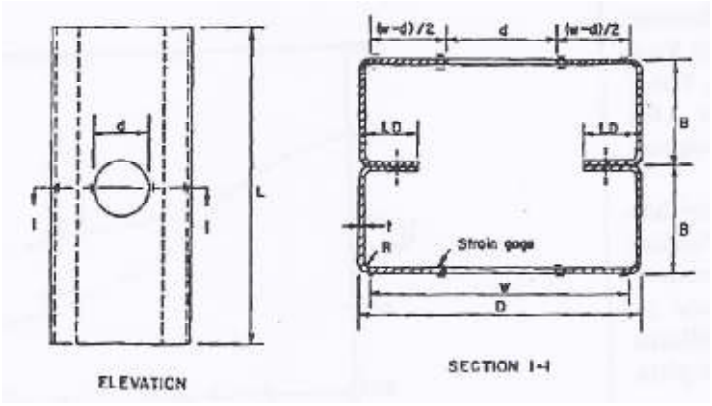

Figure 2.1 Typical I-section specimens tested by Yu and Davis (1973)

The test programme comprised both circular and square holes; the holes were located and centred beneath the bearing plate shows as in Figure 2.1. The following two strength reduction factors were proposed.

For web having circular opening with $0< d/h \leq 0.5$

$$RF = 1 - 0.6\frac{d}{h} \qquad \text{Equation 2.1}$$

where

d is diameter of the circular hole,

h is the clear distance between flanges measured in the plane web.

For web having square opening with $0< h_s/h \leq 0.642$

$$RF = 1 - 0.77\frac{h_s}{h} \qquad \text{Equation 2.2}$$

where

h_s is the width of the square hole,

h is the clear distance between flanges measured in the plane web.

2.3.2 Sivakumaran and Zinlonka (1989)

Sivakumaran and Zielonka (1989) described 103 tests on single lipped channel sections, but again for the IOF loading condition and with the rectangular holes located and centred beneath the bearing plate shown in Figure 2.2.

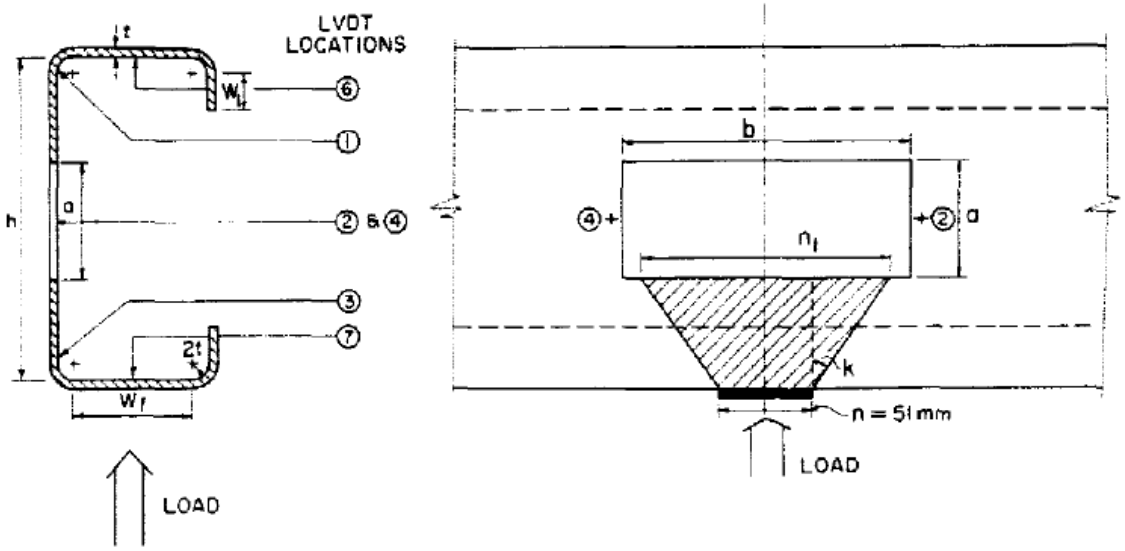

Figure 2.2 Typical cross-section of C-section specimens tested by Sivakumaran and Zielonka (1989)

The height of the opening varied from 3 mm to 151 mm; the length of bearing plate was 51mm. Following strength reduction factor equation was proposed.

$$R = \frac{P(with-opening)}{P(without-opening)} = \left[1-0.197\left(\frac{a}{h}\right)^2\right]\left[1-0.127\left(\frac{b}{n_1}\right)^2\right] \qquad \text{Equation 2.3}$$

where

n_1 is (N+h-a); N= bearing load length,

h is flat height of web,

a = height of web opening ,

b =longitudinal length of web opening.

This equation has a limitation on web openings with a/h less than or equal to 0.75 and b/n_1 less than or equal to 2.0. Sivakumaran *et al* did not investigate the case of other web crippling loading conditions, different shapes and location of the web openings. The effect of varying the bearing plate length was also not investigated.

2.3.3 Lagan (1994)

Langan (1994) presented 168 tests investigating the web crippling behaviour of single unreinforced webs for C-sections subjected to IOF and EOF loading condition (shown in Fig 2.3) with rectangular with fillet corners holes and located at mid height of the web.

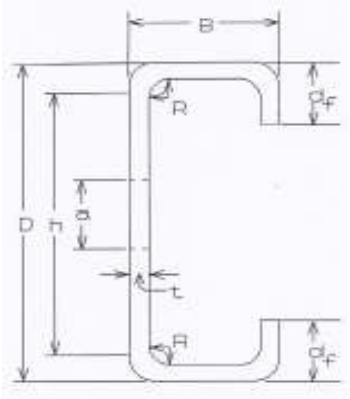

(a) Specimen cross-section

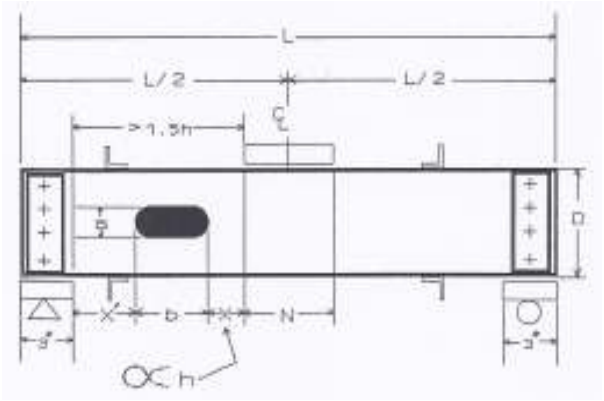

(b) IOF specimen

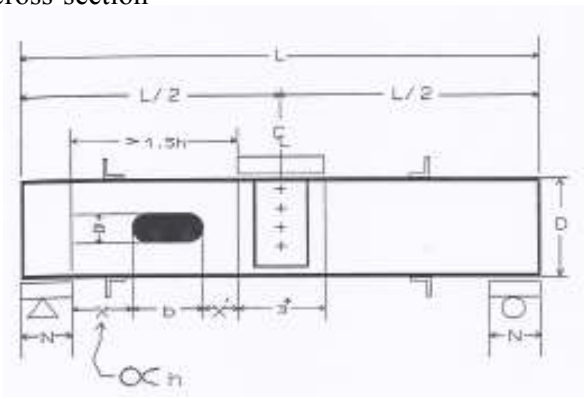

(c) EOF specimen

Figure 2.3 Typical C-section specimens tested by Langan (1994)

Lagan (1994) demonstrated that the main factors influencing the web crippling strength are the ratio of the hole depth to the depth of the web, and the ratio of the distance from the edge of the bearing to the flat depth of web. 0.74 x 4 inches and 1.54 x 4 inches sizes of web opening were used in this research. The x/h ratio were 0, 0.5, 0.7, 1.0 and 1.5.

The bearing plate lengths were 3.0, 4.0, 5.0 and 6.0 inches during the investigation. The following two reduction factor equations were proposed.

For the IOF loading condition:

$$RF = 1.08 - 0.630\ (\frac{a}{h}) + 0.120\ (\alpha) \quad \leq\ 1 \qquad \text{Equation 2.4}$$

For the EOF loading condition:

$$RF = 0.964 - 0.272\ (\frac{a}{h}) + 0.0631\ (\alpha) \quad \leq\ 1 \qquad \text{Equation 2.5}$$

where

a is height of the web opening,

h is height of the web,

α is x/h ; x is distance from the outer edge of the opening to the interior edge of the support bearing plate.

2.3.4 Chung (1995)

Chung (1995a) presented 57 tests on the web crippling behaviour of lipped channel sections and Sigma sections considering single and multiple opening subjected to IOF loading condition shown in Figure 2.4. Four different opening shape i.e. circular, elongated circular, square and rectangular openings were considered in this research. Design recommendations were provided in Chung (1995b).

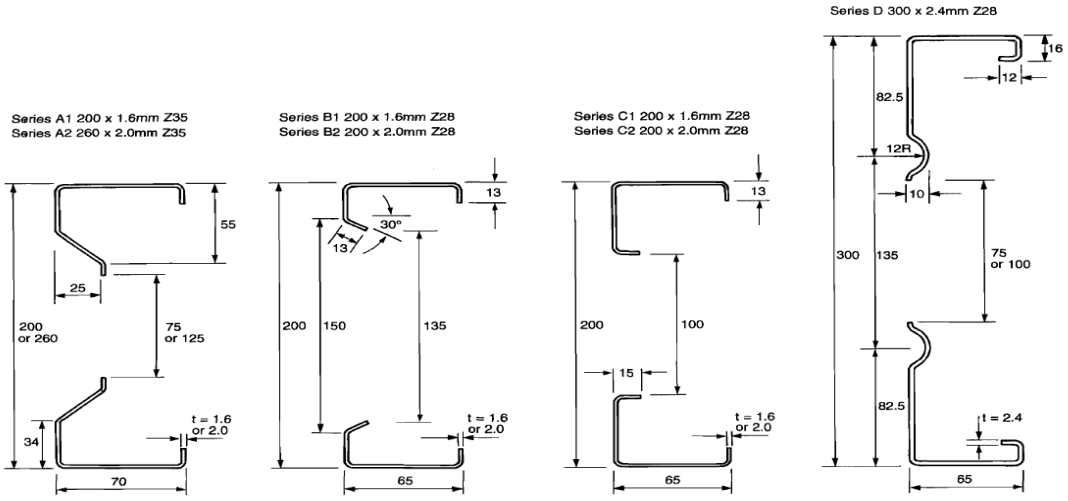

Figure 2.4 Typical cross-section of the specimens tested by Chung (1995a)

2.3.5 Deshmukh (1996) & Uphoff (1996)

At the University of Missouri-Rolla, Deshmukh (1996) performed 56 tests under IOF loading conditions and Uphoff (1996) performed a total of 52 tests under EOF loading conditions on cold-formed steel channel sections with circular web openings shown in Figure 2.5 and Figure 2.6. The inside corner radius-to-thickness ratio r_i/t ranged from 3.2 to 5.3, the web slenderness h/t ranged from 98.7 to 224.2, the bearing length-to-thickness ratio N/t ranged from 53.6 to 91.7, the yield stresses f_y of the material ranged from 324 to 392 MPa and the hole depth-to-the depth of flat portion of the web ratio a/h ranged from 0.36 to 0.81.

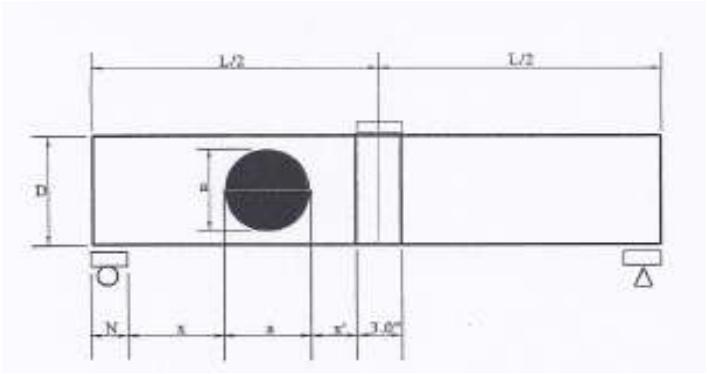

Figure 2.5 Typical cross-section of the specimens tested by Deshmukh (1996)

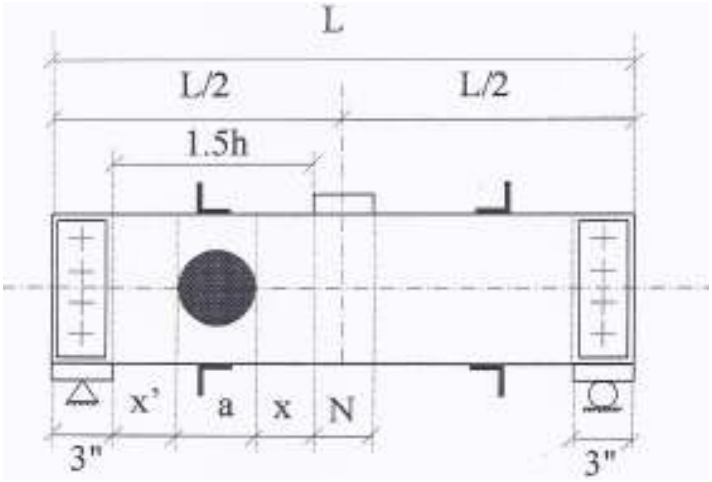

Figure 2.6 Typical cross-section of the specimens tested by Uphoff (1996)

Based on these test results, reduction factor equations were proposed to consider the effect of the web opening on the web crippling capacity under IOF loading condition. Both experimental investigations were also reported by LaBoube et al. (1997) and LaBoube et al. (1999).

2.3.6 Zhou and Young (2010)

Zhou and Young (2010) conducted 84 tests and 132 numerical simulations on aluminium alloy square hollow sections with circular holes located at the centred beneath the bearing plates. The web crippling tests were conducted under loading conditions of (ETF) and (ITF). Based on the experimental and numerical results following reduction factor equations were also proposed for aluminium alloy square hollow sections.

For the ETF loading condition:

$$R = 1.03 - 0.98\,(\frac{a}{h}) + 0.26\,(\frac{N}{h}) \quad \leq 1 \qquad \text{Equation 2.6}$$

For the ITF loading condition:

$$R = 1.00 - 0.64\,(\frac{a}{h}) + 0.18\,(\frac{N}{h}) \quad \leq 1 \qquad \text{Equation 2.7}$$

where

a is height of the web opening,

h is height of the web,

N is length of bearing plate.

Table 2.1 and Table 2.2 summarized the literature review on web crippling behaviour on cold-formed steel section with and without holes.

2.4 Concluding remarks

The above literature on web crippling clearly shows that no research has been carried out on (ETF) and (ITF) loading condition considering web holes. In practice, web holes can be punched either centred beneath the bearing plates or with offset distance to the bearing plates and flanges can be either fastened or unfastened to the support. The NAS (2001) specifications and all the researchers provide design recommendations for only end-one-flange (EOF) and interior-one-flange (IOF). The design equations were limited to the web holes located with an offset distance to the bearing plates and flanges have to be unfastened. In this thesis, a combination of experimental tests and non-linear elasto-plastic finite element analyses (FEA) are used to investigate the effects web holes on the web crippling strength of lipped channel sections under the end two flange (ETF) and interior-two-flange (ITF) loading condition; the cases of both flanges fastened and flanges unfastened to the support are considered.

Table 2.1 Summary of research on web crippling behaviour without holes

Researcher	Load cases	Type of specimen	Number of tests	Description
Winter and Pian (1946)	IOF,EOF,ITF and ETF	I-Section,	136	Develop expressions for computing the web crippling capacity of I-section
Cornell (1953)	IOF	Hat-section, U section	128 for Hat-section 26 for U-section	Web crippling of cold formed steel members having single unreinforced webs
Ratliff (1975)	IOF	C-section	26	Interaction of Concentrated Loads and Bending in C-Shaped Beams
Baehre (1975)	IOF	Unreinforced multi-web section	-	Web crippling of single unreinforced multi-web sections
Hetrakul and Yu (1978)	IOF,EOF,ITF and ETF	Hat-section, U section	Used Cornell (1953) test data	Developed new expressions for computing web crippling of cold formed steel sections having single unreinforced webs.
Wing (1981), Wing and Schuster (1986)	IOF,ITF and ETF	multi-web sections	-	Interaction of bending and web crippling of multi-web Section. Specimen fastened to the reaction supports
Davies and Packer (1987)	IOF and EOF	Rectangular Hollow Sections	-	Analysis of Web Crippling in a Rectangular Hollow Sections
Santaputra et al. (1989)	IOF,EOF,ITF and ETF	I-Section, Hat section	36 for Hat-section 24 for I-beams	Web crippling strength of high strength steel beam
Sivakumaran (1989)	IOF	C-section	103	Finite element analysis of web crippling behaviour C-sections
Studnicka (1991)	IOF and EOF	Multi-web Deck Sections	40	Web Crippling of Multi-web Deck Sections
Bakker (1992), Bhakta et al. (1992)	IOF,EOF,ITF and ETF	Steel deck section	-	Web Crippling of Cold-Formed Steel deck section and The effect of flange restraint on web crippling strength
Parabakaran and Schuster (1993)	IOF,EOF,ITF and ETF	multi-web sections	Used test data found in literature	Statistical analysis of the web crippling capacity of cold formed steel sections by using the available experimental data found in the literature
Setiyono (1994)	IOF,EOF,ITF and ETF	Plain C-sections	221	Web crippling behaviour of plain channel sections under combined and concentrated loading based on plastic mechanism approach
Cain *et al*. (1995)	EOF and IOF	Z-section and I-Section	28 for Z section 14 for I section	Experimentally investigated the conservative and unconservative aspects of the AISI design provisions for web crippling of Z and I section.
Korvink et al. (1995)	EOF	Stainless C-section	139	Web crippling of stainless steel cold-formed beams
Vaessen (1995)	IOF	C-section	FEA	On the Elastic Web Crippling Stiffness of Thin-Walled Cold-Formed Steel Members
Rhodes and Nash (1998)	ITF and ETF	Plain C-sections	Used Setiyono (1994) tests data for FEA	Theoretical examinations of the behaviour of channel sections under single or two flange loading are derived and compared with the predictions of different

Researcher	Load cases	Type of specimen	Number of tests	Description
Gerges and Schuster (1998), Gerges (1997)	EOF	C-section	72	Investigated design expressions for predicting the web crippling resistance of single web cold formed members with large inside bend radius to thickness ratio
Wu et al. (1998)	IOF and EOF	Hat-section	136	Web Crippling Strength of Cold-formed single-rib and double-rib hat-shaped section.
Beshara (1999), Beshara and Schuster (2000a)	IOF,EOF,ITF and ETF	C-section , Z-section , Hat-section	-	Web crippling data and calibrations of cold formed steel members
Beshara and Schuster (2000b)	ETF and ITF	C-section , Z-section ,	72	Web crippling of cold-formed steel C- and Z- sections
Hofmeyer (2000)	IOF,EOF,ITF and ETF	Trapezoidal Steel Sheeting	72	Combined Web Crippling and Bending Moment Failure of First-Generation Trapezoidal Steel Sheeting
Young and Hancock (2000a), Young and Hancock (2002)	IOF and EOF	Plain C-sections	25	Experimental investigation of cold-formed channels subjected to combined bending and web crippling
Young and Hancock (1998), Young and Hancock (2000b), Young and Hancock (2001)	IOF,EOF,ITF and ETF	Plain C-sections	50	Test Results are compared with Australian/New Zealand Standard and developed plastic mechanism formula for web crippling strength of plain channels.
Young and Hancock (2000c), Young and Hancock (2004)	ETF and ITF	Plain C-sections	32	Web crippling of cold-formed unlipped channels with flanges restrained
Kaspers (2001)	IOF,EOF,ITF and ETF	Trapezoidal Steel Sheeting	-	Combined Web Crippling and Bending Moment Failure of Second-Generation Trapezoidal Steel Sheeting
Holesapple and Laboube (2003), Stephens and Laboube (2003)	EOF	C-section , Z-section ,	29	Web crippling of cold-formed steel beams at end supports
Young and Hancock (2003)	ETF and ITF	Plain C-sections	40	Cold-formed steel channels subjected to concentrated bearing load
Avci and Easterling (2004)	EOF	Steel Deck section	78	Web crippling strength of steel deck subjected to end one flange loading
Kaitila (2004)	IOF,EOF,ITF and ETF	Steel Cassettes	52 and FEM	Web Crippling of Cold-Formed Thin-Walled Steel Cassettes
Ren *et al*. (2006)	EOF and IOF	Plain C-sections	Used Young (2001) tests data for FEA	Finite element analysis conducted on Plain channels subject to combined bending and web crippling.
Zhou (2006)	IOF,EOF,ITF and ETF	Square and rectangular hollow section	155- Web crippling 36- Combine bending and web crippling	Web crippling of cold-formed stainless steel tubular sections
Heiyantuduwa (2008)	IOF,EOF,ITF and ETF	C-section	252	Web Crippling behaviour of cold-formed steel lipped channel employing experimental, numerical and theoretic techniques.

Table 2.2 Summary of research on web crippling behaviour with holes

Researcher	Load cases	Type of specimen	Number of tests	Web holes	Description
Yu and Davis (1973)	IOF	I-section	20	Circular and square holes were located and centred beneath the bearing plate	Limited study that contained 20 test specimens subjected to an IOF loading condition
Sivakumaran and Zielonka (1989)	IOF	C-section	103	Rectangular holes were located and centred beneath the bearing plate	Effect of web openings on the web crippling strength of unreinforced cold-formed
Langan (1994), LaBoube et al. (1997)	IOF EOF	C-section	90 for IOF 78 for EOF	Rectangular with fillet corners holes and located at mid height of the web	Experimental investigation of web crippling effect subject to IOF and EOF
Chung (1995a), Chung (1995b)	IOF	C-section and Sigma section	57	Four different opening shape i.e. circular, elongated circular, square and rectangular openings	Experimental test on cold formed sections with single and multiple web openings of different sizes and shapes, both stiffened and unstiffened.
Deshmukh (1996)	IOF	C-section	56	Circular web hole were located with a horizontal clear distance to the near edge of the bearing plates	Experimental investigation of web crippling effect subject to IOF
Uphoff (1996)	EOF	C-section	55	Circular web hole were located with a horizontal clear distance to the near edge of the bearing plates	Experimental investigation of web crippling effect subject to EOF
Zhou and Young (2010)	ETF ITF	Aluminium alloy square hollow sections	84	Circular holes were located at the centred beneath the bearing plates	Experimental and numerical investigations of aluminium alloy square hollow sections with circular hole in the webs subjected to web crippling

CHAPTER 3. EXPERIMENTAL INVESTIGATION

3.1 Introductory remarks

This Chapter describes the experimental investigation of the web crippling behaviour of cold-formed steel sections with web opening. The details of tests and results are presented in this chapter. It also includes the details of tests carried out to determine the material properties of the channel section and the results. In this research interior-two-flange (ITF) and end-two-flange (ETF) loading conditions were considered with the cases of both flanges fastened and unfastened to the support.

3.2 Test specimens

A test programme was conducted on lipped channel sections, as shown in Figure 3.1, with circular web holes subjected to web crippling. The size of the web holes was varied in order to investigate the effect of the web holes on the web crippling strength. The circular holes with nominal diameters (a) ranging from 40 to 240 mm were considered in the experimental investigation. The ratio of the diameter of the holes to the depth of the flat portion of the webs (a/h) was 0.2, 0.4, 0.6 and 0.8.

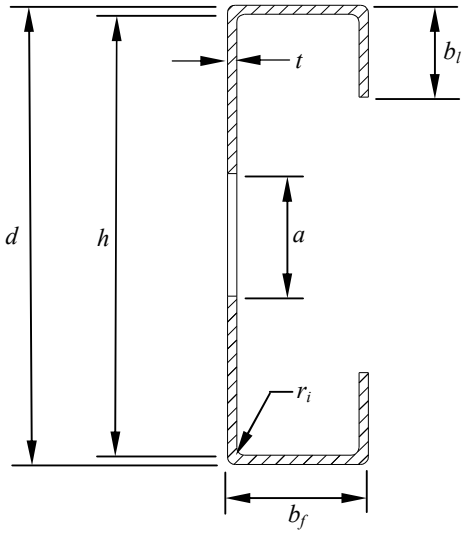

Figure 3.1 Definition of symbols

All the test specimens were fabricated with web holes located at the mid-depth of the webs. In practice, web holes can be punched either centred beneath the bearing plates or with offset distance to the bearing plates. Therefore, both types of web holes position were considered into the web. The experimental investigation consists of two types of test series for each specimen which were:

- Type 1 web holes: Where web holes located with a horizontal clear distance to the near edge of the bearing plates (Figure 3.2 (a) & Figure 3.2 (b)).
- Type 2 web holes: Where web holes located centred beneath the bearing plates. (Figure 3.2 (c) & Figure 3.2 (d)).

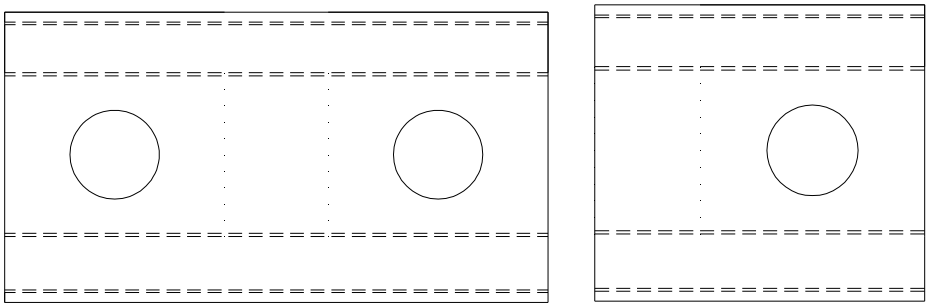

(a) Type 1 web holes section for ITF (b) Type 1 web hole section for ETF

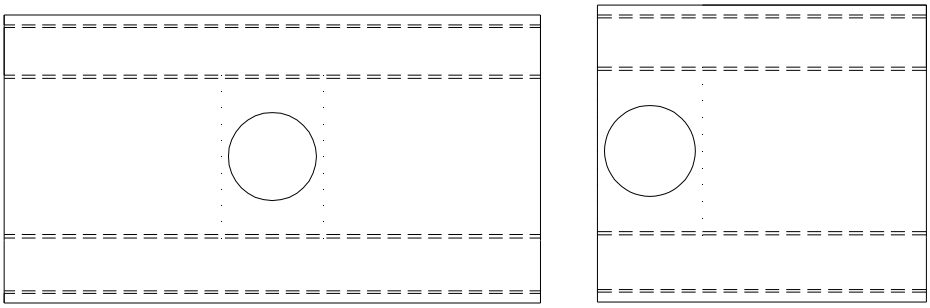

(c) Type 2 web hole section for ITF (d) Type 2 web holes section for ETF

Figure 3.2 Types of web holes location into web of the section

Channel sections without web holes were also tested for comparison of web crippling strength. The test specimens comprised five different section sizes, having the nominal thicknesses ranging from 1.3 to 2.0 mm; the nominal depth of the webs and the flange widths

ranged from 142 to 302 mm. The measured web slenderness (*h/t*) values of the channel sections ranged from 116 to 176. The bearing plates were fabricated using high strength steel having a thickness of 25 mm. Two lengths of bearing plates (N) were used: the full flange width of the channel section and half width of the channel for Type 1 holes. While 90 mm, 120 mm and 150 mm length bearing plates (N) were used for Type 2 holes.

3.3 Material properties

Tensile coupon tests were carried out to determine the material properties of the channel specimens. The tensile coupons were taken from the centre of the web plate in the longitudinal direction of the untested specimens. The tensile coupons were prepared and tested according to the British Standard for Testing and Materials EN (2001) for the tensile testing of metals using 12.5 mm wide coupons of a gauge length 50 mm. The coupons were tested in a MTS displacement controlled testing machine using friction grips as shown in Figure 3.3.

Figure 3.3 Tensile test setup

Two strain gauges and a calibrated extensometer of 50 mm gauge length were used to measure the longitudinal strain. The material properties obtained from the tensile coupon tests are summarised in Table 3.1, which includes the measured static 2% proof stress ($\sigma_{0.2}$), the static tensile strength (σ_u) and the elongation after fracture (ε_f) based on gauge length of 50 mm.

Table 3.1 Material properties obtained from tensile tests

Section	Test number	Coupon thickness t (mm)	2% Proof Stress $\sigma_{0.2}$ (MPa)	Average 2% Proof Stress $\sigma_{0.2}$ (MPa)	Ultimate Stress σ_u (MPa)	Average Ultimate Stress σ_u (MPa)	Elongation, (%)
142 x 60 x 13 x 1.3	1	1.26	457	455	536	532	23.00
	2	1.26	440		521		23.00
	3	1.26	462		535		23.00
	4	1.26	459		535		23.00
172 x 65 x 16 x 1.3	1	1.25	539	534	568	566	11.00
	2	1.25	532		564		9.00
	3	1.45	533		568		10.00
	4	1.53	533		564		11.00
202 x 65 x 13 x 1.4	1	1.44	518	513	555	552	11.00
	2	1.43	512		552		11.00
	3	1.44	513		551		11.00
	4	1.44	510		551		11.00
262 x 65 x 13 x 1.6	1	1.52	529	525	555	546	9.00
	2	1.53	523		528		10.00
	3	1.53	528		552		10.00
	4	1.53	520		550		10.00
302 x 88 x 18 x 2.0	1	1.93	483	483	525	523	11.00
	2	1.94	485		522		11.00
	3	1.93	482		525		11.00
	4	1.94	483		519		11.00

Figure 3.4 shows the photograph of sample test specimens after failure. The stress-strain curve obtained from the tensile coupon tests can be found in Appendix A in this thesis.

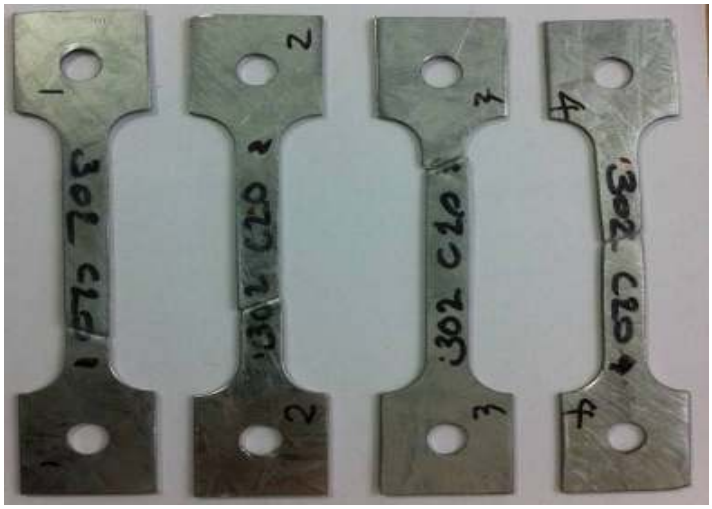

Figure 3.4 Photograph of sample tensile coupon test specimen after failure

3.4 Interior-two-flange (ITF) web opening study

3.4.1 Test specimens

The specimen lengths (L) were determined according to the NAS Specification (NAS (2001)). Generally, the distance from the edge of the bearing plate to the end of the member was set to be 1.5 times the overall depth of the web (d) rather than 1.5 times the depth of the flat portion of the web (h), the latter being the minimum specified in the specifications.

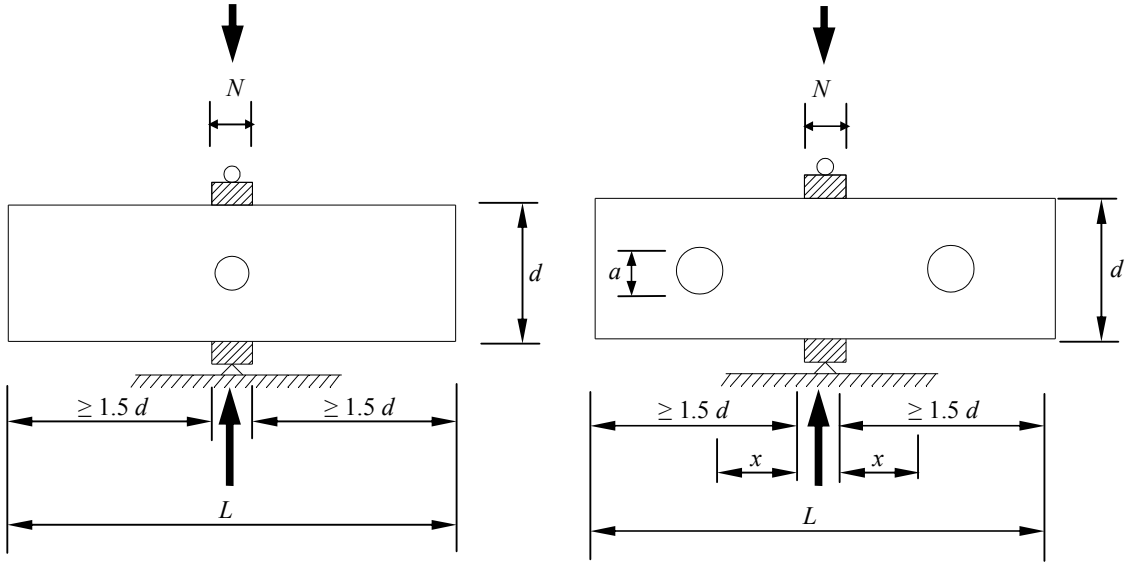

(a) With holes (Type 2) (b) With holes (Type 1)

Figure 3.5 ITF loading condition

Table 3.2 and Table 3.3 show the measured test specimen dimensions for the flange unfastened case. Table 3.4 and Table 3.5 show the measured test specimen dimensions for the fastened case. Above mentioned tables using the nomenclature defined in Figure 3.5 (a) and Figure 3.5 (b) for the ITF loading condition.

3.4.2 Specimens labelling

In all tables the specimens were labelled such that the loading condition, the nominal dimension of the specimen and the length of the bearing as well as the ratio of the diameter of the holes to the depth of the flat portion of the webs (*a/h*) could be identified from the label. For example, the labels, "ITF202x65x13-t1.4N90MA0FX" define the following specimens:

- The first three letter indicates the loading condition of interior-two-flange were used in test.
- The following symbols are the nominal dimensions ($d \times b_f \times b_l$–t1.4) of the specimens in millimetres. (202×65×13-t1.4 means d = 202 mm; b_f = 65 mm; b_l = 13 mm and t = 1.4 mm).
- The notation "N32.5" indicates the length of bearing in millimetres (32.5 mm).
- The last notations "A0.2", "A0.4", "A0.6" and "A0.8" stand for the ratios of the diameter of the holes to the depth of the flat portion of the webs (*a/h*) were 0.2, 0.4, 0.6 and 0.8, respectively. (A0.2 means *a/h* = 0.2; A0.8 means *a/h* = 0:8).
- "MA0","MA0.2", "MA0.4", "MA0.6" and "MA0.8" indicate Type-2 holes.
- Channel section specimens without web holes are denoted by "A0". FR means flanges unfastened to the support and FX means flanges fastened to the support.

3.4.3 Test rig and procedure

The specimens were tested under the ITF loading condition specified in the NAS Specification NAS (2001), as shown in Figure 3.6 (a) and Figure 3.6 (b). For the ITF loading condition, two identical bearing plates of the same width were positioned at the end and the mid-length of each specimen, respectively. Hinge supports were simulated by two half rounds in the line of action of the force.

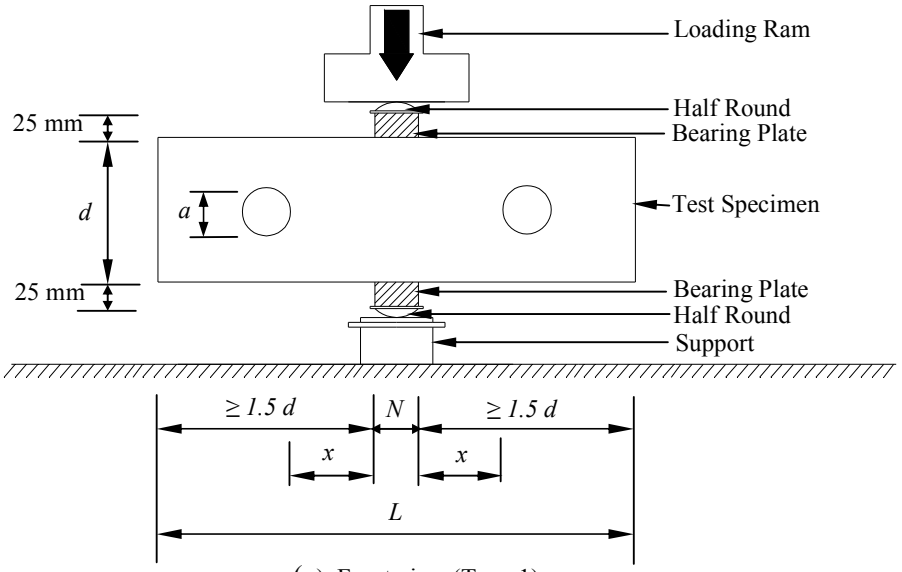

(a) Front view (Type 1)

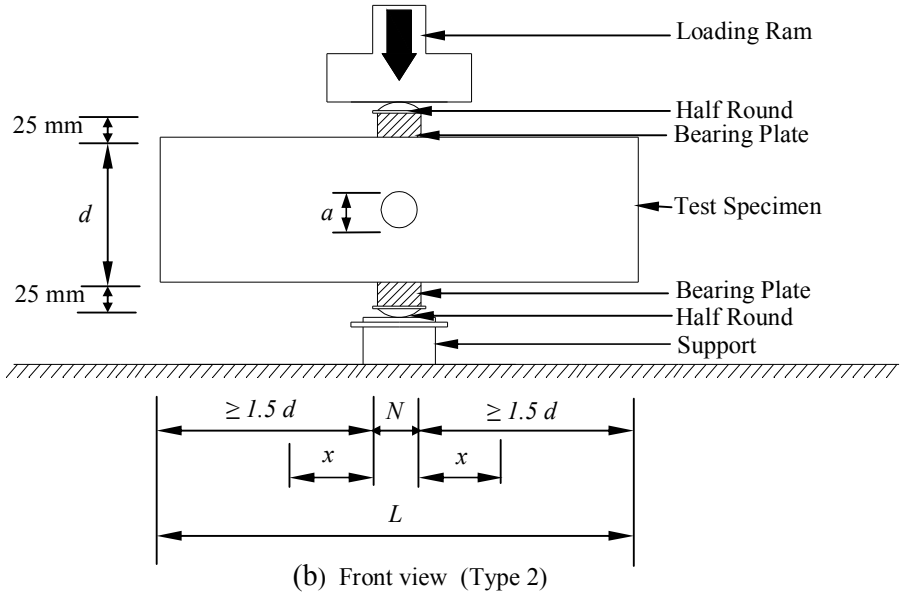

(b) Front view (Type 2)

Figure 3.6 Schematic view of Interior-Two-Flange loading test arrangement (Front view)

A servo-controlled Tinius-Olsen testing machine was used to apply a concentrated compressive force to the test specimens. Displacement control was used to drive the hydraulic actuator at a constant speed of 0.05 mm/min for all the test specimens. The load or reaction force was applied by means of bearing plates. The bearing plates were fabricated using a high strength steel. All the bearing plates were machined to specified dimensions and the thickness was 25 mm. The flanges of the channel section specimens were unfastened and fastened to the bearing plates during testing as shown in Figure 3.7 (a) and Figure 3.7 (b). In the flanges fastened test setup, the flanges were bolted to the bearing plate. Figure 3.8 shows the photograph of ITF loading condition test setups.

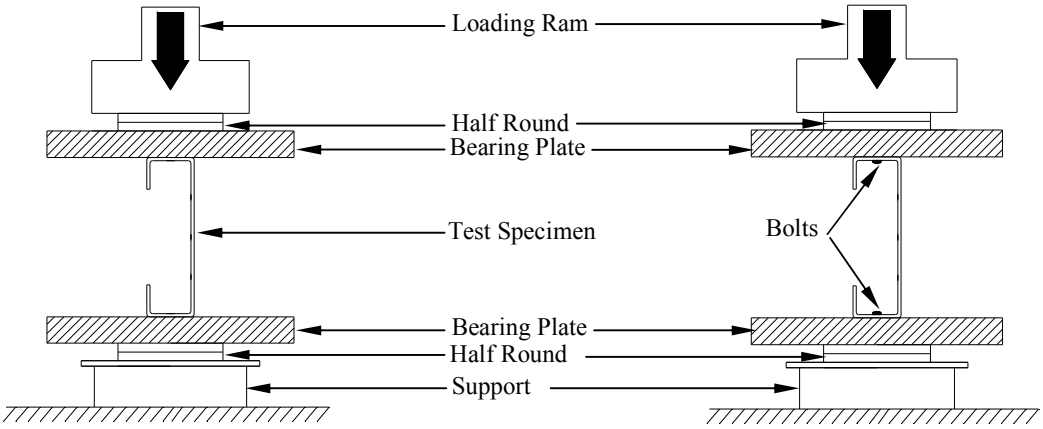

(a) End View (Unfastened flanges) (b) End View (Fastened flanges)

Figure 3.7 Schematic view of Interior-Two-Flange loading test arrangement (End view)

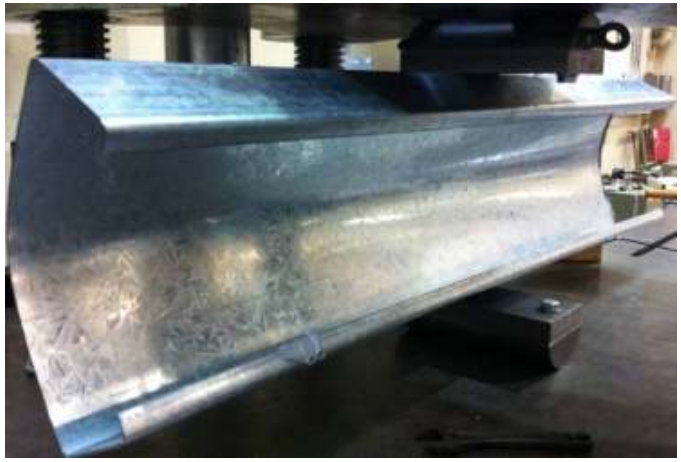

(a) Flanges unfastened (Without holes)

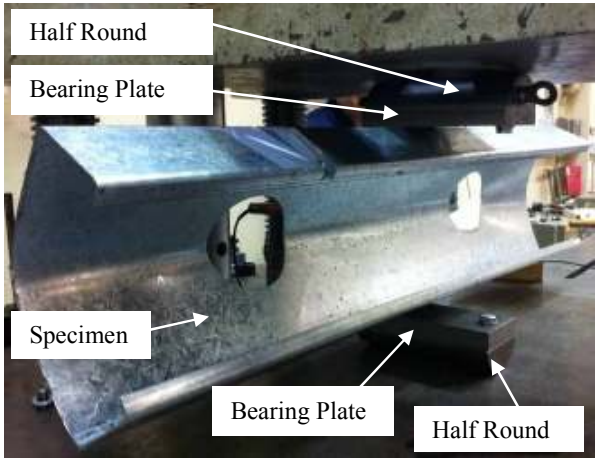

(b) Flanges unfastened (Type 1 holes)

(a) Flanges unfastened (Type 2 holes)

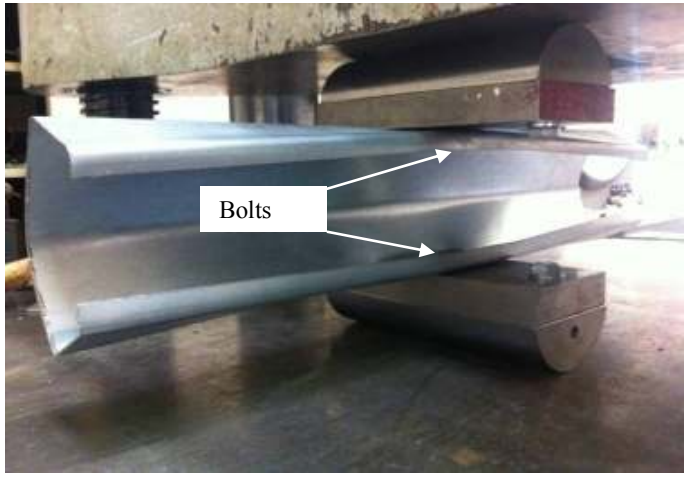

(a) Flanges fastened (Without holes)

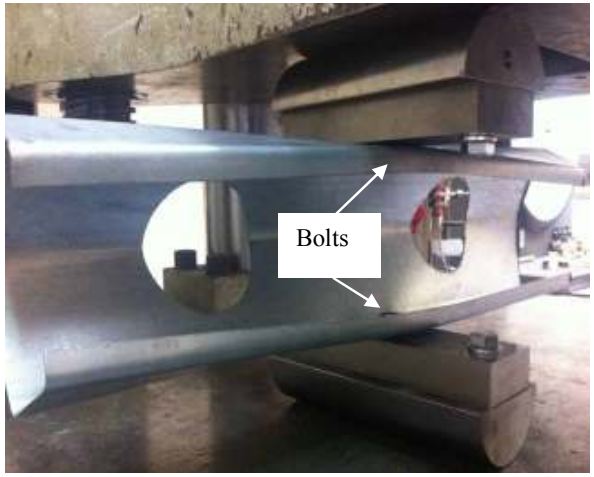

(b) Flanges fastened (Type 1 holes)

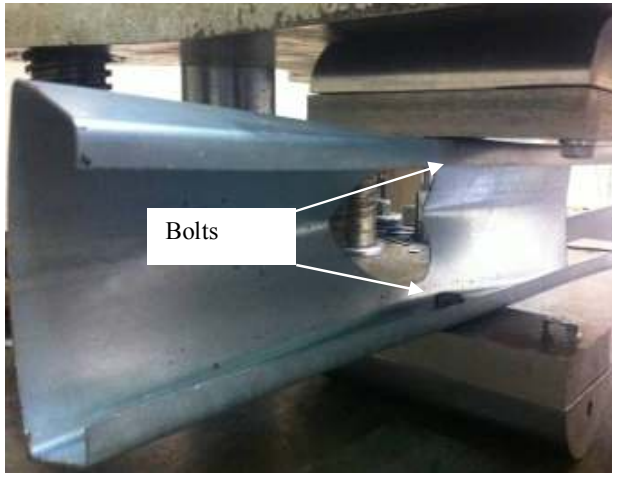

(a) Flanges fastened (Type 2 holes)

Figure 3.8 Test setup Interior-Two-Flange loading condition.

3.4.4 Test results

A total of 81 specimens were tested under the ITF loading condition considering both holes type with flanges unfastened and fastened conditions. The experimental ultimate web crippling loads per web (P_{EXP}) for the flanges fastened and unfastened condition are given in Table 3.2, Table 3.3, Table 3.4 and Table 3.5 respectively for both types web holes. All load-displacement curves obtained from tests considering both without and with web holes, and the comparisons with the numerical results is shown in Appendix B. The typical failure mode of web crippling of the specimens is shown in Appendix C.

Table 3.2 Measured specimen dimensions and experimental ultimate loads for flanges fastened under ITF loading condition (Type 1 web holes)

Specimen	Web d (mm)	Flange b_f (mm)	Lip b_l (mm)	Thickness t (mm)	Fillet r_i (mm)	Holes a (mm)	Length L (mm)	Exp. load per web P_{EXP} (kN)
ITF142x60x13-t1.3N30A0FX	142.2	59.4	15.5	1.22	4.8	0.0	502.3	7.5
ITF142x60x13-t1.3N30A0.4FX	142.1	59.3	14.4	1.20	4.8	55.6	499.1	7.0
ITF142x60x13-t1.3N60A0FX	142.5	60.1	16.0	1.21	4.8	0.0	555.0	8.1
ITF142x60x13-t1.3N60A0.4FX	142.5	60.1	15.1	1.21	4.8	55.4	552.3	7.3
ITF172x65x13-t1.3N32.5A0FX	172.8	63.6	15.1	1.26	4.8	0.0	601.1	8.9
ITF172x65x13-t1.3N32.5A0.4FX	172.6	64.5	15.1	1.20	4.8	67.8	603.8	7.7
ITF172x65x13-t1.3N65A0FX	172.5	64.4	14.8	1.25	4.5	0.0	649.1	9.5
ITF172x65x13-t1.3N65A0.4FX	173.0	64.9	14.9	1.22	4.8	67.7	649.5	8.5
ITF202x65x13-t1.4N32.5A0FX	202.1	64.7	15.1	1.44	4.5	0.0	677.6	11.5
ITF202x65x13-t1.4N32.5A0.4FX	202.3	63.4	15.2	1.44	4.8	79.5	676.7	9.6
ITF202x65x13-t1.4N65A0FX	202.4	63.5	14.9	1.43	4.5	0.0	699.9	11.7
ITF202x65x13-t1.4N65A0.4FX	202.5	63.7	15.0	1.44	4.8	79.5	702.4	10.3
ITF262x65x13-t1.6N32.5A0FX	263.1	63.5	15.0	1.51	5.0	0.0	849.0	11.5
ITF262x65x13-t1.6N32.5A0.4FX	263.4	62.6	15.8	1.52	5.0	103.0	850.9	9.6
ITF262x65x13-t1.6N65A0.4FX	262.8	65.1	13.8	1.51	5.0	103.0	899.7	10.2
ITF302x90x18-t2N44A0.4FX	305.0	89.0	18.0	1.98	5.0	118.3	999.6	17.9
ITF302x90x18-t2N90A0FX	303.7	87.5	18.3	1.95	5.0	0.0	1050.7	22.3
ITF302x90x18-t2N90A0.4FX	303.6	88.3	18.5	1.87	5.0	118.9	1052.9	19.4

Note: 1 kip = 4.45 kN

Table 3.3 Measured specimen dimensions and experimental ultimate loads for flanges fastened under ITF loading condition (Type 2 web holes)

Specimen	Web d (mm)	Flange b_f (mm)	Lip b_l (mm)	Thickness t (mm)	Fillet r_i (mm)	Holes a (mm)	Length L (mm)	Exp. load per web P_{EXP} (kN)
ITF142x60x13-t1.3N90MA0FX	142.2	58.6	15.9	1.23	4.8	0.0	337.5	8.97
ITF142x60x13-t1.3N90MA0.2FX	142.2	58.6	15.9	1.23	4.8	27.9	337.5	8.96
ITF142x60x13-t1.3N90MA0.4FX	142.2	59.5	16.3	1.25	4.8	55.8	337.5	7.75
ITF142x60x13-t1.3N90MA0.6FX	142.2	59.5	16.3	1.25	4.8	83.6	337.5	6.64
ITF142x60x13-t1.3N90MA0.8FX	142.2	59.5	16.3	1.25	4.8	111.5	337.5	5.55
ITF142x60x13-t1.3N120MA0FX	141.8	58.9	15.6	1.24	4.8	0.0	350.0	9.44
ITF142x60x13-t1.3N120MA0.2FX	141.8	58.9	15.6	1.24	4.8	27.9	350.0	9.26
ITF142x60x13-t1.3N120MA0.4FX	141.3	58.8	16.3	1.24	4.8	55.7	350.0	8.19
ITF142x60x13-t1.3N120MA0.6FX	141.3	58.8	16.3	1.24	4.8	83.6	350.0	7.06
ITF142x60x13-t1.3N120MA0.8FX	142.2	59.5	16.3	1.25	4.8	111.5	337.5	5.94
ITF172x65x13-t1.3N120MA0FX	172.8	64.1	15.6	1.27	5.0	0.0	400.0	10.72
ITF172x65x13-t1.3N120MA0.4FX	172.3	63.6	15.5	1.27	5.0	67.6	400.0	9.31
ITF172x65x13-t1.3N120MA0.6FX	172.6	64.3	15.3	1.28	5.0	101.6	400.0	7.87
ITF202x65x13-t1.4N150MA0FX	202.1	63.1	17.5	1.45	5.0	0.0	450.0	13.51
ITF202x65x13-t1.4N150MA0.4FX	202.7	64.3	16.3	1.45	5.0	79.5	450.0	11.42
ITF202x65x13-t1.4N150MA0.6FX	202.4	64.2	16.5	1.45	5.0	119.5	450.0	10.10
ITF262x65x13-t1.6N150MA0FX	263.4	63.4	14.4	1.56	5.5	0.0	550.0	12.78
ITF262x65x13-t1.6N150MA0.2FX	262.8	63.4	14.7	1.55	5.5	51.8	550.0	12.41
ITF262x65x13-t1.6N150MA0.4FX	262.8	63.4	14.7	1.55	5.5	103.5	550.0	11.31

Note: 1 kip = 4.45 kN

Table 3.4 Measured specimen dimensions and experimental ultimate loads for flanges unfastened under ITF loading condition (Type 1 web holes)

Specimen	Web d (mm)	Flange b_f (mm)	Lip b_l (mm)	Thickness t (mm)	Fillet r_i (mm)	Holes a (mm)	Length L (mm)	Exp. load per web P_{EXP} (kN)
ITF142x60x13-t1.3N30A0FR	142.9	59.0	15.2	1.21	4.8	0.0	501.0	5.6
ITF142x60x13t1.3N30A0.2FR	142.9	59.0	15.2	1.21	4.8	27.9	501.0	4.9
ITF142x60x13t1.3N30A0.4FR	144.6	57.0	15.4	1.22	4.8	55.2	502.7	4.5
ITF142x60x13t1.3N30A0.6FR	144.6	59.0	15.2	1.21	4.8	83.6	501.0	3.5
ITF142x60x13t1.3N30A0.8FR	144.6	59.0	15.2	1.21	4.8	111.5	501.0	2.7
ITF142x60x13-t1.3N60A0FR	142.4	60.0	16.0	1.21	4.8	0.0	551.3	6.0
ITF142x60x13-t1.3N60A0.2FR	142.5	59.8	14.5	1.20	4.8	27.9	551.3	5.3
ITF142x60x13-t1.3N60A0.4FR	142.5	59.8	14.5	1.20	4.8	54.8	550.9	4.9
ITF142x60x13-t1.3N60A0.6FR	142.5	59.8	14.5	1.20	4.8	83.6	551.3	3.9
ITF142x60x13-t1.3N60A0.8FR	142.5	59.8	14.5	1.20	4.8	111.5	551.3	3.1
ITF172x65x13-t1.3N32.5A0FR	172.7	64.8	14.9	1.23	4.8	0.0	599.9	5.7
ITF172x65x13-t1.3N32.5A0.4FR	172.7	64.3	14.9	1.24	4.8	67.1	606.8	4.6
ITF172x65x13-t1.3N65A0FR	172.8	64.0	14.8	1.26	4.8	0.0	649.8	6.3
ITF172x65x13-t1.3N65A0.4FR	173.0	64.3	14.9	1.27	4.8	67.0	650.9	5.2
ITF202x65x13-t1.4N32.5A0FR	202.5	63.6	16.0	1.40	4.8	0.0	678.3	6.8
ITF202x65x13-t1.4N32.5A0.4FR	202.3	64.0	15.3	1.44	4.8	79.1	675.6	5.6
ITF202x65x13-t1.4N65A0FR	202.5	64.0	17.5	1.44	4.8	0.0	701.0	7.4
ITF202x65x13-t1.4N65A0.4FR	202.4	63.9	17.0	1.39	4.8	79.1	701.4	5.8
ITF262x65x13-t1.6N32.5A0FR	262.6	64.6	15.8	1.48	5.5	0.0	850.5	6.6
ITF262x65x13-t1.6N32.5A0.4FR	263.4	63.4	14.4	1.52	5.0	102.5	836.0	5.3
ITF262x65x13-t1.6N65A0FR	263.1	65.9	15.1	1.54	5.0	0.0	907.3	7.7
ITF262x65x13-t1.6N65A0.4FR	262.5	63.8	14.4	1.47	5.5	102.5	896.7	5.5
ITF302x90x18-t2N44A0.4FR	304.0	87.9	18.0	1.93	4.8	118.2	998.9	10.2
ITF302x90x18-t2N90A0FR	303.8	88.8	18.7	1.96	4.8	0.0	1052.2	14.1
ITF302x90x18-t2N90A0.4FR	303.1	87.8	19.1	1.94	4.8	118.0	1050.9	11.3

Note: 1 kip = 4.45 kN

Table 3.5 Measured specimen dimensions and experimental ultimate loads for flanges unfastened under ITF loading condition (Type 2 web holes)

Specimen	Web d (mm)	Flange b_f (mm)	Lip b_l (mm)	Thickness t (mm)	Fillet r_i (mm)	Holes a (mm)	Length L (mm)	Exp. load per web P_{EXP} (kN)
ITF142x60x13-t1.3N90MA0FR	142.2	58.6	15.9	1.23	4.8	0.0	337.5	6.03
ITF142x60x13-t1.3N90MA0.2FR	142.2	58.6	15.9	1.23	4.8	27.9	337.5	5.96
ITF142x60x13-t1.3N90MA0.4FR	142.2	59.5	16.3	1.25	4.8	55.8	337.5	5.45
ITF142x60x13-t1.3N90MA0.6FR	142.2	59.5	16.3	1.25	4.8	83.6	337.5	4.52
ITF142x60x13-t1.3N90MA0.8FR	142.2	59.5	16.3	1.25	4.8	111.5	337.5	3.52
ITF142x60x13-t1.3N120MA0FR	141.8	58.9	15.6	1.24	4.8	0.0	350.0	6.32
ITF142x60x13-t1.3N120MA0.2FR	141.8	58.9	15.6	1.24	4.8	27.9	350.0	6.05
ITF142x60x13-t1.3N120MA0.4FR	141.3	58.8	16.3	1.24	4.8	55.7	350.0	5.45
ITF142x60x13-t1.3N120MA0.6FR	141.3	58.8	16.3	1.24	4.8	83.6	350.0	4.75
ITF142x60x13-t1.3N120MA0.8FR	142.2	59.5	16.3	1.25	4.8	111.5	337.5	3.79
ITF172x65x13-t1.3N120MA0FR	172.8	64.1	15.6	1.27	5.0	0.0	400.0	7.05
ITF172x65x13-t1.3N120MA0.4FR	172.3	63.6	15.5	1.27	5.0	67.6	400.0	6.20
ITF172x65x13-t1.3N120MA0.6FR	172.6	64.3	15.3	1.28	5.0	101.6	400.0	5.67
ITF202x65x13-t1.4N150MA0FR	202.1	63.1	17.5	1.45	5.0	0.0	450.0	8.40
ITF202x65x13-t1.4N150MA0.4FR	202.7	64.3	16.3	1.45	5.0	79.5	450.0	7.37
ITF202x65x13-t1.4N150MA0.6FR	202.4	64.2	16.5	1.45	5.0	119.5	450.0	6.79
ITF262x65x13-t1.6N150MA0FR	263.4	63.4	14.4	1.56	5.5	0.0	550.0	8.19
ITF262x65x13-t1.6N150MA0.2FR	262.8	63.4	14.7	1.55	5.5	51.8	550.0	7.88
ITF262x65x13-t1.6N150MA0.4FR	262.8	63.4	14.7	1.55	5.5	103.5	550.0	7.29

Note: 1 kip = 4.45 kN

3.5 End-two-flange (ETF) web opening study

3.5.1 Test specimens

The specimen lengths (L) were determined according to the NAS Specification NAS (2001). Generally, the distance from the edge of the bearing plate to the end of the member was set to be 1.5 times the overall depth of the web (d) rather than 1.5 times the depth of the flat portion of the web (h), the latter being the minimum specified in the specifications. Table 3.6 and Table 3.7 shows the measured test specimen dimensions for the flange unfastened. Table 3.8 and Table 3.9 shows the measured test specimen dimensions for the fastened conditions. The above tables using the nomenclature defined in Figure 3.9 (a) and (b) for the ETF loading condition.

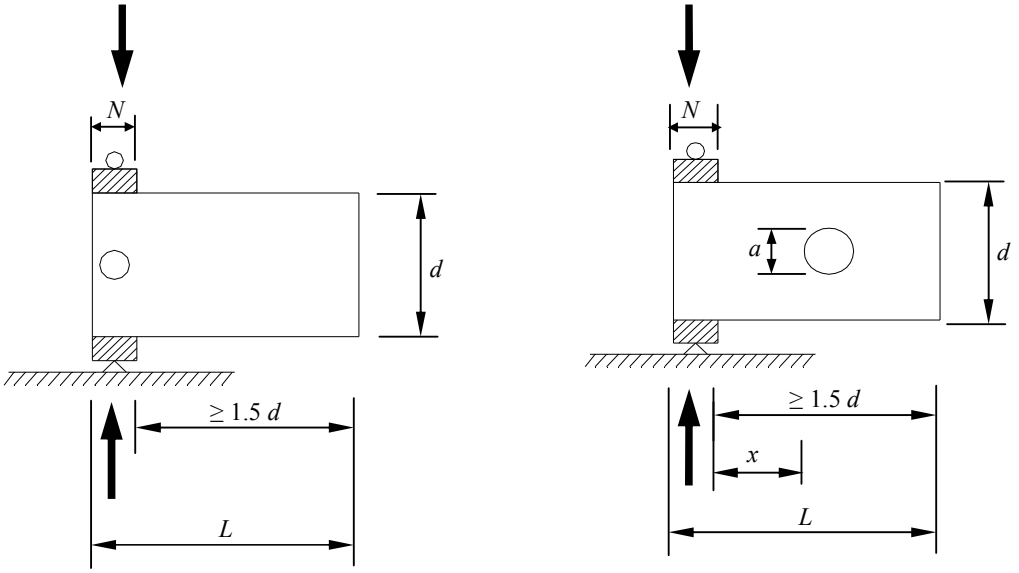

(a) Without holes (b) With holes

Figure 3.9 ETF loading condition

3.5.2 Specimens labelling

In the specimen label, the first three letters ETF indicate the loading condition of end-two-flange that were used in the test and the rest of symbols are explained in sub section 3.4.1 specimens labelling.

3.5.3 Test rig and procedure

The specimens were tested under the ETF loading condition specified in the NAS Specification NAS (2001), as shown in Figure 3.10 (a) and Figure 3.10 (b). For the ETF loading conditions, two identical bearing plates of the same width were positioned at the end of each specimen, respectively.

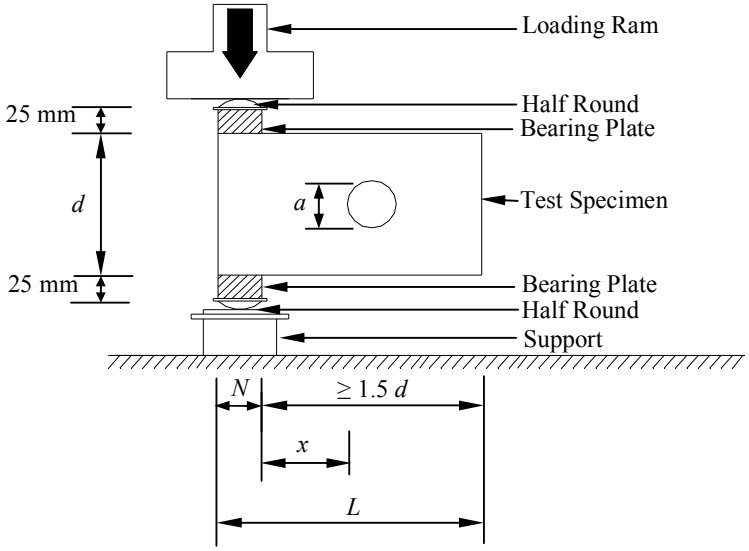

(a) Front view

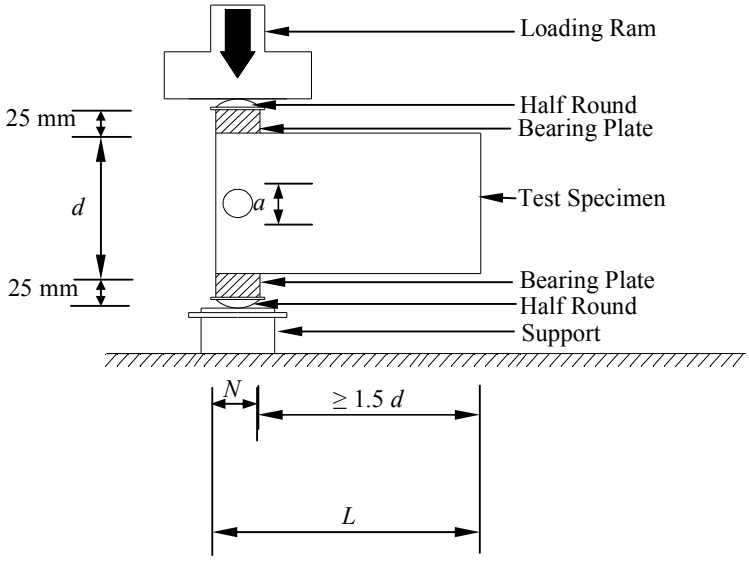

(a) Front view

Figure 3.10 Schematic view End-Two-Flange loading test arrangement (Front view)

Hinge supports were simulated by two half rounds in the line of action of the force. Testing procedure was similar to the ITF loading condition which was described sub section 3.4.3. The flanges of the channel section specimens were unfastened and fastened to the bearing plates during testing is shown in Figure 3.11 (a) and Figure 3.11 (b). In the flanges fastened test setup, the flanges were bolted to the bearing plate. Figure 3.12 show photographs of ETF loading condition test setups.

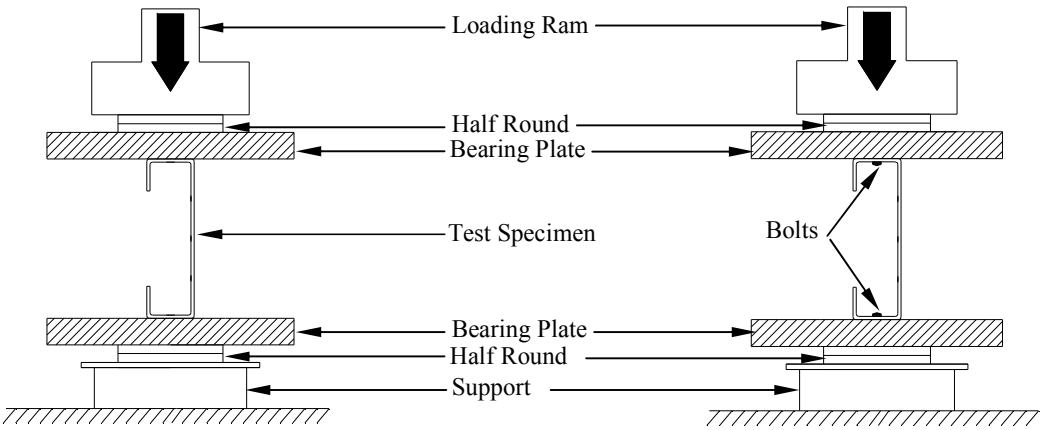

(b) End View (Unfastened flanges) (c) End View (Fastened flanges)

Figure 3.11 Schematic view End-Two-Flange loading test arrangement (End view)

(a) Flanges unfastened (Without hole)

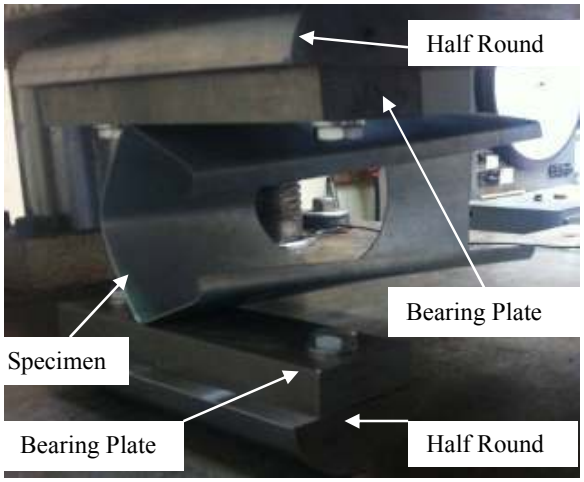

(b) Flanges unfastened (Type 1 hole)

(a) Flanges unfastened (Type 2 hole)

(a) Flanges unfastened (Without hole)

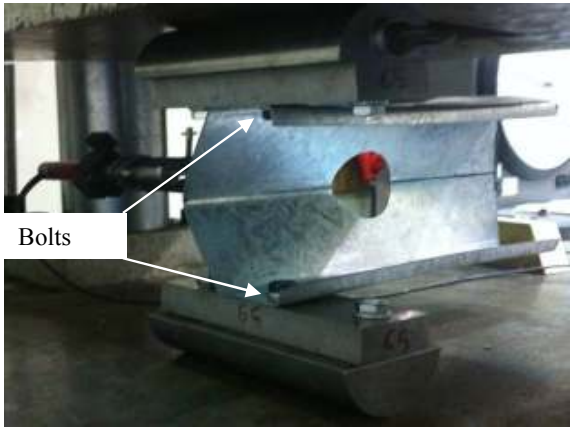

(b) Flanges unfastened (Type 1 hole)

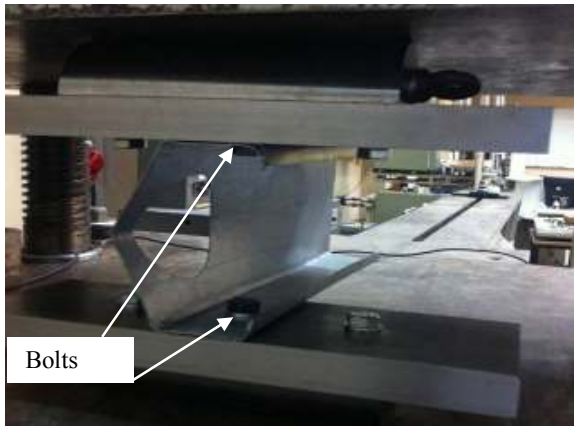

(a) Flanges unfastened (Type 2 hole)

Figure 3.12 Test setup End-Two-Flange loading condition

3.5.4 Test results

A total of 100 specimens were tested under the ETF loading condition considering both types of holes with flanges unfastened and fastened conditions. The experimental ultimate web crippling loads per web (P_{EXP}) for the flanges unfastened and fastened condition are given in Table 3.6, Table 3.7, Table 3.8 and Table 3.9 respectively for both types web holes. In order to demonstrate the reliability of the test results, four tests were repeated three times and the specimens are ETF142x60x13-t1.3N60A0FR, ETF142x60x13-t1.3N60A0.4FR ETF142x60x13-t1.3N60A0FX, and ETF142x60x13-t1.3N60A0.4FX. The tests results for the repeated tests are very close to their first test values. All load-displacement curves obtained from the tests considering both without and with web holes, and the comparisons with the numerical results are shown in Appendix B. The typical failure mode of web crippling of the specimens is shown in Appendix C.

Table 3.6 Measured specimen dimensions and experimental ultimate loads for flanges unfastened under ETF loading condition (Type 1 web holes)

Specimen	Web d (mm)	Flange b_f (mm)	Lip b_l (mm)	Thickness t (mm)	Fillet r_i (mm)	Hole a (mm)	Length L (mm)	Exp. load per web P_{EXP} (kN)
ETF142x60x13-t1.3N30A0FR	142.15	58.57	15.85	1.23	4.75	0.00	275.40	1.68
ETF142x60x13-t1.3N30A0.2FR	142.15	58.57	15.85	1.23	4.75	27.88	275.40	1.62
ETF142x60x13-t1.3N30A0.4FR	142.15	59.48	16.32	1.25	4.75	55.81	275.59	1.44
ETF142x60x13-t1.3N30A0.6FR	142.15	59.48	16.32	1.25	4.75	83.64	275.59	1.30
ETF142x60x13-t1.3N30A0.8FR	142.15	59.48	16.32	1.25	4.75	111.52	275.59	1.08
ETF142x60x13-t1.3N60A0FR-1	141.75	58.94	15.56	1.24	4.75	0.00	300.56	1.95
ETF142x60x13-t1.3N60A0FR-2	141.75	58.94	15.56	1.24	4.75	0.00	300.56	1.83
ETF142x60x13-t1.3N60A0FR-3	141.75	58.94	15.56	1.24	4.75	0.00	300.56	1.91
ETF142x60x13-t1.3N60A0.2FR	141.75	58.94	15.56	1.24	4.75	27.88	301.91	1.68
ETF142x60x13-t1.3N60A0.4FR-1	141.33	58.84	16.29	1.24	4.75	55.72	301.91	1.64
ETF142x60x13-t1.3N60A0.4FR-2	141.33	58.84	16.29	1.24	4.75	55.72	301.91	1.61
ETF142x60x13-t1.3N60A0.4FR-3	141.33	58.84	16.29	1.24	4.75	55.72	301.91	1.60
ETF142x60x13-t1.3N60A0.6FR	141.33	58.84	16.29	1.24	4.75	83.64	301.91	1.53
ETF172x65x13-t1.3N32.5A0FR	172.76	64.05	15.61	1.27	5.00	0.00	327.41	1.70
ETF172x65x13-t1.3N32.5A0.4FR	172.26	63.55	15.49	1.27	5.00	67.64	326.85	1.55
ETF172x65x13-t1.3N65A0FR	172.58	64.28	15.25	1.28	5.00	0.00	356.39	1.88
ETF172x65x13-t1.3N65A0.4FR	172.26	63.55	15.49	1.27	5.00	67.74	326.85	1.64
ETF202x65x13-t1.4N32.5A0FR	202.06	63.11	17.51	1.45	5.00	0.00	375.84	1.98
ETF202x65x13-t1.4N32.5A0.4FR	202.69	64.25	16.32	1.45	5.00	79.53	376.29	1.82
ETF202x65x13-t1.4N65A0FR	202.44	64.20	16.50	1.45	5.00	0.00	400.91	2.39
ETF202x65x13-t1.4N65A0.4FR	202.58	64.09	16.54	1.46	5.00	79.66	399.57	1.98
ETF262x65x13-t1.6N32.5A0FR	263.43	63.35	14.42	1.56	5.50	0.00	450.93	2.04
ETF262x65x13-t1.6N32.5A0.4FR	262.75	63.42	14.69	1.55	5.50	103.40	450.32	1.82
ETF262x65x13-t1.6N65A0FR	262.39	64.05	15.33	1.55	5.50	0.00	497.18	2.19
ETF262x65x13-t1.6N65A0.4FR	262.47	63.76	14.45	1.54	5.50	103.38	498.19	2.00
ETF302x90x18-t2N44A0FR	305.47	86.78	20.77	1.94	5.00	0.00	549.73	3.96
ETF302x90x18-t2N44A0.4FR	303.33	86.45	20.50	1.94	5.50	119.00	601.78	3.35
ETF302x90x18-t2N90A0FR	303.55	87.06	21.29	1.97	5.50	0.00	596.45	4.30

Note: 1 kip = 4.45 kN

Table 3.7 Measured specimen dimensions and experimental ultimate loads for flanges unfastened under ETF loading condition (Type 2 web holes)

Specimen	Web d (mm)	Flange b_f (mm)	Lip b_l (mm)	Thickness t (mm)	Fillet r_i (mm)	Holes a (mm)	Length L (mm)	Exp. load per web P_{EXP} (kN)
ETF142x60x13-t1.3N90MA0FR	142.2	58.6	15.9	1.23	4.8	0.0	337.5	2.21
ETF142x60x13-t1.3N90MA0.2FR	142.2	58.6	15.9	1.23	4.8	27.9	337.5	1.98
ETF142x60x13-t1.3N90MA0.4FR	142.2	59.5	16.3	1.25	4.8	55.8	337.5	1.62
ETF142x60x13-t1.3N90MA0.6FR	142.2	59.5	16.3	1.25	4.8	83.6	337.5	1.32
ETF142x60x13-t1.3N120MA0FR	141.8	58.9	15.6	1.24	4.8	0.0	350.0	2.35
ETF142x60x13-t1.3N120MA0.2FR	141.8	58.9	15.6	1.24	4.8	27.9	350.0	1.95
ETF142x60x13-t1.3N120MA0.4FR	141.3	58.8	16.3	1.24	4.8	55.7	350.0	1.78
ETF142x60x13-t1.3N120MA0.6FR	141.3	58.8	16.3	1.24	4.8	83.6	350.0	1.49
ETF172x65x13-t1.3N120MA0FR	172.8	64.1	15.6	1.27	5.0	0.0	400.0	2.37
ETF172x65x13-t1.3N120MA0.4FR	172.3	63.6	15.5	1.27	5.0	67.6	400.0	1.70
ETF172x65x13-t1.3N120MA0.6FR	172.6	64.3	15.3	1.28	5.0	101.6	400.0	1.36
ETF202x65x13-t1.4N120MA0FR	202.1	63.1	17.5	1.45	5.0	0.0	425.0	2.70
ETF202x65x13-t1.4N120MA0.2FR	202.7	64.3	16.3	1.45	5.0	39.8	425.0	2.41
ETF202x65x13-t1.4N120MA0.4FR	202.4	64.2	16.5	1.45	5.0	79.5	425.0	1.88
ETF202x65x13-t1.4N150MA0FR	202.1	63.1	17.5	1.45	5.0	0.0	450.0	2.84
ETF202x65x13-t1.4N150MA0.4FR	202.7	64.3	16.3	1.45	5.0	79.5	450.0	2.19
ETF202x65x13-t1.4N150MA0.6FR	202.4	64.2	16.5	1.45	5.0	119.5	450.0	1.77
ETF262x65x13-t1.6N120MA0FR	263.4	63.4	14.4	1.56	5.5	0.0	525.0	2.55
ETF262x65x13-t1.6N120MA0.2FR	263.4	63.4	14.4	1.56	5.5	51.8	525.0	2.29
ETF262x65x13-t1.6N120MA0.4FR	262.8	63.4	14.7	1.55	5.5	103.4	525.0	1.77
ETF262x65x13-t1.6N150MA0FR	263.4	63.4	14.4	1.56	5.5	0.0	550.0	2.82
ETF262x65x13-t1.6N150MA0.4FR	262.8	63.4	14.7	1.55	5.5	103.4	550.0	2.04

Note: 1 kip = 4.45 kN

Table 3.8 Measured specimen dimensions and experimental ultimate loads for flanges fastened under ETF loading condition (Type 1 web holes)

Specimen	Web d (mm)	Flange b_f (mm)	Lip b_l (mm)	Thickness t (mm)	Fillet r_i (mm)	Holes a (mm)	Length L (mm)	Exp. load per web P_{EXP} (kN)
ETF142x60x13-t1.3N30A0FX	143.5	59.8	15.8	1.24	4.8	0.0	275.5	2.96
ETF142x60x13-t1.3N30A0.2FX	143.5	59.8	15.8	1.24	4.8	27.9	275.5	2.80
ETF142x60x13-t1.3N30A0.4FX	142.1	58.0	16.1	1.25	4.8	55.7	275.5	2.53
ETF142x60x13-t1.3N30A0.6FX	142.1	58.0	16.1	1.25	4.8	83.6	275.5	2.27
ETF142x60x13-t1.3N30A0.8FX	142.1	58.0	16.1	1.25	4.8	111.5	275.5	1.93
ETF142x60x13-t1.3N60A0FX-1	143.0	61.0	14.9	1.21	4.8	0.0	302.5	3.32
ETF142x60x13-t1.3N60A0FX-2	143.0	61.0	14.9	1.21	4.8	0.0	302.5	3.31
ETF142x60x13-t1.3N60A0FX-3	143.0	61.0	14.9	1.21	4.8	0.0	302.5	3.27
ETF142x60x13-t1.3N60A0.2FX	143.0	61.0	14.9	1.21	4.8	27.9	300.0	3.23
ETF142x60x13-t1.3N60A0.4FX-1	142.0	59.6	15.7	1.23	4.8	55.6	304.5	2.99
ETF142x60x13-t1.3N60A0.4FX-2	142.0	59.6	15.7	1.23	4.8	55.6	300.0	3.11
ETF142x60x13-t1.3N60A0.4FX-3	142.0	59.6	15.7	1.23	4.8	55.6	300.0	3.07
ETF142x60x13-t1.3N60A0.6FX	142.0	59.6	15.7	1.23	4.8	83.6	300.0	2.64
ETF142x60x13-t1.3N60A0.8FX	142.0	59.6	15.7	1.23	4.8	111.5	300.0	2.47
ETF172x65x13-t1.3N32.5A0FX	173.2	63.5	15.4	1.26	5.0	0.0	325.0	2.88
ETF172x65x13-t1.3N32.5A0.4FX	172.6	63.6	16.4	1.26	5.0	67.6	325.2	2.71
ETF172x65x13-t1.3N65A0FX	173.3	64.3	14.6	1.26	5.0	0.0	351.5	3.31
ETF172x65x13-t1.3N65A0.4FX	173.1	64.2	14.2	1.26	5.0	67.7	349.7	3.03
ETF202x65x13-t1.4N32.5A0FX	202.4	64.0	16.2	1.38	5.0	0.0	376.4	3.63
ETF202x65x13-t1.4N65A0FX	202.4	63.9	16.4	1.45	5.0	0.0	401.8	4.37
ETF202x65x13-t1.4N65A0.4FX	202.6	64.2	16.5	1.45	5.0	79.6	400.1	3.80
ETF262x65x13-t1.6N32.5A0FX	263.6	63.4	14.8	1.55	5.5	0.0	452.2	3.63
ETF262x65x13-t1.6N32.5A0.4FX	262.8	63.3	15.2	1.53	5.5	103.3	451.4	3.16
ETF262x65x13-t1.6N65A0FX	262.7	65.3	15.2	1.52	5.5	0.0	499.2	3.94
ETF262x65x13-t1.6N65A0.4FX	262.7	63.4	15.3	1.55	5.5	103.3	496.8	3.68
ETF302x90x18-t2N44A0FX	304.5	86.6	19.8	1.96	5.5	0.0	544.5	6.95
ETF302x90x18-t2N44A0.4FX	303.2	87.2	21.0	1.96	5.5	119.1	545.4	6.03
ETF302x90x18-t2N90A0.4FX	303.6	86.9	20.6	1.96	5.5	119.1	550.1	6.85

Note: 1 kip = 4.45 kN

Table 3.9 Measured specimen dimensions and experimental ultimate loads for flanges fastened under ETF loading condition (Type 2 web holes)

Specimen	Web d (mm)	Flange b_f (mm)	Lip b_l (mm)	Thickness t (mm)	Fillet r_i (mm)	Holes a (mm)	Length L (mm)	Exp. load per web P_{EXP} (kN)
ETF142x60x13-t1.3N90MA0FX	142.2	58.6	15.9	1.23	4.8	0.0	337.5	3.75
ETF142x60x13-t1.3N90MA0.2FX	142.2	58.6	15.9	1.23	4.8	27.9	337.5	3.16
ETF142x60x13-t1.3N90MA0.4FX	142.2	59.5	16.3	1.25	4.8	55.8	337.5	2.79
ETF142x60x13-t1.3N90MA0.6FX	142.2	59.5	16.3	1.25	4.8	83.6	337.5	2.55
ETF142x60x13-t1.3N120MA0FX	141.8	58.9	15.6	1.24	4.8	0.0	350.0	4.06
ETF142x60x13-t1.3N120MA0.2FX	141.8	58.9	15.6	1.24	4.8	27.9	350.0	3.58
ETF142x60x13-t1.3N120MA0.4FX	141.3	58.8	16.3	1.24	4.8	55.7	350.0	3.44
ETF142x60x13-t1.3N120MA0.6FX	141.3	58.8	16.3	1.24	4.8	83.6	350.0	2.94
ETF172x65x13-t1.3N120MA0FX	172.8	64.1	15.6	1.27	5.0	0.0	400.0	4.16
ETF172x65x13-t1.3N120MA0.4FX	172.3	63.6	15.5	1.27	5.0	67.6	400.0	3.48
ETF172x65x13-t1.3N120MA0.6FX	172.6	64.3	15.3	1.28	5.0	101.6	400.0	3.00
ETF202x65x13-t1.4N120MA0FX	202.1	63.1	17.5	1.45	5.0	0.0	425.0	5.24
ETF202x65x13-t1.4N120MA0.2FX	202.7	64.3	16.3	1.45	5.0	39.8	425.0	4.88
ETF202x65x13-t1.4N120MA0.4FX	202.4	64.2	16.5	1.45	5.0	79.5	425.0	4.27
ETF202x65x13-t1.4N150MA0FX	202.1	63.1	17.5	1.45	5.0	0.0	450.0	5.82
ETF202x65x13-t1.4N150MA0.4FX	202.7	64.3	16.3	1.45	5.0	79.5	450.0	4.73
ETF202x65x13-t1.4N150MA0.6FX	202.4	64.2	16.5	1.45	5.0	119.5	450.0	4.24
ETF262x65x13-t1.6N120MA0FX	263.4	63.4	14.4	1.56	5.5	0.0	525.0	5.06
ETF262x65x13-t1.6N120MA0.2FX	263.4	63.4	14.4	1.56	5.5	51.8	525.0	4.60
ETF262x65x13-t1.6N120MA0.4FX	262.8	63.4	14.7	1.55	5.5	103.4	525.0	3.89
ETF262x65x13-t1.6N150MA0FX	263.4	63.4	14.4	1.56	5.5	0.0	550.0	5.37
ETF262x65x13-t1.6N150MA0.4FX	262.8	63.4	14.7	1.55	5.5	103.4	550.0	4.25

Note: 1 kip = 4.45 kN

3.6 Concluding remarks

A series of web crippling tests were conducted on cold-formed lipped channel sections with and without web holes under ITF and ETF loading conditions. The cases of the flanges of the channel sections being fastened and unfastened to the bearing plates were also considered. The results of the tests showed that the reduction in web crippling strength due to presence of the web holes. Web crippling test setup and results will be used in Chapter 4 to develop and verify the finite element models.

CHAPTER 4. NUMERICAL INVESTIGATION

4.1 Introductory remarks

In the Chapter, The ANSYS (2011) finite element analysis software package was used in this research. ANSYS has its own pre-processor, solver and post-processors build into it, including a full range of nonlinear capabilities. Finite element models that incorporated the geometric and the material nonlinearities of the channel sections with and without holes subjected to web crippling were developed. The bearing plates, the channel section with circular holes and the interfaces between the bearing plates and the channel section have been modelled. In the finite element model, the measured cross-section dimensions and the material properties obtained from the tests were used. The model was based on the centreline dimensions of the cross-sections. All the finite element models were validated using experiment results. The results of the finite element analysis load-displacement curves and ultimate strength values were compared with experimental results. The models developed were then employed in a parametric study to examine the effects of various section parameters and web holes on web crippling behaviour. Ren *et al*. (2006) and Heiyantuduwa (2008) developed finite element models for web crippling behaviour of cold-formed steel without holes. In this research similar techniques were adopted to develop finite element models for the channel sections with and without holes subjected to web crippling. Specific modelling issues are described in the following subsection.

4.2 Geometry and material properties

The correct definition of material properties is very important for the accuracy of results obtained from a finite element analysis. Young's modulus and Poisson's ratio were used as the basic material properties. The value of Young's modulus was 203 kN/mm^2 and Poisson's ratio was 0.3. To represent the nonlinear material behaviour, stress-strain curves were directly

obtained from the tensile tests and converted into true stress vs true strain curves using the following equation 4.1 & equation 4.2 specified in the ANSYS manual (2011). The typical converted true stress vs. true strain curves for section C142 obtained from above equations is shown in Figure 4.1.

$$\sigma_{true} = \sigma_{eng}(\varepsilon_{eng} + 1) \qquad \text{Equation 4.1}$$

$$\varepsilon_{true} = \ln(\varepsilon_{eng} + 1) \qquad \text{Equation 4.2}$$

Where

ε_{true} = True strain

ε_{eng} = Engineering strain

σ_{true} = True stress (N/mm^2)

σ_{eng} = Engineering stress (N/mm^2)

The full section true stress vs. true curves obtained from the above relationships were represented using data points and entered into ANSYS using material data table. The type of material model was defined as Multi-linear Isotropic hardening material model (MISO).

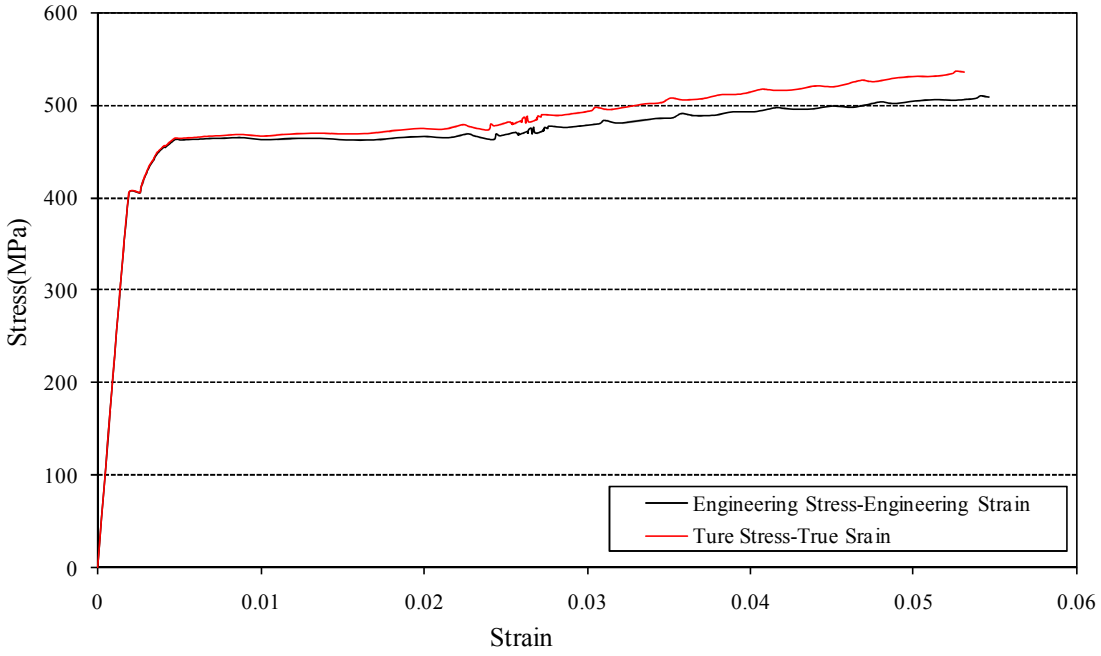

Figure 4.1 Typical true stress vs. true strain curves for section C142

One-quarter of the test set-up was modelled for ITF loading condition using symmetry about both the vertical transverse and horizontal planes is shown in Figure 4.2. For the ETF loading condition one-half of the test set-up was modelled using symmetry about horizontal planes is shown in Figure 4.3.

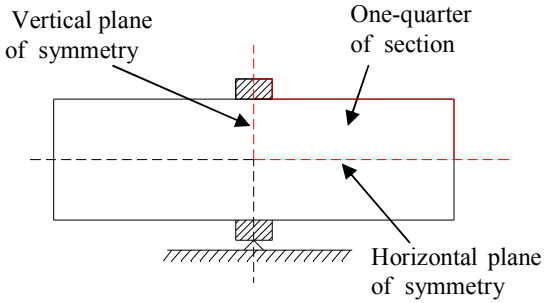

Test Setup geometry (no holes)

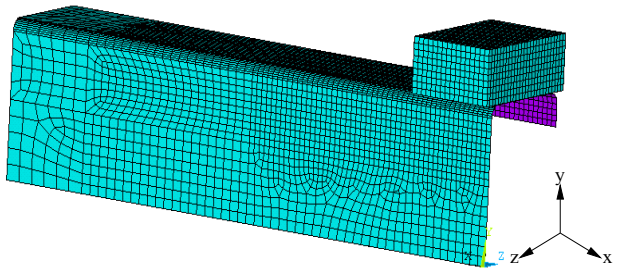

One-quarter unfastened FEA model (no holes)

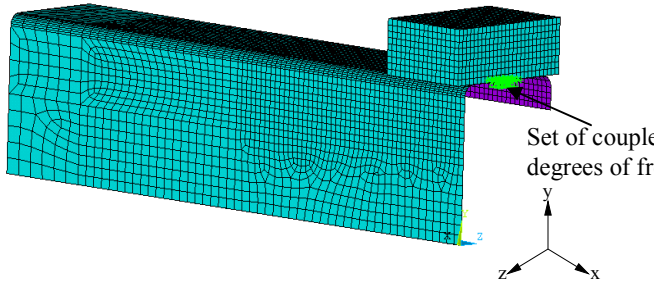

One-quarter fastened FEA model (no holes)

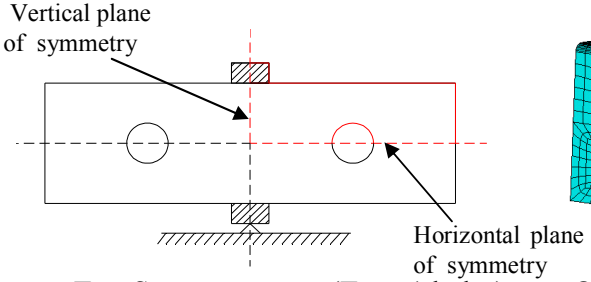

Test Setup geometry (Type 1 holes)

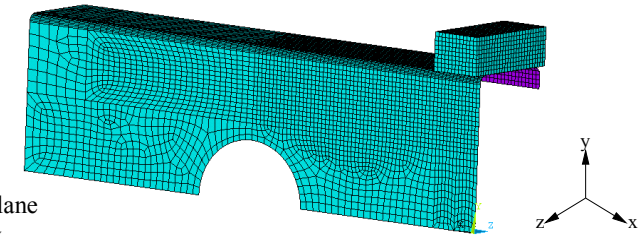

One-quarter unfastened FEA model (Type 1 holes)

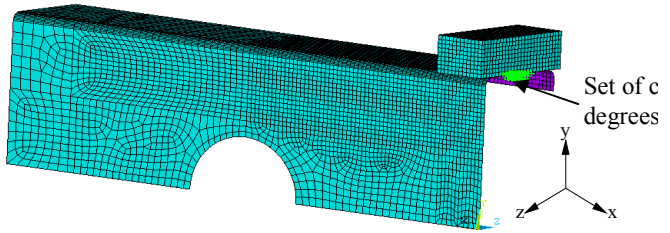

One-quarter fastened FEA model (Type 1 holes)

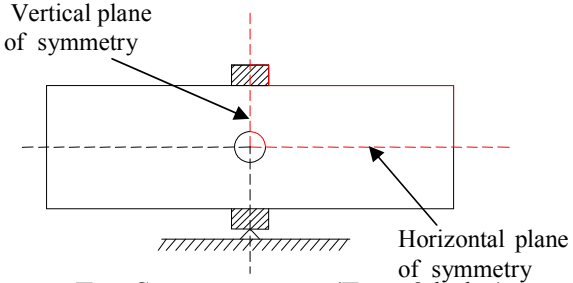

Test Setup geometry (Type 2 holes)

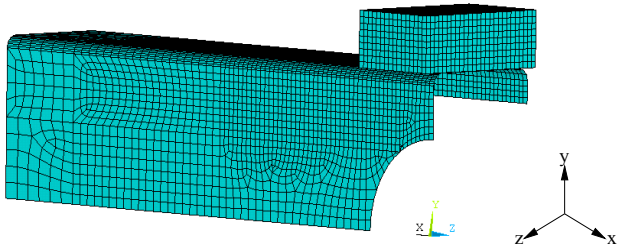

One-quarter unfastened FEA model (Type 2 holes)

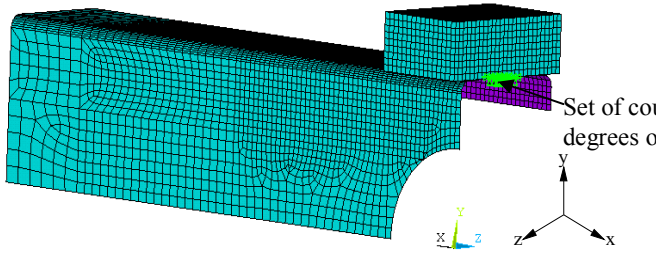

One-quarter fastened FEA model (Type 2 holes)

Figure 4.2 ITF finite element models showing different regions element mesh

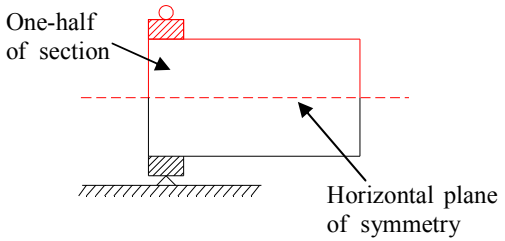

Test Setup geometry (no hole)

One-half unfastened FEA model (no hole)

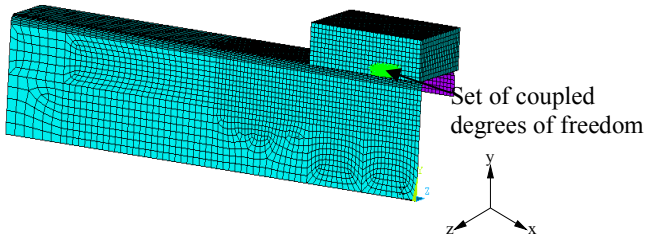

One-half fastened FEA model (no hole)

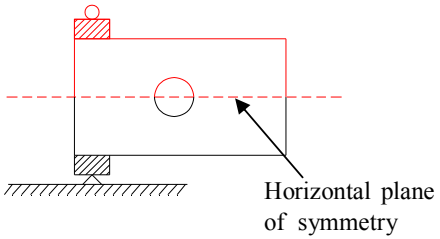

Test Setup geometry (Type 1 holes)

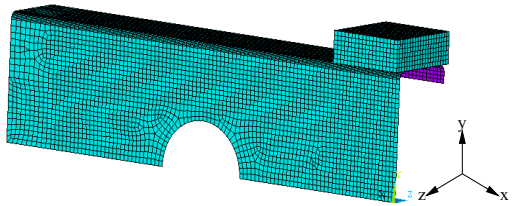

One-half unfastened FEA model (Type 1 hole)

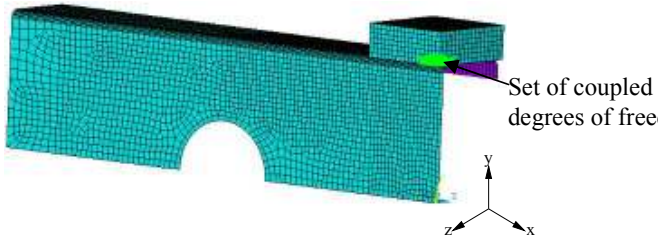

One-half fastened FEA model (Type 1 hole)

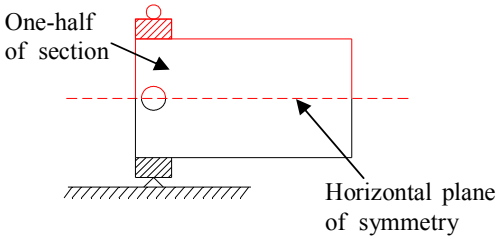

Test Setup geometry (Type 2 hole)

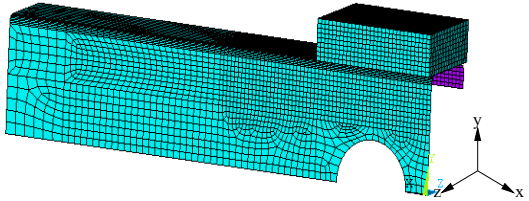

One-half unfastened FEA model (Type 2 hole)

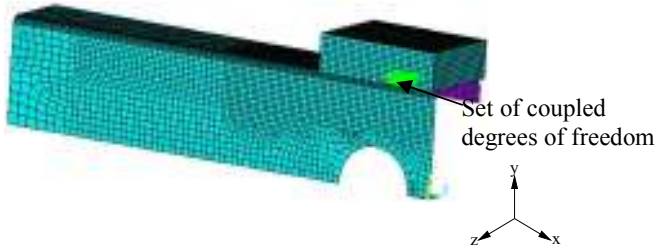

One-half fastened FEA model (Type 2 hole)

Figure 4.3 ETF finite element models showing different regions element mesh

4.3 Element type and mesh sensitivity

Figure 4.2 and Figure 4.3 shows details of a typical finite element mesh of the channel section and the bearing plate. With finite element analysis, it is good practice to carry out a mesh sensitivity check to ensure that results are accurate. Mesh density should be checked to ensure enough elements of the type chosen are being used. Coarse mesh patterns could produce under estimate the results; fine mesh patterns may take longer to solve and be no more accurate. Mesh sensitivity analyses were performed to verify the number of elements. The effect of different element sizes in the cross-section of the channel section was investigated to provide both accurate results and reduced computation time. Depending on the size of the section, the finite element mesh sizes ranged from 3×3 mm (length by width) to 5×5 mm.

It is necessary to finely mesh the corners of the section due to the transfer of stress from the flange to the web. Nine elements were used around the inside corner radius that forms the bend between the flange and web. Three elements were used at the rounded corners between the flange and lip of the section. The number of elements was chosen so that the aspect ratio of the elements was as close to one as possible. Where holes were modelled, finer mesh sizes were used around the web holes..

Shell elements are often used to model thin-walled structures and provide more accurate results with a reasonable solution time compared to volume elements. SHELL181 is defined in the ANSYS element library along with many other shell elements such as SHELL43, SHELL93, etc. ANSYS recommends SHELL181 for analysing thin to moderately-thick shell structures. SHELL181 is a four-noded element with six degrees-of-freedom at each node and has special features such as plasticity, large deformation, large rotation, stress stiffening,

The bearing plates were modelled using a 3D structure solid element SOLID45. The solid element is suitable for the three-dimensional modelling of structure with plasticity. The solid element is defined by eight nodes having three translational degree of freedom at each node.

CONTAT173 and TARGET170 elements were used for modelling contact between the flanges and the load bearing plates.

4.4 Loading and boundary conditions

The nodes of the cold-formed section and the bearing plate were restrained to represent the vertical and horizontal symmetry condition. The vertical symmetry boundary conditions were represented using displacement constraints at a transverse plane passing through the mid-span. The nodes were restrained by X, ROTY and ROTZ. The horizontal symmetry boundary condition was symmetrical about the horizontal plane passing through the centre line of the beam. The nodes were restrained by Y, ROTX and ROTZ. The interface between the bearing plate and the cold-formed steel section were modelled using the surface-to-surface contact option. The contact modelling properties and techniques were obtained from Heiyantuduwa (2008). The bearing plate was the target surface, while the cold-formed steel section was the contact surface. The two contact surfaces were not allowed to penetrate each other.

The vertical load applied to the channel sections in the laboratory tests was modelled using displacement control method; an imposed displacement is applied to the nodes of the top bearing plate where the vertical load is applied. The top bearing plate was restrained against all degrees of freedom, except for the translational degree of freedom in the Y direction. In the flanges fastened condition, the node coupling method was used in the region where the flanges connected to the bearing plates. The nodes were coupled together in all degrees of freedom.

4.5 Verification of finite element model

In order to validate the finite element model, the experimental failure loads were compared against the failure load predicted by the finite element analysis. The main objective of this comparison was to verify and check the accuracy of the finite element model.

4.5.1 ITF loading condition

A comparison of the test results (P_{EXP}) with the numerical results (P_{FEA}) of web crippling strengths per web is shown in Table 4.1, Table 4.2, Table 4.3 and Table 4.4. Load-deflection curves comparing the experimental results and the finite element results are shown in Appendix-B covering the cases of both with and without the web holes. It can be seen that good agreement has been achieved between both the results for all specimens.

Type 1 web holes case, The mean value of the P_{EXP}/P_{FEA} ratio is 1.00 and 1.00 with the corresponding coefficient of variation (COV) of 0.03 and 0.04 for the flanges unfastened and fastened condition, respectively. A maximum difference of 6% and 13% was observed between the experimental and the numerical results for the specimen ITF142x60x13-t1.3N60A0.4FR and ITF302x90x18-t2N90A0.4FX, respectively.

Type 2 web holes case, The mean value of the P_{EXP}/P_{FEA} ratio is 0.99 and 0.98 with the corresponding coefficient of variation (COV) of 0.02 and 0.01 for the flanges unfastened and fastened condition, respectively. A maximum difference of 5% and 4% was observed between the experimental and the numerical results for the specimen ITF142x60x13-t1.3N90MA0.8FR and ITF142x60x13-t1.3N90MA0.4FX, respectively.

The web crippling failure modes observed from the tests have been also verified by the finite element model for the ITF loading conditions are shown in appendix-C. It is shown that good agreement is achieved between the experimental and finite element results for both the web crippling strength and the failure mode.

Table 4.1 Comparison of the web crippling strength predicted from the finite element analysis with the experiment results for flanges unfastened under ITF loading condition (Type 1 holes)

Specimen	Web slenderness	Hole diameter ratio	Exp. load per web	Web crippling strength per web predicted from FEA	Comparison
	h/t	a/h	P_{EXP} (kN)	P_{FEA} (kN)	P_{EXP}/P_{FEA}
ITF142x60x13-t1.3N30A0FR	116.3	0.0	5.6	5.5	1.02
ITF142x60x13-t1.3N30A0.2FR	116.2	0.2	4.9	5.0	0.98
ITF142x60x13-t1.3N30A0.4FR	116.2	0.4	4.5	4.3	1.03
ITF142x60x13-t1.3N30A0.6FR	116.2	0.6	3.5	3.6	0.97
ITF142x60x13-t1.3N30A0.8FR	116.2	0.8	2.7	2.8	0.96
ITF142x60x13-t1.3N60A0FR	115.5	0.0	6.0	5.9	1.02
ITF142x60x13-t1.3N60A0.2FR	116.5	0.2	5.3	5.3	1.00
ITF142x60x13-t1.3N60A0.4FR	116.5	0.4	4.9	4.7	1.06
ITF142x60x13-t1.3N60A0.6FR	116.5	0.6	3.9	3.9	0.98
ITF142x60x13-t1.3N60A0.8FR	116.5	0.8	3.1	3.2	0.99
ITF172x65x13-t1.3N32.5A0FR	138.4	0.0	5.7	5.6	1.02
ITF172x65x13-t1.3N32.5A0.4FR	137.2	0.4	4.6	4.6	0.98
ITF172x65x13-t1.3N65A0FR	135.4	0.0	6.3	6.4	0.98
ITF172x65x13-t1.3N65A0.4FR	134.5	0.4	5.2	5.3	0.97
ITF202x65x13-t1.4N32.5A0FR	143.1	0.0	6.8	6.9	0.99
ITF202x65x13-t1.4N32.5A0.4FR	138.3	0.4	5.6	5.9	0.96
ITF202x65x13-t1.4N65A0FR	139.0	0.0	7.4	7.7	0.96
ITF202x65x13-t1.4N65A0.4FR	143.7	0.4	5.8	5.6	1.03
ITF262x65x13-t1.6N32.5A0FR	175.9	0.0	6.6	6.5	1.01
ITF262x65x13-t1.6N32.5A0.4FR	170.8	0.4	5.3	5.5	0.96
ITF262x65x13-t1.6N65A0FR	169.3	0.0	7.7	7.8	0.99
ITF262x65x13-t1.6N65A0.4FR	176.9	0.4	5.5	5.4	1.02
ITF302x90x18-t2N44A0.4FR	155.7	0.4	10.2	9.9	1.03
ITF302x90x18-t2N90A0FR	153.4	0.0	14.1	13.5	1.04
ITF302x90x18-t2N90A0.4FR	154.5	0.4	11.3	10.7	1.06
Mean					1.00
COV					0.03

Table 4.2 Comparison of the web crippling strength predicted from the finite element analysis with the experiment results for flanges unfastened under ITF loading condition (Type 2 holes)

Specimen	Web slenderness	Hole diameter ratio	Exp. load per web	Web crippling strength per web predicted from FEA	Comparison
	h/t	a/h	P_{EXP} (kN)	P_{FEA} (kN)	P_{EXP}/P_{FEA}
ITF142x60x13-t1.3N90MA0FR	113.8	0.0	6.03	6.06	1.00
ITF142x60x13-t1.3N90MA0.2FR	113.8	0.2	5.96	5.80	1.03
ITF142x60x13-t1.3N90MA0.4FR	112.2	0.4	5.45	5.33	1.02
ITF142x60x13-t1.3N90MA0.6FR	112.2	0.6	4.52	4.65	0.97
ITF142x60x13-t1.3N90MA0.8FR	112.2	0.8	3.52	3.71	0.95
ITF142x60x13-t1.3N120MA0FR	112.5	0.0	6.32	6.28	1.01
ITF142x60x13-t1.3N120MA0.2FR	112.5	0.2	6.05	6.00	1.01
ITF142x60x13-t1.3N120MA0.4FR	112.4	0.4	5.45	5.54	0.98
ITF142x60x13-t1.3N120MA0.6FR	112.4	0.6	4.75	4.90	0.97
ITF142x60x13-t1.3N120MA0.8FR	112.2	0.8	3.79	4.00	0.95
ITF172x65x13-t1.3N120MA0FR	134.5	0.0	7.05	7.17	0.98
ITF172x65x13-t1.3N120MA0.4FR	134.1	0.4	6.20	6.40	0.97
ITF172x65x13-t1.3N120MA0.6FR	133.3	0.6	5.67	5.68	1.00
ITF202x65x13-t1.4N150MA0FR	137.4	0.0	8.40	8.52	0.99
ITF202x65x13-t1.4N150MA0.4FR	137.8	0.4	7.37	7.56	0.97
ITF202x65x13-t1.4N150MA0.6FR	137.6	0.6	6.79	6.80	1.00
ITF262x65x13-t1.6N150MA0FR	166.9	0.0	8.19	8.04	1.02
ITF262x65x13-t1.6N150MA0.2FR	167.5	0.2	7.88	7.78	1.01
ITF262x65x13-t1.6N150MA0.4FR	167.5	0.4	7.29	7.26	1.00
Mean					0.99
COV					0.02

Table 4.3 Comparison of the web crippling strength predicted from the finite element analysis with the experiment results for flanges fastened under ITF loading condition (Type 1 holes)

Specimen	Web slenderness	Hole diameter ratio	Exp. load per web	Web crippling strength per web predicted from FEA	Comparison
	h/t	a/h	P_{EXP} (kN)	P_{FEA} (kN)	P_{EXP}/P_{FEA}
ITF142x60x13-t1.3N30A0FX	114.52	0.00	7.48	7.84	0.95
ITF142x60x13-t1.3N30A0.4FX	116.42	0.40	6.95	6.95	1.00
ITF142x60x13-t1.3N60A0FX	115.75	0.00	8.14	8.23	0.99
ITF142x60x13-t1.3N60A0.4FX	115.80	0.40	7.29	7.63	0.96
ITF172x65x13-t1.3N32.5A0FX	135.16	0.00	8.92	8.99	0.99
ITF172x65x13-t1.3N32.5A0.4FX	141.83	0.40	7.68	7.51	1.02
ITF172x65x13-t1.3N65A0FX	135.98	0.00	9.48	9.58	0.99
ITF172x65x13-t1.3N65A0.4FX	139.82	0.40	8.46	8.30	1.02
ITF202x65x13-t1.4N32.5A0FX	138.33	0.00	11.46	11.07	1.04
ITF202x65x13-t1.4N32.5A0.4FX	138.51	0.40	9.59	10.06	0.95
ITF202x65x13-t1.4N65A0FX	139.51	0.00	11.65	11.94	0.98
ITF202x65x13-t1.4N65A0.4FX	138.61	0.40	10.25	10.71	0.96
ITF262x65x13-t1.6N32.5A0FX	172.26	0.00	11.46	11.17	1.03
ITF262x65x13-t1.6N32.5A0.4FX	171.28	0.40	9.64	9.65	1.00
ITF262x65x13-t1.6N65A0.4FX	172.01	0.40	10.16	10.17	1.00
ITF302x90x18-t2N44A0.4FX	152.04	0.39	17.92	17.84	1.00
ITF302x90x18-t2N90A0FX	153.75	0.00	22.31	21.72	1.03
ITF302x90x18-t2N90A0.4FX	160.35	0.40	19.35	17.10	1.13
Mean					1.00
COV					0.04

Table 4.4 Comparison of the web crippling strength predicted from the finite element analysis with the experiment results for flanges fastened under ITF loading condition (Type 2 holes)

Specimen	Web slenderness h/t	Hole diameter ratio a/h	Exp. load per web P_{EXP} (kN)	Web crippling strength per web predicted from FEA P_{FEA} (kN)	Comparison P_{EXP}/P_{FEA}
ITF142x60x13-t1.3N90MA0FX	113.8	0.0	8.97	9.10	0.99
ITF142x60x13-t1.3N90MA0.2FX	113.8	0.2	8.96	9.06	0.99
ITF142x60x13-t1.3N90MA0.4FX	112.2	0.4	7.75	8.08	0.96
ITF142x60x13-t1.3N90MA0.6FX	112.2	0.6	6.64	6.81	0.98
ITF142x60x13-t1.3N90MA0.8FX	112.2	0.8	5.55	5.72	0.97
ITF142x60x13-t1.3N120MA0FX	112.5	0.0	9.44	9.70	0.97
ITF142x60x13-t1.3N120MA0.2FX	112.5	0.2	9.26	9.34	0.99
ITF142x60x13-t1.3N120MA0.4FX	112.4	0.4	8.19	8.40	0.98
ITF142x60x13-t1.3N120MA0.6FX	112.4	0.6	7.06	7.23	0.98
ITF142x60x13-t1.3N120MA0.8FX	112.2	0.8	5.94	6.15	0.97
ITF172x65x13-t1.3N120MA0FX	134.5	0.0	10.72	11.12	0.96
ITF172x65x13-t1.3N120MA0.4FX	134.1	0.4	9.31	9.62	0.97
ITF172x65x13-t1.3N120MA0.6FX	133.3	0.6	7.87	8.12	0.97
ITF202x65x13-t1.4N150MA0FX	137.4	0.0	13.51	13.66	0.99
ITF202x65x13-t1.4N150MA0.4FX	137.8	0.4	11.42	11.82	0.97
ITF202x65x13-t1.4N150MA0.6FX	137.6	0.6	10.10	10.10	1.00
ITF262x65x13-t1.6N150MA0FX	166.9	0.0	12.78	12.95	0.99
ITF262x65x13-t1.6N150MA0.2FX	167.5	0.2	12.41	12.56	0.99
ITF262x65x13-t1.6N150MA0.4FX	167.5	0.4	11.31	11.53	0.98
Mean					0.98
COV					0.01

4.5.2 ETF loading condition

A comparison of the test results (P_{EXP}) with the numerical results (P_{FEA}) of web crippling strengths per web is shown in Table 4.5, Table 4.6, Table 4.7 and Table 4.8. Load-deflection curves comparing the experimental results and the finite element results are shown in Appendix-B covering the cases of both with and without the web holes. It can be seen that good agreement has been achieved between both results for all specimens.

Type 1 web hole case, The mean value of the P_{EXP}/P_{FEA} ratio is 0.98 and 0.98 with the corresponding coefficient of variation (COV) of 0.05 and 0.04 for the flanges unfastened and fastened condition, respectively. A maximum difference of 9% and 8% was observed between the experimental and the numerical results for the specimen ETF172x65x13-t1.3N65A0FR and ETF202x65x13-t1.4N65A0.4FX, respectively.

Type 2 web hole case, The mean value of the P_{EXP}/P_{FEA} ratio is 0.94 and 0.95 with the corresponding coefficient of variation (COV) of 0.05 and 0.05 for the flanges unfastened and fastened condition, respectively. A maximum difference of 15% and 12% was observed between the experimental and the numerical results for the specimen ETF142x60x13-t1.3N120MA0.2FR and ETF142x60x13-t1.3N120MA0.6FX, respectively.

The web crippling failure mode observed from the tests has been also verified by the finite element model for the ETF loading conditions are shown Appendix-C. It is shown that good agreement is achieved between the experimental and finite element results for both the web crippling strength and the failure mode.

Table 4.5 Comparison of the web crippling strength predicted from the finite element analysis with the experiment results for flanges unfastened under ETF loading condition (Type 1 holes)

Specimen	Web slenderness	Hole diameter ratio	Exp. load per web	Web crippling strength per web predicted from FEA	Comparison
	h/t	a/h	P_{EXP} (kN)	P_{FEA} (kN)	P_{EXP}/P_{FEA}
ETF142x60x13-t1.3N30A0FR	112.18	0.00	1.68	1.65	1.02
ETF142x60x13-t1.3N30A0.2FR	112.18	0.20	1.62	1.62	1.00
ETF142x60x13-t1.3N30A0.4FR	112.18	0.40	1.44	1.46	0.99
ETF142x60x13-t1.3N30A0.6FR	112.18	0.60	1.30	1.28	1.02
ETF142x60x13-t1.3N30A0.8FR	112.18	0.80	1.08	1.09	0.99
ETF142x60x13-t1.3N60A0FR	112.50	0.00	1.95	2.02	0.97
ETF142x60x13-t1.3N60A0.2FR	112.44	0.20	1.68	1.68	1.00
ETF142x60x13-t1.3N60A0.4FR	112.44	0.40	1.64	1.65	0.99
ETF142x60x13-t1.3N60A0.6FR	112.44	0.60	1.60	1.65	0.97
ETF142x60x13-t1.3N60A0.8FR	112.44	0.80	1.53	1.56	0.98
ETF172x65x13-t1.3N32.5A0FR	134.46	0.00	1.70	1.70	1.00
ETF172x65x13-t1.3N32.5A0.4FR	134.07	0.40	1.55	1.47	1.05
ETF172x65x13-t1.3N65A0FR	133.25	0.00	1.88	2.07	0.91
ETF172x65x13-t1.3N65A0.4FR	134.07	0.40	1.64	1.77	0.93
ETF202x65x13-t1.4N32.5A0FR	137.54	0.00	1.98	2.16	0.92
ETF202x65x13-t1.4N32.5A0.4FR	137.98	0.40	1.82	1.85	0.98
ETF202x65x13-t1.4N65A0FR	137.81	0.00	2.39	2.49	0.96
ETF202x65x13-t1.4N65A0.4FR	136.94	0.40	1.98	2.20	0.90
ETF262x65x13-t1.6N32.5A0FR	167.41	0.00	2.04	2.09	0.98
ETF262x65x13-t1.6N32.5A0.4FR	167.52	0.40	1.82	1.75	1.04
ETF262x65x13-t1.6N65A0FR	166.96	0.00	2.19	2.40	0.91
ETF262x65x13-t1.6N65A0.4FR	168.21	0.40	2.00	2.03	0.99
ETF302x90x18-t2N44A0FR	155.30	0.00	3.96	3.64	1.09
ETF302x90x18-t2N44A0.4FR	154.19	0.40	3.35	3.32	1.01
ETF302x90x18-t2N90A0FR	152.24	0.00	4.30	4.41	0.98
Mean					0.98
COV					0.05

Table 4.6 Comparison of the web crippling strength predicted from the finite element analysis with the experiment results for flanges unfastened under ETF loading condition (Type 2 holes)

Specimen	Web slenderness	Hole diameter ratio	Exp. load per web	Web crippling strength per web predicted from FEA	Comparison
	h/t	a/h	P_{EXP} (kN)	P_{FEA} (kN)	P_{EXP}/P_{FEA}
ETF142x60x13-t1.3N90MA0FR	113.8	0.0	2.21	2.18	1.01
ETF142x60x13-t1.3N90MA0.2FR	113.8	0.2	1.98	1.94	1.02
ETF142x60x13-t1.3N90MA0.4FR	112.2	0.4	1.62	1.69	0.96
ETF142x60x13-t1.3N90MA0.6FR	112.2	0.6	1.32	1.41	0.94
ETF142x60x13-t1.3N120MA0FR	112.5	0.0	2.35	2.63	0.89
ETF142x60x13-t1.3N120MA0.2FR	112.5	0.2	1.95	2.30	0.85
ETF142x60x13-t1.3N120MA0.4FR	112.4	0.4	1.78	1.95	0.91
ETF142x60x13-t1.3N120MA0.6FR	112.4	0.6	1.49	1.62	0.92
ETF172x65x13-t1.3N120MA0FR	134.5	0.0	2.37	2.28	1.04
ETF172x65x13-t1.3N120MA0.4FR	134.1	0.4	1.70	1.81	0.94
ETF172x65x13-t1.3N120MA0.6FR	133.3	0.6	1.36	1.48	0.92
ETF202x65x13-t1.4N120MA0FR	137.4	0.0	2.70	2.87	0.94
ETF202x65x13-t1.4N120MA0.2FR	137.8	0.2	2.41	2.46	0.98
ETF202x65x13-t1.4N120MA0.4FR	137.6	0.4	1.88	2.01	0.94
ETF202x65x13-t1.4N150MA0FR	137.4	0.0	2.84	3.29	0.86
ETF202x65x13-t1.4N150MA0.4FR	137.8	0.4	2.19	2.35	0.93
ETF202x65x13-t1.4N150MA0.6FR	137.6	0.6	1.77	1.90	0.93
ETF262x65x13-t1.6N120MA0FR	166.9	0.0	2.55	2.88	0.89
ETF262x65x13-t1.6N120MA0.2FR	166.9	0.2	2.29	2.29	1.00
ETF262x65x13-t1.6N120MA0.4FR	167.5	0.4	1.77	1.85	0.96
ETF262x65x13-t1.6N150MA0FR	166.9	0.0	2.82	3.19	0.88
ETF262x65x13-t1.6N150MA0.4FR	167.5	0.4	2.04	2.09	0.98
Mean					0.94
COV					0.05

Table 4.7 Comparison of the web crippling strength predicted from the finite element analysis with the experiment results for flanges fastened under ETF loading condition (Type 1 holes)

Specimen	Web slenderness	Hole diameter ratio	Exp. load per web	Web crippling strength per web predicted from FEA	Comparison
	h/t	a/h	P_{EXP} (kN)	P_{FEA} (kN)	P_{EXP}/P_{FEA}
ETF142x60x13-t1.3N30A0FX	113.82	0.00	2.96	2.92	1.01
ETF142x60x13-t1.3N30A0.2FX	113.82	0.20	2.80	2.84	0.99
ETF142x60x13-t1.3N30A0.4FX	113.82	0.40	2.53	2.66	0.95
ETF142x60x13-t1.3N30A0.6FX	113.82	0.59	2.27	2.34	0.97
ETF142x60x13-t1.3N30A0.8FX	113.82	0.79	1.93	2.00	0.97
ETF142x60x13-t1.3N60A0FX	116.57	0.00	3.32	3.32	1.00
ETF142x60x13-t1.3N60A0.2FX	116.57	0.20	3.23	3.20	1.01
ETF142x60x13-t1.3N60A0.4FX	116.57	0.39	3.11	3.10	1.00
ETF142x60x13-t1.3N60A0.6FX	116.57	0.59	2.64	2.94	0.90
ETF142x60x13-t1.3N60A0.8FX	116.57	0.79	2.47	2.65	0.93
ETF172x65x13-t1.3N32.5A0FX	135.48	0.00	2.88	2.96	0.97
ETF172x65x13-t1.3N32.5A0.4FX	134.73	0.40	2.71	2.64	1.03
ETF172x65x13-t1.3N65A0FX	135.30	0.00	3.31	3.56	0.93
ETF172x65x13-t1.3N65A0.4FX	135.03	0.40	3.03	3.25	0.93
ETF202x65x13-t1.4N32.5A0FX	144.69	0.00	3.63	3.40	1.07
ETF202x65x13-t1.4N65A0FX	137.76	0.00	4.37	4.51	0.97
ETF202x65x13-t1.4N65A0.4FX	137.33	0.40	3.80	4.15	0.92
ETF262x65x13-t1.6N32.5A0FX	168.03	0.00	3.63	3.54	1.03
ETF262x65x13-t1.6N32.5A0.4FX	170.00	0.40	3.16	3.10	1.02
ETF262x65x13-t1.6N65A0FX	170.58	0.00	3.94	4.08	0.97
ETF262x65x13-t1.6N65A0.4FX	167.90	0.40	3.68	3.88	0.95
ETF302x90x18-t2N44A0FX	153.37	0.00	6.95	6.54	1.06
ETF302x90x18-t2N44A0.4FX	152.36	0.40	6.03	5.98	1.01
ETF302x90x18-t2N90A0.4FX	152.92	0.40	6.85	7.07	0.97
Mean					0.98
COV					0.04

Table 4.8 Comparison of the web crippling strength predicted from the finite element analysis with the experiment results for flanges fastened under ETF loading condition (Type 2 holes)

Specimen	Web slenderness	Hole diameter ratio	Exp. load per web	Web crippling strength per web predicted from FEA	Comparison
	h/t	a/h	P_{EXP} (kN)	P_{FEA} (kN)	P_{EXP}/P_{FEA}
ETF142x60x13-t1.3N90MA0FX	113.8	0.0	3.75	3.73	1.01
ETF142x60x13-t1.3N90MA0.2FX	113.8	0.2	3.16	3.48	0.91
ETF142x60x13-t1.3N90MA0.4FX	112.2	0.4	2.79	3.13	0.89
ETF142x60x13-t1.3N90MA0.6FX	112.2	0.6	2.55	2.73	0.93
ETF142x60x13-t1.3N120MA0FX	112.5	0.0	4.06	4.51	0.90
ETF142x60x13-t1.3N120MA0.2FX	112.5	0.2	3.58	4.19	0.85
ETF142x60x13-t1.3N120MA0.4FX	112.4	0.4	3.44	3.78	0.91
ETF142x60x13-t1.3N120MA0.6FX	112.4	0.6	2.94	3.36	0.88
ETF172x65x13-t1.3N120MA0FX	134.5	0.0	4.16	4.51	0.92
ETF172x65x13-t1.3N120MA0.4FX	134.1	0.4	3.48	3.69	0.94
ETF172x65x13-t1.3N120MA0.6FX	133.3	0.6	3.00	3.24	0.93
ETF202x65x13-t1.4N120MA0FX	137.4	0.0	5.24	5.29	0.99
ETF202x65x13-t1.4N120MA0.2FX	137.8	0.2	4.88	4.78	1.02
ETF202x65x13-t1.4N120MA0.4FX	137.6	0.4	4.27	4.22	1.01
ETF202x65x13-t1.4N150MA0FX	137.4	0.0	5.82	6.10	0.95
ETF202x65x13-t1.4N150MA0.4FX	137.8	0.4	4.73	4.97	0.95
ETF202x65x13-t1.4N150MA0.6FX	137.6	0.6	4.24	4.35	0.97
ETF262x65x13-t1.6N120MA0FX	166.9	0.0	5.06	5.05	1.00
ETF262x65x13-t1.6N120MA0.2FX	166.9	0.2	4.60	4.51	1.02
ETF262x65x13-t1.6N120MA0.4FX	167.5	0.4	3.89	3.88	1.00
ETF262x65x13-t1.6N150MA0FX	166.9	0.0	5.37	5.72	0.94
ETF262x65x13-t1.6N150MA0.4FX	167.5	0.4	4.25	4.51	0.94
Mean					0.95
COV					0.05

4.6 Parametric study

The finite element model developed closely predicts the behaviour of the channel sections with circular web holes subjected to web crippling. Using this model, parametric studies were carried out to study the effects of web holes and cross-section sizes on the web crippling strengths of channel sections subjected to web crippling.

Zhou and Young (2010) and LaBoube et al. (1999) investigates and shows that the ratios *a/h*, *x/h* and *N/h* are the primary parameters influencing the web crippling behaviour of the sections with web holes. The web crippling strength predicted was influenced primarily by the ratio of the hole depth to the flat portion of the web, *a/h*, the ratio of the bearing length to the flat portion of the web *N/h* and the location of the hole as defined by the distance of the hole from the edge of the bearing divided by the flat portion of the web, *x/h*. In order to find the effect of *a/h* and *x/h* on web crippling strength for Type 1 web holes and the effect of *a/h* and *N/h* on web crippling strength for Type 2 web holes, two separate parametric studies were carried out considering the web holes sizes, the cross-section sizes and location of the holes.

The specimens consisted of two different section sizes, having the thicknesses (t) ranging from 1.4 to 6.0 mm and the web slenderness (h/t) value ranging from 31.8 to 176.9. The ratios of the diameter of the holes (a) to the depth of the flat portion of the webs (h) were 0.2, 0.4, 0.6 and 0.8. The ratio of the distance of the web holes (x) to the depth of the flat portion of the webs (h) were 0.2, 0.4 and 0.6. For each series of specimens, the web crippling strengths of the sections without the web holes were obtained. Thus, the ratio of the web crippling strengths for sections with the web holes divided by the sections without the web holes, which is the strength reduction factor (R), was used to quantify the degrading influence of the web holes on the web crippling strengths.

4.6.1 Effects of a/h and x/h on web crippling strength reduction for Type 1 web holes

For the ITF loading condition, A total of 200 specimens were analysed in the parametric study to investigate the effect of the ratio *a/h*. The cross-section dimensions as well as the web crippling strengths (P_{FEA}) per web predicted from the FEA are summarised in Table 4.9 and Table 4.10 for flanges unfastened and fastened condition, respectively. A total of 160 specimens were analysed in the parametric study investigating the effect of *x/h*. The cross-section dimensions as well as the web crippling strengths (P_{FEA}) per web predicted from the FEA are summarised in Table 4.11 and Table 4.12 for flanges unfastened and fastened condition, respectively. The effects of *a/h* and *x/h* ratio on the web crippling strength on the reduction factor for flanges unfastened and fastened condition are shown in Figure 4.4 and Figure 4.5 for the C202 specimen, respectively. It is seen from these graphs that the parameter *a/h* and *x/h* noticeably affects the web crippling strength and the reduction factor.

For the ETF loading condition, a total of 140 specimens wee analysed in the parametric study to investigate the effect of the ratio *a/h*. The cross-section dimensions as well as the web crippling strengths (P_{FEA}) per web predicted from the FEA are summarised in Table 4.13 and Table 4.14 for flanges unfastened and fastened condition, respectively. A total of 160 specimens were analysed in the parametric study investigating the effect of *x/h*. The cross-section dimensions as well as the web crippling strengths (P_{FEA}) per web predicted from the FEA are summarised in Table 4.15 and Table 4.16 for flanges unfastened and fastened condition, respectively. The effects of *a/h* and *x/h* ratio on the web crippling strength on the reduction factor for flanges unfastened and fastened condition are shown in Figure 4.6 and Figure 4.7 for the C202 specimen, respectively. It can be seen from these graphs that the parameter *a/h* and *x/h* noticeably affects the web crippling strength and the reduction factor.

Table 4.9 Dimensions and web crippling strength predicted from the finite element analysis of parametric study of *a/h* for flanges unfastened under ITF loading condition (Type 1 holes)

Specimen	Web	Flange	Lip	Thickness	Length	FEA load per web, P_{FEA}				
	d (mm)	b_f (mm)	b_l (mm)	t (mm)	L (mm)	A0 (kN)	A0.2 (kN)	A0.4 (kN)	A0.6 (kN)	A0.8 (kN)
ITF202x65x13-t1.4N32.5FR	202.5	63.6	16.0	1.40	678.3	6.9	6.3	5.4	4.5	3.6
ITF202x65x13-t2.0N32.5FR	202.5	63.6	16.0	2.00	678.3	17.8	15.9	13.5	11.1	8.4
ITF202x65x13-t2.5N32.5FR	202.5	63.6	16.0	2.50	678.3	30.6	27.3	22.8	18.4	14.1
ITF202x65x13-t3.0N32.5FR	202.5	63.6	16.0	3.00	678.3	43.8	41.4	34.1	27.5	21.2
ITF202x65x13-t4.0N32.5FR	202.5	63.6	16.0	4.00	678.3	86.6	74.2	61.9	49.7	38.6
ITF202x65x13-t5.0N32.5FR	202.5	63.6	16.0	5.00	678.3	129.1	112.7	96.4	76.5	59.3
ITF202x65x13-t6.0N32.5FR	202.5	63.6	16.0	6.00	678.3	185.5	161.5	137.5	107.7	83.7
ITF202x65x13-t1.4N65FR	202.5	64.0	17.5	1.44	701.0	7.6	7.0	6.1	5.1	4.0
ITF202x65x13-t2.0N65FR	202.5	64.0	17.5	2.00	701.0	17.8	16.2	13.9	11.5	8.9
ITF202x65x13-t2.5N65FR	202.5	64.0	17.5	2.50	701.0	30.0	27.2	23.4	19.2	14.9
ITF202x65x13-t3.0N65FR	202.5	64.0	17.5	3.00	701.0	44.6	40.3	34.5	28.4	22.3
ITF202x65x13-t4.0N65FR	202.5	64.0	17.5	4.00	701.0	80.4	72.4	62.1	51.7	41.0
ITF202x65x13-t5.0N65FR	202.5	64.0	17.5	5.00	701.0	124.8	111.8	95.7	79.7	63.8
ITF202x65x13-t6.0N65FR	202.5	64.0	17.5	6.00	701.0	176.2	158.6	135.0	112.8	89.8
ITF302x90x18-t2N44FR	304.0	87.9	18.0	1.93	998.9	12.4	11.4	9.8	8.2	6.4
ITF302x90x18-t2.5N44FR	304.0	87.9	18.0	2.50	998.9	24.9	22.7	19.5	16.0	12.1
ITF302x90x18-t3.0N44FR	304.0	87.9	18.0	3.00	998.9	39.9	36.0	30.5	24.7	18.6
ITF302x90x18-t4.0N44FR	304.0	87.9	18.0	4.00	998.9	74.5	70.4	59.1	47.5	36.2
ITF302x90x18-t5.0N44FR	304.0	87.9	18.0	5.00	998.9	115.1	112.9	94.8	76.2	58.7
ITF302x90x18-t6.0N44FR	304.0	87.9	18.0	6.00	998.9	160.1	158.5	137.4	109.8	84.8
ITF302x90x18-t2N90FR	303.8	88.8	18.7	1.96	1052.2	13.6	12.5	10.9	9.1	7.2
ITF302x90x18-t2.5N90FR	303.8	88.8	18.7	2.50	1052.2	25.9	23.8	20.6	17.0	13.1
ITF302x90x18-t3.0N90FR	303.8	88.8	18.7	3.00	1052.2	40.8	37.3	32.2	26.4	20.3
ITF302x90x18-t4.0N90FR	303.8	88.8	18.7	4.00	1052.2	78.5	71.4	61.5	50.6	39.4
ITF302x90x18-t5.0N90FR	303.8	88.8	18.7	5.00	1052.2	125.0	113.7	97.8	81.2	64.2
ITF302x90x18-t6.0N90FR	303.8	88.8	18.7	6.00	1052.2	180.0	163.3	140.6	117.3	93.3

Table 4.10 Dimensions and web crippling strength predicted from the finite element analysis of parametric study of *a/h* for flanges fastened under ITF loading condition (Type 1 holes)

Specimen	Web	Flange	Lip	Thickness	Length	FEA load per web, P_{FEA}				
	d (mm)	b_f (mm)	b_l (mm)	t (mm)	L (mm)	A0 (kN)	A0.2 (kN)	A0.4 (kN)	A0.6 (kN)	A0.8 (kN)
ITF202x65x13-t1.4N32.5FX	202.5	63.6	16.0	1.40	678.3	10.5	10.2	9.5	8.4	7.0
ITF202x65x13-t2.0N32.5FX	202.5	63.6	16.0	2.00	678.3	21.3	20.7	19.7	18.1	15.6
ITF202x65x13-t4.0N32.5FX	202.5	63.6	16.0	4.00	678.3	77.2	75.8	73.3	68.4	60.2
ITF202x65x13-t6.0N32.5FX	202.5	63.6	16.0	6.00	678.3	159.2	155.6	151.4	141.5	125.7
ITF202x65x13-t1.4N65FX	202.5	64.0	17.5	1.44	701.0	11.9	11.6	10.7	9.5	7.9
ITF202x65x13-t2.0N65FX	202.5	64.0	17.5	2.00	701.0	23.5	22.7	21.7	19.7	16.8
ITF202x65x13-t4.0N65FX	202.5	64.0	17.5	4.00	701.0	86.4	85.5	83.9	79.5	69.3
ITF202x65x13-t6.0N65FX	202.5	64.0	17.5	6.00	701.0	185.7	184.5	179.3	162.7	140.4
ITF302x90x18-t2N44FX	304.0	87.9	18.0	1.93	998.9	18.6	18.2	16.9	15.2	12.8
ITF302x90x18-t4.0N44FX	304.0	87.9	18.0	4.00	998.9	75.9	75.6	74.5	70.6	62.9
ITF302x90x18-t6.0N44FX	304.0	87.9	18.0	6.00	998.9	162.0	161.7	158.8	150.9	130.6
ITF302x90x18-t2N90FX	303.9	88.8	18.7	1.96	1052.2	22.2	21.1	19.2	17.0	14.3
ITF302x90x18-t4.0N90FX	303.9	88.8	18.7	4.00	1052.2	90.5	90.1	88.9	82.2	70.7
ITF302x90x18-t6.0N90FX	303.9	88.8	18.7	6.00	1052.2	193.6	192.9	190.1	178.0	154.6

Table 4.11 Dimensions and web crippling strength predicted from the finite element analysis of parametric study of *x/h* for flanges unfastened under ITF loading condition (Type 1 web holes)

Specimen	Web	Flange	Lip	Thickness	Length	FEA load per web P_{FEA}			
	d (mm)	b_f (mm)	b_l (mm)	t (mm)	L (mm)	X0 (kN)	X0.2 (kN)	X0.4 (kN)	X0.6 (kN)
ITF202x65x13-t1.4N32.5A0FR	202.5	63.6	16.0	1.40	678.3	6.9	6.9	6.9	6.9
ITF202x65x13-t1.4N32.5A0.2FR	202.5	63.6	16.0	1.40	678.3	6.3	6.3	6.3	6.3
ITF202x65x13-t1.4N32.5A0.4FR	202.5	63.6	16.0	1.40	678.3	5.3	5.4	5.4	5.5
ITF202x65x13-t1.4N32.5A0.6FR	202.5	63.6	16.0	1.40	678.3	4.3	4.4	4.5	4.6
ITF202x65x13-t1.4N32.5A0.8FR	202.5	63.6	16.0	1.40	678.3	3.1	3.3	3.6	3.7
ITF202x65x13-t1.4N65A0FR	202.5	64.0	17.5	1.44	701.0	7.6	7.6	7.6	7.6
ITF202x65x13-t1.4N65A0.2FR	202.5	64.0	17.5	1.44	701.0	7.0	7.0	7.0	7.0
ITF202x65x13-t1.4N65A0.4FR	202.5	64.0	17.5	1.44	702.0	5.9	6.0	6.1	6.1
ITF202x65x13-t1.4N65A0.6FR	202.5	64.0	17.5	1.44	703.0	4.8	5.0	5.1	5.2
ITF202x65x13-t1.4N65A0.8FR	202.5	64.0	17.5	1.44	704.0	3.5	3.8	4.1	4.3
ITF302x90x18-t2N44A0FR	304.0	87.9	18.0	1.93	997.9	12.4	12.4	12.4	12.4
ITF302x90x18-t2N44A0.2FR	304.0	87.9	18.0	1.93	998.9	11.4	11.4	11.4	11.4
ITF302x90x18-t2N44A0.4FR	304.0	87.9	18.0	1.93	999.9	9.6	9.7	9.8	9.8
ITF302x90x18-t2N44A0.6FR	304.0	87.9	18.0	1.93	1000.9	7.7	7.9	8.1	8.3
ITF302x90x18-t2N44A0.8FR	304.0	87.9	18.0	1.93	1001.9	5.5	5.9	6.4	6.7
ITF302x90x18-t2N90A0FR	303.8	88.8	18.7	1.96	1051.2	13.6	13.6	13.6	13.6
ITF302x90x18-t2N90A0.2FR	303.8	88.8	18.7	1.96	1052.2	12.5	12.5	12.5	12.5
ITF302x90x18-t2N90A0.4FR	303.8	88.8	18.7	1.96	1053.2	10.6	10.7	10.8	10.9
ITF302x90x18-t2N90A0.6FR	303.8	88.8	18.7	1.96	1054.2	8.6	8.9	9.1	9.3
ITF302x90x18-t2N90A0.8FR	303.8	88.8	18.7	1.96	1055.2	6.2	6.8	7.4	7.6

Table 4.12 Dimensions and web crippling strength predicted from the finite element analysis of parametric study of *x/h* for flanges fastened under ITF loading condition (Type 1 holes)

Specimen	Web	Flange	Lip	Thickness	Length	FEA load per web P_{FEA}			
	d (mm)	b_f (mm)	b_l (mm)	t (mm)	L (mm)	X0 (kN)	X0.2 (kN)	X0.4 (kN)	X0.6 (kN)
ITF202x65x13-t1.4N32.5A0-FX	202.5	63.6	16.0	1.40	678.3	10.5	10.5	10.5	10.5
ITF202x65x13-t1.4N32.5A0.2-FX	202.5	63.6	16.0	1.40	678.3	10.0	10.0	10.0	10.2
ITF202x65x13-t1.4N32.5A0.4-FX	202.5	63.6	16.0	1.40	678.3	8.6	9.0	9.2	9.5
ITF202x65x13-t1.4N32.5A0.6-FX	202.5	63.6	16.0	1.40	678.3	7.1	7.7	8.2	8.7
ITF202x65x13-t1.4N32.5A0.8-FX	202.5	63.6	16.0	1.40	678.3	5.1	6.3	7.1	7.9
ITF202x65x13-t1.4N65A0-FX	202.5	64.0	17.5	1.44	701.0	11.9	11.9	11.9	11.9
ITF202x65x13-t1.4N65A0.2-FX	202.5	64.0	17.5	1.44	701.0	11.5	11.4	11.5	11.6
ITF202x65x13-t1.4N65A0.4-FX	202.5	64.0	17.5	1.44	702.0	10.0	10.3	10.5	10.8
ITF202x65x13-t1.4N65A0.6-FX	202.5	64.0	17.5	1.44	703.0	8.2	8.9	9.5	10.0
ITF202x65x13-t1.4N65A0.8-FX	202.5	64.0	17.5	1.44	704.0	6.2	7.4	8.3	9.1
ITF302x90x18-t2N44A0-FX	304.0	87.9	18.0	1.93	997.9	18.6	18.6	18.6	18.6
ITF302x90x18-t2N44A0.2-FX	304.0	87.9	18.0	1.93	998.9	17.8	17.8	17.9	18.1
ITF302x90x18-t2N44A0.4-FX	304.0	87.9	18.0	1.93	999.9	15.6	16.1	16.5	17.0
ITF302x90x18-t2N44A0.6-FX	304.0	87.9	18.0	1.93	1000.9	12.9	14.1	15.0	15.8
ITF302x90x18-t2N44A0.8-FX	304.0	87.9	18.0	1.93	1001.9	9.0	11.5	13.1	14.5
ITF302x90x18-t2N90A0-FX	303.9	88.8	18.7	1.96	1051.2	22.2	22.2	22.2	22.2
ITF302x90x18-t2N90A0.2-FX	303.9	88.8	18.7	1.96	1052.2	20.7	20.7	20.8	21.1
ITF302x90x18-t2N90A0.4-FX	303.9	88.8	18.7	1.96	1053.2	17.8	18.4	18.8	19.4
ITF302x90x18-t2N90A0.6-FX	303.9	88.8	18.7	1.96	1054.2	14.5	15.9	16.9	17.8
ITF302x90x18-t2N90A0.8-FX	303.9	88.8	18.7	1.96	1055.2	10.9	13.2	14.9	16.4

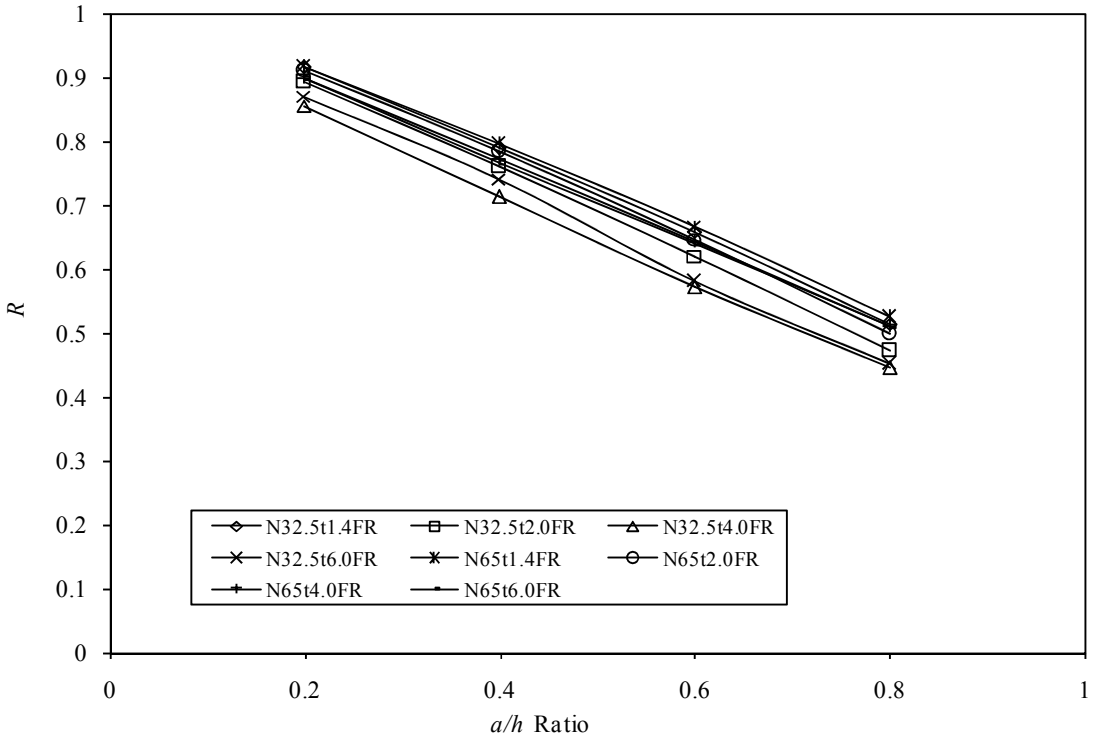

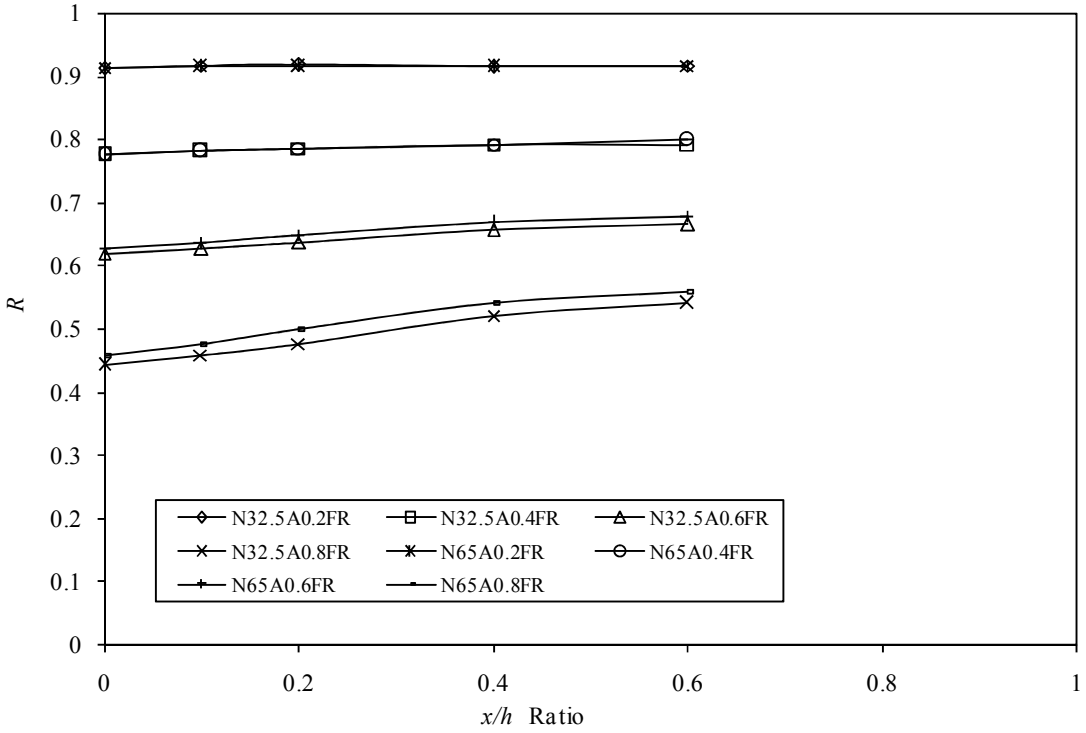

Figure 4.4 Variation in reduction factors with *a/h* and *x/h* for flanges unfastened under ITF loading condition for C202 section

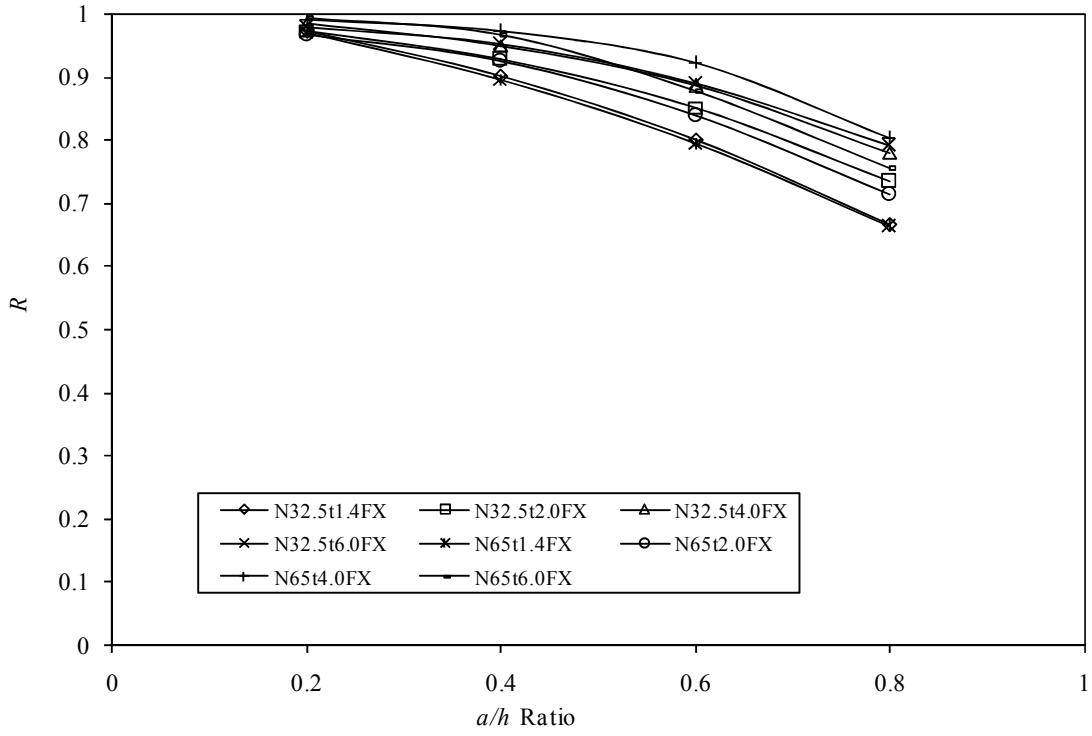

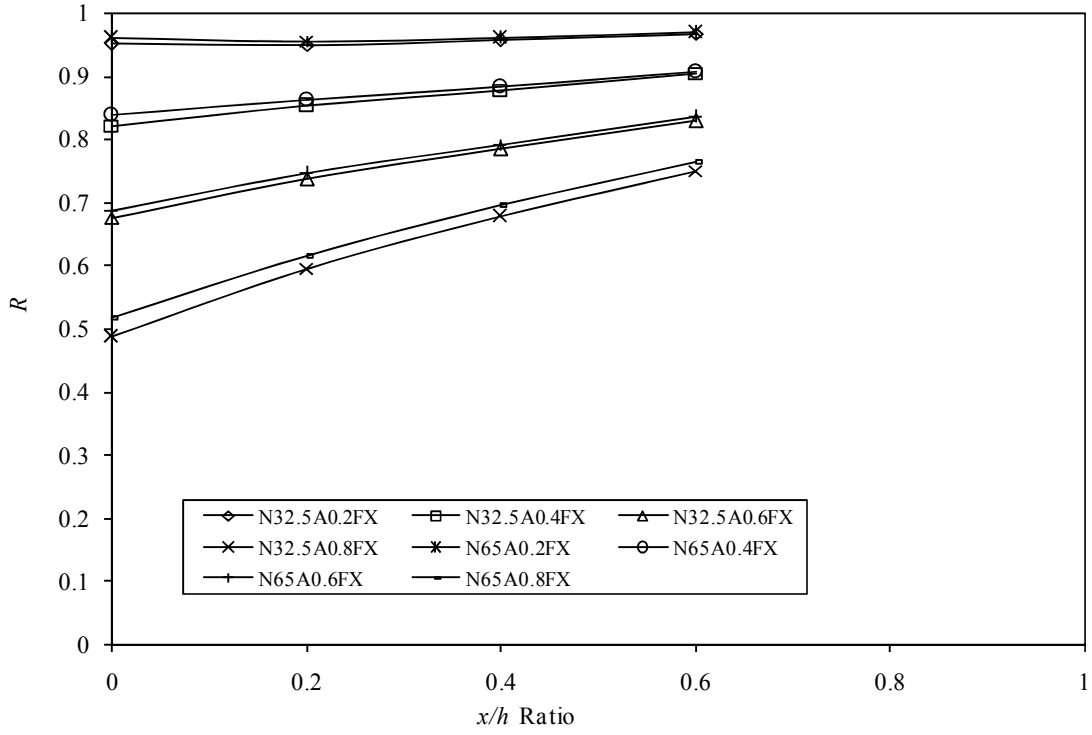

Figure 4.5 Variation in reduction factors with *a/h* and *x/h* for flanges fastened under ITF loading condition for C202 section

Table 4.13 Dimensions and web crippling strength predicted from the finite element analysis of parametric study of *a/h* for flanges unfastened under ETF loading condition (Type 1 holes)

Specimen	Web	Flange	Lip	Thickness	Length	FEA load per web, P_{FEA}				
	d (mm)	b_f (mm)	b_l (mm)	t (mm)	L (mm)	A0 (kN)	A0.2 (kN)	A0.4 (kN)	A0.6 (kN)	A0.8 (kN)
ETF202x65x13-t1.4N32.5FR	202.5	63.6	16.0	1.40	376.4	1.9	1.8	1.6	1.4	1.2
ETF202x65x13-t2.0N32.5FR	202.5	63.6	16.0	2.00	376.4	5.5	5.2	4.7	4.1	3.4
ETF202x65x13-t4.0N32.5FR	202.5	63.6	16.0	4.00	376.4	26.9	25.8	23.3	20.5	17.4
ETF202x65x13-t6.0N32.5FR	202.5	63.6	16.0	6.00	376.4	62.2	60.4	54.9	48.2	41.1
ETF202x65x13-t1.4N65FR	202.5	64.0	17.5	1.44	401.8	2.5	2.4	2.2	1.9	1.7
ETF202x65x13-t2.0N65FR	202.5	64.0	17.5	2.00	401.8	6.3	6.0	5.5	4.8	4.2
ETF202x65x13-t4.0N65FR	202.5	64.0	17.5	4.00	401.8	30.4	29.2	26.7	23.7	20.6
ETF202x65x13-t6.0N65FR	202.5	64.0	17.5	6.00	401.8	70.2	68.1	62.6	55.6	48.0
ETF302x90x18-t2N44FR	304.0	87.9	18.0	1.93	544.5	3.7	3.5	3.2	2.8	2.3
ETF302x90x18-t4.0N44FR	304.0	87.9	18.0	4.00	544.5	24.0	22.8	20.5	17.8	15.0
ETF302x90x18-t6.0N44FR	304.0	87.9	18.0	6.00	544.5	59.1	56.7	51.2	44.7	37.8
ETF302x90x18-t2N90FR	303.8	88.8	18.7	1.96	601.8	4.3	4.1	3.7	3.3	2.8
ETF302x90x18-t4.0N90FR	303.8	88.8	18.7	4.00	601.8	27.7	26.6	24.2	21.5	18.7
ETF302x90x18-t6.0N90FR	303.8	88.8	18.7	6.00	601.8	67.0	64.3	59.8	53.4	46.6

Table 4.14 Dimensions and web crippling strength predicted from the finite element analysis of parametric study of *a/h* for flanges fastened under ETF loading condition (Type 1 holes)

Specimen	Web	Flange	Lip	Thickness	Length	FEA load per web, P_{FEA}				
	d (mm)	b_f (mm)	b_l (mm)	t (mm)	L (mm)	A0 (kN)	A0.2 (kN)	A0.4 (kN)	A0.6 (kN)	A0.8 (kN)
ETF202x65x13-t1.4N32.5FX	202.5	63.6	16.0	1.40	376.4	3.4	3.2	3.0	2.7	2.3
ETF202x65x13-t2.0N32.5FX	202.5	63.6	16.0	2.00	376.4	8.9	8.6	8.0	7.1	6.2
ETF202x65x13-t4.0N32.5FX	202.5	63.6	16.0	4.00	376.4	36.3	35.6	33.4	30.7	27.8
ETF202x65x13-t6.0N32.5FX	202.5	63.6	16.0	6.00	376.4	75.2	74.8	71.6	66.4	60.5
ETF202x65x13-t1.4N65FX	202.5	64.0	17.5	1.44	401.8	4.5	4.4	4.1	3.8	3.4
ETF202x65x13-t2.0N65FX	202.5	64.0	17.5	2.00	401.8	10.5	10.2	9.6	8.8	8.0
ETF202x65x13-t4.0N65FX	202.5	64.0	17.5	4.00	401.8	43.1	42.5	40.8	38.5	36.0
ETF202x65x13-t6.0N65FX	202.5	64.0	17.5	6.00	401.8	92.0	91.2	88.3	83.6	78.0
ETF302x90x18-t2N44FX	304.0	87.9	18.0	1.93	544.5	6.5	6.3	5.9	5.4	4.6
ETF302x90x18-t4.0N44FX	304.0	87.9	18.0	4.00	544.5	35.3	34.4	32.1	29.2	26.1
ETF302x90x18-t6.0N44FX	304.0	87.9	18.0	6.00	544.5	78.1	76.9	72.4	66.3	59.8
ETF302x90x18-t2N90FX	303.9	88.8	18.7	1.96	601.8	7.9	7.7	7.2	6.7	6.0
ETF302x90x18-t4.0N90FX	303.9	88.8	18.7	4.00	601.8	42.5	41.7	39.6	37.1	34.6
ETF302x90x18-t6.0N90FX	303.9	88.8	18.7	6.00	601.8	94.2	93.1	89.8	85.1	79.6

Table 4.15 Dimensions and web crippling strength predicted from the finite element analysis of parametric study of *x/h* for flanges unfastened under ETF loading condition (Type 1 holes)

Specimen	Web	Flange	Lip	Thickness	Length	FEA load per web, P_{FEA}			
	d (mm)	b_f (mm)	b_l (mm)	t (mm)	L (mm)	X0 (kN)	X0.2 (kN)	X0.4 (kN)	X0.6 (kN)
ETF202x65x13-t1.4N32.5A0FR	202.5	63.6	16.0	1.40	376.4	1.9	1.9	1.9	1.9
ETF202x65x13-t1.4N32.5A0.2FR	202.5	63.6	16.0	1.40	376.4	1.6	1.7	1.7	1.8
ETF202x65x13-t1.4N32.5A0.4FR	202.5	63.6	16.0	1.40	376.4	1.4	1.5	1.5	1.6
ETF202x65x13-t1.4N32.5A0.6FR	202.5	63.6	16.0	1.40	376.4	1.1	1.2	1.4	1.5
ETF202x65x13-t1.4N32.5A0.8FR	202.5	63.6	16.0	1.40	376.4	0.9	1.0	1.2	1.4
ETF202x65x13-t1.4N65A0FR	202.5	64.0	17.5	1.44	401.8	2.5	2.5	2.5	2.5
ETF202x65x13-t1.4N65A0.2FR	202.5	64.0	17.5	1.44	401.8	2.2	2.3	2.3	2.4
ETF202x65x13-t1.4N65A0.4FR	202.5	64.0	17.5	1.44	401.8	1.9	2.0	2.1	2.2
ETF202x65x13-t1.4N65A0.6FR	202.5	64.0	17.5	1.44	401.8	1.6	1.8	1.9	2.1
ETF202x65x13-t1.4N65A0.8FR	202.5	64.0	17.5	1.44	401.8	1.3	1.6	1.8	1.9
ETF302x90x18-t2N44A0FR	304.0	87.9	18.0	1.93	544.5	3.7	3.7	3.7	3.7
ETF302x90x18-t2N44A0.2FR	304.0	87.9	18.0	1.93	544.5	3.2	3.3	3.4	3.5
ETF302x90x18-t2N44A0.4FR	304.0	87.9	18.0	1.93	544.5	2.6	2.8	3.0	3.2
ETF302x90x18-t2N44A0.6FR	304.0	87.9	18.0	1.93	544.5	2.1	2.4	2.7	2.9
ETF302x90x18-t2N44A0.8FR	304.0	87.9	18.0	1.93	544.5	1.7	2.0	2.4	2.7
ETF302x90x18-t2N90A0FR	303.8	88.8	18.7	1.96	601.8	4.3	4.3	4.3	4.3
ETF302x90x18-t2N90A0.2FR	303.8	88.8	18.7	1.96	601.8	3.8	3.9	4.0	4.1
ETF302x90x18-t2N90A0.4FR	303.8	88.8	18.7	1.96	601.8	3.2	3.5	3.6	3.8
ETF302x90x18-t2N90A0.6FR	303.8	88.8	18.7	1.96	601.8	2.7	3.0	3.3	3.5
ETF302x90x18-t2N90A0.8FR	303.8	88.8	18.7	1.96	601.8	2.3	2.7	3.0	3.3

Table 4.16 Dimensions and web crippling strength predicted from the finite element analysis of parametric study of *x/h* for flanges fastened under ETF loading condition (Type 1 holes)

Specimen	Web	Flange	Lip	Thickness	Length	FEA load per web, P_{FEA}			
	d (mm)	b_f (mm)	b_l (mm)	t (mm)	L (mm)	X0 (kN)	X0.2 (kN)	X0.4 (kN)	X0.6 (kN)
ETF202x65x13-t1.4N32.5A0FX	202.5	63.6	16.0	1.40	376.4	3.4	3.4	3.4	3.4
ETF202x65x13-t1.4N32.5A0.2FX	202.5	63.6	16.0	1.40	376.4	3.1	3.1	3.2	3.2
ETF202x65x13-t1.4N32.5A0.4FX	202.5	63.6	16.0	1.40	376.4	2.7	2.8	2.9	3.0
ETF202x65x13-t1.4N32.5A0.6FX	202.5	63.6	16.0	1.40	376.4	2.3	2.5	2.7	2.8
ETF202x65x13-t1.4N32.5A0.8FX	202.5	63.6	16.0	1.40	376.4	1.8	2.1	2.4	2.6
ETF202x65x13-t1.4N65A0FX	202.5	64.0	17.5	1.44	401.8	4.5	4.5	4.5	4.5
ETF202x65x13-t1.4N65A0.2FX	202.5	64.0	17.5	1.44	401.8	4.2	4.3	4.3	4.4
ETF202x65x13-t1.4N65A0.4FX	202.5	64.0	17.5	1.44	401.8	3.9	4.0	4.1	4.2
ETF202x65x13-t1.4N65A0.6FX	202.5	64.0	17.5	1.44	401.8	3.5	3.6	3.8	4.0
ETF202x65x13-t1.4N65A0.8FX	202.5	64.0	17.5	1.44	401.8	3.0	3.3	3.6	3.8
ETF302x90x18-t2N44A0FX	304.0	87.9	18.0	1.93	544.5	6.5	6.5	6.5	6.5
ETF302x90x18-t2N44A0.2FX	304.0	87.9	18.0	1.93	544.5	6.0	6.1	6.2	6.3
ETF302x90x18-t2N44A0.4FX	304.0	87.9	18.0	1.93	544.5	5.3	5.5	5.8	6.0
ETF302x90x18-t2N44A0.6FX	304.0	87.9	18.0	1.93	544.5	4.4	4.9	5.3	5.7
ETF302x90x18-t2N44A0.8FX	304.0	87.9	18.0	1.93	544.5	3.4	4.2	4.7	5.3
ETF302x90x18-t2N90A0FX	303.8	88.8	18.7	1.96	601.8	7.9	7.9	7.9	7.9
ETF302x90x18-t2N90A0.2FX	303.8	88.8	18.7	1.96	601.8	7.4	7.5	7.6	7.7
ETF302x90x18-t2N90A0.4FX	303.8	88.8	18.7	1.96	601.8	6.7	6.9	7.1	7.3
ETF302x90x18-t2N90A0.6FX	303.8	88.8	18.7	1.96	601.8	6.0	6.4	6.7	7.0
ETF302x90x18-t2N90A0.8FX	303.8	88.8	18.7	1.96	601.8	5.3	5.8	6.3	6.7

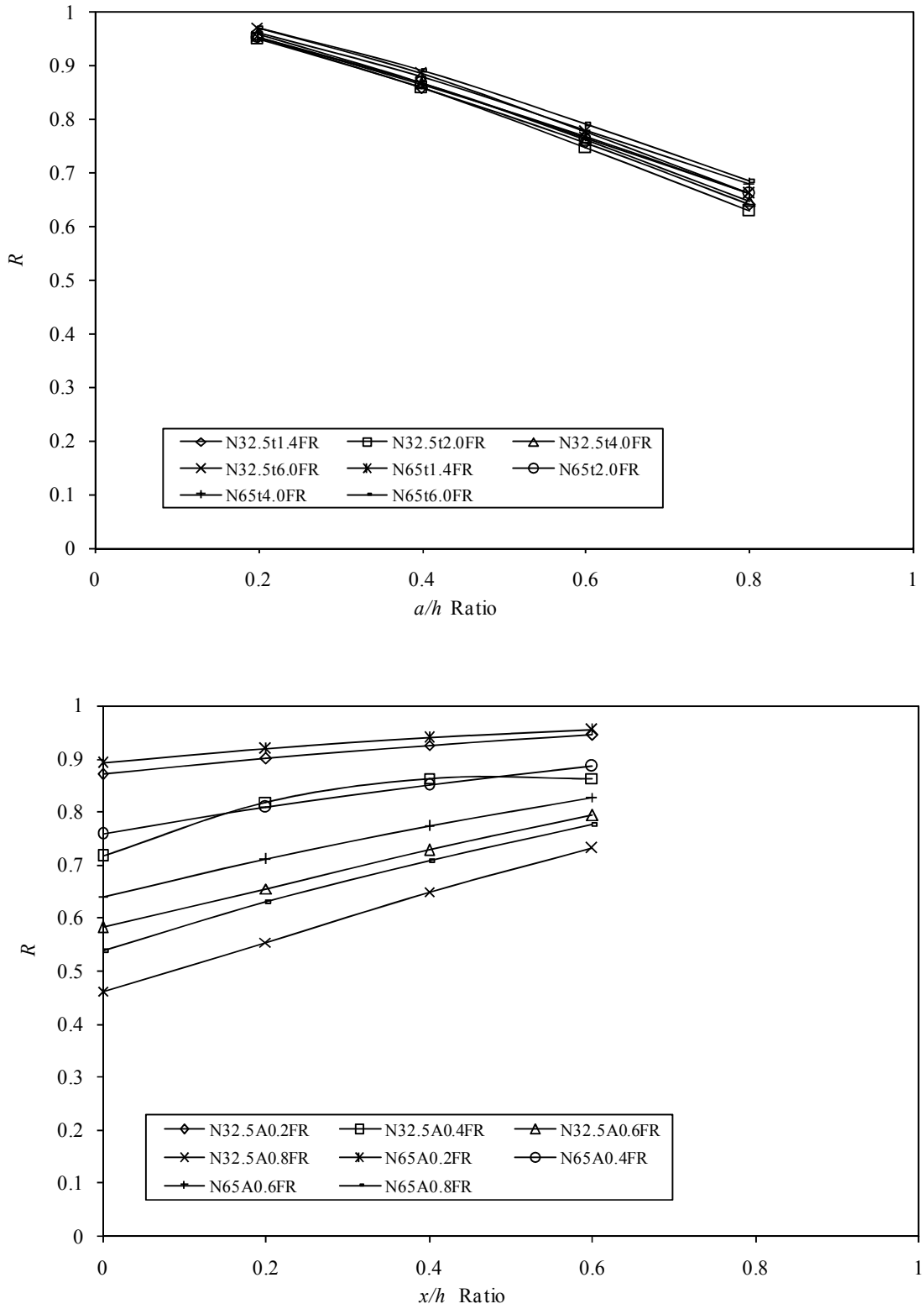

Figure 4.6 Variation in reduction factors with *a/h* and *x/h* for flanges fastened under ETF loading condition for C202 section

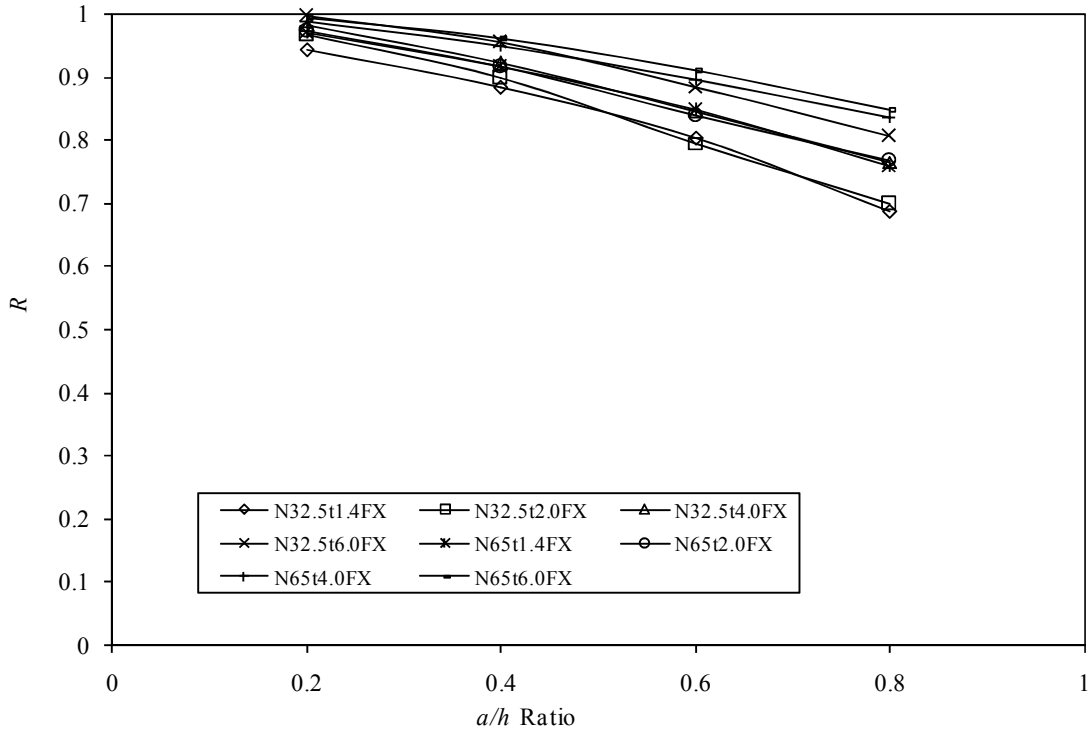

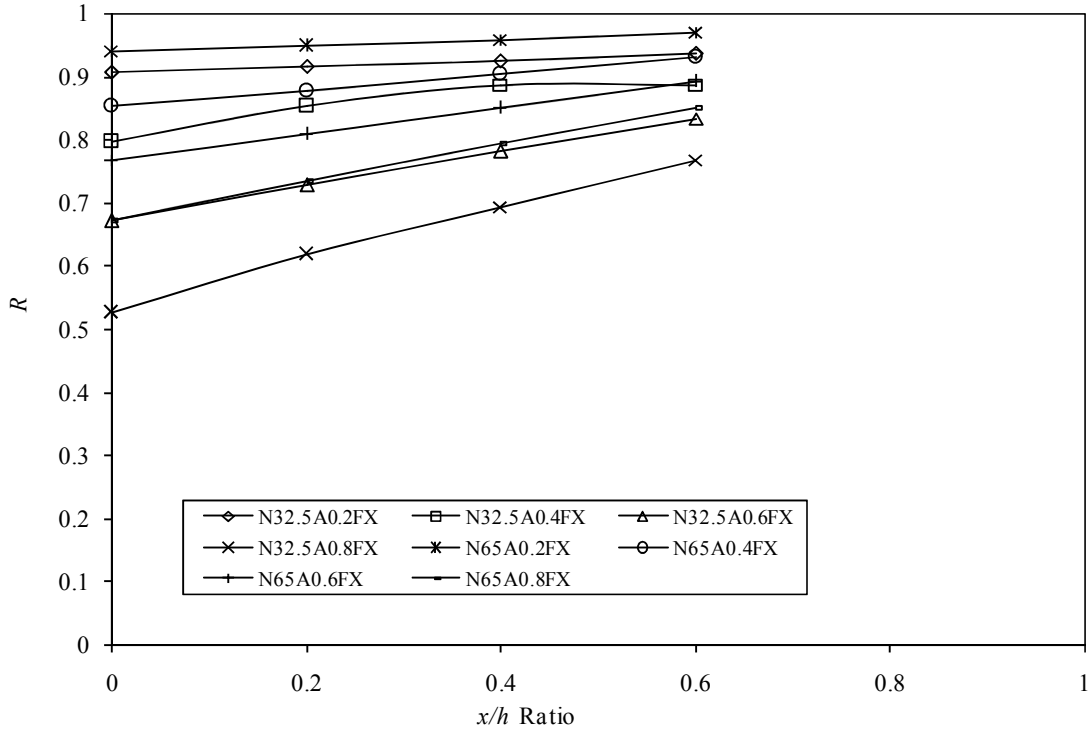

Figure 4.7 Variation in reduction factors with *a/h* and *x/h* for flanges fastened under ETF loading condition for C202 section

4.6.2 Effects of a/h and N/h when web hole is located centred beneath the bearing plates

For ITF loading condition, a total of 146 specimens were analysed in the parametric study to investigate the effects of the ratio *a/h* and *N/h*. The cross-section dimensions as well as the web crippling strengths (P_{FEA}) per web predicted from the FEA are summarised in Table 4.17 and Table 4.18 for flanges unfastened and fastened condition, respectively. The effects of *a/h* and *N/h* ratio on the web crippling strength on the reduction factor for flanges unfastened and fastened condition are shown in Figure 4.8 and Figure 4.9 for the C202 specimen, respectively. It can be seen from these graphs that the parameter *a/h* and *N/h* noticeably affects the web crippling strength and the reduction factor.

For ETF loading condition, a total of 146 specimens was analysed in the parametric study to investigate the effects of the ratio *a/h* and *N/h*. The cross-section dimensions as well as the web crippling strengths (P_{FEA}) per web predicted from the FEA are summarised in Table 4.19 and Table 4.20 for flanges unfastened and fastened condition, respectively. The effects of *a/h* and *N/h* ratio on the web crippling strength on the reduction factor for flanges unfastened and fastened condition are shown in Figure 4.10 and Figure 4.11 for the C202 Specimen, respectively. It can be seen from these graphs that the parameter *a/h* and *N/h* noticeably affects the web crippling strength and the reduction factor.

Table 4.17 Dimensions and web crippling strength predicted from the finite element analysis of parametric study of *a/h* for flanges unfastened under ITF loading condition (Type 2 holes)

Specimen	Web	Flange	Lip	Thickness	Length	FEA load per web, P_{FEA}				
	d (mm)	b_f (mm)	b_l (mm)	t (mm)	L (mm)	A0 (kN)	A0.2 (kN)	A0.4 (kN)	A0.6 (kN)	A0.8 (kN)
ITF202x65x13-t1.4N100FR	202.5	63.6	16.0	1.40	736.4	18.4	17.4	15.7	-	-
ITF202x65x13-t4.0N100FR	202.5	63.6	16.0	4.00	736.4	81.8	76.0	66.2	-	-
ITF202x65x13-t6.0N100FR	202.5	63.6	16.0	6.00	736.4	176.3	163.0	142.0	-	-
ITF202x65x13-t1.4N150FR	202.5	64.0	17.5	1.44	786.4	19.3	18.2	16.5	14.2	-
ITF202x65x13-t4.0N150FR	202.5	64.0	17.5	4.00	786.4	84.4	78.9	69.8	58.9	-
ITF202x65x13-t6.0N150FR	202.5	64.0	17.5	6.00	786.4	183.0	170.6	151.0	129.2	-
ITF202x65x13-t1.4N200FR	202.5	64.0	17.5	1.44	836.4	20.2	19.1	17.5	15.3	12.2
ITF202x65x13-t4.0N200FR	202.5	64.0	17.5	4.00	836.4	87.5	82.1	73.9	63.8	54.1
ITF202x65x13-t6.0N200FR	202.5	64.0	17.5	6.00	836.4	190.0	178.0	160.2	139.2	120.4
ITF302x90x18-t2N150FR	304.0	87.9	18.0	2.00	1112.2	15.0	14.5	13.4	-	-
ITF302x90x18-t4.0N150FR	304.0	87.9	18.0	4.00	1112.2	80.5	75.1	65.6	-	-
ITF302x90x18-t6.0N150FR	304.0	87.9	18.0	6.00	1112.2	184.3	170.6	147.9	-	-
ITF302x90x18-t2N220FR	303.8	88.8	18.7	2.00	1182.2	15.9	15.3	14.2	12.8	-
ITF302x90x18-t4.0N220FR	303.8	88.8	18.7	4.00	1182.2	83.2	77.8	68.8	57.4	-
ITF302x90x18-t6.0N220FR	303.8	88.8	18.7	6.00	1182.2	190.0	176.9	155.6	130.3	-
ITF302x90x18-t2N300FR	303.8	88.8	18.7	2.00	1262.2	16.9	16.3	15.2	13.7	10.9
ITF302x90x18-t4.0N300FR	303.8	88.8	18.7	4.00	1262.2	86.6	81.2	73.0	62.8	51.4
ITF302x90x18-t6.0N300FR	303.8	88.8	18.7	6.00	1262.2	197.7	184.7	165.1	142.1	120.1

Table 4.18 Dimensions and web crippling strength predicted from the finite element analysis of parametric study of *a/h* for flanges fastened under ITF loading condition (Type 2 holes)

Specimen	Web	Flange	Lip	Thickness	Length	FEA load per web, P_{FEA}				
	d	b_f	b_l	t	L	A0	A0.2	A0.4	A0.6	A0.8
	(mm)	(mm)	(mm)	(mm)	(mm)	(kN)	(kN)	(kN)	(kN)	(kN)
ITF202x65x13-t1.4N100FX	202.5	63.6	16.0	1.4	736.4	26.7	26.0	22.9	-	-
ITF202x65x13-t4.0N100FX	202.5	63.6	16.0	4.0	736.4	99.6	97.6	88.5	-	-
ITF202x65x13-t6.0N100FX	202.5	63.6	16.0	6.0	736.4	207.7	206.0	178.3	-	-
ITF202x65x13-t1.4N150FX	202.5	64.0	17.5	1.4	786.4	28.4	27.0	24.2	20.6	-
ITF202x65x13-t4.0N150FX	202.5	64.0	17.5	4.0	786.4	114.1	107.2	95.0	82.0	-
ITF202x65x13-t6.0N150FX	202.5	64.0	17.5	6.0	786.4	232.2	218.7	195.3	170.7	-
ITF202x65x13-t1.4N200FX	202.5	64.0	17.5	1.4	836.4	29.6	28.1	25.6	22.4	19.0
ITF202x65x13-t4.0N200FX	202.5	64.0	17.5	4.0	836.4	119.3	112.7	101.9	89.7	78.1
ITF202x65x13-t6.0N200FX	202.5	64.0	17.5	6.0	836.4	245.9	232.9	212.2	189.6	167.4
ITF302x90x18-t2N150FX	304.0	87.9	18.0	2.0	1112.2	24.5	23.7	21.3	-	-
ITF302x90x18-t4.0N150FX	304.0	87.9	18.0	4.0	1112.2	111.1	104.7	91.1	-	-
ITF302x90x18-t6.0N150FX	304.0	87.9	18.0	6.0	1112.2	233.7	225.1	195.0	-	-
ITF302x90x18-t2N220FX	303.8	88.8	18.7	2.0	1182.2	25.6	24.5	22.2	18.9	-
ITF302x90x18-t4.0N220FX	303.8	88.8	18.7	4.0	1182.2	115.5	108.5	96.1	81.9	-
ITF302x90x18-t6.0N220FX	303.8	88.8	18.7	6.0	1182.2	250.8	234.8	207.8	179.0	-
ITF302x90x18-t2N300FX	303.8	88.8	18.7	2.0	1262.2	26.7	25.5	23.4	20.7	17.6
ITF302x90x18-t4.0N300FX	303.8	88.8	18.7	4.0	1262.2	120.9	113.8	102.8	89.8	76.5
ITF302x90x18-t6.0N300FX	303.8	88.8	18.7	6.0	1262.2	264.3	248.3	224.5	197.4	170.6

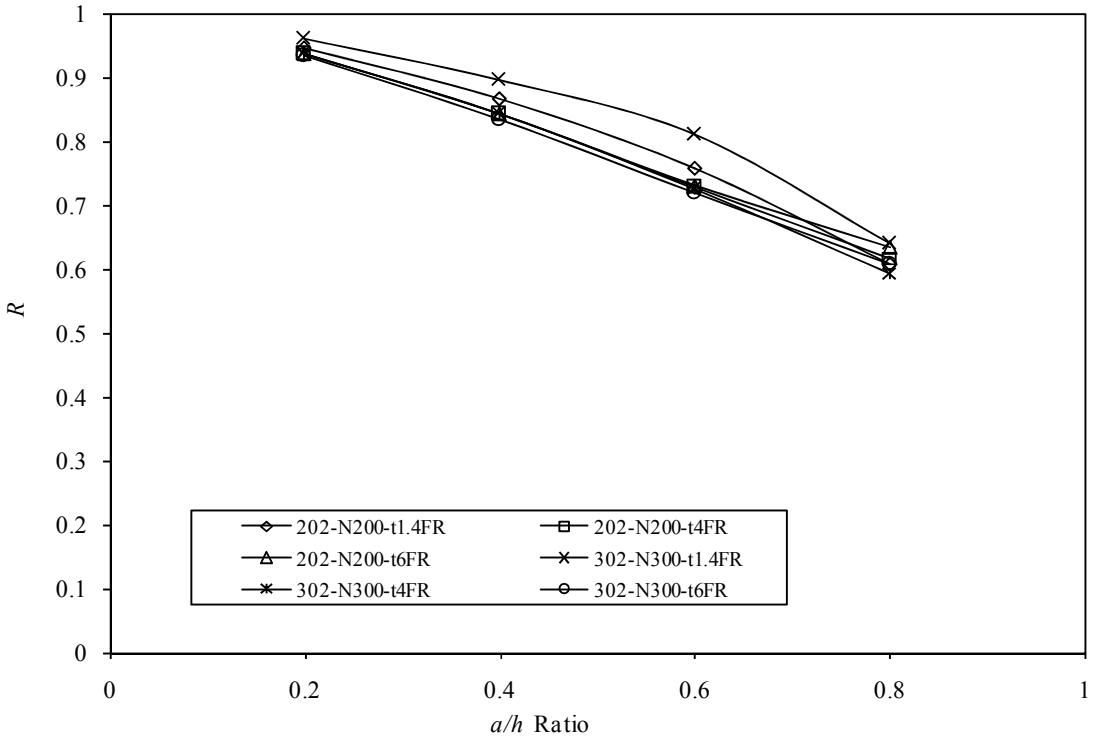

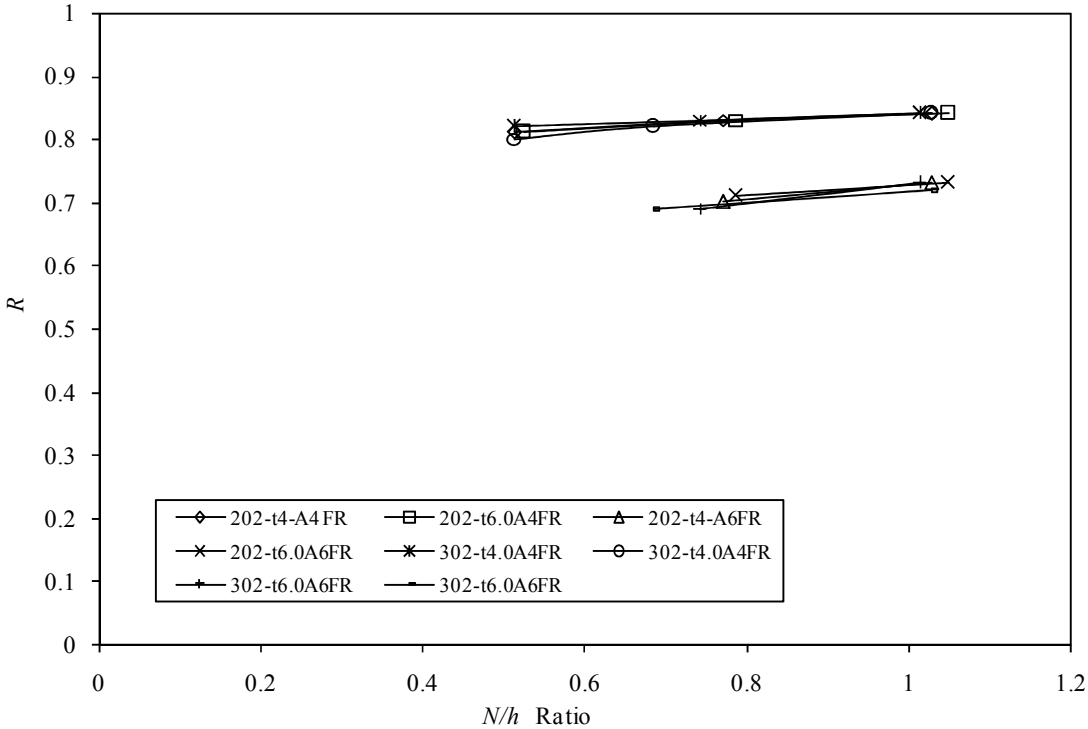

Figure 4.8 Variation in reduction factors with *a/h* and *N/h* for flanges unfastened under ITF loading condition

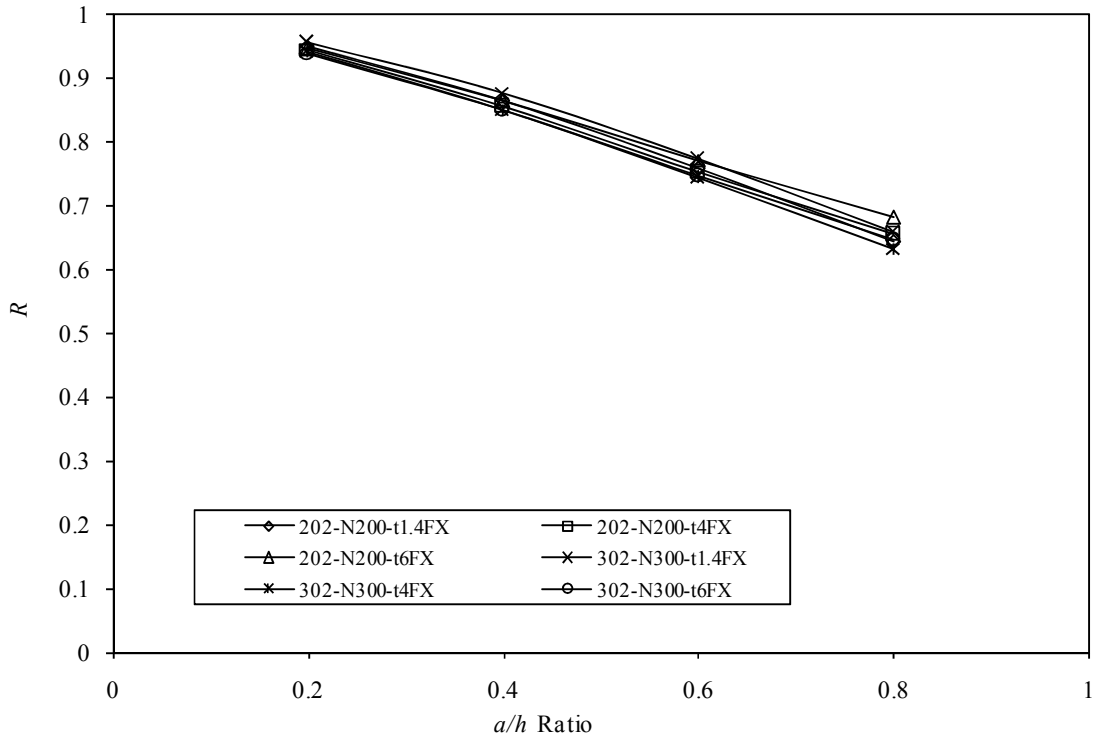

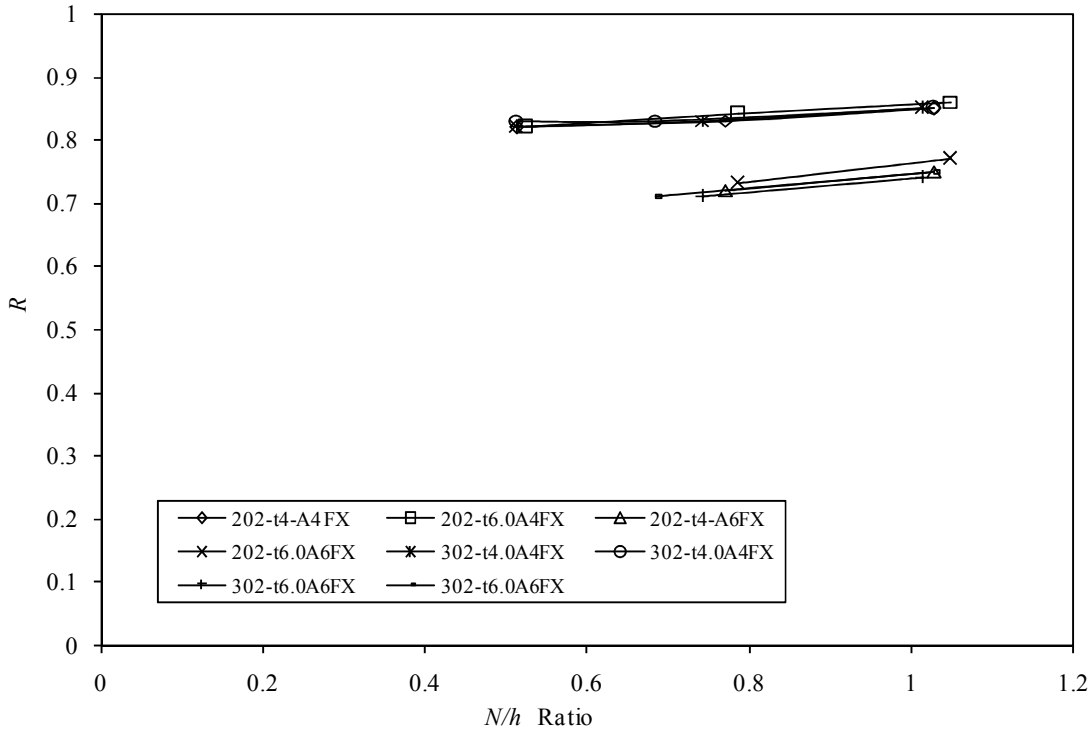

Figure 4.9 Variation in reduction factors with *a/h* and *N/h* for flanges fastened under ITF loading condition

Table 4.19 Dimensions and web crippling strength predicted from the finite element analysis of parametric study of *a/h* for flanges unfastened under ETF loading condition (Type 2 holes)

Specimen	Web	Flange	Lip	Thickness	Length,	FEA load per web, P_{FEA}				
	d (mm)	b_f (mm)	b_l (mm)	t (mm)	L (mm)	A0 (kN)	A0.2 (kN)	A0.4 (kN)	A0.6 (kN)	A0.8 (kN)
ETF202x65x13-t1.4N100FR	202.5	63.6	16.0	1.40	410.0	2.9	2.5	2.1	-	-
ETF202x65x13-t4.0N100FR	202.5	63.6	16.0	4.00	410.0	35.2	30.0	25.2	-	-
ETF202x65x13-t6.0N100FR	202.5	63.6	16.0	6.00	410.0	80.1	67.8	57.3	-	-
ETF202x65x13-t1.4N150FR	202.5	64.0	17.5	1.44	460.0	3.2	2.8	2.4	1.9	-
ETF202x65x13-t4.0N150FR	202.5	64.0	17.5	4.00	460.0	43.0	37.4	31.9	26.8	-
ETF202x65x13-t6.0N150FR	202.5	64.0	17.5	6.00	460.0	95.8	83.5	72.2	61.3	-
ETF202x65x13-t1.4N200FR	202.5	64.0	17.5	1.44	510.0	3.9	3.5	3.0	2.6	2.2
ETF202x65x13-t4.0N200FR	202.5	64.0	17.5	4.00	510.0	50.9	45.2	39.5	33.9	28.4
ETF202x65x13-t6.0N200FR	202.5	64.0	17.5	6.00	510.0	111.9	99.1	87.4	75.8	64.3
ETF302x90x18-t2N150FR	304.0	87.9	18.0	2.00	662.0	5.1	4.5	3.6	-	-
ETF302x90x18-t4.0N150FR	304.0	87.9	18.0	4.00	662.0	33.2	28.2	23.4	-	-
ETF302x90x18-t6.0N150FR	304.0	87.9	18.0	6.00	662.0	79.6	67.4	56.3	-	-
ETF302x90x18-t2N220FR	303.8	88.8	18.7	2.00	732.0	6.4	5.6	4.7	3.8	-
ETF302x90x18-t4.0N220FR	303.8	88.8	18.7	4.00	732.0	40.0	34.5	29.0	24.0	-
ETF302x90x18-t6.0N220FR	303.8	88.8	18.7	6.00	732.0	94.8	81.8	69.4	56.9	-
ETF302x90x18-t2N300FR	303.8	88.8	18.7	2.00	812.0	7.9	7.1	6.1	5.1	4.1
ETF302x90x18-t4.0N300FR	303.8	88.8	18.7	4.00	812.0	48.2	42.7	36.9	31.2	25.8
ETF302x90x18-t6.0N300FR	303.8	88.8	18.7	6.00	812.0	112.5	99.3	86.6	74.1	61.9

Table 4.20 Dimensions and web crippling strength predicted from the finite element analysis of parametric study of *a/h* for flanges fastened under ETF loading condition (Type 2 holes)

Specimen	Web	Flange	Lip	Thickness	Length	FEA load per web, P_{FEA}				
	d	b_f	b_l	t	L	A0	A0.2	A0.4	A0.6	A0.8
	(mm)	(mm)	(mm)	(mm)	(mm)	(kN)	(kN)	(kN)	(kN)	(kN)
ETF202x65x13-t1.4N100FX	202.5	63.6	16.0	1.40	410.0	5.4	4.9	4.3	-	-
ETF202x65x13-t4.0N100FX	202.5	63.6	16.0	4.00	410.0	52.4	46.6	41.2	-	-
ETF202x65x13-t6.0N100FX	202.5	63.6	16.0	6.00	410.0	112.3	98.5	86.7	-	-
ETF202x65x13-t1.4N150FX	202.5	64.0	17.5	1.44	460.0	6.0	5.6	5.0	4.4	-
ETF202x65x13-t4.0N150FX	202.5	64.0	17.5	4.00	460.0	67.1	60.4	54.1	47.9	-
ETF202x65x13-t6.0N150FX	202.5	64.0	17.5	6.00	460.0	143.9	128.7	114.9	102.2	-
ETF202x65x13-t1.4N200FX	202.5	64.0	17.5	1.44	510.0	7.2	6.7	6.1	5.5	4.6
ETF202x65x13-t4.0N200FX	202.5	64.0	17.5	4.00	510.0	82.0	75.4	67.9	60.3	50.8
ETF202x65x13-t6.0N200FX	202.5	64.0	17.5	6.00	510.0	175.6	159.7	144.4	129.1	109.0
ETF302x90x18-t2N150FX	304.0	87.9	18.0	2.00	662.0	9.8	8.9	7.7	-	-
ETF302x90x18-t4.0N150FX	304.0	87.9	18.0	4.00	662.0	53.0	47.1	41.3	-	-
ETF302x90x18-t6.0N150FX	304.0	87.9	18.0	6.00	662.0	119.1	104.6	91.8	-	-
ETF302x90x18-t2N220FX	303.8	88.8	18.7	2.00	732.0	12.3	11.3	10.0	8.6	-
ETF302x90x18-t4.0N220FX	303.8	88.8	18.7	4.00	732.0	65.7	59.5	52.7	46.1	-
ETF302x90x18-t6.0N220FX	303.8	88.8	18.7	6.00	732.0	148.9	133.2	117.6	103.5	-
ETF302x90x18-t2N300FX	303.8	88.8	18.7	2.00	812.0	14.9	13.9	12.6	11.2	9.2
ETF302x90x18-t4.0N300FX	303.8	88.8	18.7	4.00	812.0	81.0	74.9	67.3	58.9	47.7
ETF302x90x18-t6.0N300FX	303.8	88.8	18.7	6.00	812.0	183.4	167.5	150.1	132.5	109.5

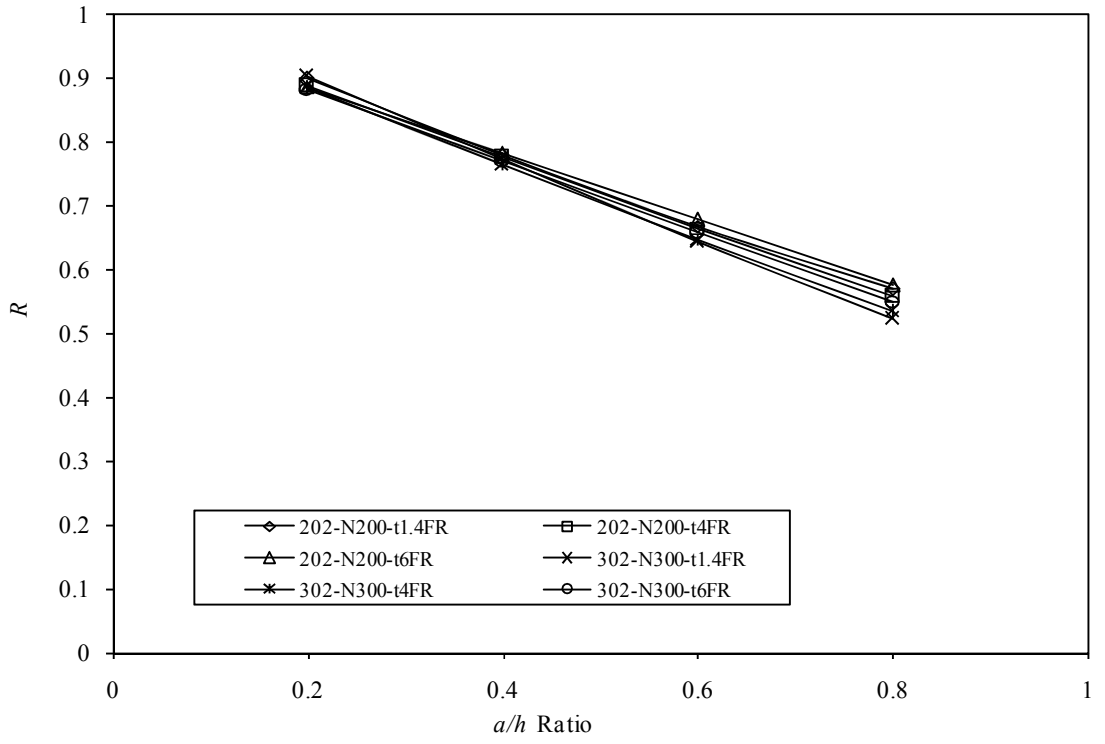

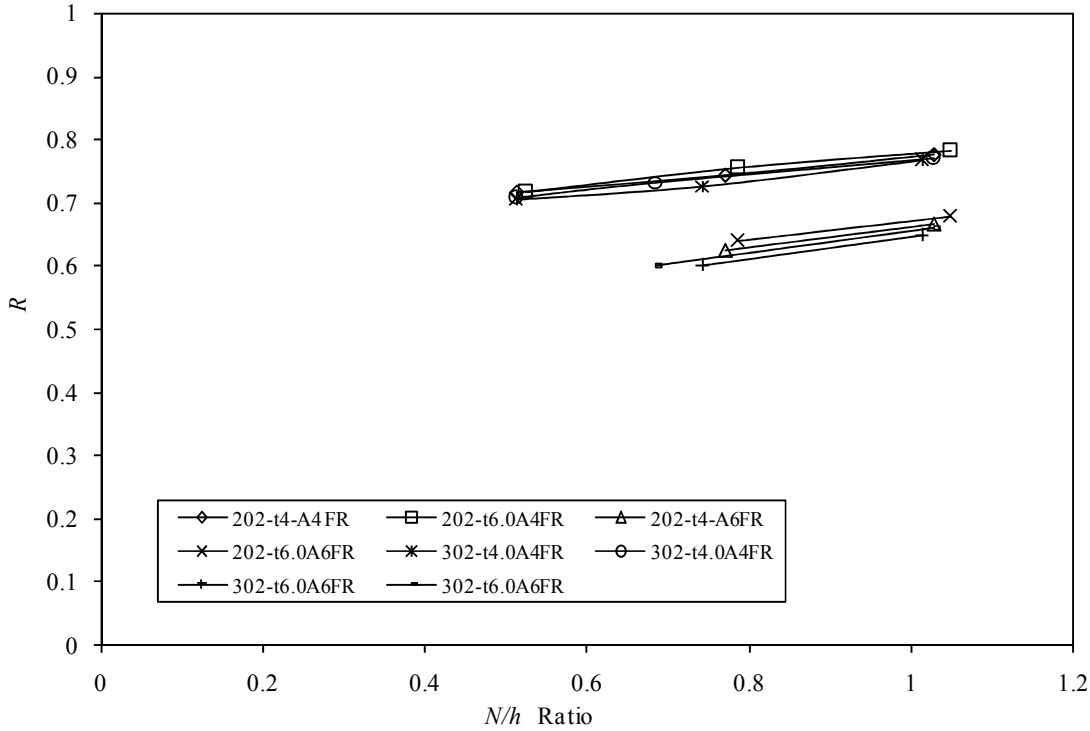

Figure 4.10 Variation in reduction factors with *a/h* and *N/h* for flanges unfastened under ETF loading condition

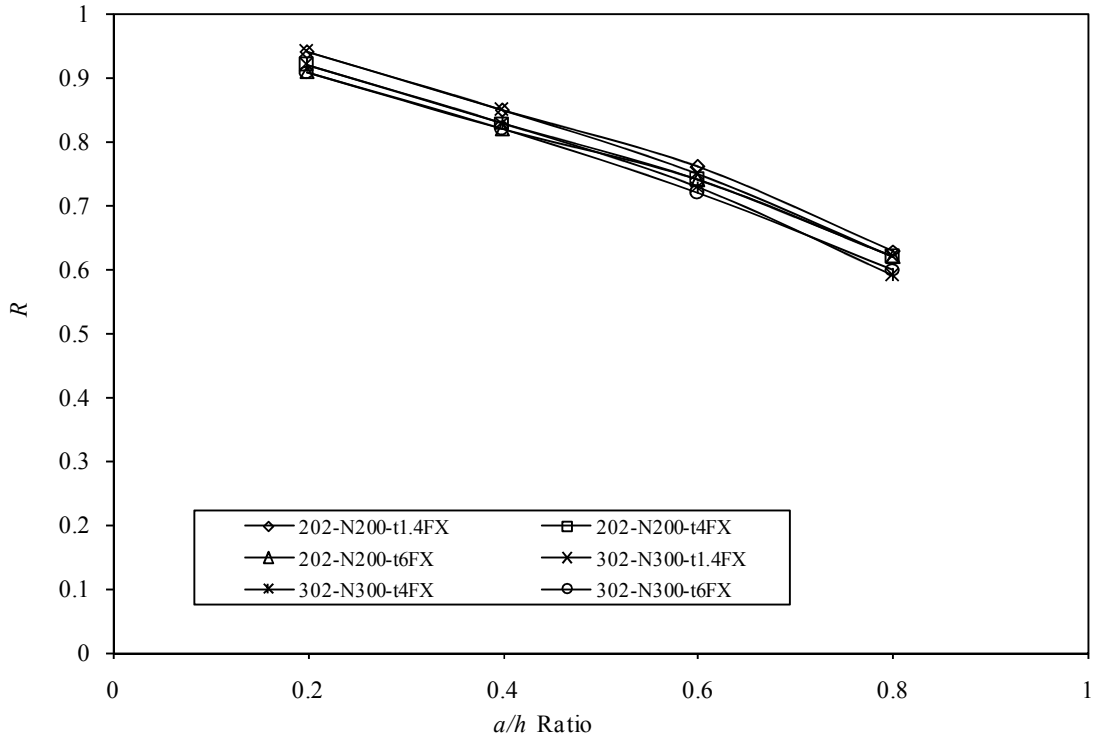

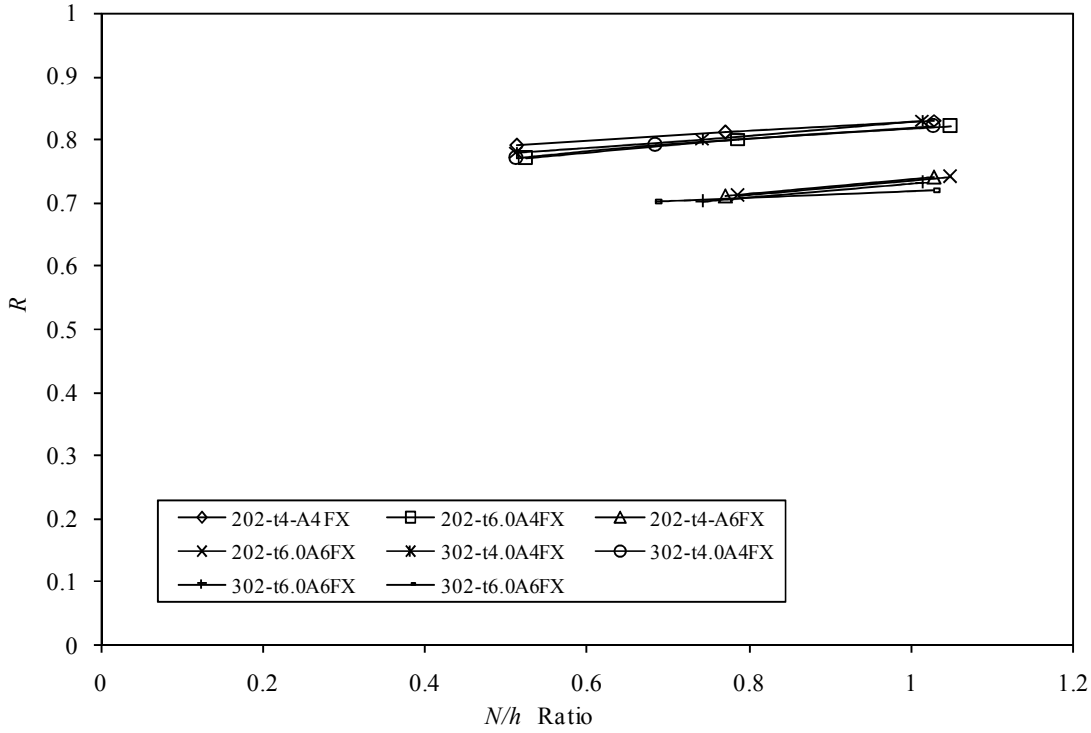

Figure 4.11 Variation in reduction factors with *a/h* and *N/h* for flanges fastened under ETF loading condition

4.7 Concluding remarks

A finite element models that incorporated the geometric and the material nonlinearities were described, and the results compared against the laboratory test results; a good agreement was obtained in terms of both strength and failure modes. Finite element model was used for the parametric study to investigate the effects of web holes and cross-section sizes on the web crippling strength of channel sections under ITF and ETF loading conditions. It was demonstrated that the main factors influencing the web crippling strength are the ratio of the hole depth to the flat depth of the web, the ratio of the distance from the edge of the bearing plates to the flat depth of the web and the ratio of the length of bearing plates to the flat depth of the web.

CHAPTER 5. DESIGN CODE PREDICTIONS

5.1 Introductory remarks

The web crippling strength predicted from the three major design codes are described in this chapter. All the current design codes provide the design rules for the specimen without any web holes. The results of the design codes were compared with the tests and finite element analysis results.

5.2 British Standard - BS 5950 Part 5:1998

The British Standard BS5950 (1998), provided a set of equations to evaluate the resistance to local failure of webs of beams at support points or points of concentrated loads without having any web holes. The web crippling strength (P_{BS}) for sections with single webs are calculated using Equation (5.1) to Equation (5.2).

a) Two opposite loads or reactions, both are near or at free end $(c < 1.5D)$:

Stiffened and unstiffened flanges:

$$P_w = t^2 k C_3 C_4 C_{12} \{1520 - 3.57(D/t)\}\{1 + 0.01(N/t)\} \qquad \text{Equation 5.1}$$

b) Two opposite loads or reactions, both are far from free end $(c > 1.5D)$:

Stiffened and unstiffened flanges:

$$P_w = t^2 k C_1 C_2 C_{12} \{4800 - 14(D/t)\}\{1 + 0.0013(N/t)\} \qquad \text{Equation 5.2}$$

where

P_W is the concentrated load resistant of a single web in Newton (N),

D is the overall web depth in millimetres (mm),

t is the web thickness in millimetres (mm),

r is the inside bend radius in millimetres (mm),

N is the actual length of the bearing in millimetres (mm),

For the case of two equal and opposite concentrated loads distributed over unequal bearing lengths, the smaller value of N should be taken, C is the distance from the end of the beam to the load or the reaction in millimetres (mm),

C_1 to C_{12} are constants with the following values:

$C_1 = (1.22 - 0.22k)$

$C_2 = (1.06 - 0.06r/t) \leq 1.0$

$C_3 = (1.33 - 0.33k)$

$C_4 = (1.15 - 0.15r/t) \leq 1.0$ but not less than 0.50

$C_5 = (1.49 - 0.53k) \geq 0.6$

$C_6 = (0.88 + 0.12m)$

$C_7 = 1 + D/t / 750$ when $D/t < 150$

$C_7 = 1.20$ when $D/t > 150$

$C_8 = 1/k$, when $D/t < 66.5$

$C_8 = (1.10 - D/t / 665)/k$ when, $D/t > 66.5$

$C_9 = (0.82 + 0.15m)$

$C_{10} = (0.98 - D/t / 865)/k$

$C_{11} = (0.64 + 0.31m)$

$C_{12} = 0.7 + 0.3 (\Theta /90)^2$

$k = p_y/228$,

where

p_y is the design strength in N/mm^2

$m = t/1.9$

Θ = Angle between plane of web and plane of bearing surface ($45° \leq \theta \leq 90°$)

The above equations apply within the following limits:

$D/t < 200$

$r/t < 6$

5.3 Eurocode 3: Part 1.3 (ENV 1993-1-3:1996)

Eurocode-3 (1996) provides a set of equations to avoid crushing, crippling or buckling of webs subjected to support reactions or other local transverse loads applied through the flanges. For a cross-section with a single unstiffened web, the local transverse resistance of the web (P_{EURO}) is determined using Equation 5.3 and Equation 5.4 provided that the cross-sections satisfy the following criteria:

$$h_w / t \le 200$$

$$r / t \le 6$$

$$45^\circ \le \phi \le 90^\circ$$

where

h_w is the web height between the midline of the flanges,

r is the internal radius of the corner ,

ϕ is the angle of the web relative to the flange (degrees)

For two opposing local transverse forces closer together than $1.5h_w$ and:

i) When $c \le 1.5h_w$ clear from a free end:

$$R_{w,Rd} = \frac{k_1 k_2 k_3 \left[6.66 - \frac{h_w / t}{64}\right]\left[1 + 0.01\frac{S_s}{t}\right] t^2 f_{yb}}{\gamma_{M1}} \qquad \text{Equation 5.3}$$

ii) When $c > 1.5h_w$ clear from a free end:

$$R_{w,Rd} = \frac{k_3 k_4 k_5 \left[21.0 - \frac{h_w / t}{16.3}\right]\left[1 + 0.0013\frac{S_s}{t}\right] t^2 f_{yb}}{\gamma_{M1}} \qquad \text{Equation 5.4}$$

where

c is the distance from loading to the closest end of the beam.

$k_1 = (1.33\text{-}0.33k)$

$k_2 = (1.15\text{-}0.15r/t)$, but $k_2 \ge 0.5$ and $k_2 \le 1.0$

$k_3 = 0.7+0.3\,(\phi/90)^2$

$k_4 = (1.22\text{-}0.22k)$

$k_5 = (1.06\text{-}0.06r/t)$ but $k_5 \le 1.0$

$k = f_{yb}/228$ (f_{yb} in N/mm^2)

S_s is the actual length of bearing.

5.4 North American Specification

North American Cold-formed steel specification NAS (2001) provides Equation 5.5. Using this the nominal web crippling strength (P_{AISI}) of members without opening in the webs. Coefficient of this equation values are given into Table 5.1.

$$P_n = Ct^2 F_y \sin\theta \left(1 - C_R\sqrt{\frac{R}{t}}\right)\left(1 - C_N\sqrt{\frac{N}{t}}\right)\left(1 - C_h\sqrt{\frac{h}{t}}\right) \qquad \text{Equation 5.5}$$

where

C is the coefficient,

C_R is the inside corner radius coefficient,

C_N is the bearing length coefficient,

C_h is the web slenderness coefficient,

F_y is the design strength,

h is the flat dimension of the web measured in plane of web,

N is the bearing length [3/4 in.(19 mm) minimum],

R is the inside bend radius, t is the web thickness,

Θ is the angle between plane of the web and plane of bearing surface, $45° \le \theta \le 90°$.

In this specification, coefficients are separated according to the flange fastened and unfastened to the support with stiffened or partially stiffened flanges condition.

Table 5.1 Web crippling design rules coefficients for single web channel section in NAS

Supports and Flange Conditions		Load Cases		C	C_R	C_N	C_h	USA and Mexico		Canada LSD φ_W	Limits
								ASD Ω_W	LRFD φ_W		
Fastened to Support	Stiffened or Partially Stiffened Flanges	Two-Flange or Reaction	End	7.5	0.08	0.12	0.048	1.75	0.85	0.75	$R/t \leq 12$
			Interior	20	0.10	0.08	0.031	1.75	0.85	0.75	$R/t \leq 12$
Unfastened	Stiffened or Partially Stiffened Flanges	Two-Flange or Reaction	End	13	0.32	0.05	0.04	1.65	0.90	0.80	$R/t \leq 3$
			Interior	24	0.52	0.15	0.001	1.90	0.80	0.65	

Note :

(1) The above coefficients apply when $h/t \leq 200$, $N/t \leq 210$, $N/t \leq 2.0$ and $\theta = 90^{\circ}$

(2) For interior-two-flange loading or reaction of members having flanges fastened to the support, the distance from the edge of bearing to the end of the member shall be extended at least 2.5h. For unfastened cases, the distance from the edge of bearing to the end of the member shall be extended at least 1.5h.

5.5 Comparison of results with current design strengths

The web crippling strength predicted from test and FEA results were compared with the web crippling strength obtained from design codes. According to Baehre and Schuster (2000), NAS specification design expressions have section parameters ranges. For the flanges fastened to the support specimen thicknesses ranged from 1.16 mm to 1.45 mm and yield stress ranged 323 MPa to 448 MPa. For the flanges unfastened to the support specimen thicknesses ranged from 1.194 mm to 1.326 mm and yield stress ranged 301.8 MPa to 324.6 MPa. However, it should be noted, the above range of specimens were considered for the results comparison.

In the case of flanges unfastened, Table 5.2 and Table 5.3 show the comparison of web crippling strength with design strength for ETF and ITF loading condition, respectively. The NAS specification design strength was not considered due to the r_i/t ratio limit was greater than 3. In the British standard comparison, the mean values of ratio are 0.97 and 0.87 with the

corresponding coefficients of variation (COV) of 0.08 and 0.06, respectively. Euro code comparison, the mean values of ratio are 0.97 and 0.85 with the corresponding coefficients of variation (COV) of 0.08 and 0.06, respectively.

Table 5.2 Comparison of web crippling strength with design strength for flanges unfastened under ETF loading condition.

Specimen	Web slenderness	Bearing length ratio	Bearing length ratio	Inside bend radius ratio	Failure load (P_{EXP} and P_{FEA})	Web crippling strength predicted from Current design codes			Comparison		
	h/t	N/t	N/h	ri/t	P (kN)	P_{BS} (kN)	$P_{euro.}$ (kN)	P_{NAS} (kN)	P/P_{BS}	$P/P_{euro.}$	P/P_{NAS}
ETF142x60x13-t1.3N30A0FR	113.3	24.2	0.2	3.8	1.7	1.6	1.6	R/t ≤3	1.02	1.02	R/t ≤3
ETF142x60x13-t1.3N60A0FR	113.3	48.4	0.4	3.8	2.0	2.0	2.0	R/t ≤3	0.99	0.99	R/t ≤3
ETF142x60x13-t1.3N90A0FR	113.3	72.6	0.6	3.8	2.2	2.3	2.3	R/t ≤3	0.97	0.97	R/t ≤3
ETF142x60x13-t1.3N120A0FR	113.3	96.8	0.9	3.8	2.4	2.6	2.6	R/t ≤3	0.90	0.90	R/t ≤3
ETF172x65x13-t1.3N32.5A0FR	134.0	25.6	0.2	3.9	1.7	1.5	1.5	R/t ≤3	1.10	1.10	R/t ≤3
ETF172x65x13-t1.3N65A0FR	134.0	51.2	0.4	3.9	1.9	1.9	1.9	R/t ≤3	1.01	1.01	R/t ≤3
ETF172x65x13-t1.3N120A0FR	134.0	94.5	0.7	3.9	2.4	2.4	2.4	R/t ≤3	0.99	0.99	R/t ≤3
ETF202x65x13-t1.4N32.5A0FR	137.4	22.4	0.2	3.4	2.0	2.2	2.2	R/t ≤3	0.89	0.89	R/t ≤3
ETF202x65x13-t1.4N65A0FR	137.4	44.8	0.3	3.4	2.4	2.6	2.6	R/t ≤3	0.91	0.91	R/t ≤3
ETF202x65x13-t1.4N120A0FR	137.4	82.8	0.6	3.4	2.7	3.3	3.3	R/t ≤3	0.82	0.82	R/t ≤3
ETF202x65x13-t1.4N100A0FR	142.3	71.4	0.5	3.6	2.9	2.8	2.8	R/t ≤3	1.06	1.06	R/t ≤3
ETF202x65x13-t1.4N150A0FR	142.3	107.1	0.8	3.6	3.2	3.3	3.3	R/t ≤3	0.96	0.96	R/t ≤3
ETF202x65x13-t1.4N200A0FR	142.3	142.9	1.0	3.6	3.9	3.9	3.9	R/t ≤3	0.99	0.99	R/t ≤3
Mean									0.97	0.97	
COV									0.08	0.08	

Table 5.3 Comparison of web crippling strength with design strength for flanges unfastened under ITF loading condition.

Specimen	Web slenderness	Bearing length ratio	Bearing length ratio	Inside bend radius ratio	Failure load (P_{EXP} and P_{FEA})	Web crippling strength predicted from Current design codes			Comparison		
	h/t	N/t	N/h	ri/t	P (kN)	P_{BS} (kN)	$P_{euro.}$ (kN)	P_{NAS} (kN)	P/P_{BS}	$P/P_{euro.}$	P/P_{NAS}
ITF142x60x13-t1.3N30A0FR	113.3	24.2	0.2	3.8	5.6	6.6	6.7	R/t ≤3	0.85	0.83	R/t ≤3
ITF142x60x13-t1.3N60A0FR	113.3	48.4	0.4	3.8	6.0	6.8	6.9	R/t ≤3	0.88	0.86	R/t ≤3
ITF142x60x13-t1.3N90A0FR	113.3	72.6	0.6	3.8	6.0	7.0	7.2	R/t ≤3	0.86	0.84	R/t ≤3
ITF142x60x13-t1.3N120A0FR	113.3	96.8	0.9	3.8	6.3	7.2	7.4	R/t ≤3	0.88	0.86	R/t ≤3
ITF172x65x13-t1.3N32.5A0FR	134.0	25.6	0.2	3.9	5.7	6.6	6.8	R/t ≤3	0.86	0.84	R/t ≤3
ITF172x65x13-t1.3N65A0FR	134.0	51.2	0.4	3.9	6.3	6.8	7.0	R/t ≤3	0.92	0.90	R/t ≤3
ITF172x65x13-t1.3N120A0FR	134.0	94.5	0.7	3.9	7.1	7.2	7.4	R/t ≤3	0.98	0.96	R/t ≤3
ITF202x65x13-t1.4N32.5A0FR	137.4	22.4	0.2	3.4	6.8	8.7	8.9	R/t ≤3	0.78	0.77	R/t ≤3
ITF202x65x13-t1.4N65A0FR	137.4	44.8	0.3	3.4	7.4	8.9	9.1	R/t ≤3	0.83	0.81	R/t ≤3
ITF202x65x13-t1.4N150A0FR	137.4	103.4	0.8	3.4	8.4	9.6	9.8	R/t ≤3	0.88	0.86	R/t ≤3
Mean									0.87	0.85	
COV									0.06	0.06	

In the case of flanges fastened, Table 5.4 and Table 5.5 show the comparison of web crippling strength with design strength for ETF and ITF loading condition, respectively. British standard and Eurocode provide better web crippling strength predictions for flanges unfastened over flanges fastened mode. Both design codes underestimate the web crippling strength about 32% for the flanges fastened to the support case. For the NAS specification comparison, the mean values of ratio are 0.86 and 0.70 with the corresponding coefficients of variation (COV) of 0.11 and 0.03, respectively.

Table 5.4 Comparison of web crippling strength with design strength for flanges fastened under ETF loading condition

Specimen	Web slenderness	Bearing length ratio	Bearing length ratio	Inside bend radius ratio	Failure load (P_{EXP} and P_{FEA})	Web crippling strength predicted from Current design codes			Comparison		
	h/t	N/t	N/h	ri/t	P (kN)	P_{BS} (kN)	$P_{euro.}$ (kN)	P_{NAS} (kN)	P/P_{BS}	$P/P_{euro.}$	P/P_{NAS}
ETF142x60x13-t1.3N30A0FX	113.3	24.2	0.2	3.8	3.0	1.6	1.6	3.44	1.80	1.80	0.86
ETF142x60x13-t1.3N60A0FX	113.3	48.4	0.4	3.8	3.3	2.0	2.0	3.97	1.69	1.69	0.84
ETF142x60x13-t1.3N90A0FX	113.3	72.6	0.6	3.8	3.8	2.3	2.3	4.38	1.64	1.64	0.86
ETF142x60x13-t1.3N120A0FX	113.3	96.8	0.9	3.8	4.1	2.6	2.6	4.72	1.56	1.56	0.86
ETF172x65x13-t1.3N32.5A0FX	134.0	25.6	0.2	3.9	2.9	1.5	1.5	3.88	1.87	1.87	0.74
ETF172x65x13-t1.3N65A0FX	134.0	51.2	0.4	3.9	3.3	1.9	1.9	4.49	1.79	1.79	0.74
ETF172x65x13-t1.3N120A0FX	134.0	94.5	0.7	3.9	4.2	2.4	2.4	5.23	1.74	1.75	0.80
ETF202x65x13-t1.4N32.5A0FX	137.4	22.4	0.2	3.4	3.6	2.2	2.2	4.72	1.64	1.64	0.77
ETF202x65x13-t1.4N65A0FX	137.4	44.8	0.3	3.4	4.4	2.6	2.6	5.43	1.67	1.67	0.80
ETF202x65x13-t1.4N120A0FX	137.4	82.8	0.6	3.4	5.2	3.3	3.3	6.30	1.58	1.58	0.83
ETF202x65x13-t1.4N150A0FX	137.4	103.4	0.8	3.4	5.8	3.7	3.7	6.69	1.58	1.58	0.87
ETF202x65x13-t1.4N100A0FX	142.3	71.4	0.5	3.6	5.4	2.8	2.8	5.51	1.96	1.96	0.98
ETF202x65x13-t1.4N150A0FX	142.3	107.1	0.8	3.6	6.0	3.3	3.3	6.13	1.80	1.80	0.98
ETF202x65x13-t1.4N200A0FX	142.3	142.9	1.0	3.6	7.2	3.9	3.9	6.66	1.84	1.84	1.08
Mean									1.73	1.73	0.86
COV									0.07	0.07	0.11

Table 5.5 Comparison of web crippling strength with design strength for flanges fastened under ITF loading condition.

Specimen	Web slenderness	Bearing length ratio	Bearing length ratio	Inside bend radius ratio	Failure load (P_{EXP} and P_{FEA})	Web crippling strength predicted from Current design codes			Comparison		
	h/t	N/t	N/h	ri/t	P (kN)	P_{BS} (kN)	$P_{euro.}$ (kN)	P_{NAS} (kN)	P/P_{BS}	$P/P_{euro.}$	P/P_{NAS}
ITF142x60x13-t1.3N30A0FX	113.3	24.2	0.2	3.8	7.5	6.6	6.7	10.51	1.14	1.11	0.71
ITF142x60x13-t1.3N60A0FX	113.3	48.4	0.4	3.8	8.1	6.8	6.9	11.74	1.19	1.17	0.69
ITF142x60x13-t1.3N90A0FX	113.3	72.6	0.6	3.8	9.0	7.0	7.2	12.68	1.28	1.25	0.71
ITF142x60x13-t1.3N120A0FX	113.3	96.8	0.9	3.8	9.4	7.2	7.4	13.48	1.31	1.28	0.70
ITF172x65x13-t1.3N32.5A0FX	134.0	25.6	0.2	3.9	8.9	6.6	6.8	12.43	1.34	1.31	0.72
ITF172x65x13-t1.3N65A0FX	134.0	51.2	0.4	3.9	9.5	6.8	7.0	13.92	1.39	1.36	0.68
ITF172x65x13-t1.3N120A0FX	134.0	94.5	0.7	3.9	10.7	7.2	7.4	15.74	1.49	1.45	0.68
ITF202x65x13-t1.4N32.5A0FX	137.4	22.4	0.2	3.4	11.5	8.7	8.9	15.42	1.33	1.30	0.75
ITF202x65x13-t1.4N65A0FX	137.4	44.8	0.3	3.4	11.7	8.9	9.1	17.17	1.31	1.28	0.68
ITF202x65x13-t1.4N150A0FX	137.4	103.4	0.8	3.4	13.5	9.6	9.8	20.28	1.41	1.38	0.67
Mean									1.32	1.29	0.70
COV									0.08	0.08	0.03

5.6 Concluding remarks

As mentioned earlier, the current cold-formed design standards do not provide design rules for cold-formed steels with web holes subjected to web crippling under ITF and ETF loading conditions. The web crippling strength without holes predicted from test and FEA results were compared with the web crippling strength obtained from design codes. British standard and Eurocode provides better web crippling strength predictions for flanges unfastened over flanges fastened mode. It is noted that for the unfastened case agreement is very good, however, for the fastened case, the comparison is less reliable due to the post buckling strength effect was not fully considered into design codes.

CHAPTER 6. DESIGN RECOMMENDATIONS

6.1 Introductory remarks

Design recommendations in the form of web crippling strength reduction factors are proposed in this chapter. Comparing the failure loads of the channel sections having web holes with the sections without web holes has been already shown in chapter 4 section 4.3. It can be seen that, as expected, the failure load decreases as the size of the web holes increases and the failure load increases as the distance of the web holes increases. For each series of specimens, the web crippling strengths of the sections without the web holes were obtained. Thus, the ratio of the web crippling strengths for sections with the web holes divided by the sections without the web holes, which is the strength reduction factor (R), was used to quantify the degrading influence of the web holes on the web crippling strengths under the interior-two-flange loading condition. According to Zhou and Young (2010) and LaBoube et al. (1999) , evaluation of the experimental and the numerical results shows that the ratios *a/h*, *x/h* and *N/h* are the primary parameters influencing the web crippling behaviour of the sections with web holes. Therefore, based on both the experimental and the numerical results obtained from this study, (R_p) are proposed using linear regression analysis. Statistical data analysis software Origin Lab (OriginLab (2011)) was used for the regression analysis to develop the reduction factor equation.

6.2 Reliability analysis

The reliability of the cold-formed steel section design rules is evaluated using reliability analysis. The reliability index (β) is a relative measure of the safety of the design. The basic equation used to calculate β is define as follows:

$$\beta = \frac{\ln(R_m / Q_m)}{\sqrt{V_R^{\,2} + V_Q^{\,2}}} \qquad \text{Equation 6.1}$$

$$R_m = M_m \times F_m \times P_m \times R_n \qquad \text{Equation 6.2}$$

$$V_R = \sqrt{V_M{}^2 + V_F{}^2 + C_P \times V_P{}^2} \qquad \text{Equation 6.3}$$

Where,

R_m = The mean member resistance

V_R = The corresponding coefficient of variation

R_n = Equation for nominal resistance

Q_m = Mean load effect

V_Q = Coefficient of variation of load effect

R_n = Equation for nominal resistance

M_m ,F_m, P_m ,V_M, V_F, and V_P = Mean values and coefficients of variation for material properties, fabrication variables and design equations.

A target reliability index of 2.5 for cold-formed steel structural members is recommended as a lower limit in the NAS Specification NAS (2001). The design rules are considered to be reliable if the reliability index is greater than or equal to 2.5. The correction factor C_P was used to account for the influence due to a small number of test. The total load values used in the reliability study are based on a combination of dead load (DL) and live loads (LL) specified in the applicable design standards. The load combination of 1.2DL + 1.6LL as specified in the American Society of Civil Engineers Standard ASCE (2005) was used in the reliability analysis, where DL is the dead load and LL is the live load. Accordingly, the safety index may be given as

$$\beta = \frac{\ln[(M_m \times F_m \times P_m)/(0.657\phi)]}{\sqrt{V_M{}^2 + V_F{}^2 + C_P \times V_P{}^2 + 0.21^2}} \qquad \text{Equation 6.4}$$

The statistical parameters are obtained from Table F1 of the NAS Specification NAS (2001) for compression members, where M_m = 1.10, F_m = 1.00, V_M = 0.10, and V_F = 0.05, which are the mean values and coefficients of variation for material properties and fabrication factors. In calculating the reliability index, the correction factor (c) in the NAS Specification was used. Reliability analysis is detailed in the NAS Specification NAS (2001). In the reliability analysis, a constant resistance factor (ϕ) of 0.85 was used. The design rules are considered to be reliable if the reliability index (β) is greater than the value of 2.5.

6.3 Proposed strength reduction factors for flanges unfastened under ITF loading conditions

Based on both the experimental and the numerical results obtained from this study, two strength reduction factor (R_p) are proposed based on the types of web holes using nonlinear regression analysis for flanges unfastened under the interior-two-flange loading condition.

For the Type 1 web holes:

$$R_P = 1.04 - 0.68\ (\frac{a}{h}) + 0.023\ (\frac{x}{h}) \quad \leq\ 1 \qquad \text{Equation 6.5}$$

For the Type 2 web holes:

$$R_P = 1.05 - 0.54\ (\frac{a}{h}) + 0.01\ (\frac{N}{h}) \quad \leq\ 1 \qquad \text{Equation 6.6}$$

The limits for the reduction factor Equation 6.1 and Equation 6.2 are $h/t \leq$ 156, $N/t \leq$ 84, $N/h \leq$ 0.63, $a/h \leq$ 0.8, and $\theta = 90^0$.

The values of the strength reduction factor (R) obtained from the experimental and the numerical results are compared with the values of the proposed strength reduction factor (R_p) calculated using equation (6.5) and equation (6.6), as plotted against the ratios *a/h* and *h/t* in Figure 6.1 and Figure 6.2, respectively.

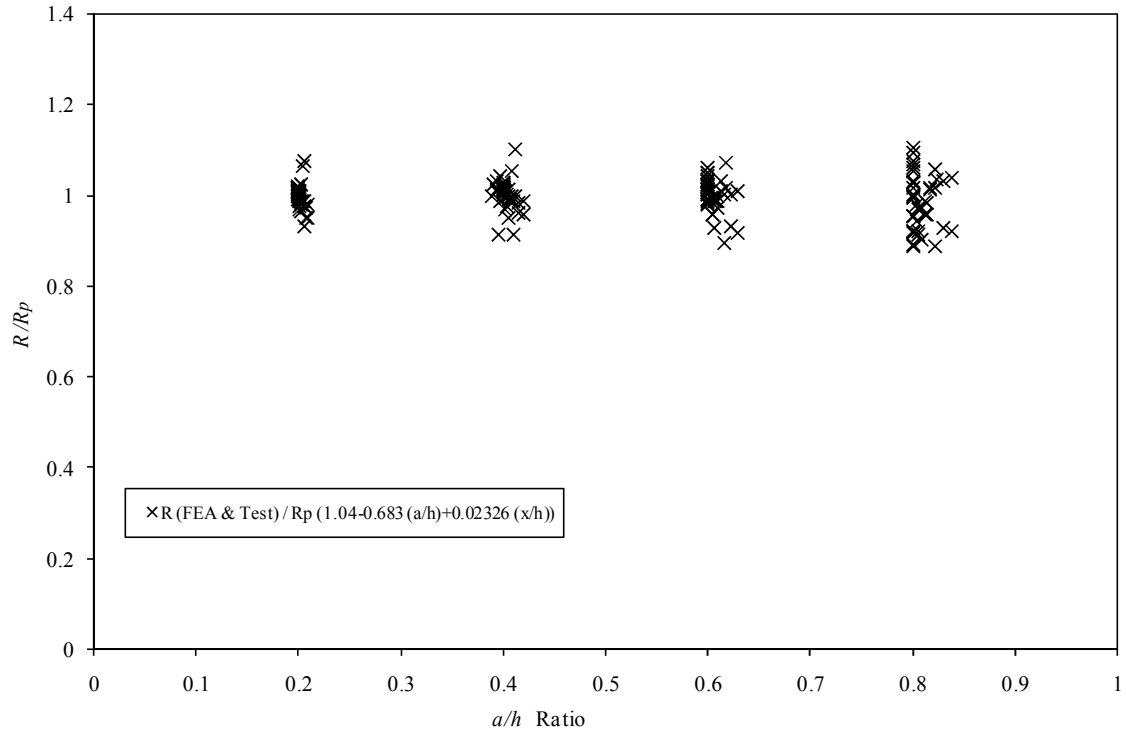

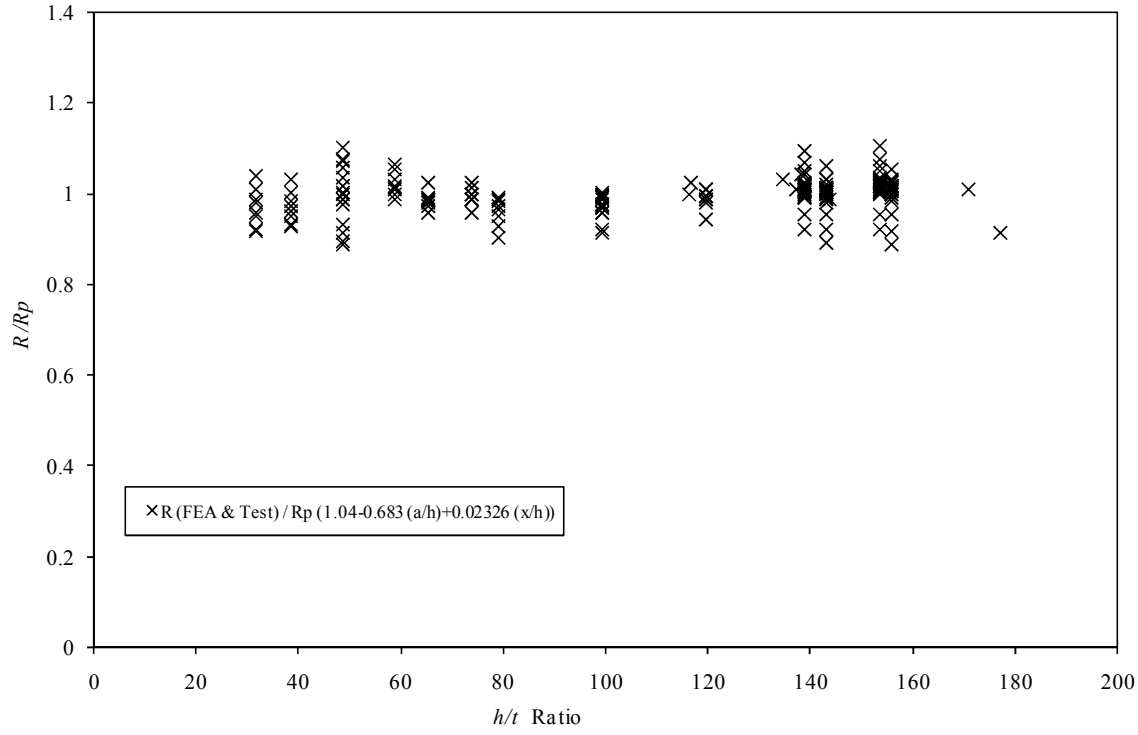

Figure 6.1 Comparison of the strength reduction factors for flanges unfastened under ITF loading condition (Type 1 holes)

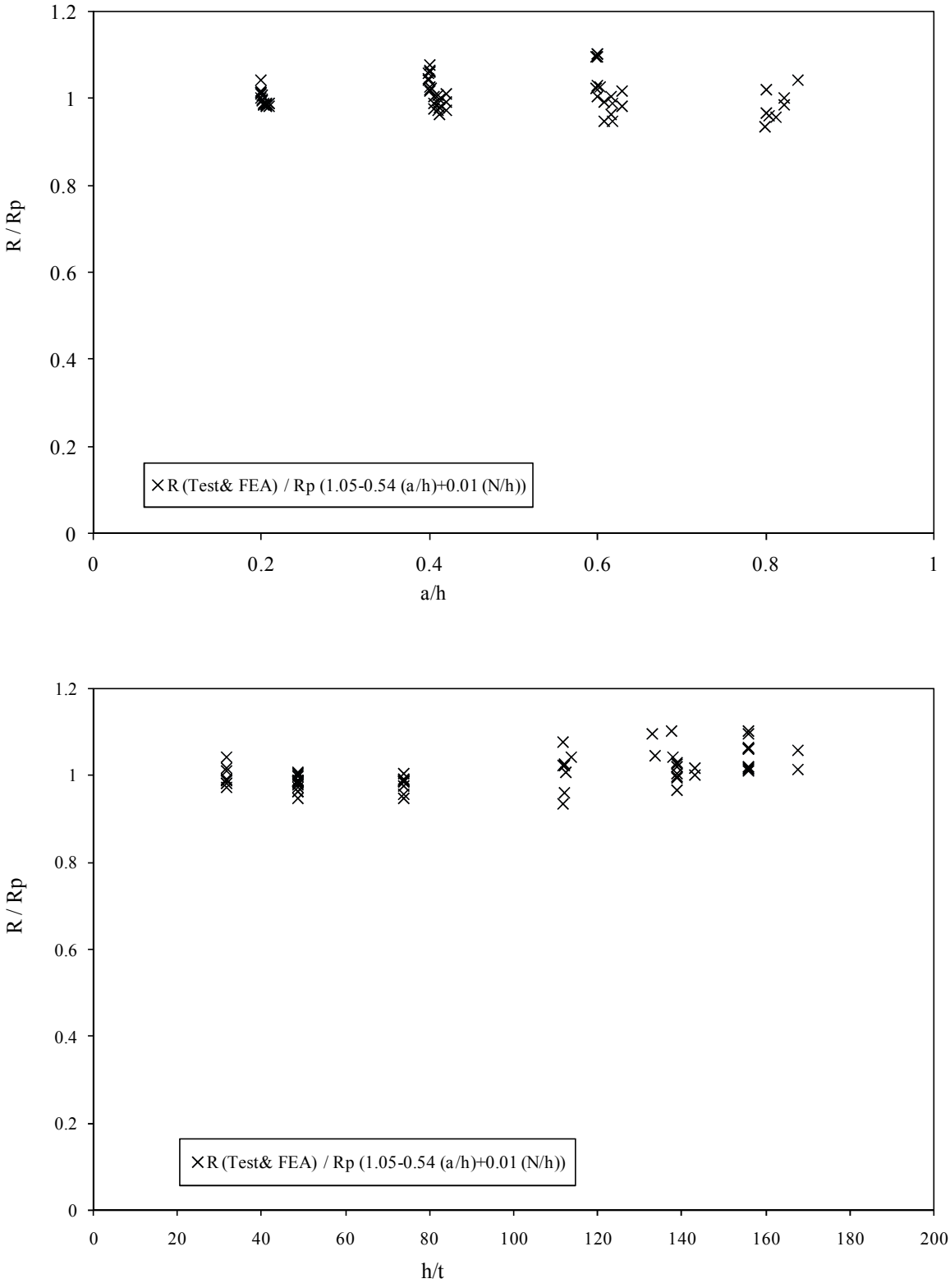

Figure 6.2 Comparison of the strength reduction factors for flanges unfastened under ITF loading condition (Type 2 holes)

As can be seen, the values of proposed reduction factor generally agreed with the experiment and the numerical results for both type of web holes. Table 6.1 and Table 6.2 summarizes a statistical analysis to define the accuracy of the proposed design equations. The mean value of the web crippling reduction factor ratio are 1.00 and 1.01 with the corresponding COV of 0.04 and 0.04, and reliability index (β) of 2.83 and 2.87 for the Type 1 web holes and Type 2 web holes, respectively. Thus, the proposed strength reduction factor equations are able to predict the influence of the web holes on the web crippling strengths of channel sections for the flanges unfastened under ITF loading condition. The comparison tables are illustrated in Appendix-D.

Table 6.1 Statistical analysis for the comparison of the strength reduction factor for flanges unfastened under ITF loading condition (Type 1 holes)

Statistical parameters	R (Test & FEA) / R_p (1.04-0.68 (a/h)+0.023 (x/h))
Mean, P_m	1.00
Coefficient of variation, V_p	0.04
Reliability index, β	2.83
Resistance factor, ϕ	0.85

Table 6.2 Statistical analysis for the comparison of the strength reduction factor for flanges unfastened under ITF loading condition (Type 2 holes)

Statistical parameters	R (Test & FEA) / R_p (1.05-0.54 (a/h)+0.01 (N/h))
Mean, P_m	1.01
Coefficient of variation, V_p	0.04
Reliability index, β	2.87
Resistance factor, ϕ	0.85

6.4 Proposed strength reduction factors for flanges fastened under ITF loading conditions

Both the experimental and the numerical results obtained from this study, two strength reduction factor (R_p) are proposed based on the types of web holes using nonlinear regression analysis for flanges unfastened under the interior-two-flange loading condition.

For the Type 1 web holes:

$$R_P = 1.00 - 0.45\ (\frac{a}{h}) + 0.09\ (\frac{x}{h}) \quad \leq\ 1 \qquad \text{Equation 6.7}$$

For the Type 2 web holes:

$$R_P = 1.01 - 0.51\ (\frac{a}{h}) + 0.06\ (\frac{N}{h}) \quad \leq\ 1 \qquad \text{Equation 6.8}$$

The limits for the reduction factor Equation 6.3 and Equation 6.4 are $h/t \leq$ 156, $N/t \leq$ 84, $N/h \leq$ 0.63, $a/h \leq$ 0.8, and $\theta = 90^0$.

The values of the strength reduction factor (R) obtained from the experimental and the numerical results are compared with the values of the proposed strength reduction factor (R_p) calculated using Equation 6.7 and Equation 6.8, as plotted against the ratios *a/h* and *h/t* in Figure 6.3 and Figure 6.4, respectively. As can be seen, the values of proposed reduction factors generally agreed with the experiment and the numerical results for both type of web holes.

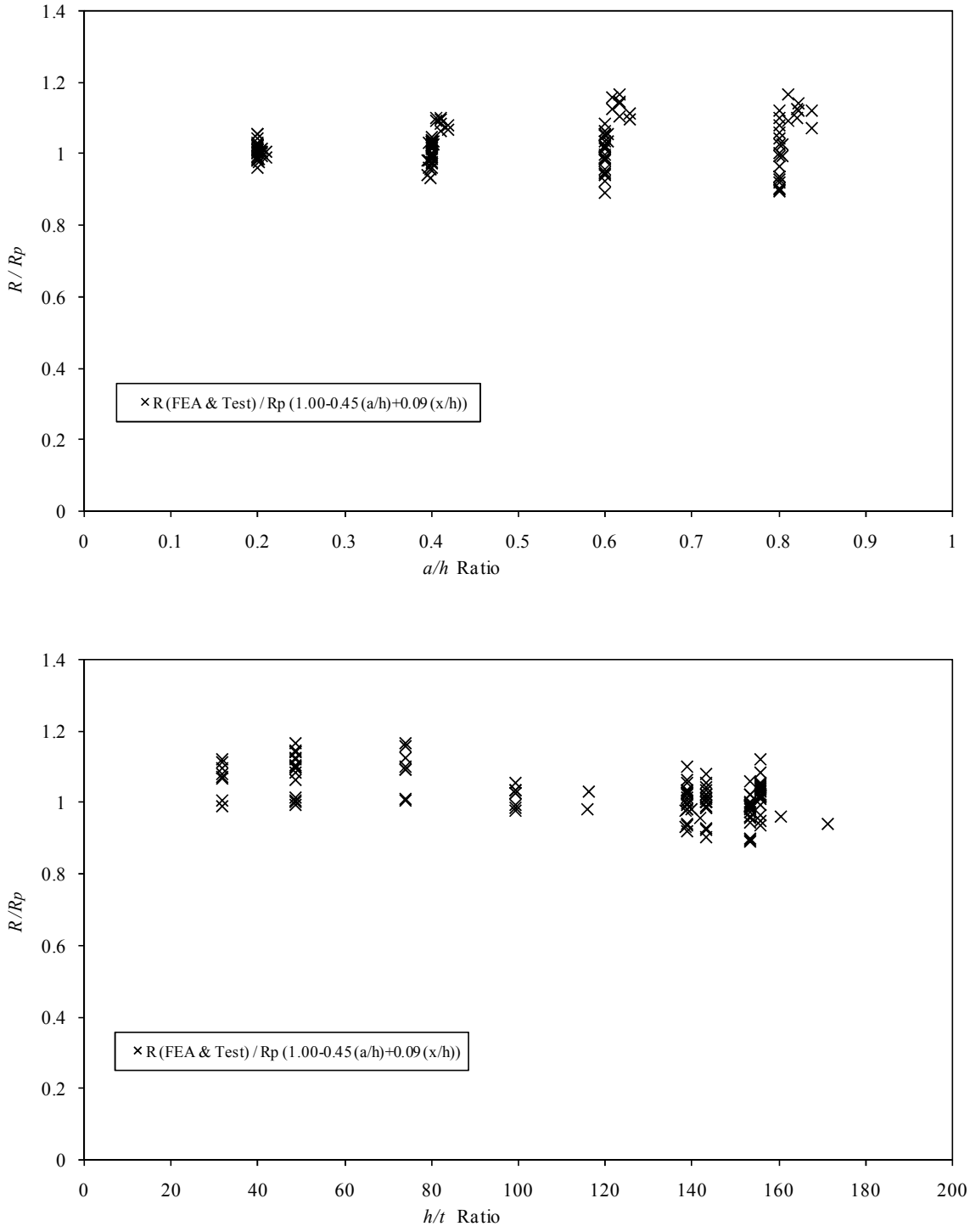

Figure 6.3 Comparison of the strength reduction factors for flanges fastened under ITF loading condition (Type 1 holes)

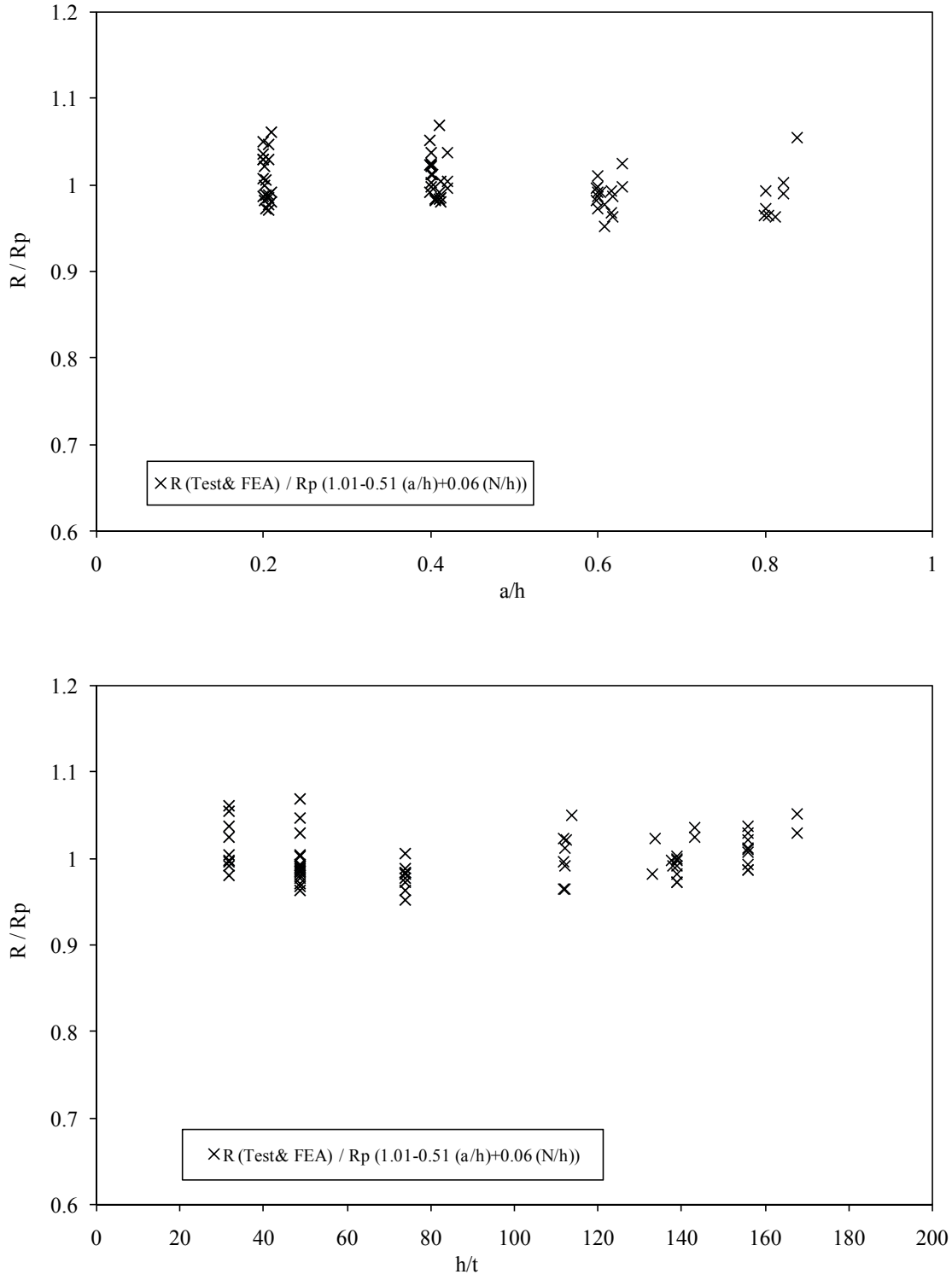

Figure 6.4 Comparison of the strength reduction factors for flanges fastened under ITF loading condition (Type 2 holes)

Table 6.3 and Table 6.4 summarizes a statistical analysis to define the accuracy of the proposed design equations. The mean value of the web crippling reduction factor ratio are 1.02 and 1.01 with the corresponding COV of 0.07 and 0.03, and reliability index (β) of 2.81 and 2.86 for the Type 1 web holes and Type 2 web holes, respectively. Thus, the proposed strength reduction factor equations are able to predict the influence of the web holes on the web crippling strengths of channel sections for the flanges unfastened under ITF loading condition. The comparison tables are illustrated in Appendix D.

Table 6.3 Statistical analysis for the comparison of the strength reduction factor for flanges fastened under ITF loading condition (Type 1 holes)

Statistical parameters	R (Test & FEA) / R_p (1.00-0.45 (a/h)+0.09 (x/h))
Mean, P_m	1.02
Coefficient of variation, V_p	0.07
Reliability index, β	2.81
Resistance factor, ϕ	0.85

Table 6.4 Statistical analysis for the comparison of the strength reduction factor for flanges fastened under ITF loading condition (Type 2 holes)

Statistical parameters	R (Test & FEA) / R_p (1.01-0.51 (a/h)+0.06 (N/h))
Mean, P_m	1.00
Coefficient of variation, V_p	0.03
Reliability index, β	2.86
Resistance factor, ϕ	0.85

6.5 Proposed strength reduction factors for flanges unfastened under ETF loading conditions

Both the experimental and the numerical results obtained from this study, two strength reduction factor (R_p) are proposed based on the types of web holes using nonlinear regression analysis for flanges unfastened under the end-two-flange loading condition.

For the Type 1 web holes:

$$R_P = 0.95 - 0.49\ (\frac{a}{h}) + 0.17\ (\frac{x}{h}) \quad \leq\ 1 \qquad \text{Equation 6.9}$$

For the Type 2 web holes:

$$R_P = 0.90 - 0.60\ (\frac{a}{h}) + 0.12\ (\frac{N}{h}) \quad \leq\ 1 \qquad \text{Equation 6.10}$$

The limits for the reduction factor Equations 6.5 and Equation 6.6 are $h/t \leq$ 156, $N/t \leq$ 84, $N/h \leq$ 0.63, $a/h \leq$ 0.8, and $\theta = 90^0$.

The values of the strength reduction factor (R) obtained from the experimental and the numerical results are compared with the values of the proposed strength reduction factor (R_p) calculated using Equation 6.9 and equation 6.10, as plotted against the ratios *a/h* and *h/t* in Figure 6.5 and Figure 6.6, respectively. As can be seen, the values of proposed reduction factors generally agreed with the experiment and the numerical results for both type of web holes.

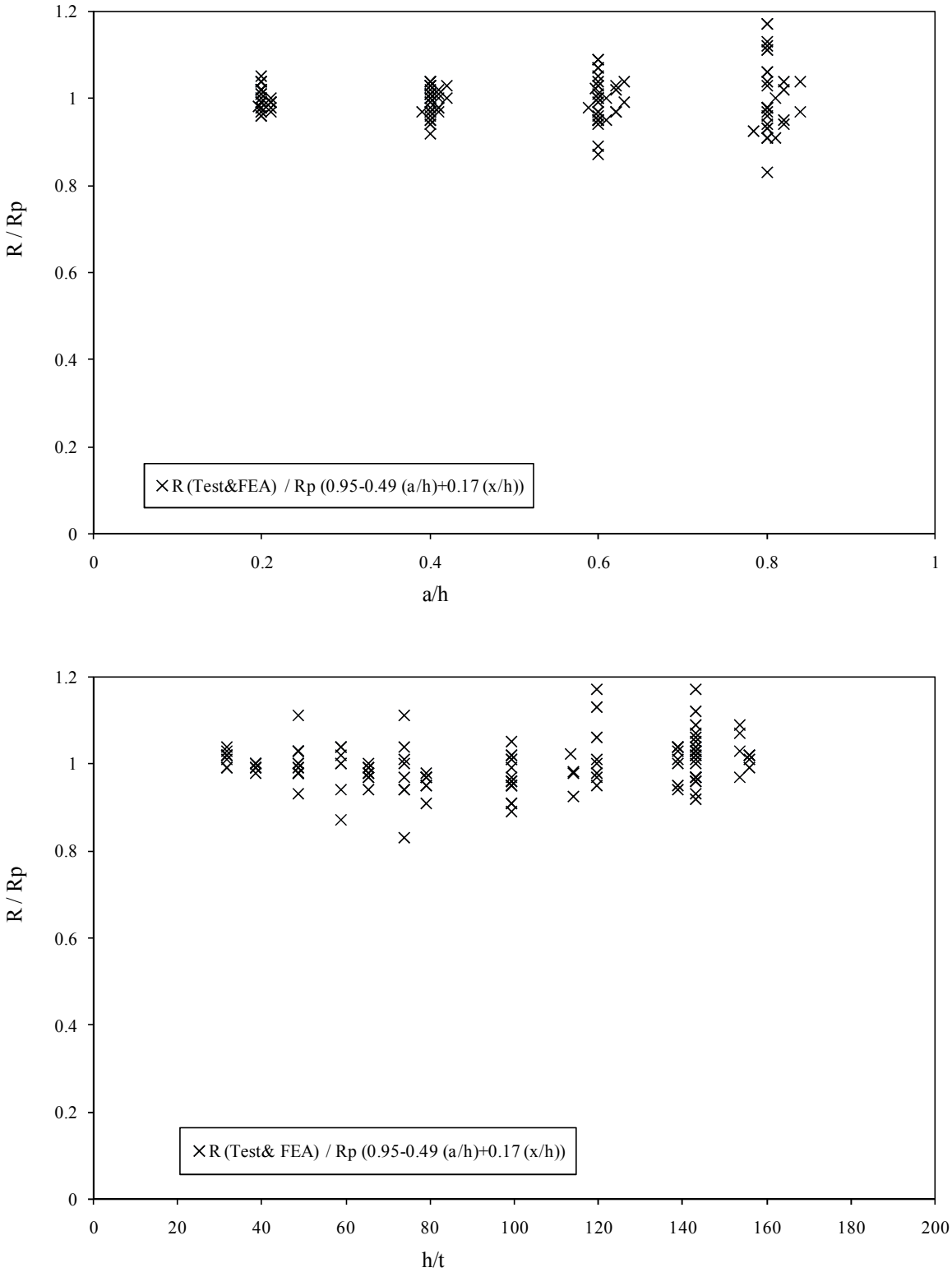

Figure 6.5 Comparison of the strength reduction factors for flanges unfastened under ETF loading condition (Type 1 holes)

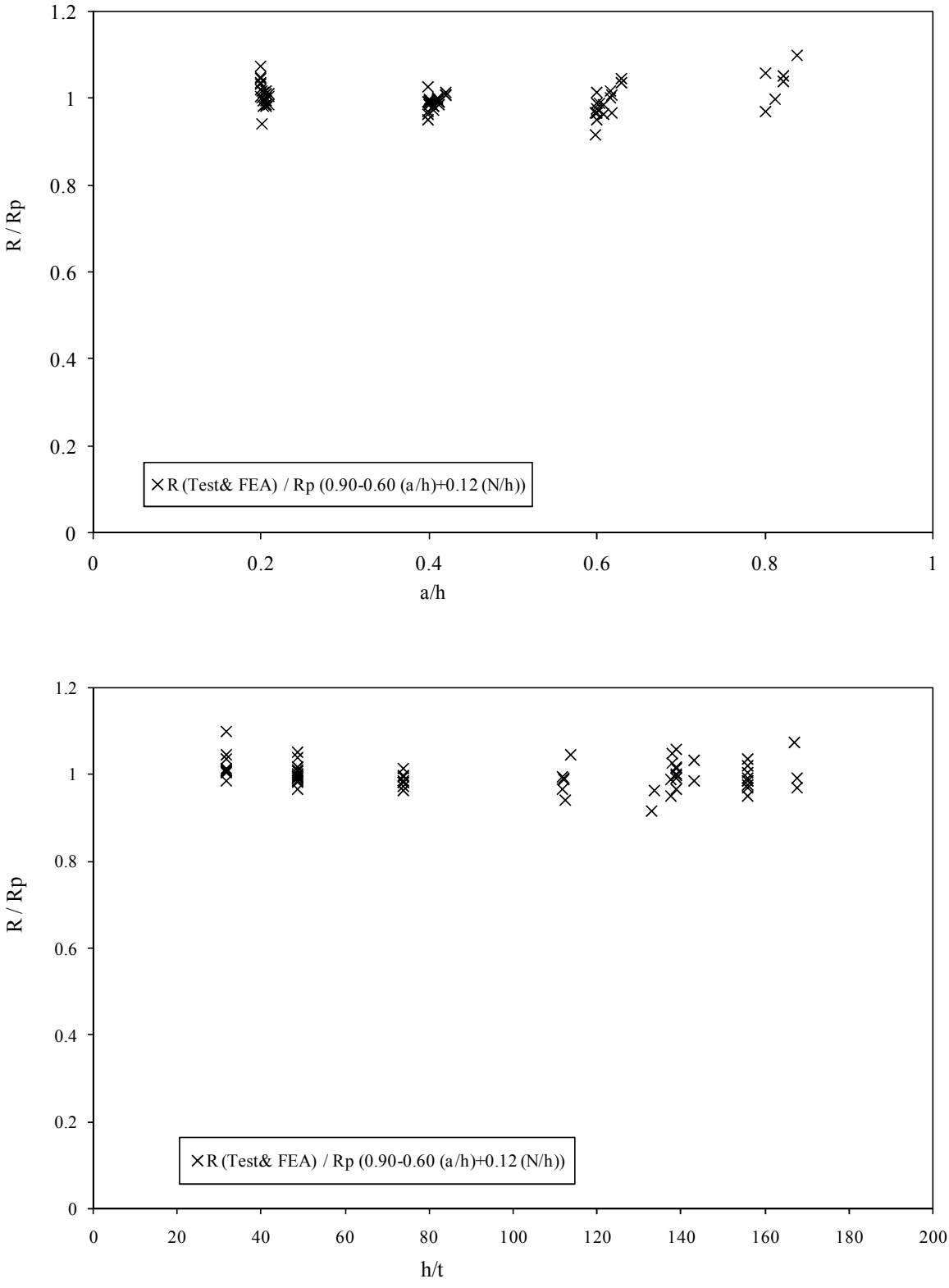

Figure 6.6 Comparison of the strength reduction factors for flanges unfastened under ETF loading condition (Type 2 holes)

Table 6.5 and Table 6.6 summarizes a statistical analysis to define the accuracy of the proposed design equations. The mean value of the web crippling reduction factor ratio are 1.00 and 1.00 with the corresponding COV of 0.05 and 0.03, and reliability index (β) of 2.80 and 2.85 for the Type 1 web holes and Type 2 web holes, respectively. Thus, the proposed strength reduction factor equations are able to predict the influence of the web holes on the web crippling strengths of channel sections for the flanges unfastened under ETF loading condition. The comparison tables are illustrated in Appendix D.

Table 6.5 Statistical analysis for the comparison of the strength reduction factor for flanges unfastened under ETF loading condition (Type 1 holes)

Statistical parameters	R (Test & FEA) / R_p (0.95-0.49 (a/h)+0.17 (x/h))
Mean, P_m	1.00
Coefficient of variation, V_p	0.05
Reliability index, β	2.80
Resistance factor, ϕ	0.85

Table 6.6 Statistical analysis for the comparison of the strength reduction factor for flanges unfastened under ETF loading condition (Type 2 holes)

Statistical parameters	R (Test & FEA) / R_p (0.90-0.60 (a/h)+0.12 (N/h))
Mean, P_m	1.00
Coefficient of variation, V_p	0.03
Reliability index, β	2.85
Resistance factor, ϕ	0.85

6.6 Proposed strength reduction factors for flanges fastened under ETF loading conditions

Both the experimental and the numerical results obtained from this study, two strength reduction factor (R_p) are proposed based on the types of web holes using nonlinear regression analysis for flanges unfastened under the end-two-flange loading condition.

For the Type 1 web holes:

$$R_P = 0.96 - 0.36\ (\frac{a}{h}) + 0.14\ (\frac{x}{h}) \quad \leq\ 1 \qquad \text{Equation 6.11}$$

For the Type 2 web holes:

$$R_P = 0.95 - 0.50\ (\frac{a}{h}) + 0.08\ (\frac{N}{h}) \quad \leq\ 1 \qquad \text{Equation 6.12}$$

The limits for the reduction factor Equation 6.7 and Equation 6.8 are $h/t \leq$ 156, $N/t \leq$ 84, $N/h \leq$ 0.63, $a/h \leq$ 0.8, and $\theta = 90^0$.

The values of the strength reduction factor (R) obtained from the experimental and the numerical results are compared with the values of the proposed strength reduction factor (R_p) calculated using equation 6.11 and equation 6.12, as plotted against the ratios *a/h* and *h/t* in Figure 6.7 and Figure 6.8, respectively. As can be seen, the values of proposed reduction factor are generally agree with the experiment and the numerical results for both type of web holes.

Table 6.7 and Table 6.8 summarizes a statistical analysis to define the accuracy of the proposed design equations. As can be seen, the values of proposed reduction factor are generally conservative and agree with the experiment and the numerical results for both type of web holes.

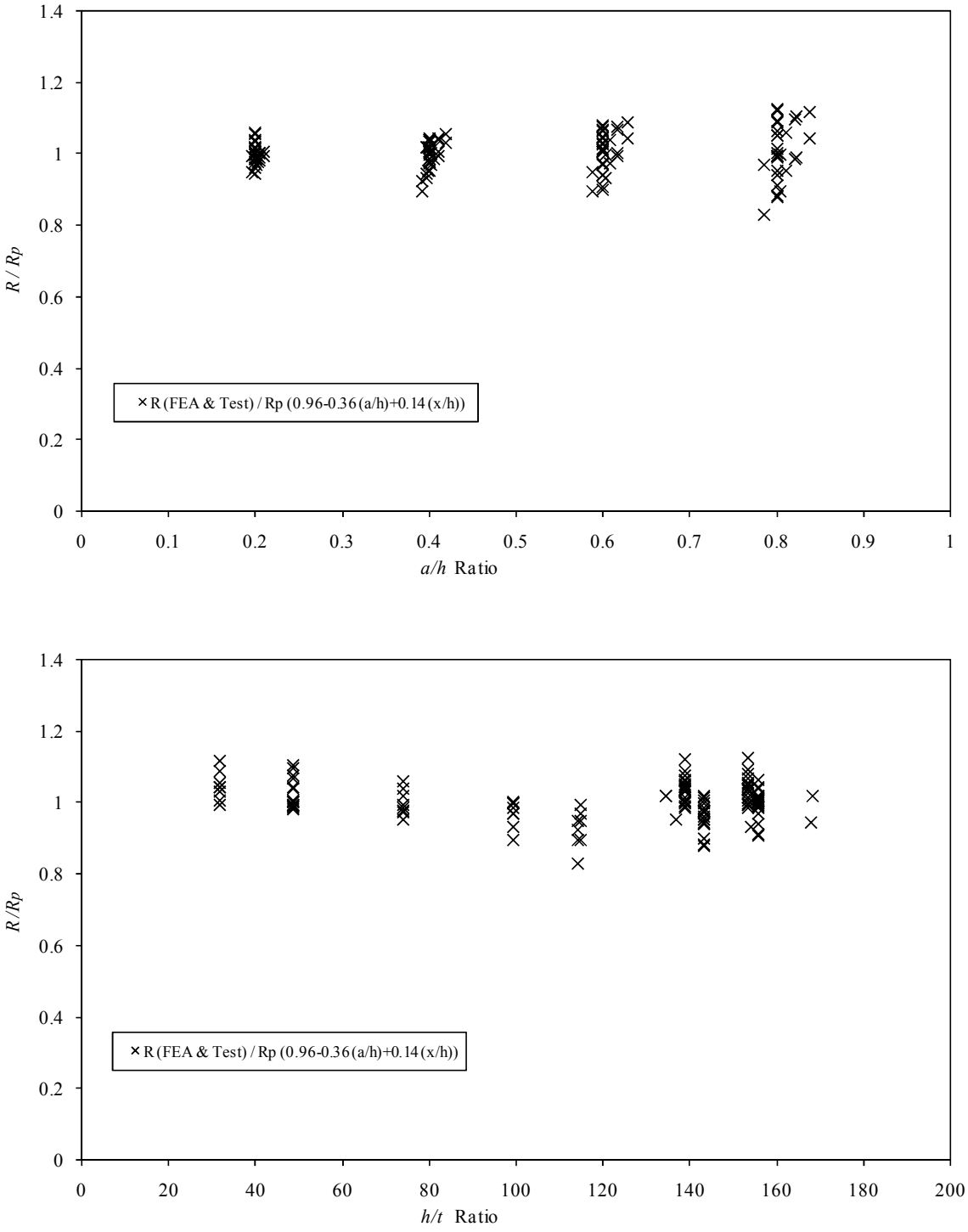

Figure 6.7 Comparison of the strength reduction factors for flanges fastened under ETF loading condition (Type 1 holes)

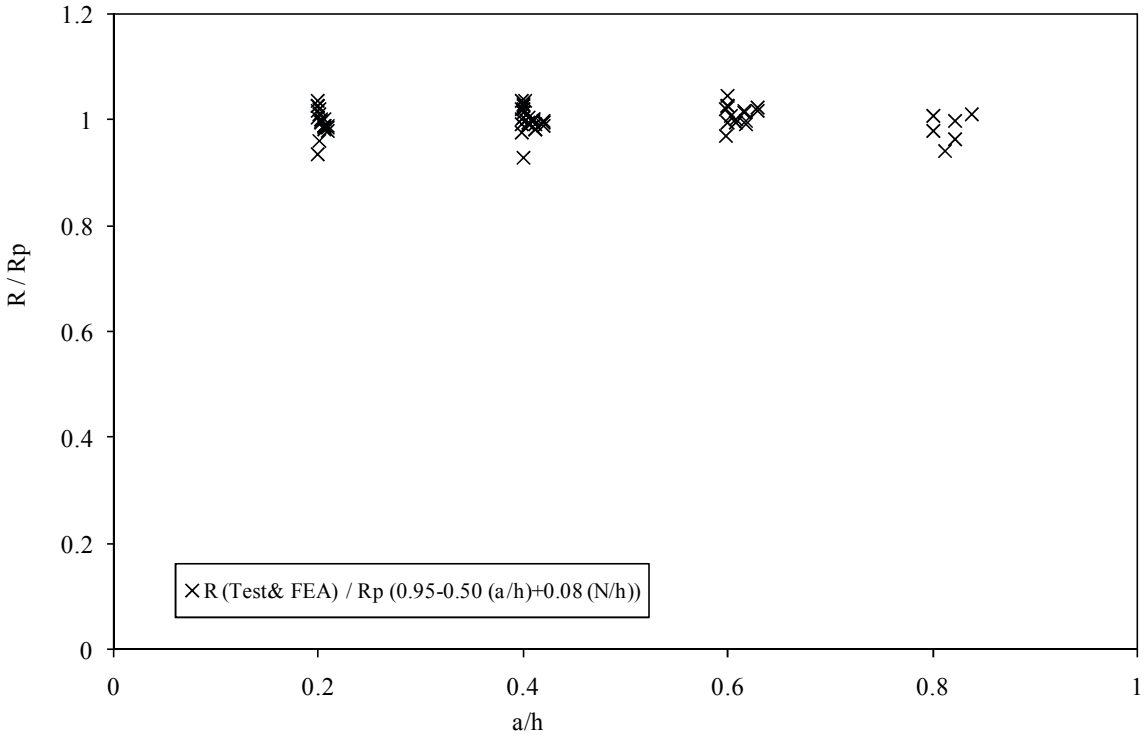

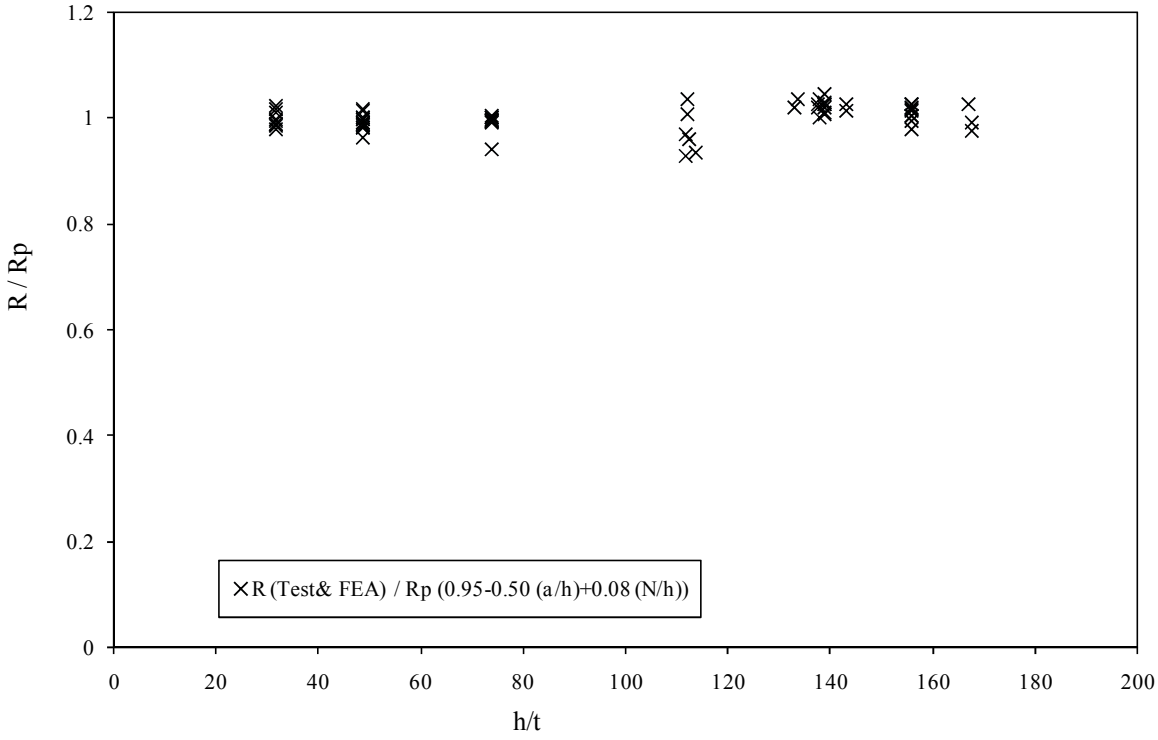

Figure 6.8 Comparison of the strength reduction factors for flanges fastened under ETF loading condition (Type 2 holes)

The mean value of the web crippling reduction factor ratio are 1.00 and 1.00 with the corresponding COV of 0.06 and 0.02, and reliability index (β) of 2.80 and 2.86 for the Type 1 web holes and Type 2 web holes, respectively. Thus, the proposed strength reduction factor equations are able to predict the influence of the web holes on the web crippling strengths of channel sections for the flanges unfastened under ETF loading condition. The comparison tables and Statistical data analysis reports are illustrated in Appendix D.

Table 6.7 Statistical analysis for the comparison of the strength reduction factor for flanges fastened under ETF loading condition (Type 1 holes)

Statistical parameters	R (Test & FEA) / R_p (0.96-0.36 (a/h)+0.14 (x/h))
Mean, P_m	1.00
Coefficient of variation, V_p	0.06
Reliability index, β	2.80
Resistance factor, ϕ	0.85

Table 6.8 Statistical analysis for the comparison of the strength reduction factor for flanges fastened under ETF loading condition (Type 2 holes)

Statistical parameters	R (Test & FEA) / R_p (0.95-0.50 (a/h)+0.08 (N/h))
Mean, P_m	1.00
Coefficient of variation, V_p	0.02
Reliability index, β	2.85
Resistance factor, ϕ	0.85

6.7 Concluding remarks

Based on the available test data obtained from experimental and numerical investigation, web crippling strength reduction factor equations were proposed for the ITF and ETF loading conditions for both the cases of flanges unfastened and fastened to the support. Reliability analysis was performed to evaluate the reliability of the proposed strength reduction factors. It is shown that the proposed strength reduction factors are generally agree well with the experimental and the numerical results.

CHAPTER 7. CONCLUSION

7.1 Introductory remarks

The principal objective of this research was to investigate the effect of web holes on web crippling strength of cold-formed steel sections. Both experimental and finite element analyses were conducted to examine the web crippling strength and strength reduction due to the presence of web holes into the section. Finally, design recommendations were proposed based on the results. The conclusion and future recommendation are summarized in this chapter.

7.2 Experimental investigation

The experimental investigations of lipped channel sections with circular web holes subjected to web crippling have been presented. A total 181 of tests were conducted on lipped channel sections with and without web holes subjected to the end-one-flange (ETF) and interior-two-flange (ITF) loading condition. The cases of the flanges of the channel sections being fastened and unfastened to the bearing plates also considered. The web slenderness value of the specimens ranged from 116 to 176 and the thickness ranged from 1.3 to 2.0 mm. Different lengths of bearing plates were used. The diameter of the web holes was varied from 40 to 240 mm in order to investigate the influence of the web holes on the web crippling strength. Web holes centred beneath the bearing plates and with offset distance to the bearing plates were considered into the web. Tensile coupon tests were carried out to determine the material properties of the channel specimens.

7.3 Numerical investigation

A finite element models that incorporated the geometric and the material nonlinearities has been developed and verified against the experimental results. Finite element program ANSYS was used throughout the numerical investigation. The finite element models were shown to be able to closely predict the web crippling behaviour of the channel sections, both

with and without circular web holes. A good arrangement were achieved between the experimental and finite element results for both the web crippling strength and the failure mode. Thereafter, a parametric study was carried out to study the effects of the different sizes of the cross- sections and the web hole on the web crippling strengths of the channel sections. A total 632 models were analysis and it was shown that the ratios *a/h*, *x/h and N/h* were the primary parametric relationships influencing the web crippling behaviour of the sections with the web holes .

7.4 Design recommendations

An extensive statistical analysis of web crippling for cold-formed steel sections with web holes was carried out using 181 test results and 632 numerical results. The web crippling strength without holes predicted from test and FEA results were compared with the web crippling strength obtained from design codes. A total eight web crippling strength reduction factor equations were proposed for the ETF and ITF loading conditions for both the cases of flanges unfastened and fastened to the support. It is shown that the proposed strength reduction factors are generally conservative and agree well with the experimental and the numerical results. These equations may be applied to the existing web crippling prediction equation contained in the design specification.

7.5 Suggestion for further study

Future research is require in order to understand and improve the web crippling behaviour considering web holes. The following gives suggestion for future research given below

1. Current design code provide reduction factor equations for IOF and EOF loading condition. This equation limited with flange unfastened to the support and web holes considered with offset distance to the bearing plates. Since fastened sections represent actual field practice, the author recommends that more research can be carried out considering web hole centred

beneath the bearing plates and flanges fastened to the bearing plates under IOF and EOF loading condition.

2. In this research lipped channel sections were considered. Different types of sections i.e.; Z-sections, Multiple web sections etc with web holes should be considered in order to widen the field of application of the research.
3. A similar research can be extended with stainless steel sections.
4. Recently, Fibre-reinforced polymer (FRP) plates are being used for on strengthening of steel sections against web crippling. A similar study may be conducted on the influence Fibre-reinforced polymer (FRP) strengthening of the steel sections with web holes subjected to web crippling.

REFERENCES

ANSYS (2011). User's manual, revision 11.0. Swanson Analysis System.

ASCE (2005). Minimum design loads for buildings and other structures. New York: American Society of Civil Engineers Standard.

Avci, O. & Easterling, W. S. (2004). Web crippling strength of steel deck subjected to end one flange loading. *Journal of Structural Engineering,* ASCE,130(5)**,** 697-707.

Baehre, B. & Schuster, R. M. (2000). Web crippling data and calibations of cold formed steel members. Canada: Uinversity of waterloo.

Baehre, R. (1975). Sheet Metal Panels for Use in Building Construction – Recent Research Projects in Sweden. *Proceeding of the Third International-Specialty Conference on Cold Formed Steel Structures.* Rolla, Missouri,U.S.A: University of Missouri-Rolla.

Bakker, M. C. M. (1992). *Web Crippling of Cold-Formed Steel Members.* PhD Thesis, Eindhoven University of Technology.

Beshara, B. (1999). *Web crippling of cold-formed steel members.* M.A.Sc. Thesis, University of Waterloo.

Beshara, B. & Schuster, R. M. (2000a). Web crippling data and calibations of cold formed steel members. Canada: Uinversity of waterloo.

Beshara, B. & Schuster, R. M. (2000b). Web crippling of cold-formed steel C- and Z- sections. *Fifteenth International Specialty Conference on Cold-Formed Steel Structures.* St. Louis, Missouri, U.S.A.

Bhakta, B. H., LaBoube, R. A. & Yu, W. W. (1992). The effect of flange restraint on web crippling strength. *Civil Engineering Study 92-1.* Rolla, Missouri, USA.: University of Missouri-Rolla.

BS5950 (1998). Structural use of steelwork in buildings. *Part 5 Code of practice for the design of cold-formed sections.* London: British Standards Institution.

Cain, D. E., LaBoube, R. A. & Yu, W. W. (1995). The effect of flange restraint on web crippling strength of cold formed steel z-and i-sections. *Civil Engineering Study 95-2.* Rolla, Missouri, U.S.A: University of Missouri-Rolla.

Chung, K. F. (1995a). Structural perfomance of cold formed sections with single and multiple web openimgs.(part-1 Experimental investigation). *The Structural engineer,* Vol 73.

Chung, K. F. (1995b). Structural perfomance of cold formed sections with single and multiple web openimgs.(part-2 Design rules). *The Structural engineer,* Vol 73.

Cornell (1953). Cornell University, “65 th and 66th Progress Reports on Light Gage Steel Beams of Cold Formed Steel. New York, NY, U.S.A.,: Cornell University.

Davies, G. & Packer, J. A. (1987). Analysis of Web Crippling in a Rectangular Hollow Sections. *Proceedings of the Institution of Civil Engineers.*

Deshmukh, S. U. (1996). *Behavior of Cold-Formed Steel Web Elements with Web Openings Subjected to Web Crippling and a Combination of Bending and Web Crippling for Interior-One-Flange.* M.S. Thesis, University of Missouri-Rolla.

EN, B. (2001). 10002-1: 2001. Tensile testing of metallic materials. Method of test at ambient temperature. *British Standards Institution*.

Eurocode-3 (1996). Design of steel structures: Part 1.3: General rules — Supplementary rules for cold-formed thin gauge members and sheeting. *ENV 1993-1-3*. Brussels, Belgium: European Committee for Standardization.

Gerges, R. R. (1997). *Web Crippling of Single Web Cold Formed Steel Members Subjected to End One-Flange Loading.* M.A.Sc. Thesis, University of Waterloo.

Gerges, R. R. & Schuster, R. M. (1998). web crippling of single web cold formed steel members subjected to end one-flange loading. *Fourth International Specialty Conference on Cold-Formed Steel Structures.* St. Louis, Missouri, U.S.A.

Heiyantuduwa, M. (2008). *Web crippling behaviour of cold-formed thin-walled steel lipped channel beams.* Ph.D. Thesis, Glasgow Caledonian University.

Hetrakul, N. & Yu, W. W. (1978). Structural Behaviour of Beam Webs Subjected to Web Crippling and a Combination of Web Crippling and Bending. *Civil Engineering Study.* Missouri, U.S.A: University of Missouri-Rolla, Rolla,.

Hofmeyer, H. (2000). *Combined Web Crippling and Bending Moment Failure of First-Generation Trapezoidal Steel Sheeting.* PhD Thesis, Eindhoven University of Technology.

Holesapple, M. W. & Laboube, R. A. (2003). Web crippling of cold-formed steel beams at end supports. *Engineering Structures,* vol. 25**,** pp. 1211-1216.

Kaitila, O. (2004). *Web Crippling of Cold-Formed Thin-Walled Steel Cassettes.* PhD Thesis, Helsinki University of Technology.

Kaspers, M. (2001). *Combined Web Crippling and Bending Moment Failure of Second-Generation Trapezoidal Steel Sheeting.* MSc Thesis, Eindhoven University of Technology.

Korvink, S. A., Van den berg, G. J. & Van der merwe, P. (1995). Web crippling of stainless steel cold-formed beams. *Journal of Constructional Steel Research,* vol. 34 pp. 225-248.

LaBoube, R. A., Yu, W. W., Deshmukh, S. U. & Uphoff, C. A. (1999). Crippling Capacity of Web Elements with Openings. *Journal of Structural Engineering,* 125**,** 137-141.

LaBoube, R. A., Yu, W. W. & Langan, J. E. (1997). Cold-formed steel web with openings:summary report. *Thin-Walled Structures,* vol. 28**,** pp. 355-372.

Langan, J. E. (1994). *Structural behaviour of perforated web elements of cold formed flexural members subjected to web crippling and a combination of web crippling and bending.* PhD Thesis, University of Missouri-Rolla.

NAS (2001). North American Specification for the design of cold-formed steel structural members. Washington,D.C.: American Iron and Steel Institute.

OriginLab (2011). Data Analysis and Graphing Software(8.5.1). OriginLab Corporation.

Parabakaran, K. & Schuster, R. M. (1993). Web crippling of cold formed steel sections. Department of Civil Engineering,Waterloo, Ontario, Canada: University of Waterloo.

Ratliff, G. D. (1975). Interaction of Concentrated Loads and Bending in C-Shaped Beams. *Third International Specialty Conference on Cold-Formed Steel Structures.* St. Louis, Missouri, U.S.A.

Ren, W., Fang, S. & Young, B. (2006). Analysis and design of cold-formed steel channels subjected to combined bending and web crippling. *Thin-Walled Structures,* vol. 44**,** pp. 314 – 320.

Ren, W., Fang, S. & Young, B. (2006). Finite element simulation and design of cold-formed steel channels subjected to web crippling. *Journal of Structural Engineering ,* vol. 132**,** pp. 1967 – 1975.

Rhodes, J. & Nash, D. (1998). An investigation of web crushing behaviour in thin-walled beams. *Thin-Walled Structures,* 32**,** 207-230.

Santaputra, C., Parks, M. B. & Yu, W. W. (1989). Web crippling strength of cold-formed steel beams. *Journal of Structural Engineering,* vol. 115**,** pp. 111-139.

Setiyono, H. (1994). *Web crippling of cold-formed plain channel steel section beams.* PhD Thesis, University of Strathclyde.

Sivakumaran, K. S. (1989). Analysis for web crippling behaviour of cold-formed steel members. *Computers and structures,* vol. 32**,** pp. 707-719.

Sivakumaran, K. S. & Zielonka, K. M. (1989). Web crippling strength of thin-walled steel members with web opening. *Thin-Walled Structures,* 8**,** 295-319.

Stephens, S. F. & Laboube, R. A. (2003). Web crippling and combined bending and web crippling of cold-formed steel beam headers. *Thin-Walled Structures,* vol. 41**,** pp. 1073-1087.

Studnicka, J. (1991). Web Crippling of Multi-web Deck Sections. *Thin-Walled Structures,* vol. 11**,** pp. 219-231.

Uphoff, C. A. (1996). *Structural Behavior of Circular Holes in Web Elements of Cold-Formed Steel Flexural Members Subjected to Web Crippling for End- One-Flange Loading.* M.S. Thesis, University of Missouri-Rolla.

Vaessen, V. (1995). *On the Elastic Web Crippling Stiffness of Thin-Walled Cold-Formed Steel Members.* MSc Thesis, Eindhoven University of Technology.

Wing, B. A. (1981). *Web Crippling and the Interaction of Bending and Web Crippling of Unreinforced Multi-Web Cold Formed steel Sections.* M.Sc. Thesis, University of Waterloo.

Wing, B. A. & Schuster, R. M. (1986). Web Crippling of Multi-Web Deck Sections. *Eighth International Specialty Conference on Cold-Formed Steel Structures.* St. Louis, Missouri, U.S.A.

Winter, G. & Pian, R. H., J., (1946). Crushing Strength of Thin Steel Webs. *Engineering Experiment Station.* N.Y,U.S.A: Cornell University.

Wu, S., Yu, W. & Laboube, R. A. (1998). Web Crippling Strength of Cold-formed Steel Structures. *Fourteenth International Specialty Conference on Cold-Formed Steel Structures.* St. Louis, Missouri U.S.A.

Young, B. & Hancock, G. J. (1998). Web crippling behaviour of cold formed unlipped channels. *Fourteenth International Specialty Conference on Cold-Formed Steel Structures.* St. Louis, Missouri U.S.A.

Young, B. & Hancock, G. J. (2000a). Experimental investigation of cold-formed channels subjected to combined bending and web crippling. *Fifteenth International Specialty Conference on Cold-Formed Steel Structures.* St. Louis, Missouri U.S.A.

Young, B. & Hancock, G. J. (2000b). Tests and design of cold-formed unlipped channels subjected to web crippling. *Fifteenth International Specialty Conference on Cold-Formed Steel Structures.* St. Louis, Missouri U.S.A.

Young, B. & Hancock, G. J. (2000c). Web crippling behaviour of channels with flanges restrained. *Fifteenth International Specialty Conference on Cold-Formed Steel Structures.* St. Louis, Missouri U.S.A.

Young, B. & Hancock, G. J. (2001). Design of Cold-Formed Channels Subjected to Web Crippling. *J. Struct. Eng.,* 127**,** 1137.

Young, B. & Hancock, G. J. (2002). Tests of channels subjected to combined bending and web crippling. *Journal of Structural Engineering,* ASCE, 128(3)**,** 300-308.

Young, B. & Hancock, G. J. (2003). Cold-formed steel channels subjected to concentrated bearing load. *Journal of Structural Engineering,* ASCE, 129(8)**,** 1003-1010.

Young, B. & Hancock, G. J. (2004). Web crippling of cold-formed unlipped channels with flanges restrained. *Thin-Walled Structures,* 42**,** 911-930.

Yu, W. W. & Davis, C. S. (1973). Cold-formed steel members with perforated elements. *Journal of the Structural Division,* 99**,** 2061-2077.

Zhou, F. (2006). *Web crippling of cold-formed stainless steel tubular sections.* PhD Thesis, The University of Hong Kong.

Zhou, F. & Young, B. (2010). Web crippling of aluminium tubes with perforated webs. *Engineering Structures,* 32**,** 1397-1410.

Appendix A

Stress-strain curves predicted from coupon tests

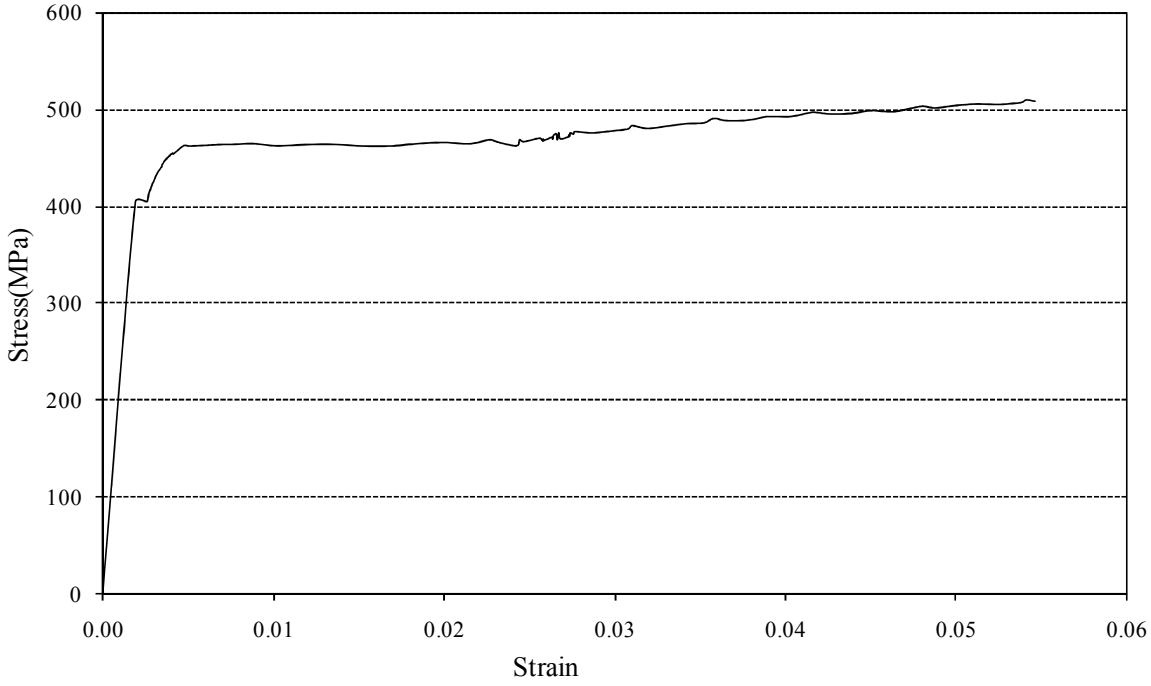

Figure A-1. Stress-strain curve for channel 142 x 60 x 13 x 1.3

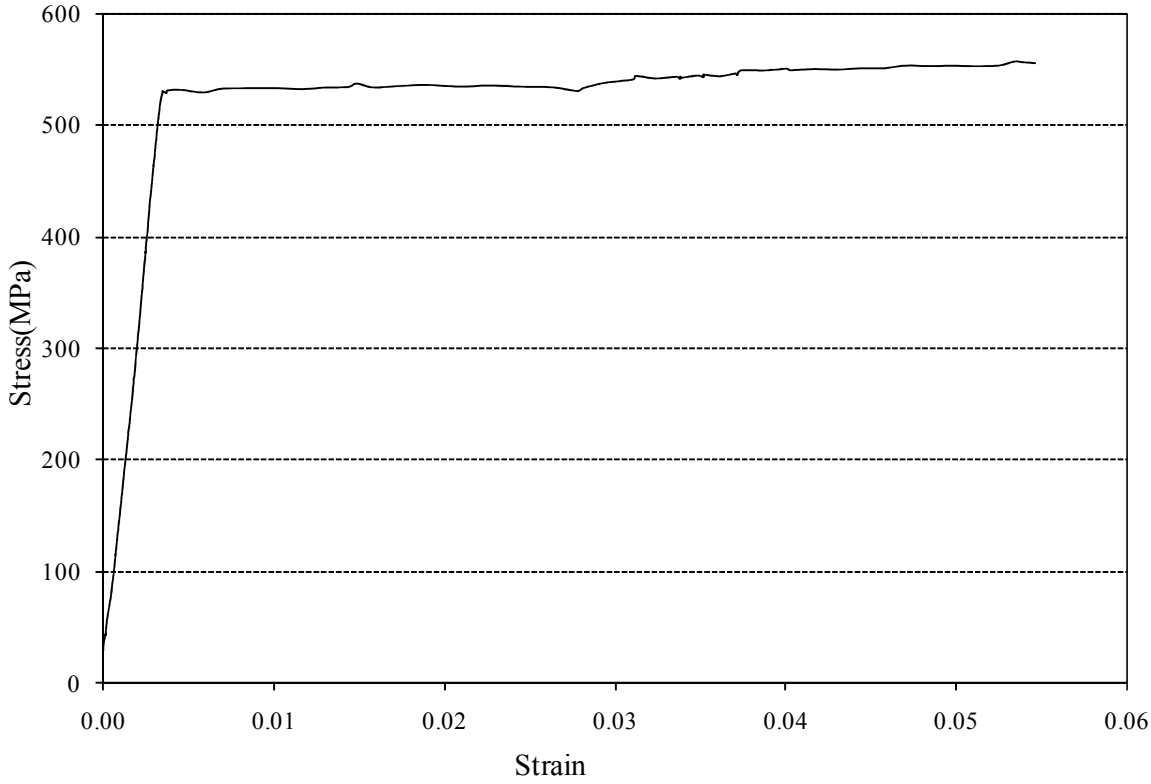

Figure A-2. Stress-strain curve for channel 172 x 65 x 13 x 1.3

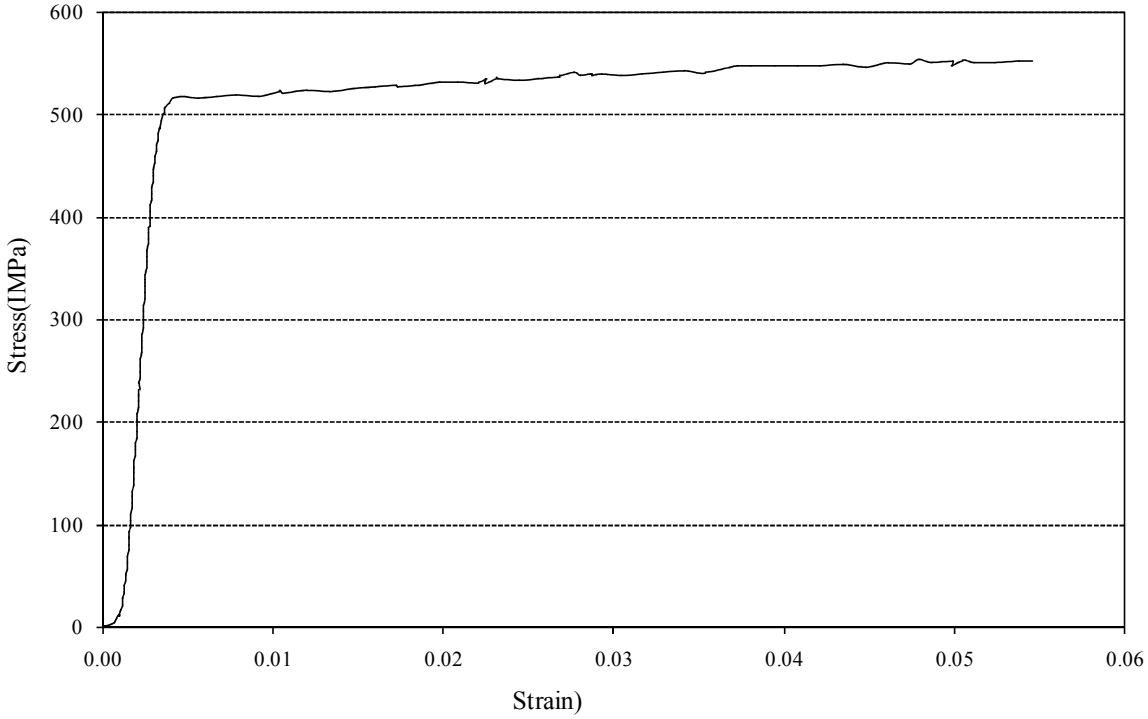

Figure A-3. Stress-strain curve for channel 202 x 65 x 13 x 1.4

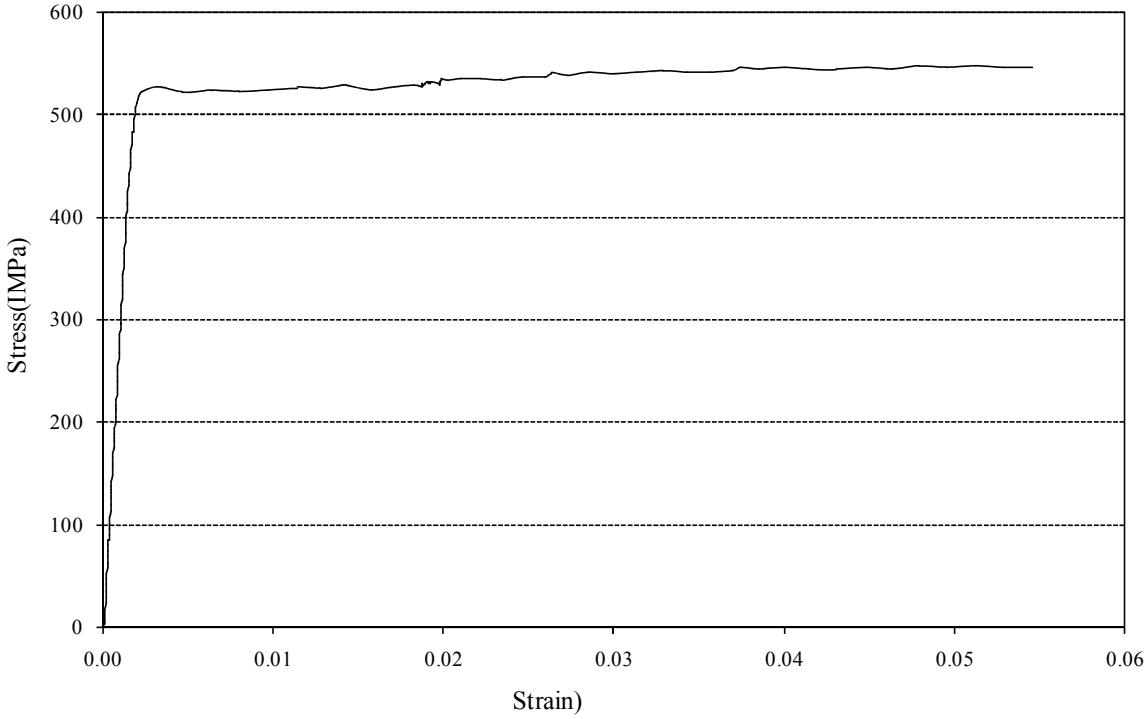

Figure A-4. Stress-strain curve for channel 262 x 65 x 13 x 1.6

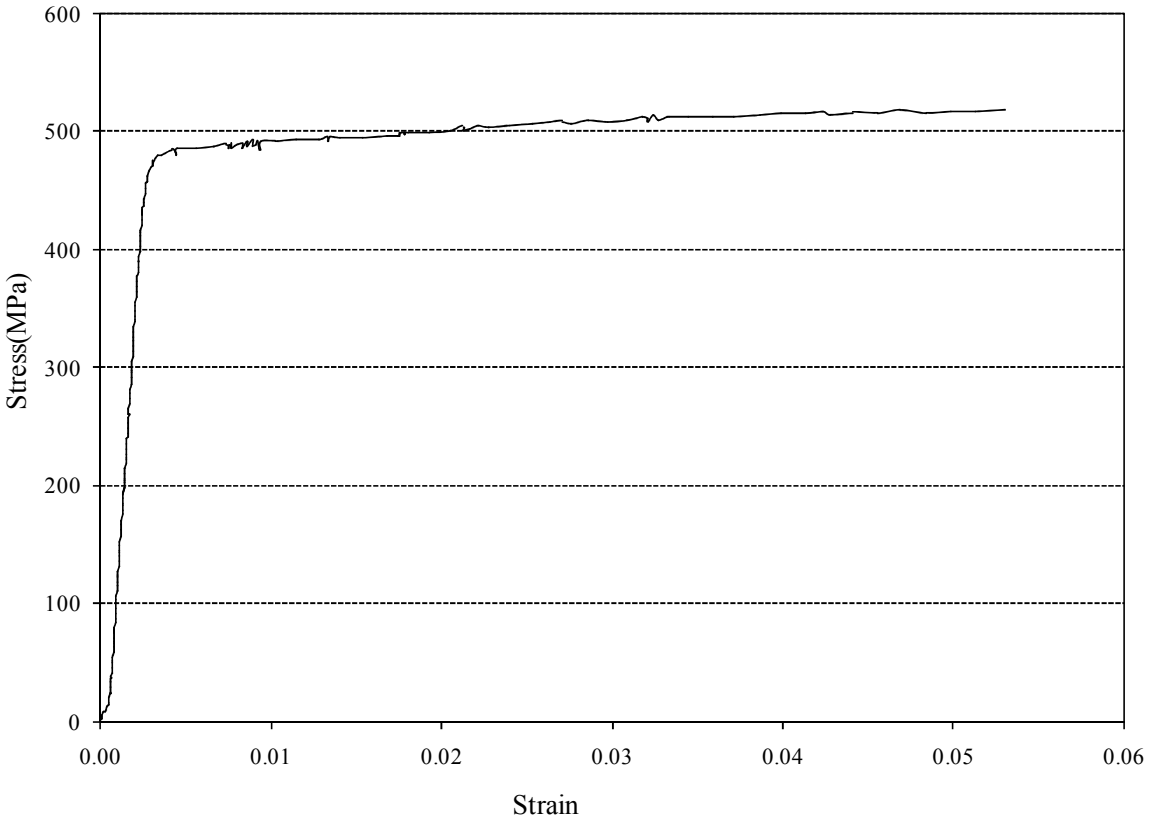

Figure A-5. Stress-strain curve for channel 302 x 88 x 18 x 2.0

Appendix B :

Comparison web deformation curves predicted from the finite element analysis with the experiment tests.

1.1 Comparison curves for flanges unfastened under ITF loading condition (Type 1 holes)

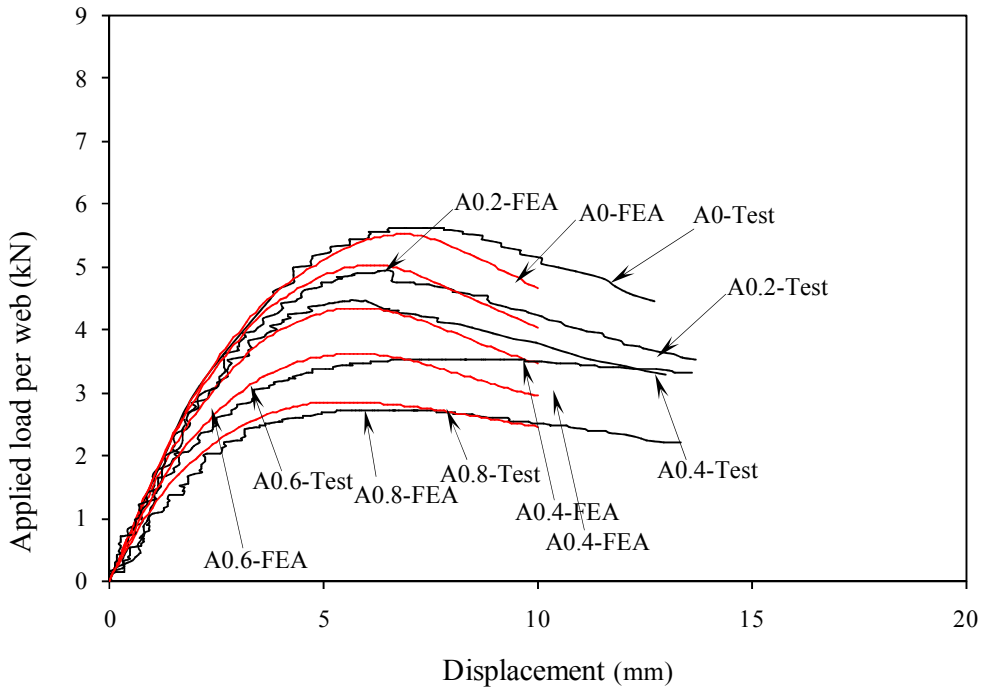

Figure B.1.1 Comparison web deformation curves for specimen ITF142×60×13-t1.3N30FR

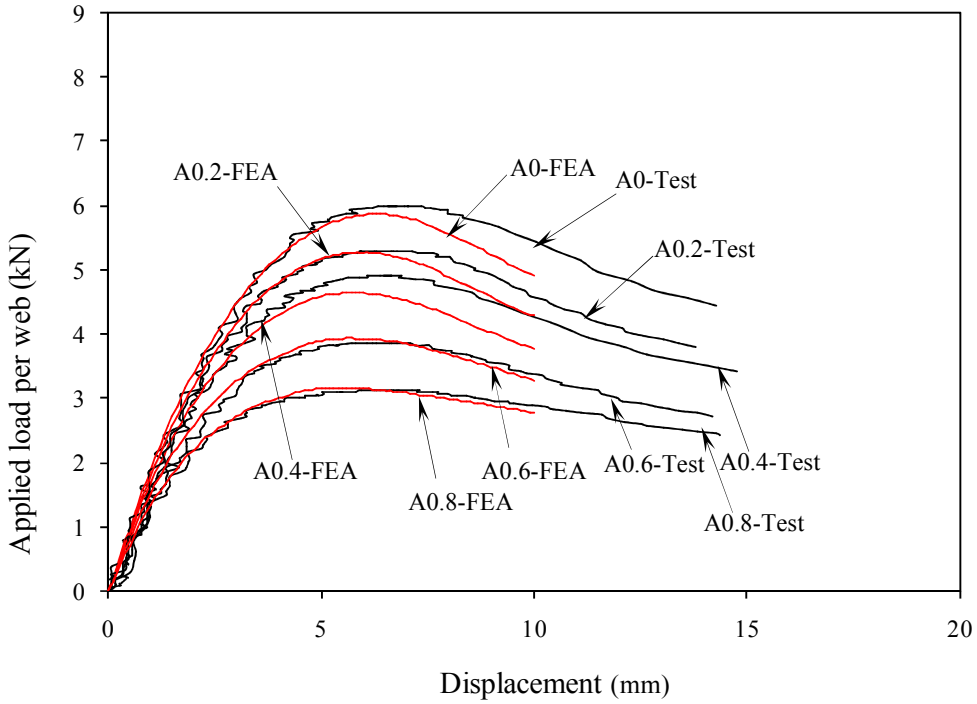

Figure B.1.2 Comparison web deformation curves for specimen ITF142×60×13-t13N60FR

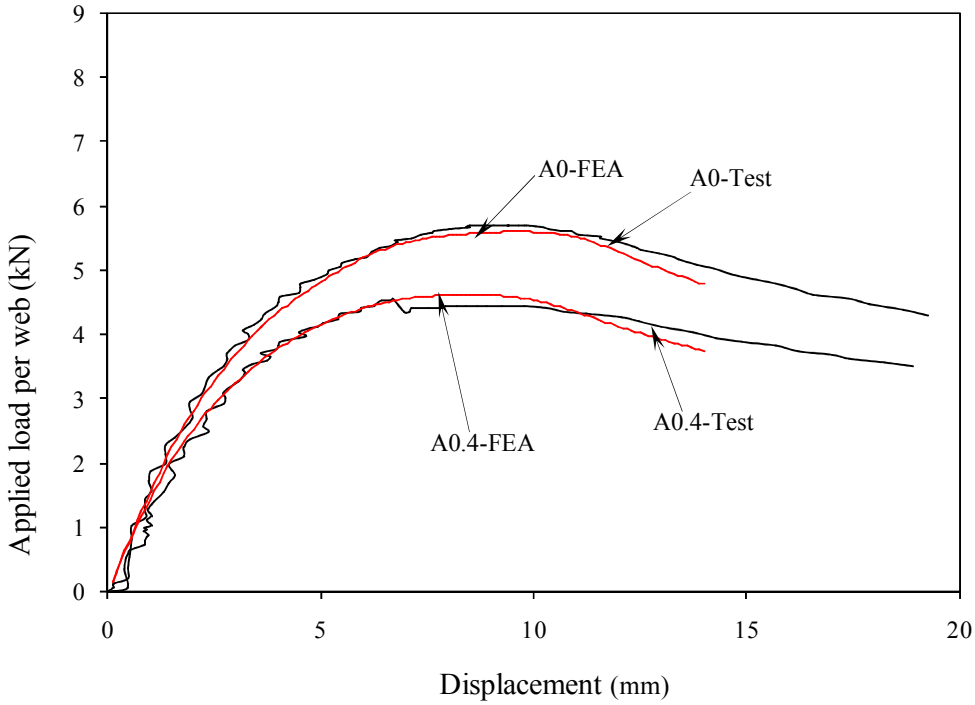

Figure B.1.3 Comparison web deformation curves for specimen ITF172×65×13-t1.3N32.5FR

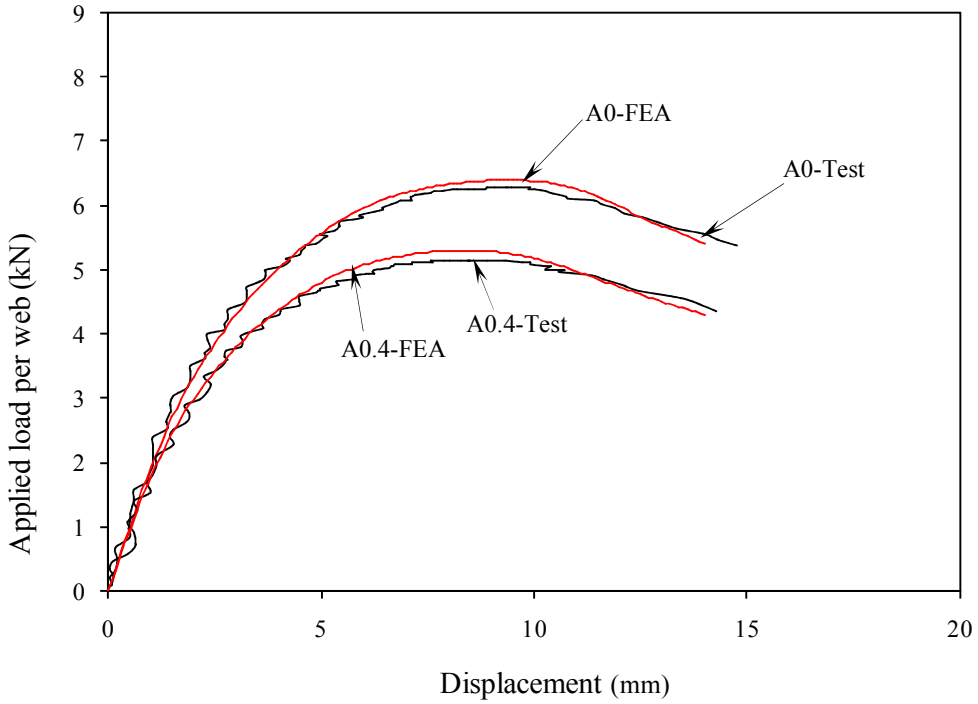

Figure B.1.4 Comparison web deformation curves for specimen ITF172×65×13-t1.3N65FR

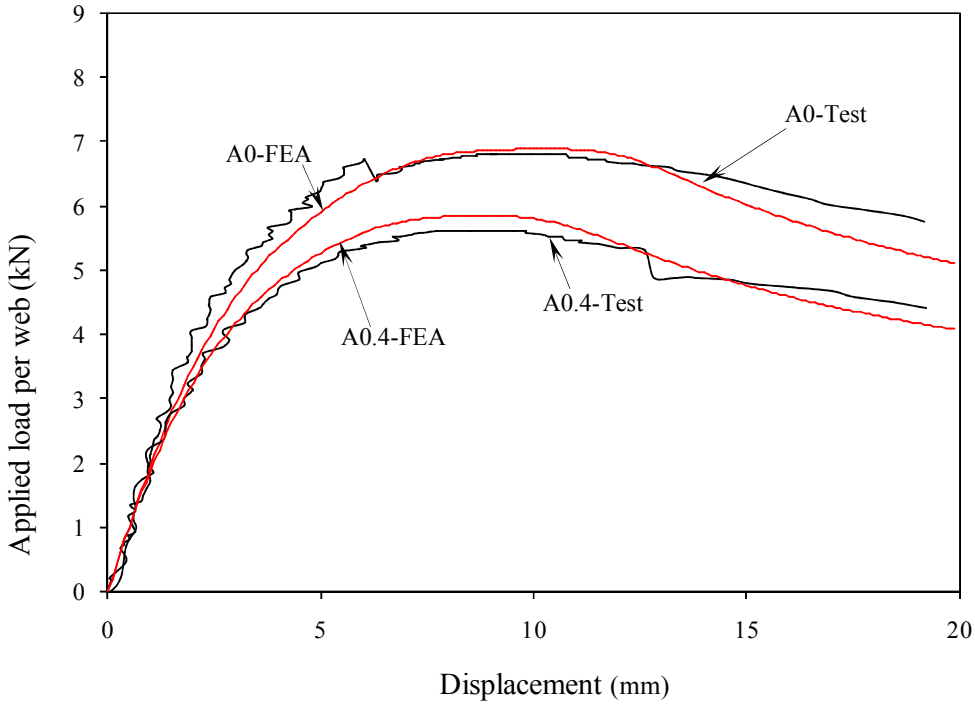

Figure B.1.5 Comparison web deformation curves for specimen ITF202×65×13-t1.4N32.5FR

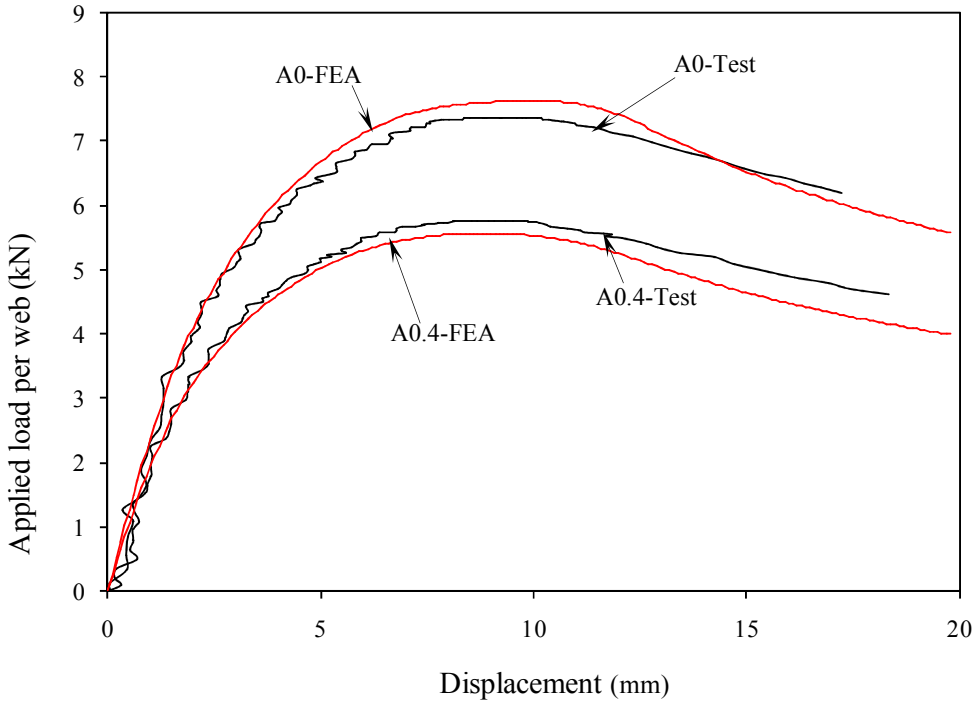

Figure B.1.6 Comparison web deformation curves for specimen ITF202×65×13-t1.4N65FR

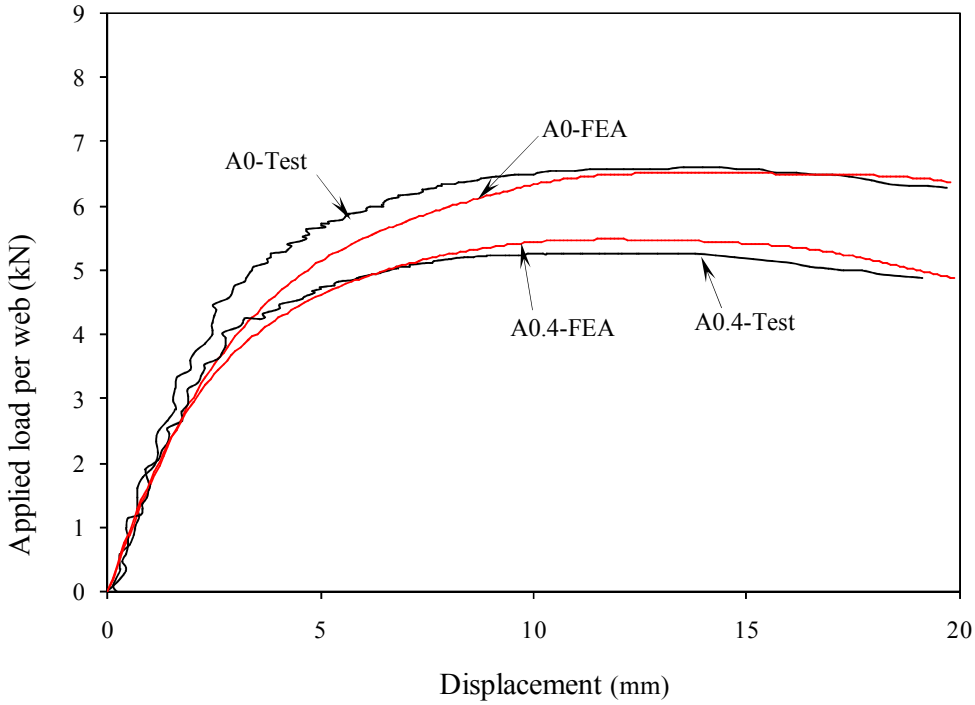

Figure B.1.7 Comparison web deformation curves for specimen ITF262×65×13-t1.6N32.5FR

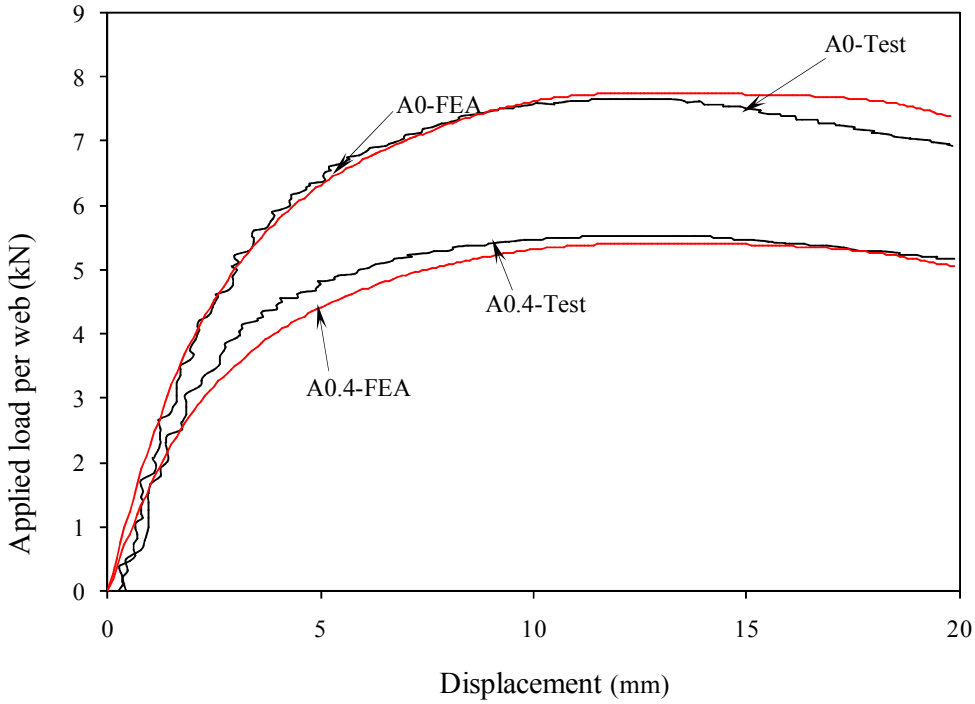

Figure B.1.8 Comparison web deformation curves for specimen ITF262×65×13-t1.6N65FR

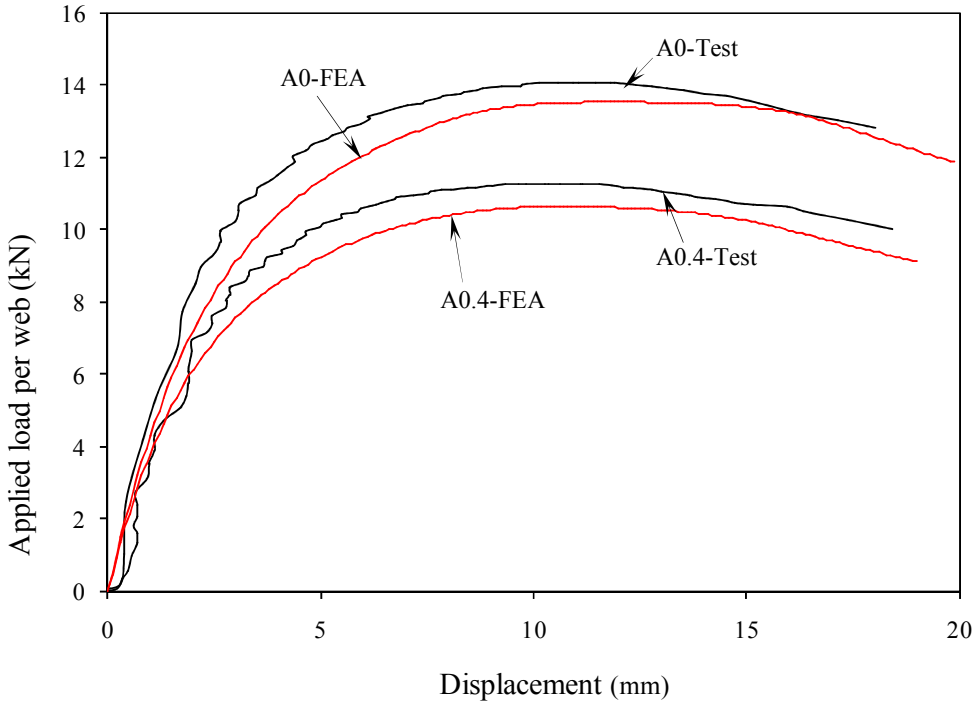

Figure B.1.9 Comparison web deformation curves for specimen ITF302×90×18-t2N90FR

1.2 Comparison curves for flanges unfastened under ITF loading condition (Type 2 holes)

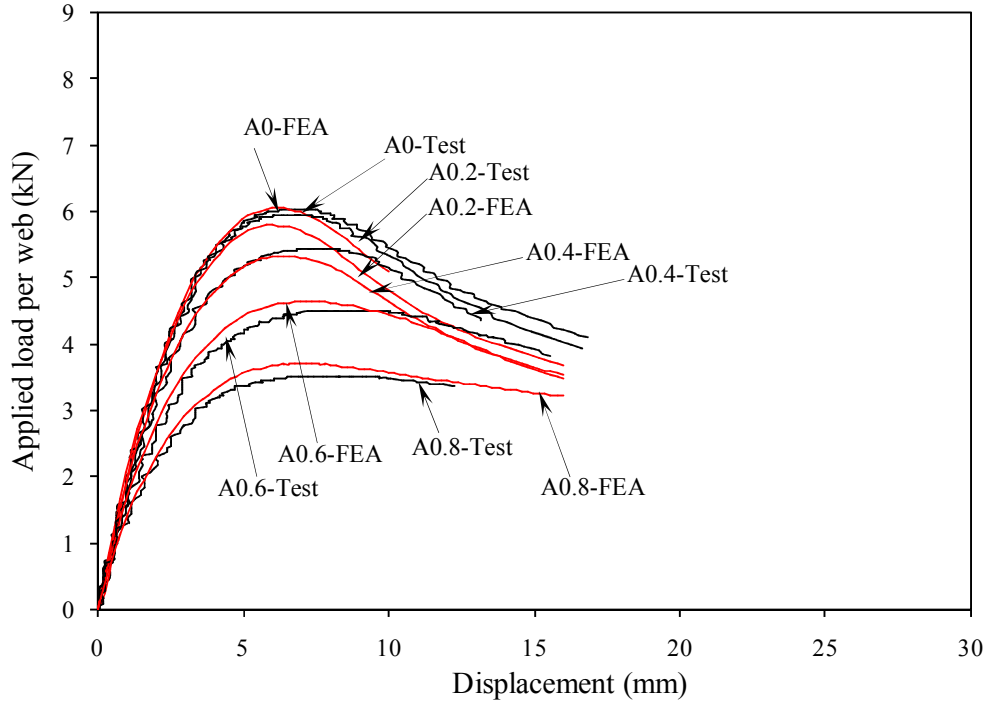

Figure B.2.1 Comparison web deformation curves for specimen ITF142×60×13-t1.3MN90FR

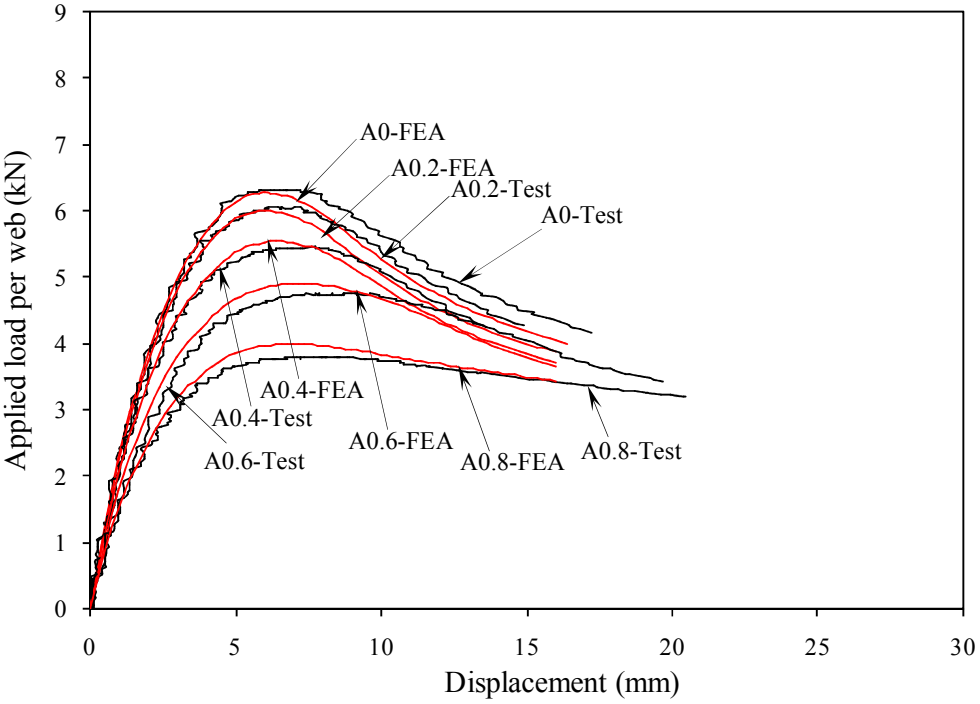

Figure B.2.2 Comparison web deformation curves for specimen ITF142×60×13-t13MN120FR

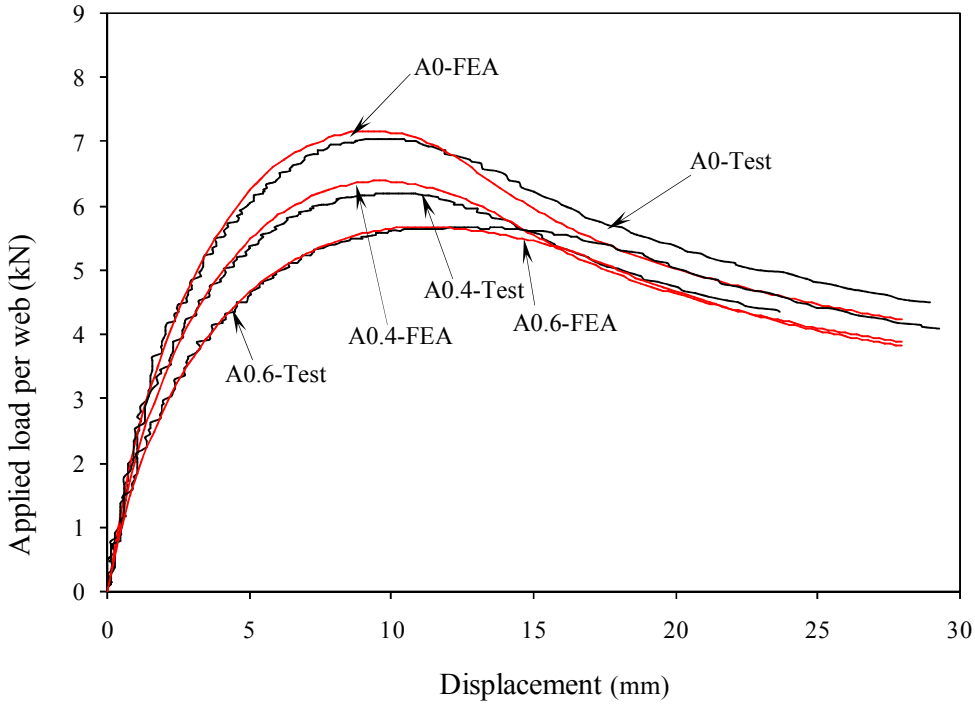

Figure B.2.3 Comparison web deformation curves for specimen ITF172×65×13-t1.3MN120FR

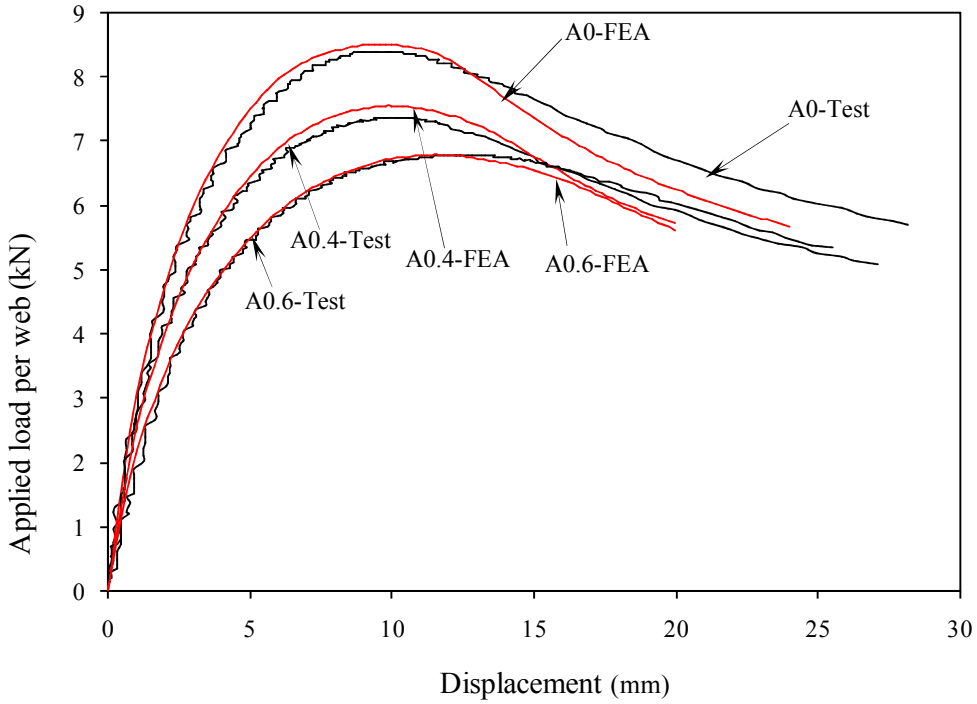

Figure B.2.4 Comparison web deformation curves for specimen ITF202×65×13-t1.4MN150FR

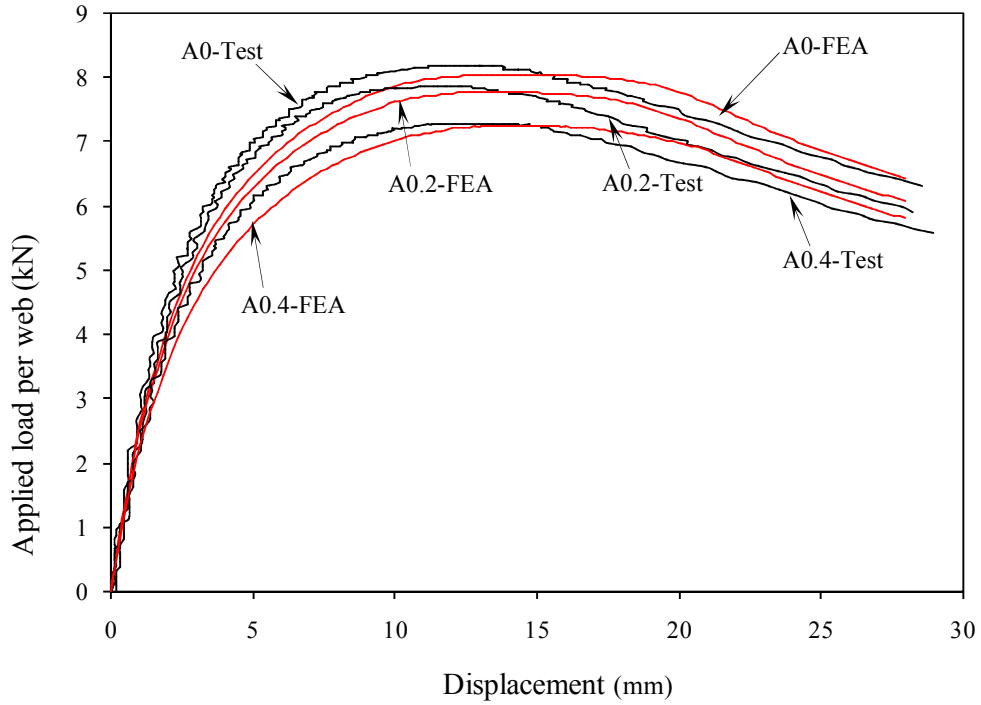

Figure B.2.5 Comparison web deformation curves for specimen ITF262×65×13-t1.6MN150FR

1.3 Comparison curves for flanges fastened under ITF loading condition (Type 1 holes)

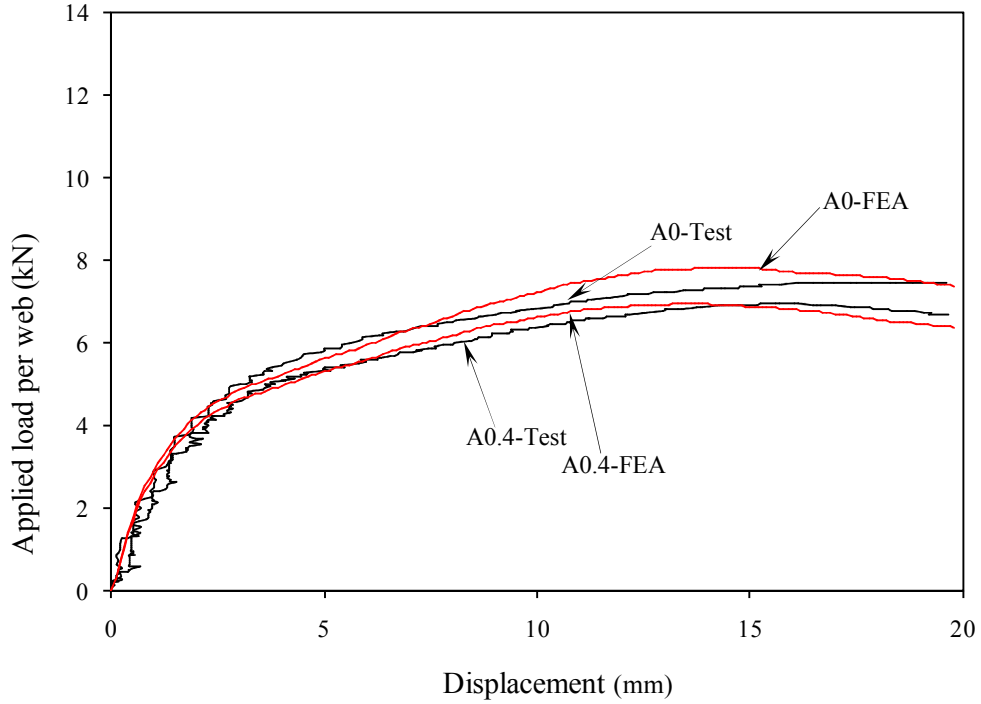

Figure B.3.1 Comparison web deformation curves for specimen ITF142×60×13-t1.3N30FX

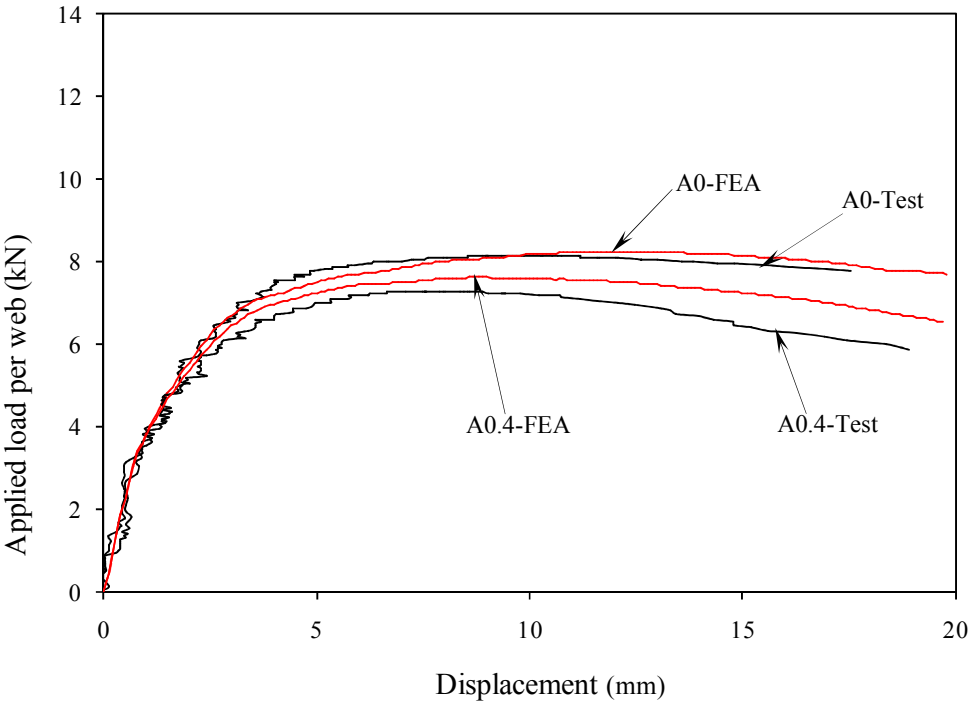

Figure B.3.2 Comparison web deformation curves for specimen ITF142×60×13-t13N60FX

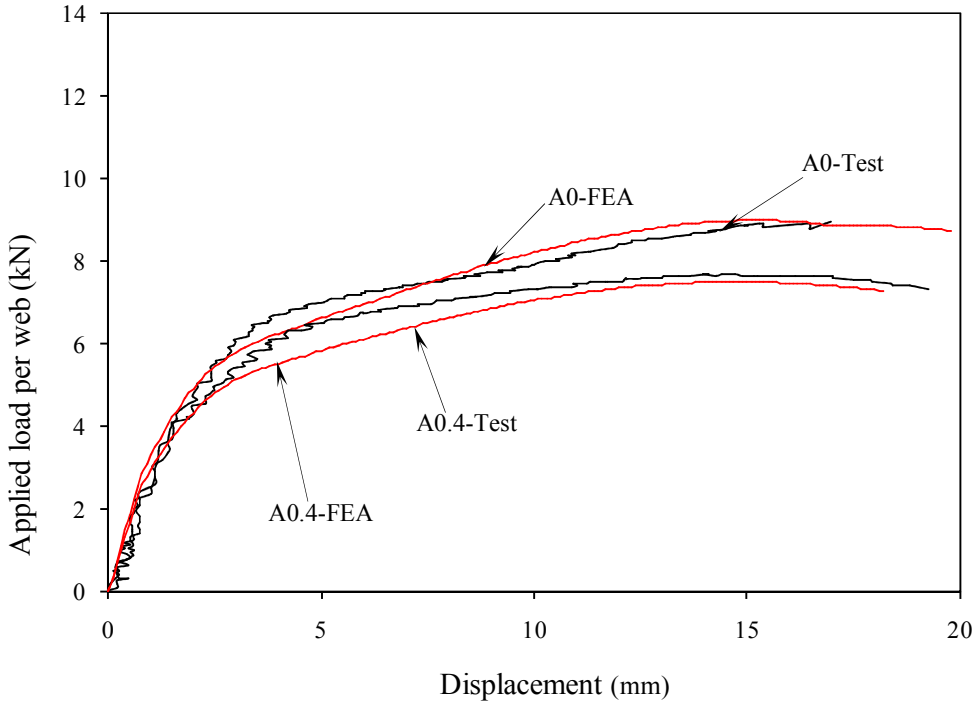

Figure B.3.3 Comparison web deformation curves for specimen ITF172×65×13-t1.3N32.5FX

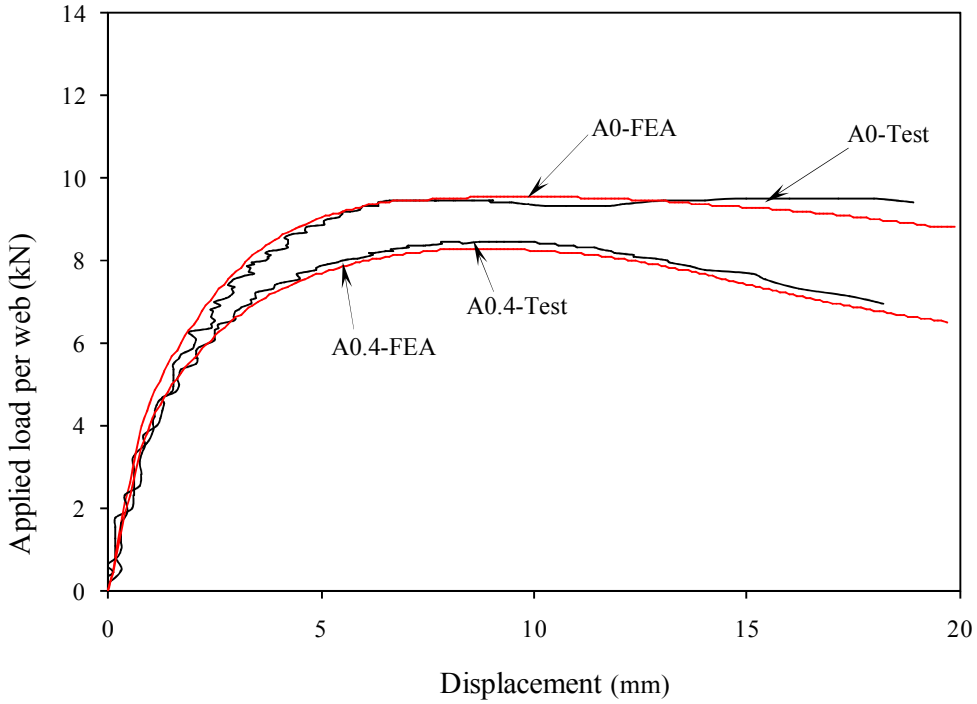

Figure B.3.4 Comparison web deformation curves for specimen ITF172×65×13-t1.3N65FX

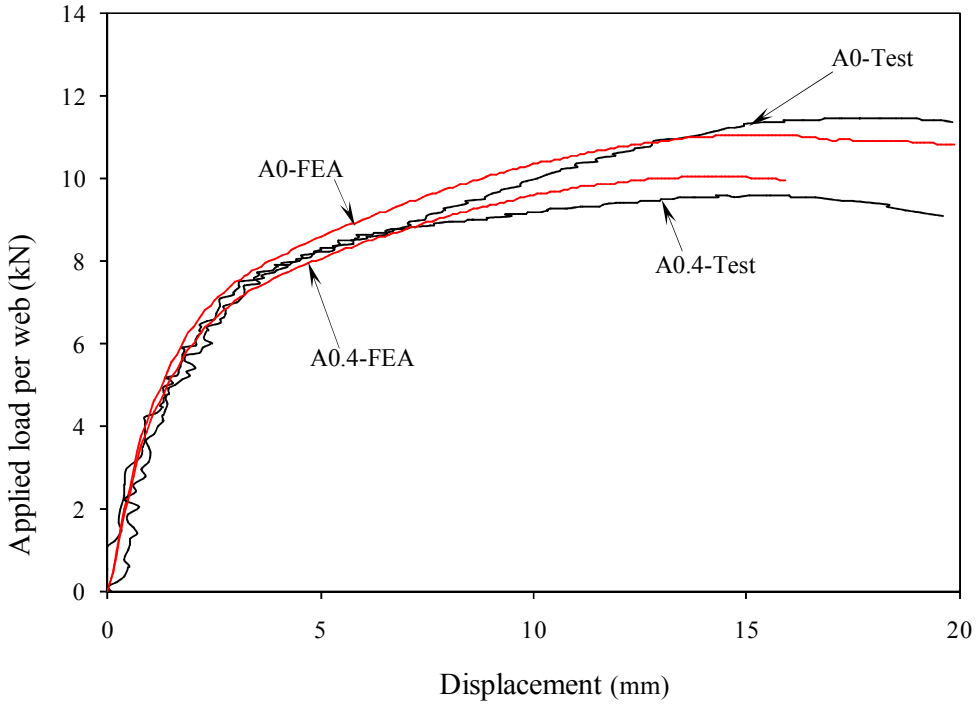

Figure B.3.5 Comparison web deformation curves for specimen ITF202×65×13-t1.4N32.5FX

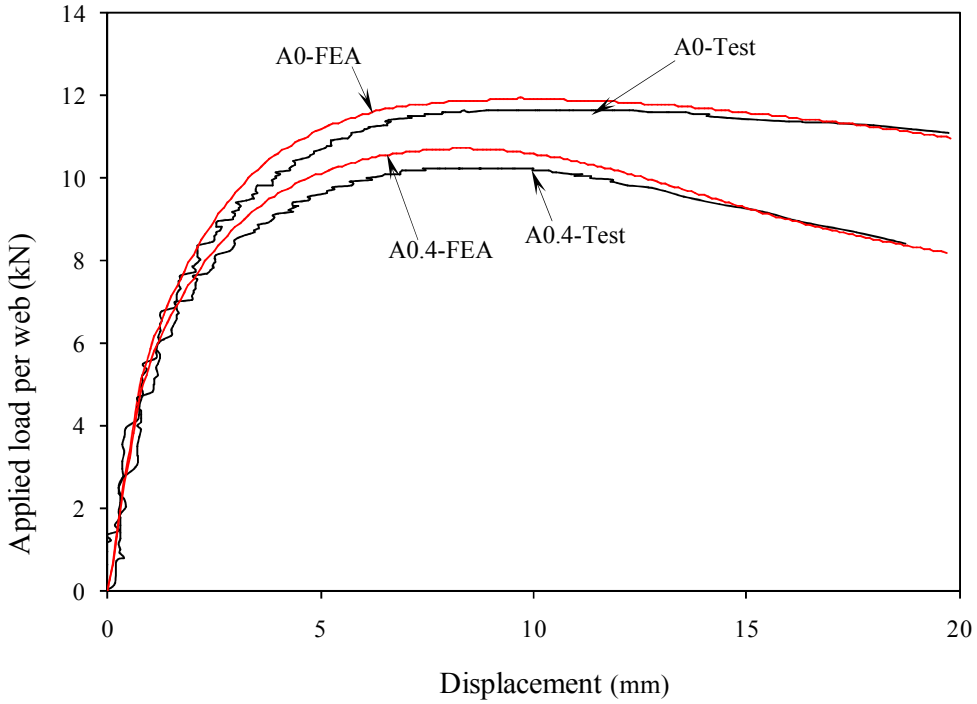

Figure B.3.6 Comparison web deformation curves for specimen ITF202×65×13-t1.4N65FX

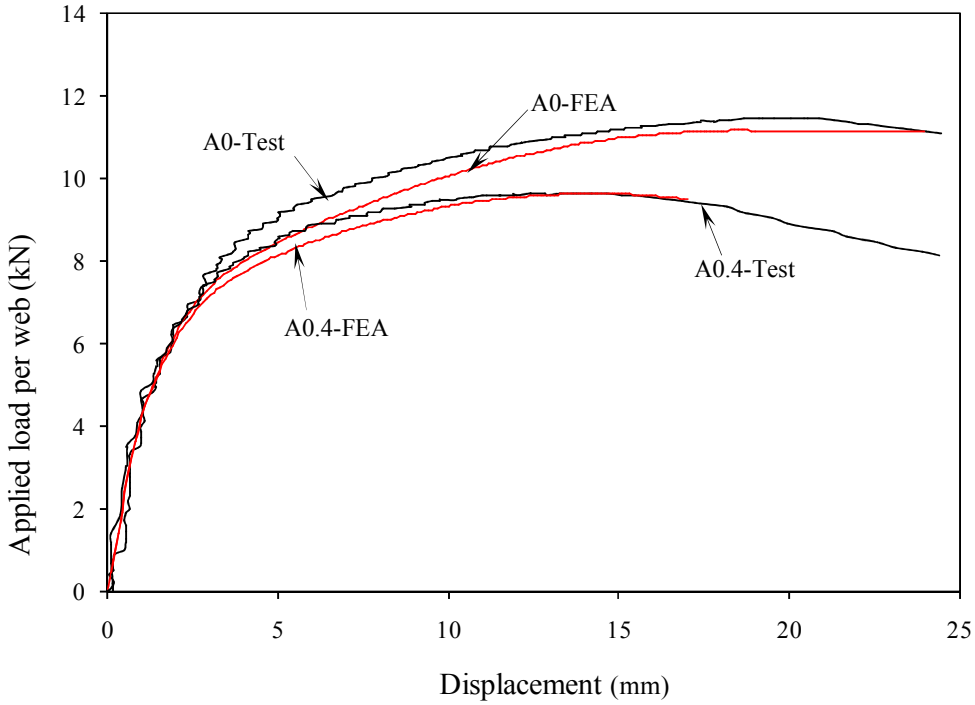

Figure B.3.7 Comparison web deformation curves for specimen ITF262×65×13-t1.6N32.5FX

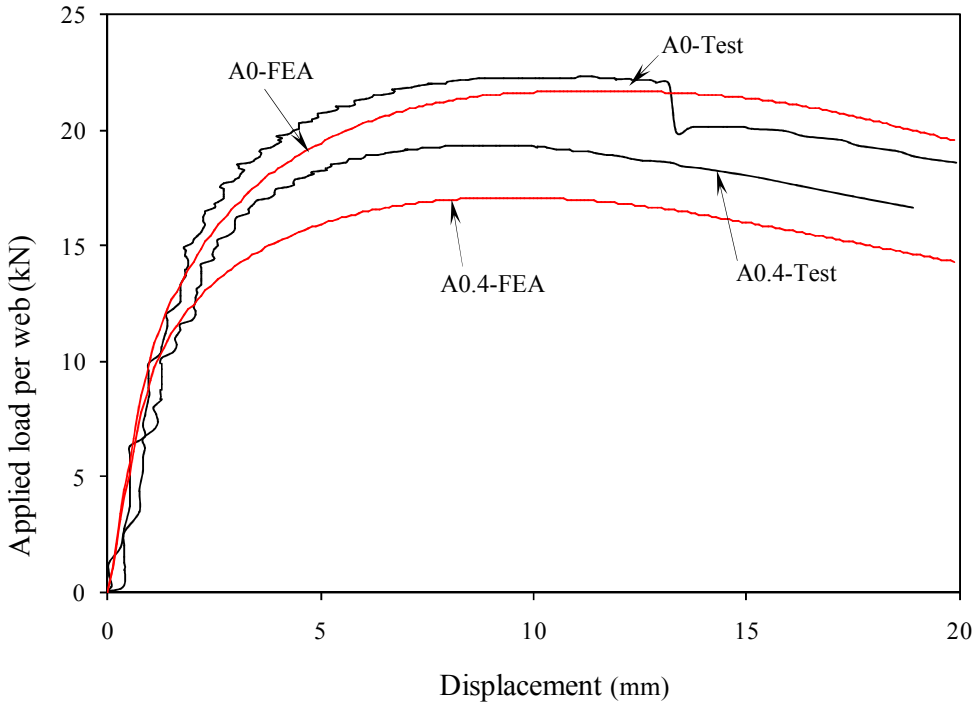

Figure B.3.8 Comparison web deformation curves for specimen ITF302×90×18-t2N90FX

1.4 Comparison curves for flanges fastened under ITF loading condition (Type 2 holes)

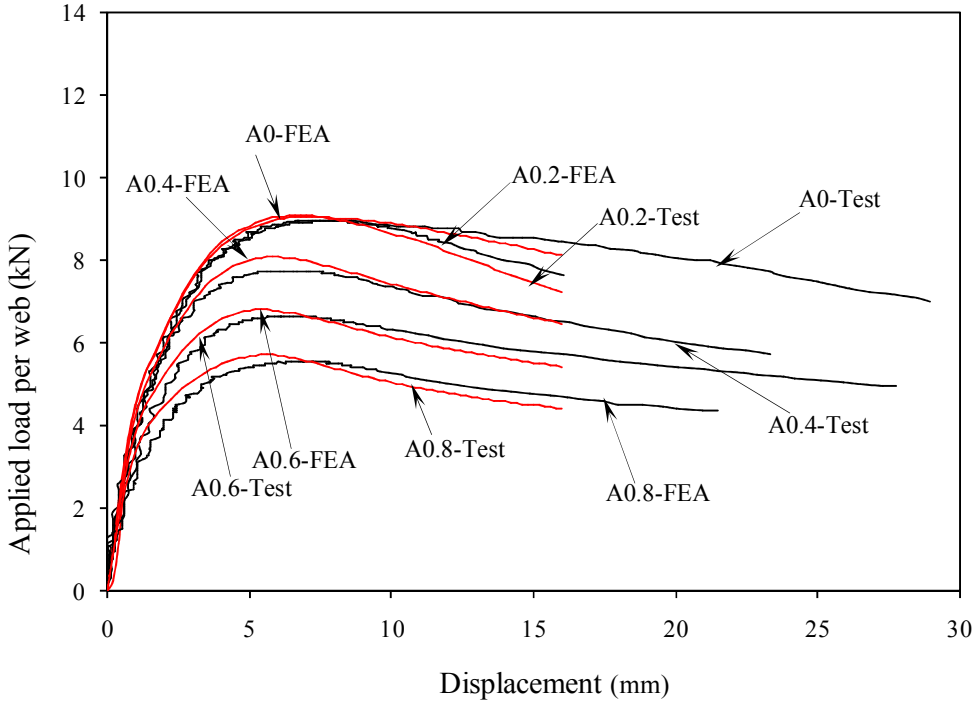

Figure B.4.1 Comparison web deformation curves for specimen ETF142×60×13-t1.3MN90FX

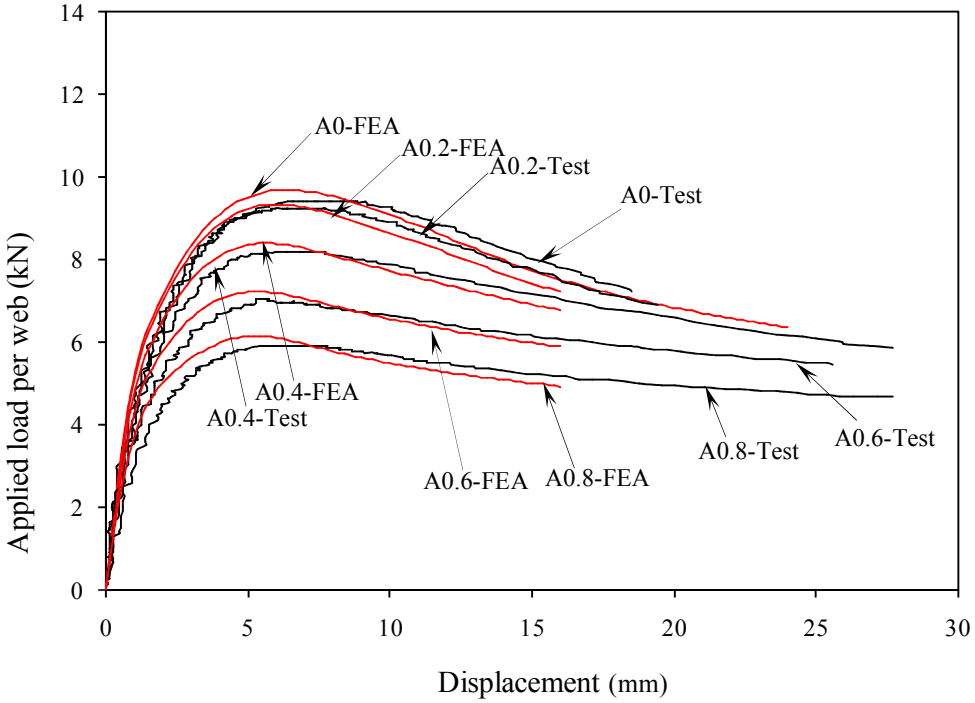

Figure B.4.2 Comparison web deformation curves for specimen ETF142×60×13-t13MN120FX

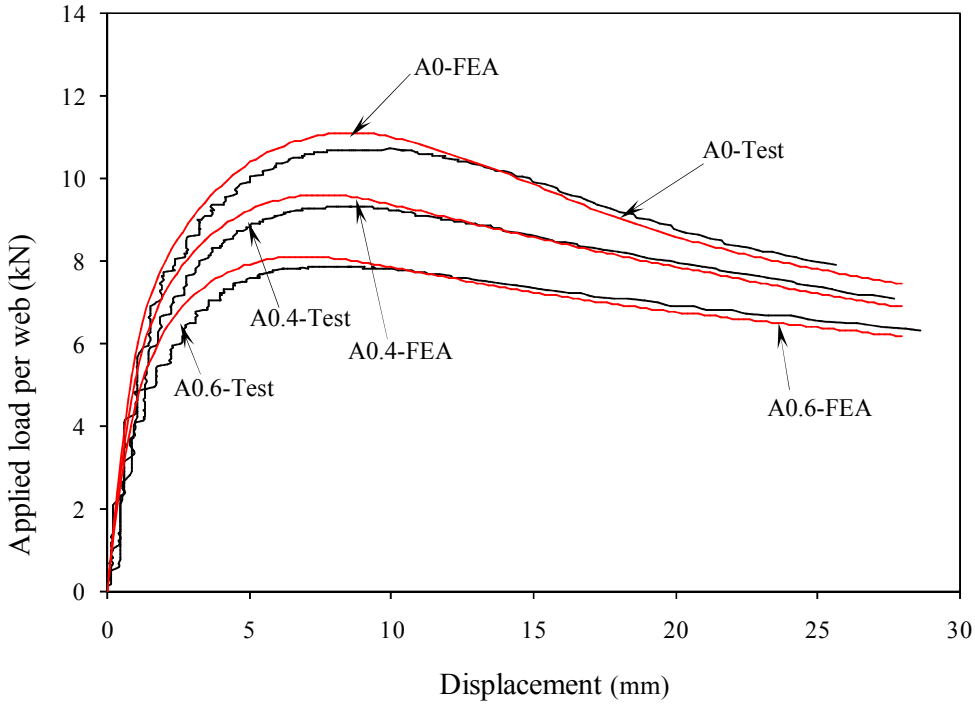

Figure B.4.3 Comparison web deformation curves for specimen ITF172×65×13-t1.3MN120FX

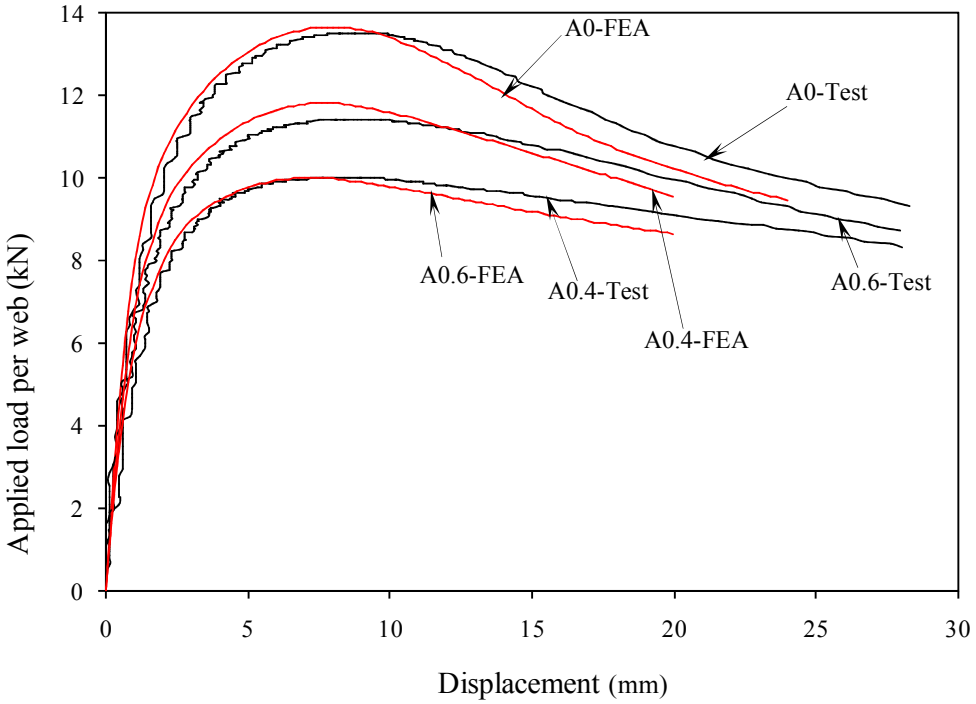

Figure B.4.4 Comparison web deformation curves for specimen ITF202×65×13-t1.4MN150FX

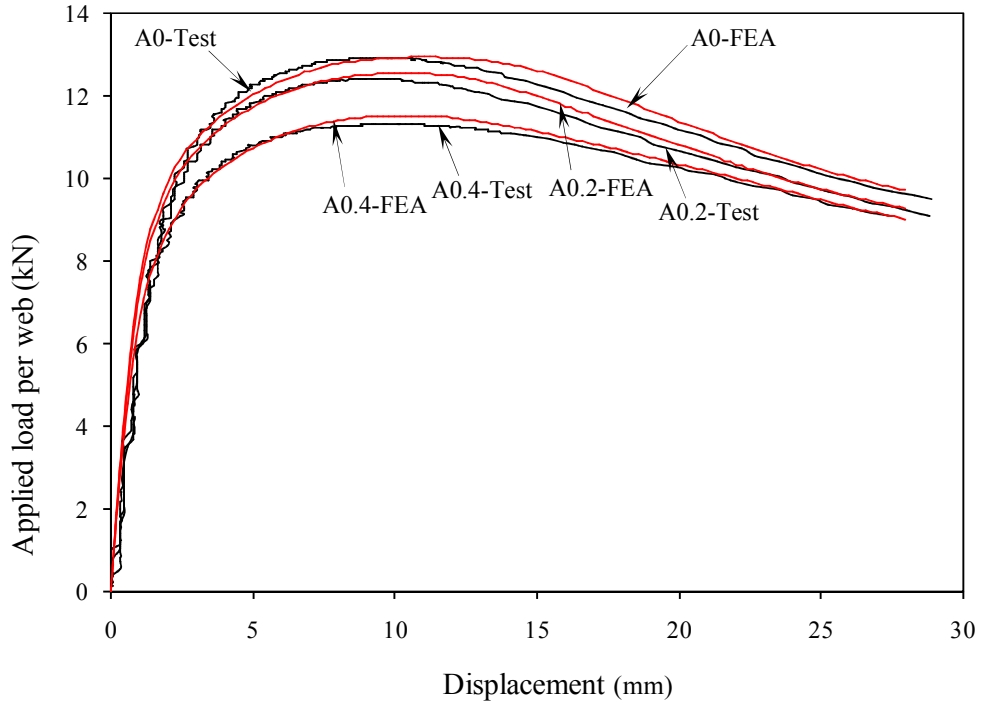

Figure B.4.5 Comparison web deformation curves for specimen ITF262×65×13-t1.6MN150FX

1.5 Comparison curves for flanges unfastened under ETF loading condition (Type 1 holes)

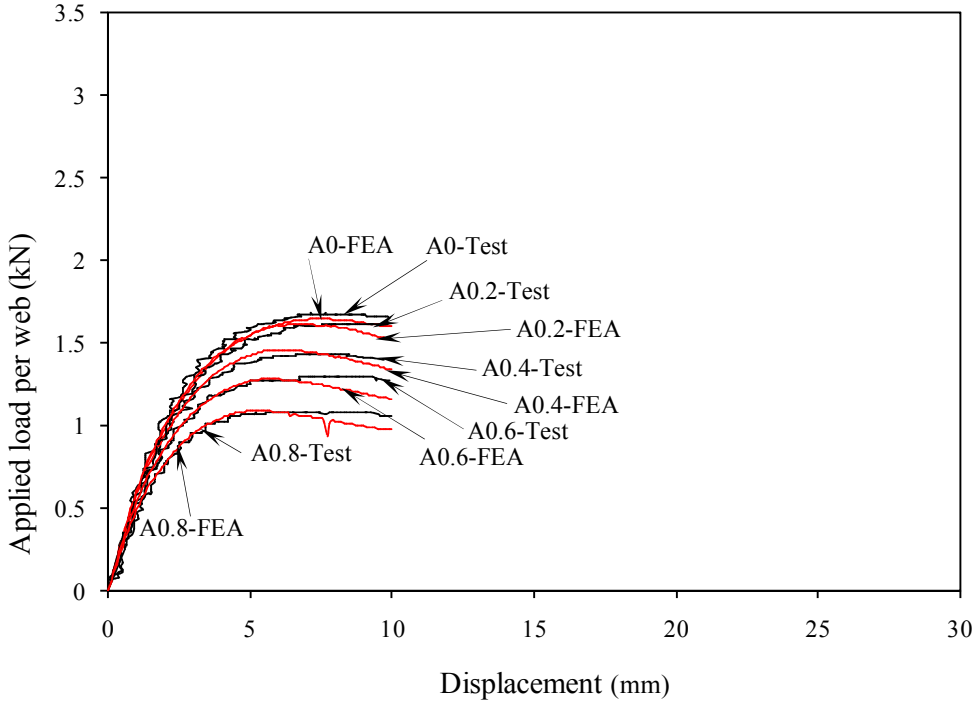

Figure B.5.1 Comparison web deformation curves for specimen ETF142×60×13-t1.3N30FR

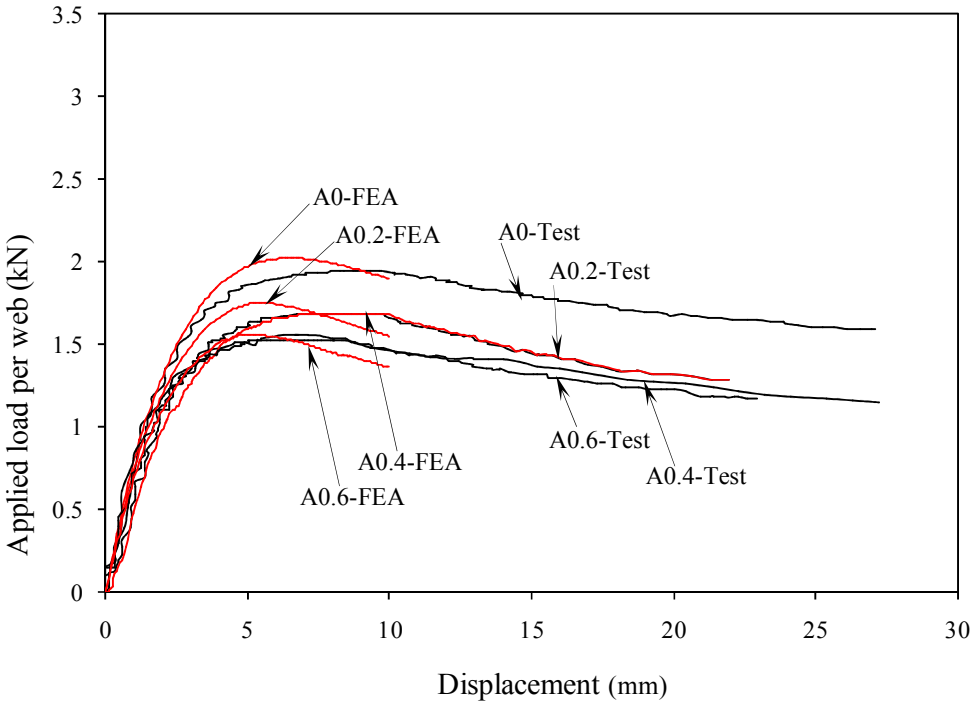

Figure B.5.2 Comparison web deformation curves for specimen ETF142×60×13-t13N60FR

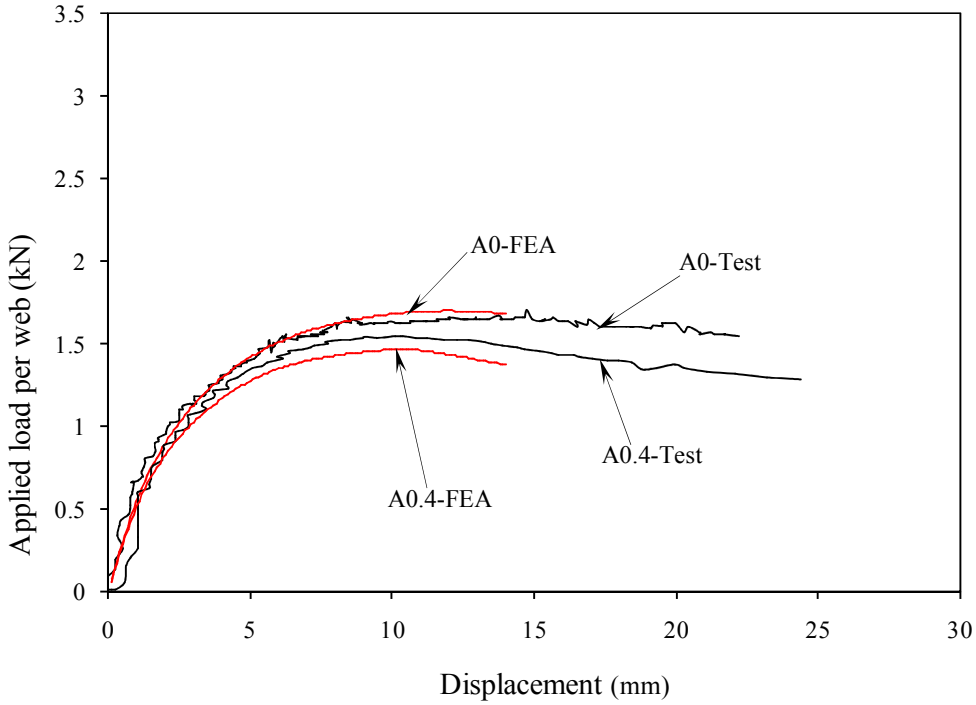

Figure B.5.3 Comparison web deformation curves for specimen ETF172×65×13-t1.3N32.5FR

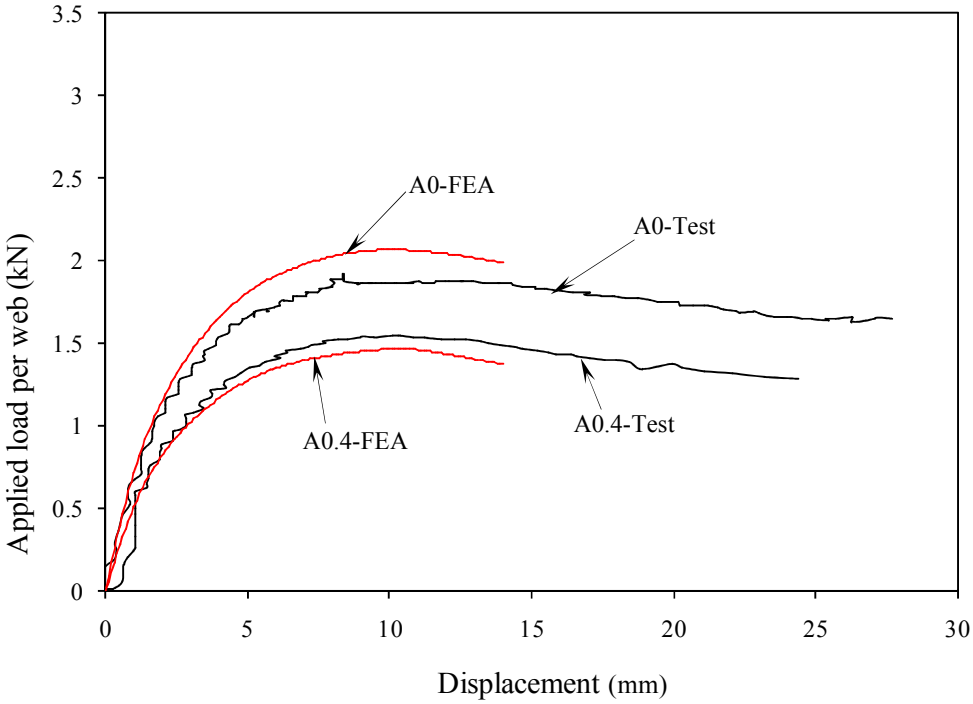

Figure B.5.4 Comparison web deformation curves for specimen ETF172×65×13-t1.3N65FR

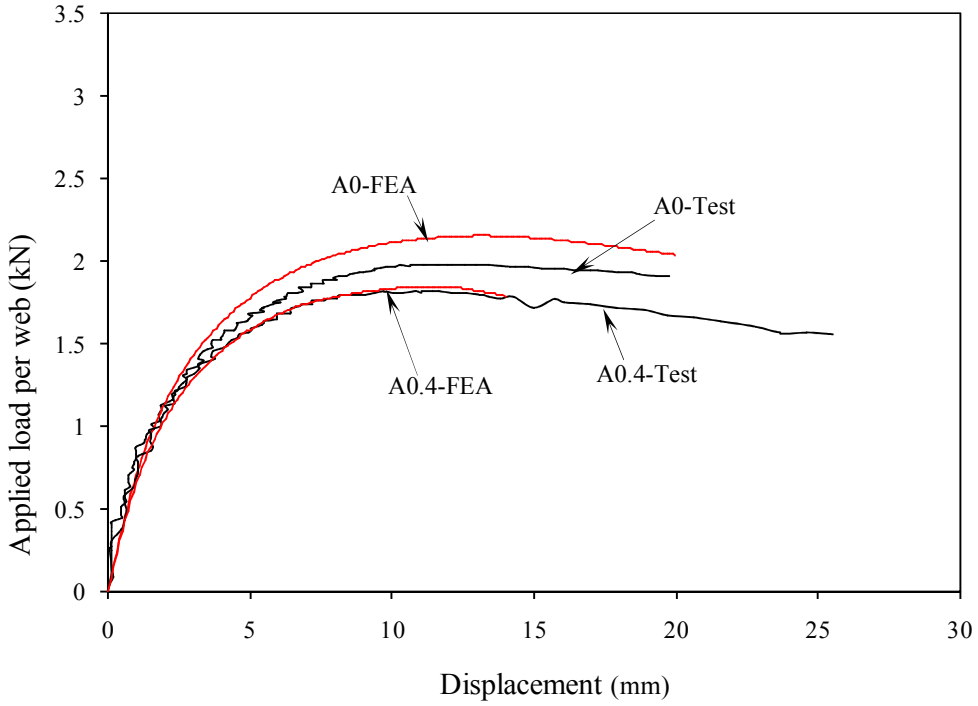

Figure B.5.5 Comparison web deformation curves for specimen ETF202×65×13-t1.4N32.5FR

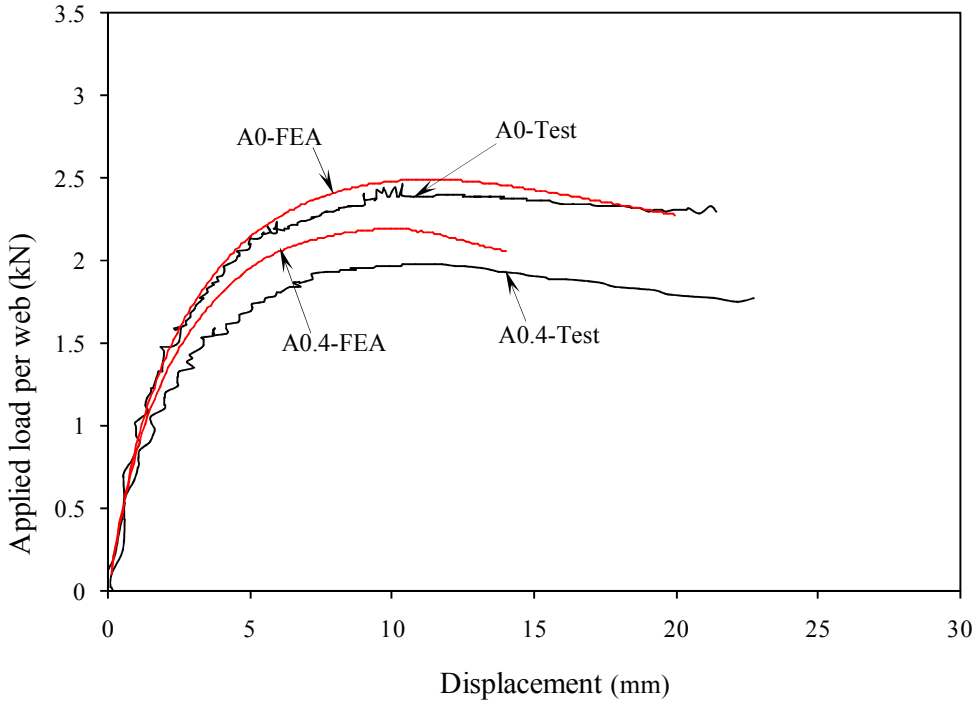

Figure B.5.6 Comparison web deformation curves for specimen ETF202×65×13-t1.4N65FR

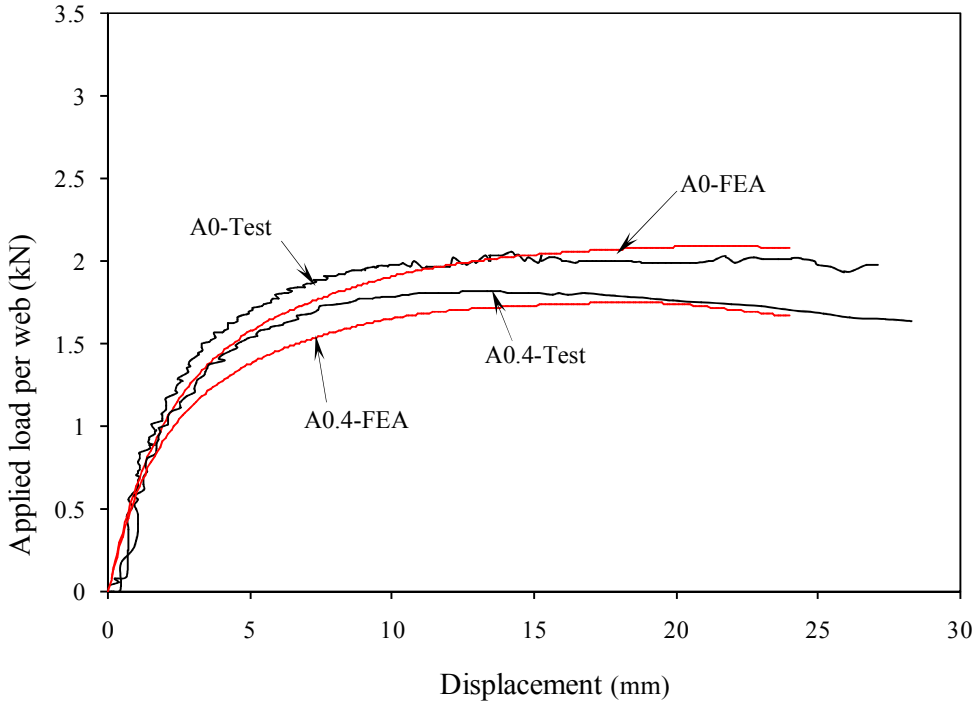

Figure B.5.7 Comparison web deformation curves for specimen ETF262×65×13-t1.6N32.5FR

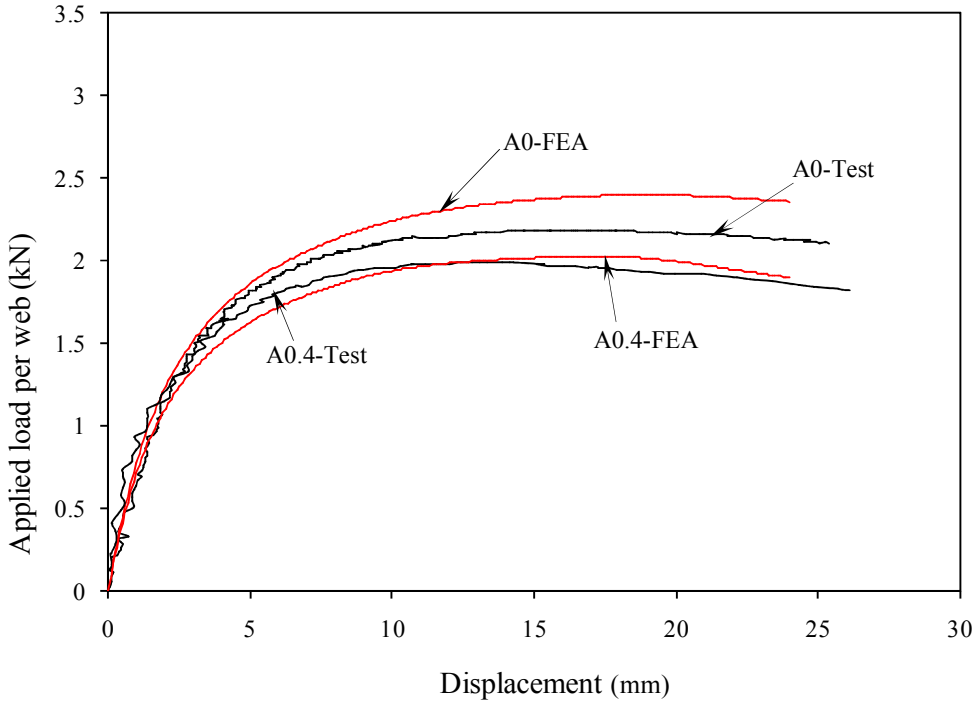

Figure B.5.8 Comparison web deformation curves for specimen ETF262×65×13-t1.6N65FR

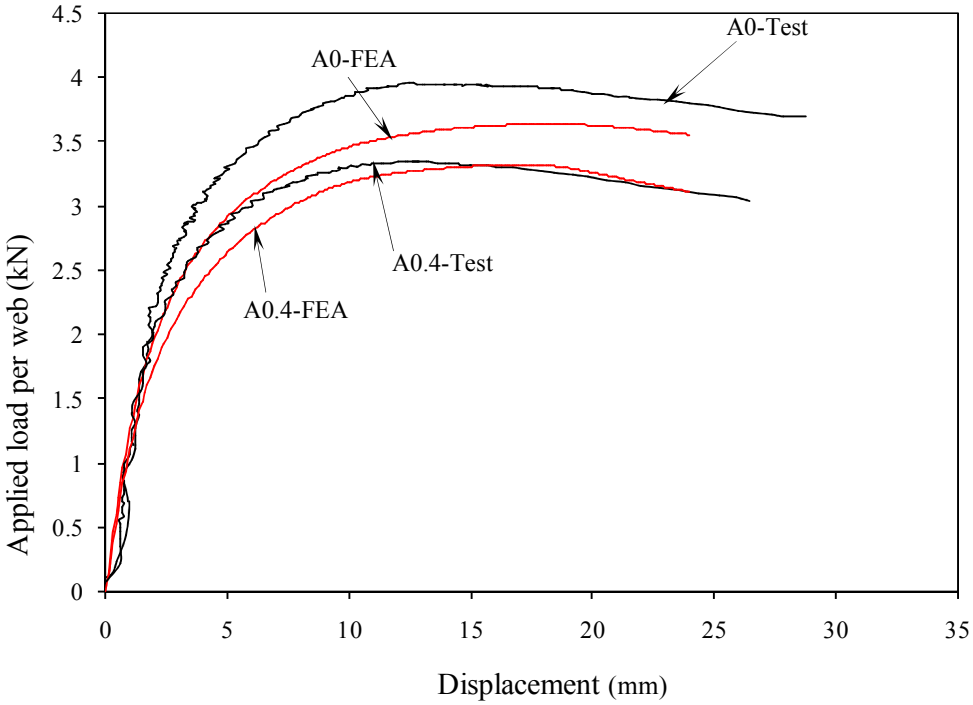

Figure B.5.9 Comparison web deformation curves for specimen ETF302×90×18-t2N90FR

1.6 Comparison curves for flanges unfastened under ETF loading condition (Type 2 holes)

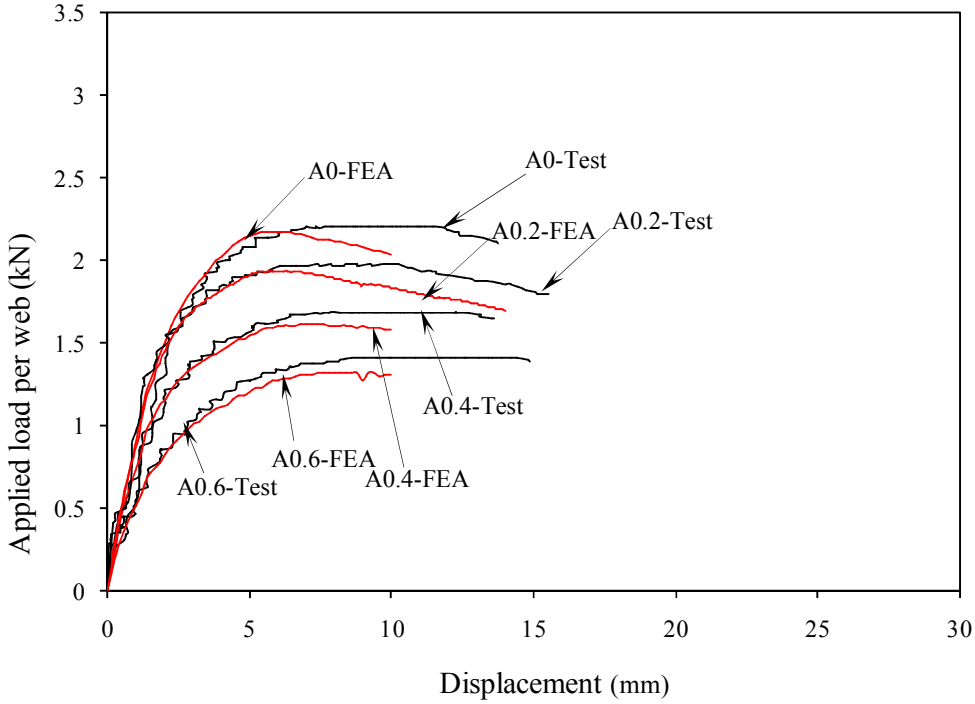

Figure B.6.1 Comparison web deformation curves for specimen ETF142×60×13-t1.3MN90FR

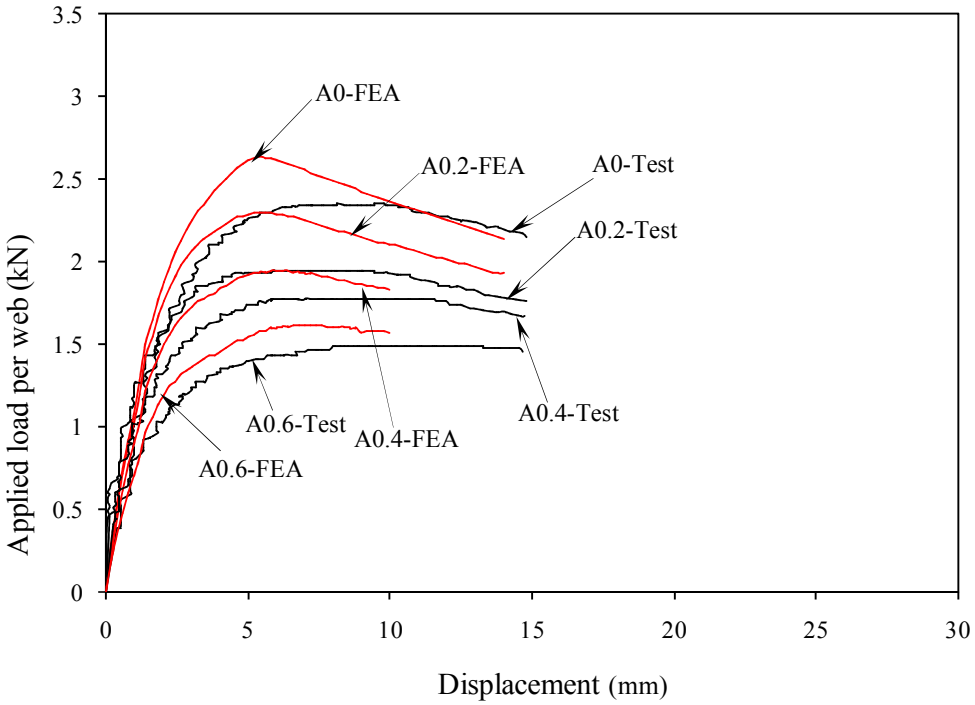

Figure B.6.2 Comparison web deformation curves for specimen ETF142×60×13-t13MN120FR

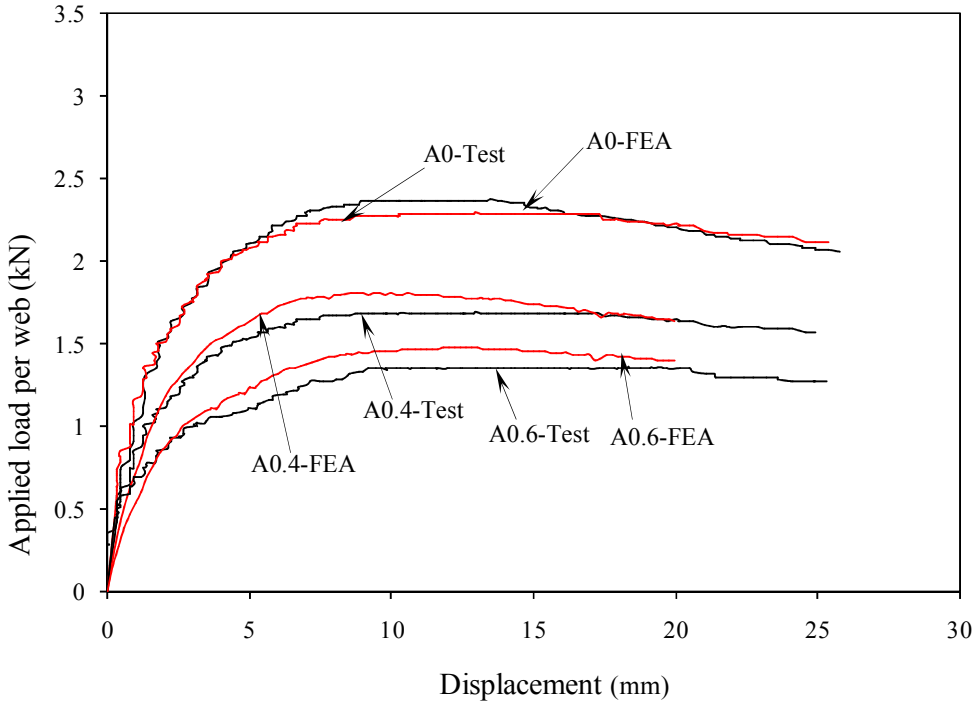

Figure B.6.3 Comparison web deformation curves for specimen ETF172×65×13-t1.3MN120FR

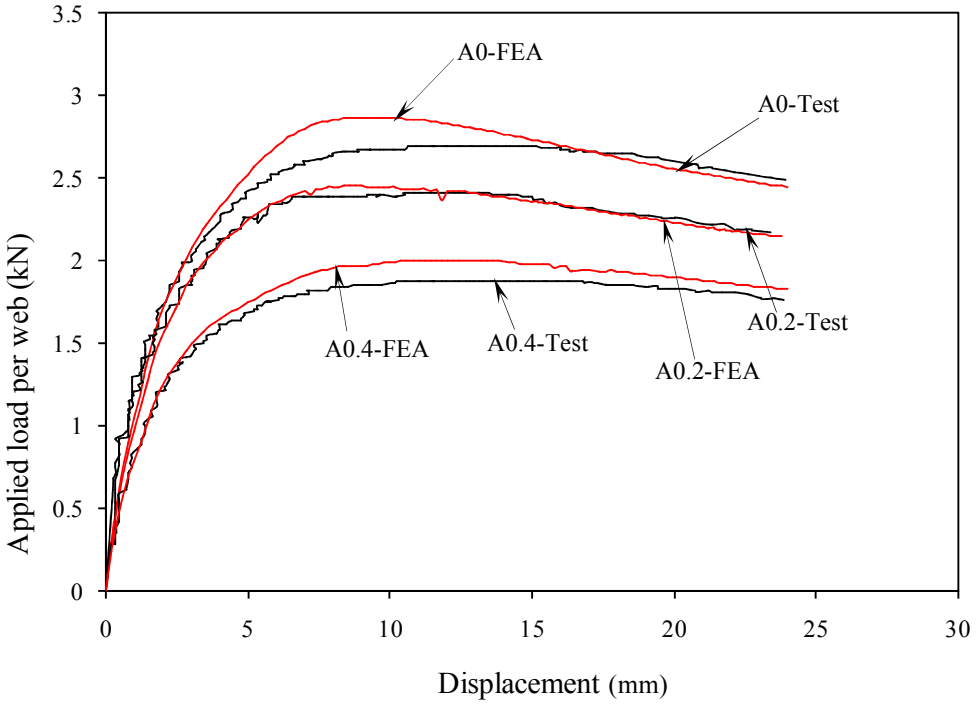

Figure B.6.4 Comparison web deformation curves for specimen ETF202×65×13-t1.4MN120FR

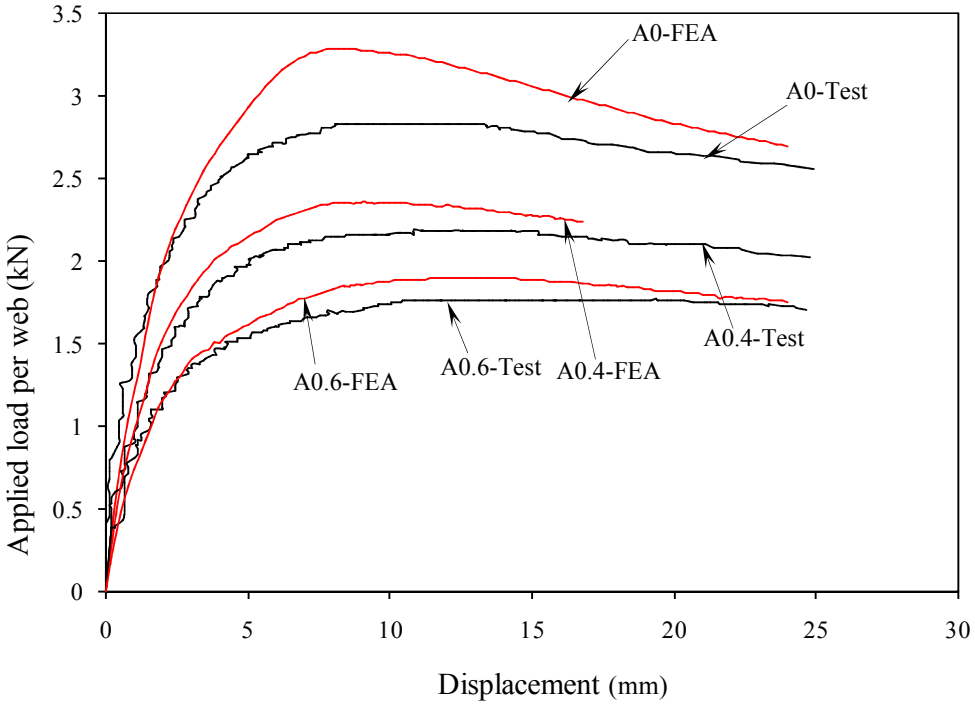

Figure B.6.5 Comparison web deformation curves for specimen 202×65×13-t1.4N150FR

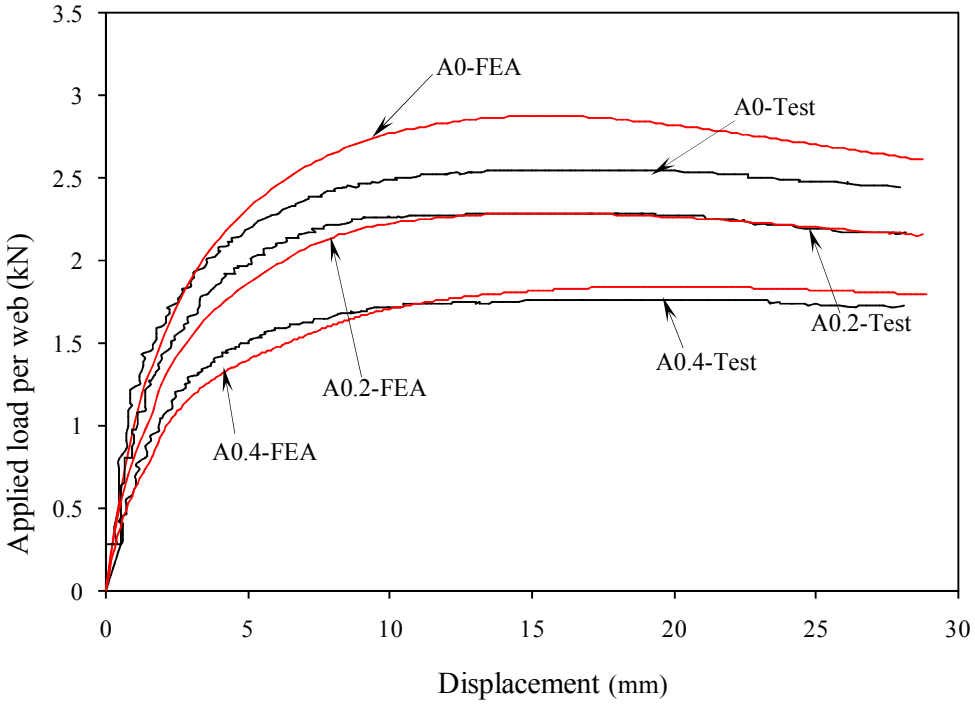

Figure B.6.6 Comparison web deformation curves for specimen ETF262×65×13-t1.6MN120FR

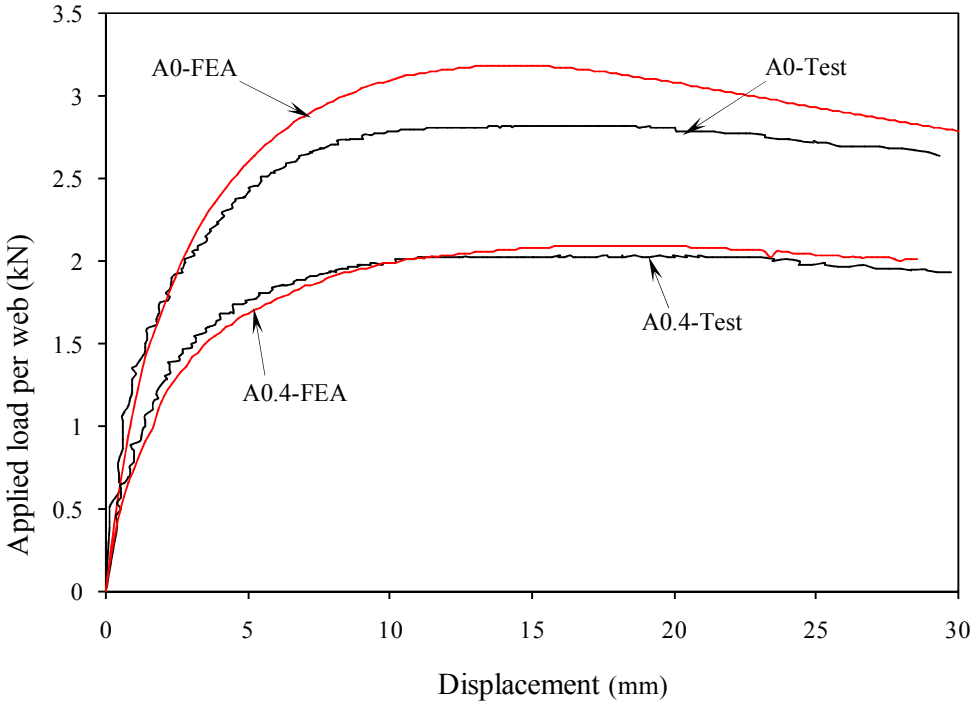

Figure B.6.7 Comparison web deformation curves for specimen ETF262×65×13-t1.6MN150FR

1.7 Comparison curves for flanges fastened under ETF loading condition (Type 1 holes)

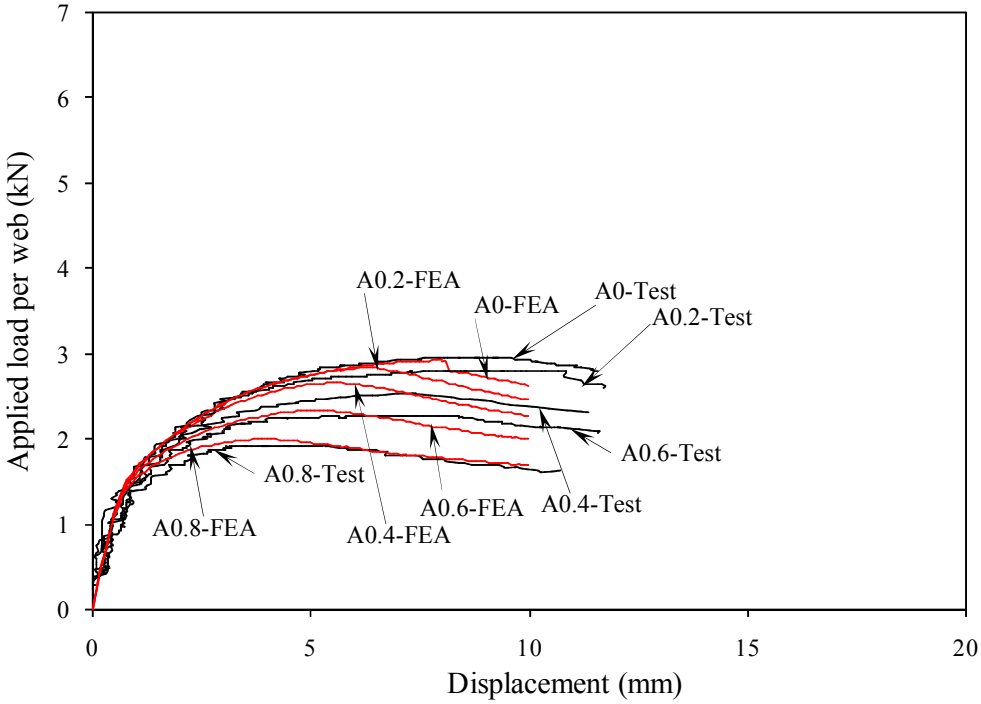

Figure B.7.1 Comparison web deformation curves for specimen ETF142×60×13-t1.3N30FX

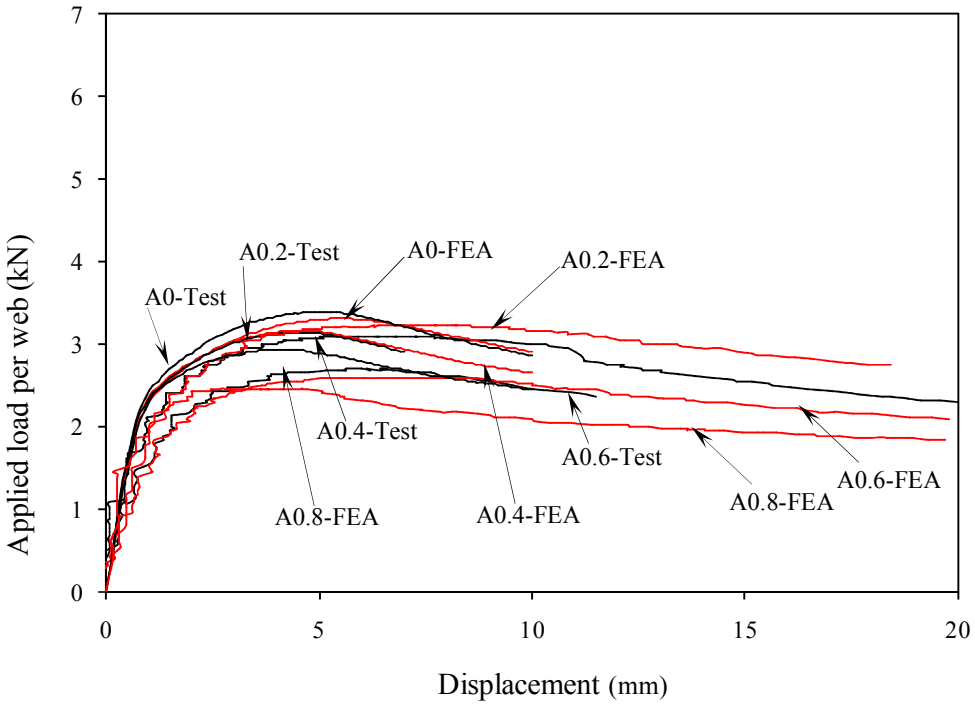

Figure B.7.2 Comparison web deformation curves for specimen ETF142×60×13-t13N60FX

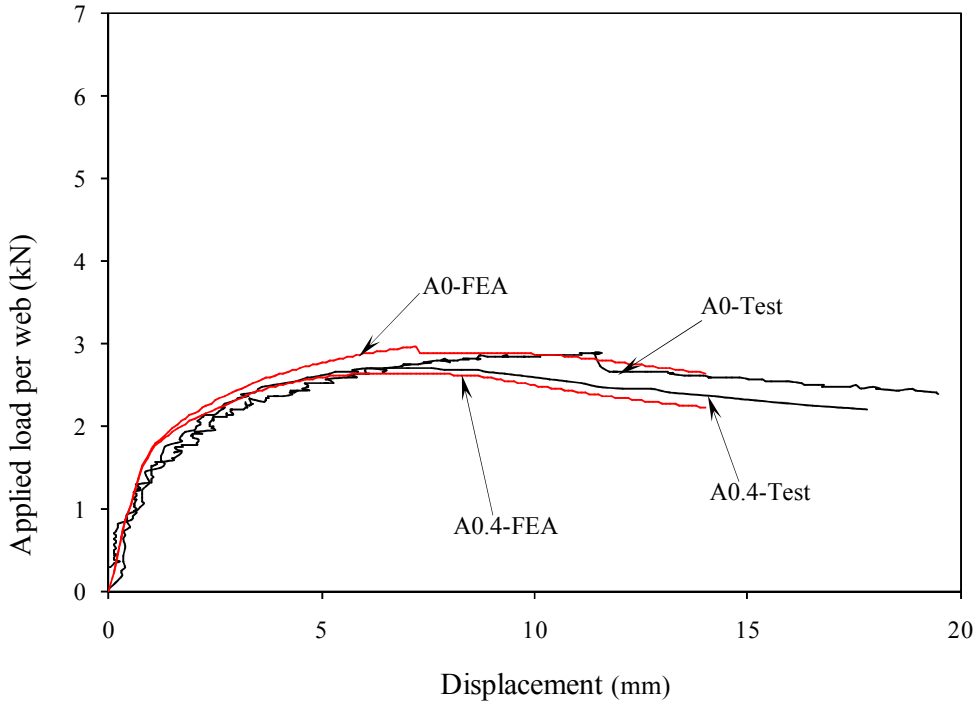

Figure B.7.3 Comparison web deformation curves for specimen ETF172×65×13-t1.3N32.5FX

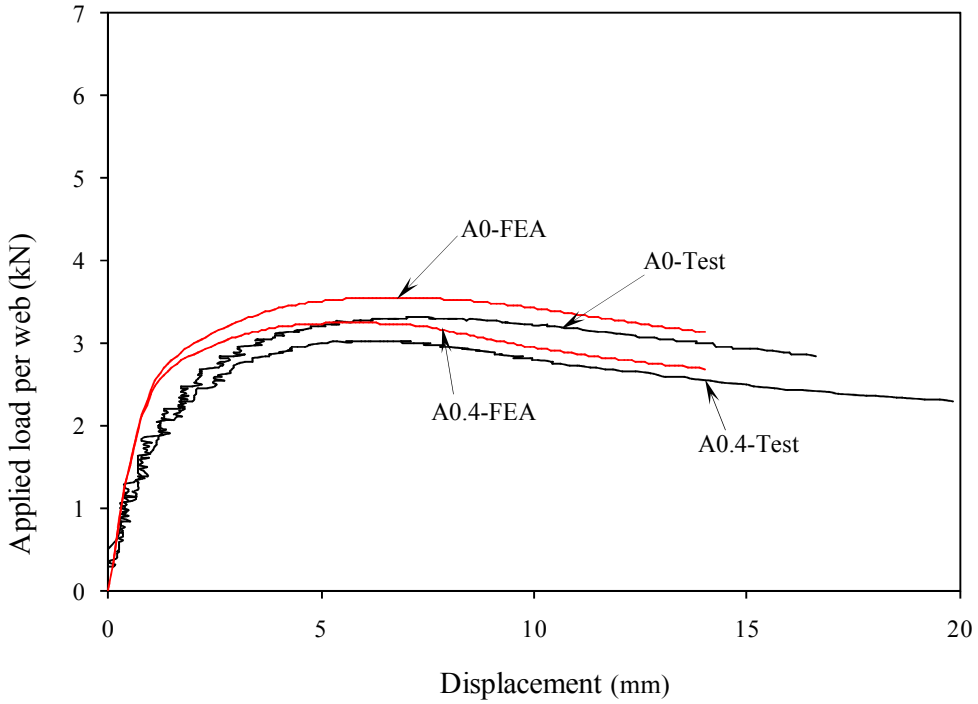

Figure B.7.4 Comparison web deformation curves for specimen ETF172×65×13-t1.3N65FX

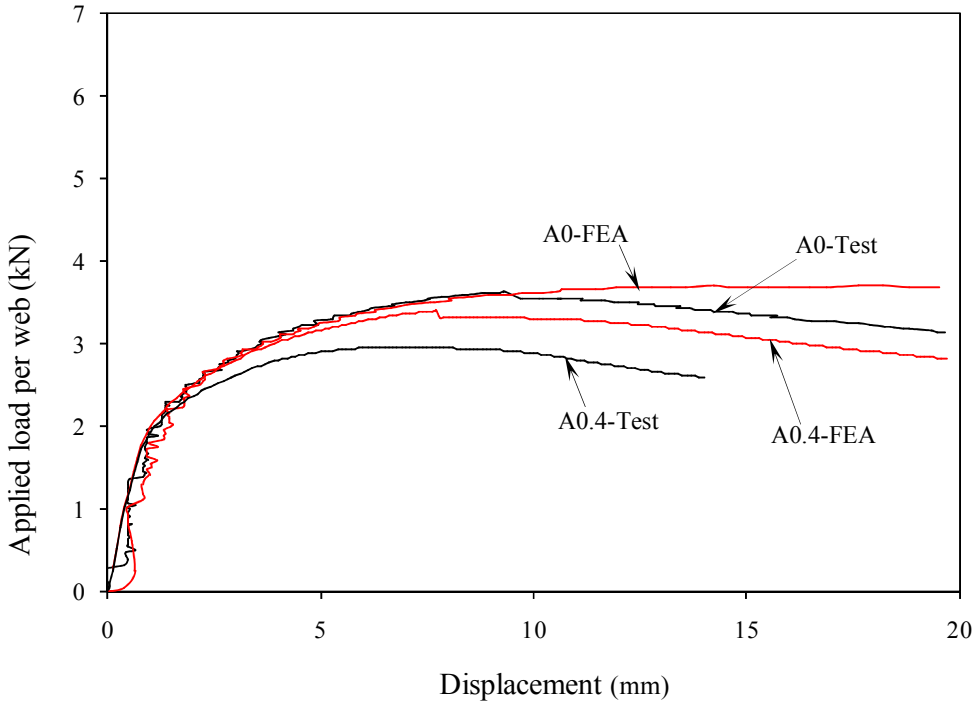

Figure B.7.5 Comparison web deformation curves for specimen ETF202×65×13-t1.4N32.5FX

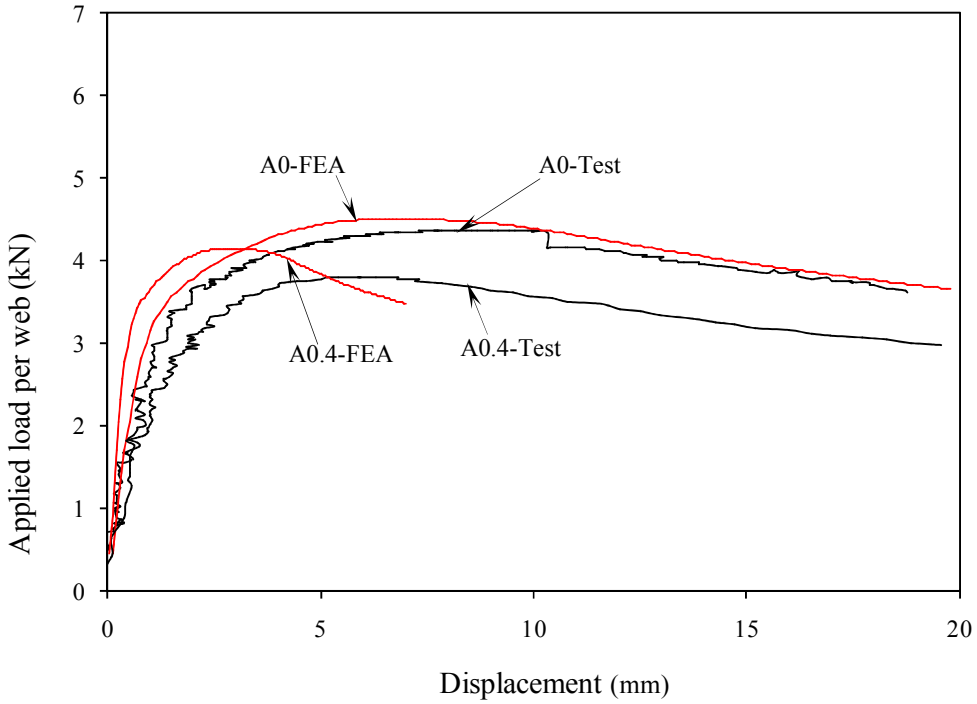

Figure B.7.6 Comparison web deformation curves for specimen ETF202×65×13-t1.4N65FX

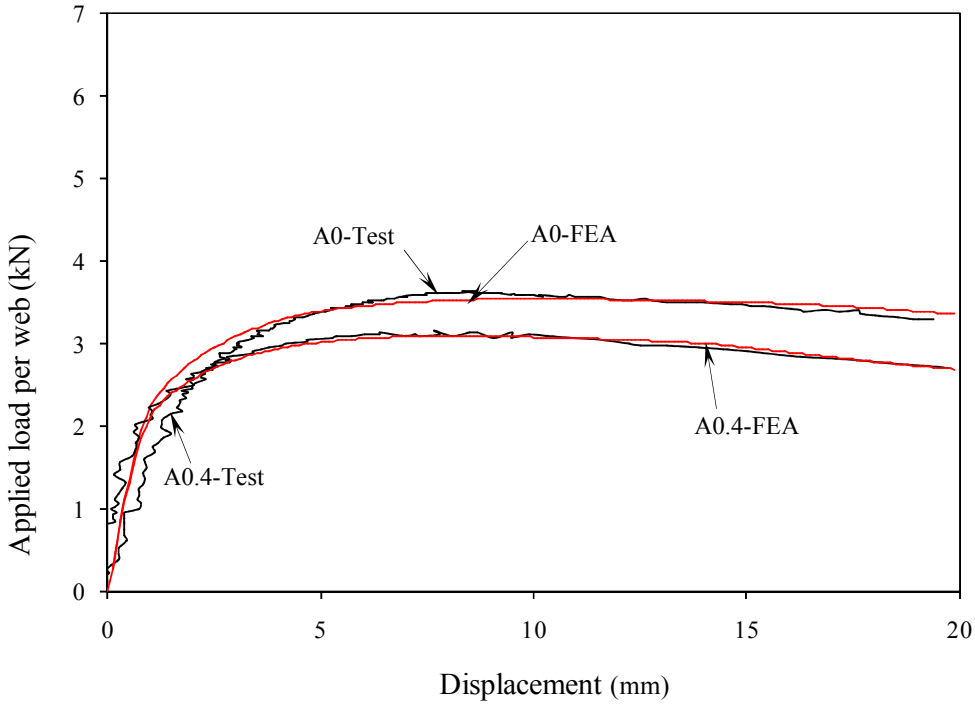

Figure B.7.7 Comparison web deformation curves for specimen ETF262×65×13-t1.6N32.5FX

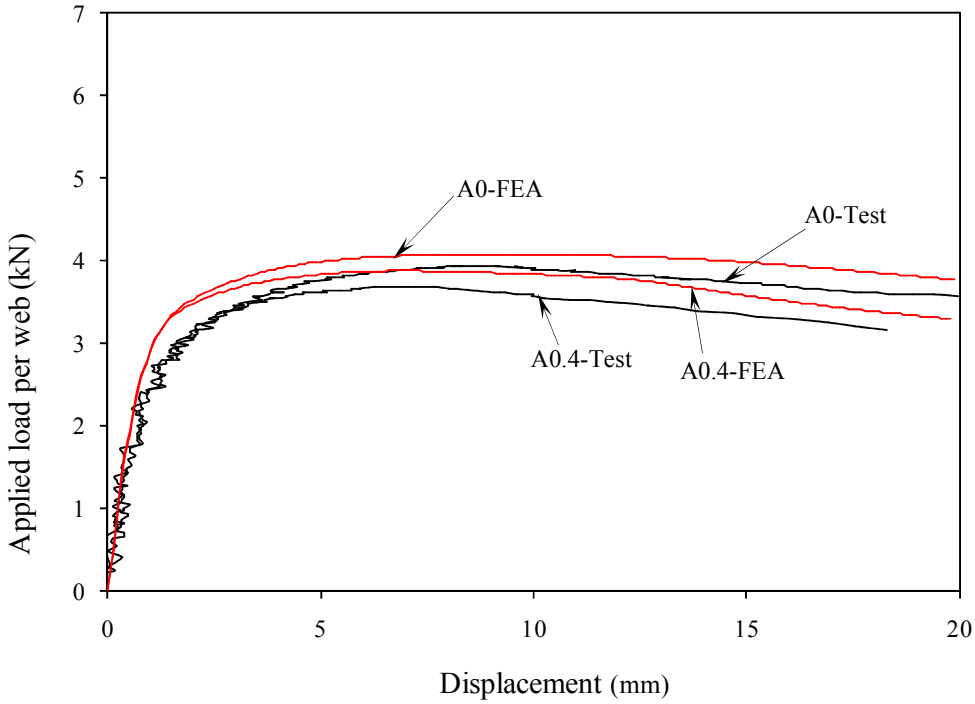

Figure B.7.8 Comparison web deformation curves for specimen ETF262×65×13-t1.6N65FX

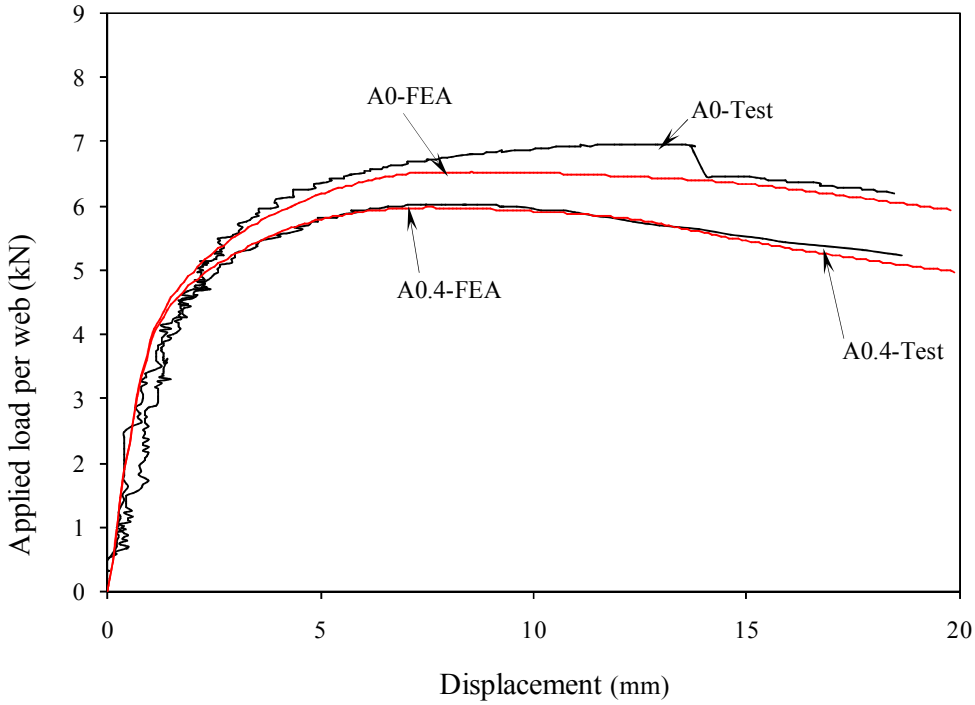

Figure B.7.9 Comparison web deformation curves for specimen ETF302×90×18-t2N44FX

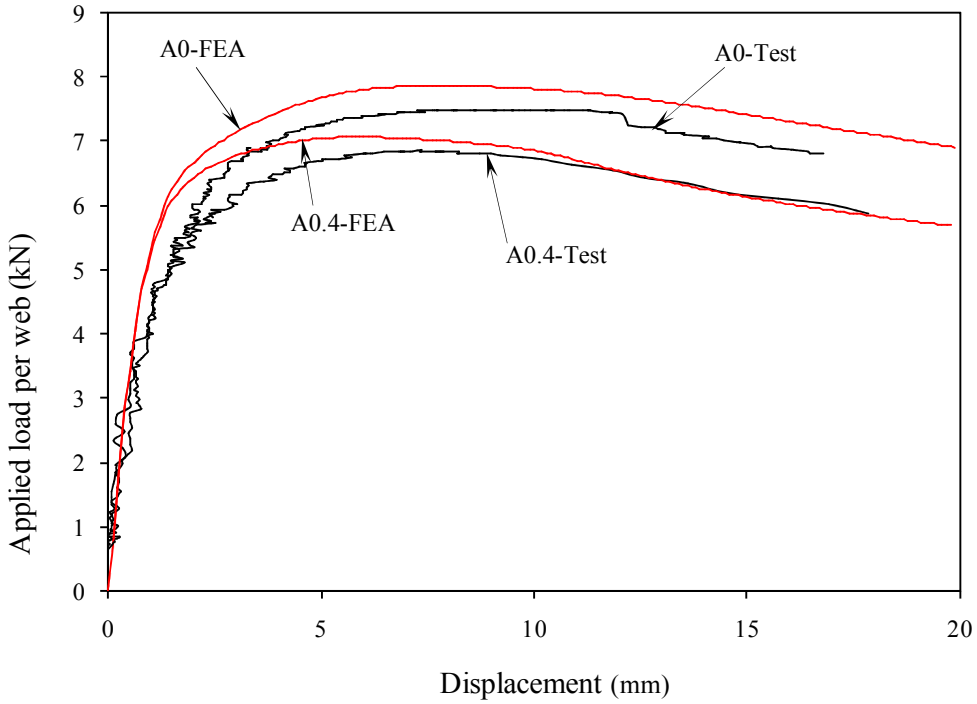

Figure B.7.10 Comparison web deformation curves for specimen ETF302×90×18-t2N90FX

1.8 Comparison curves for flanges fastened under ETF loading condition (Type 2 holes)

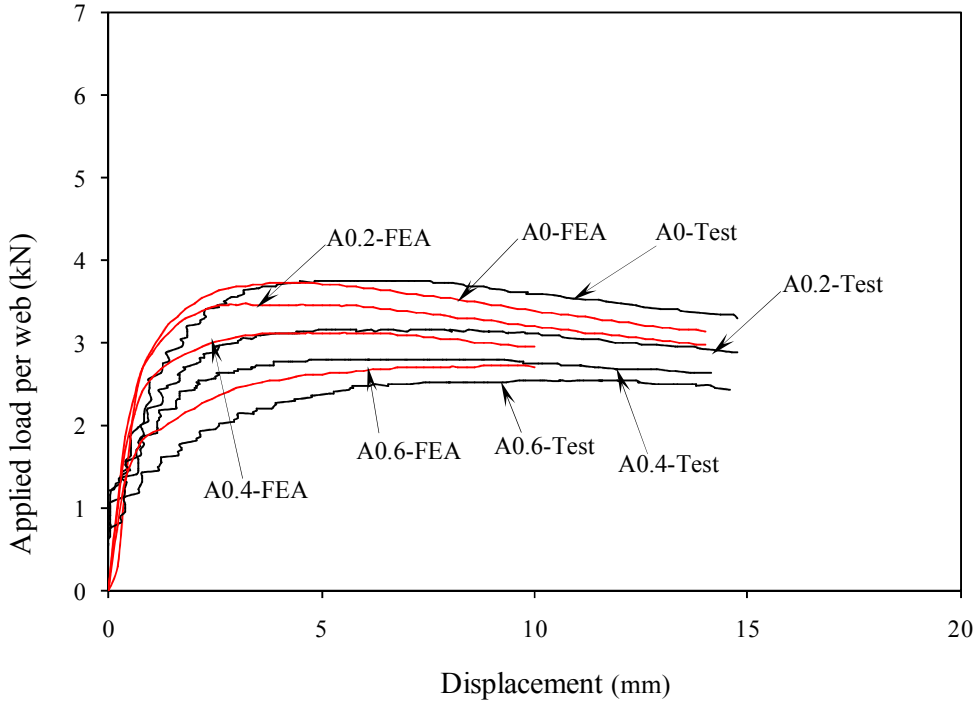

Figure B.8.1 Comparison web deformation curves for specimen ETF142×60×13-t1.3MN90FX

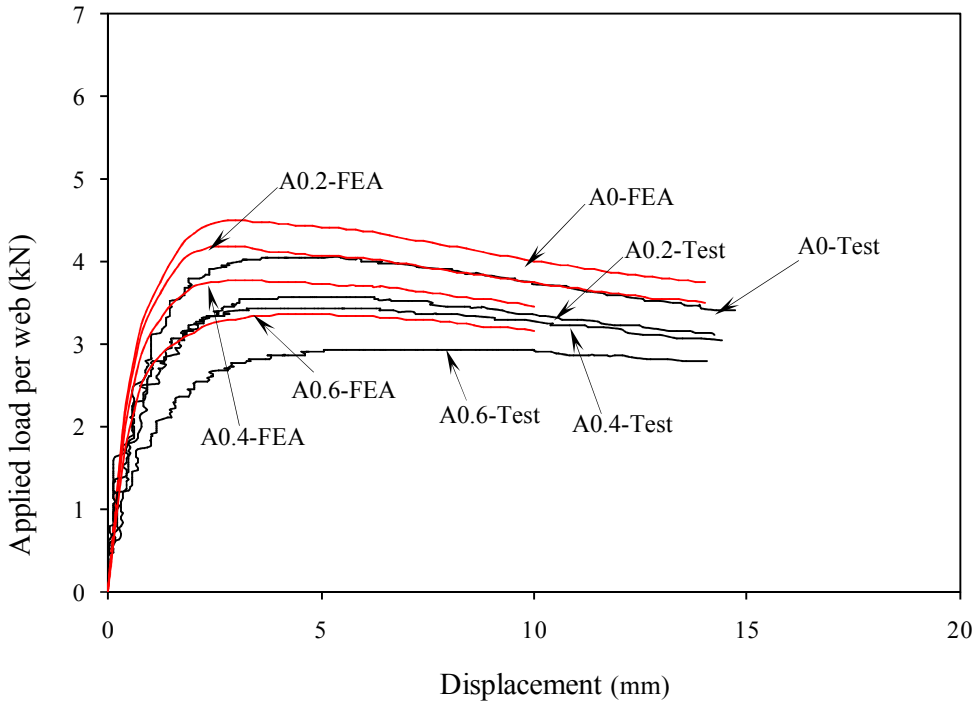

Figure B.8.2 Comparison web deformation curves for specimen ETF142×60×13-t13MN120FX

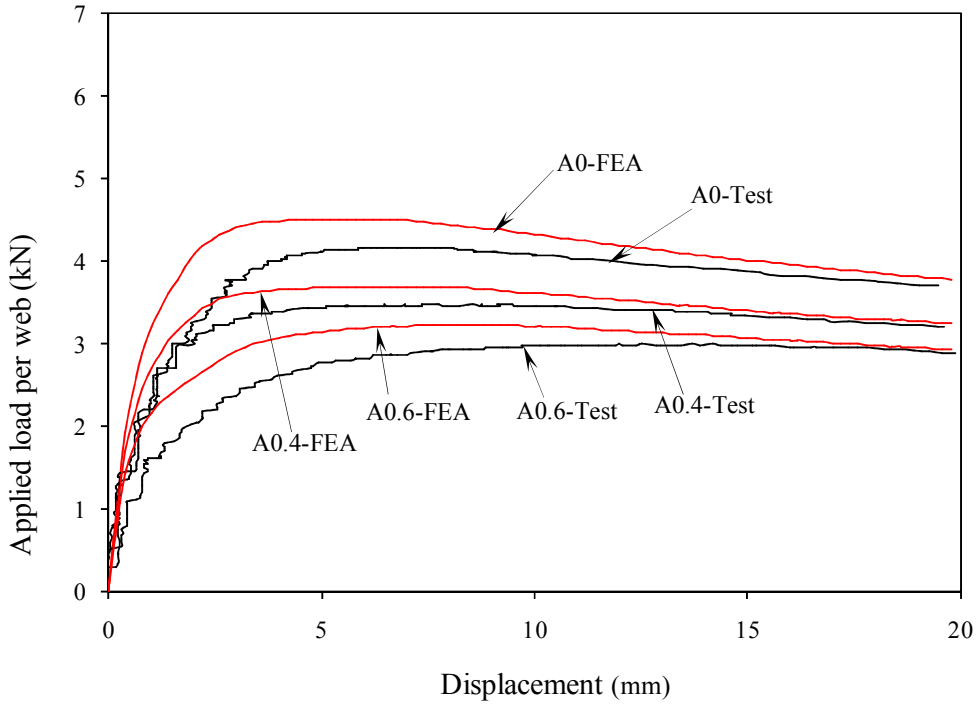

Figure B.8.3 Comparison web deformation curves for specimen ETF172×65×13-t1.3MN120FX

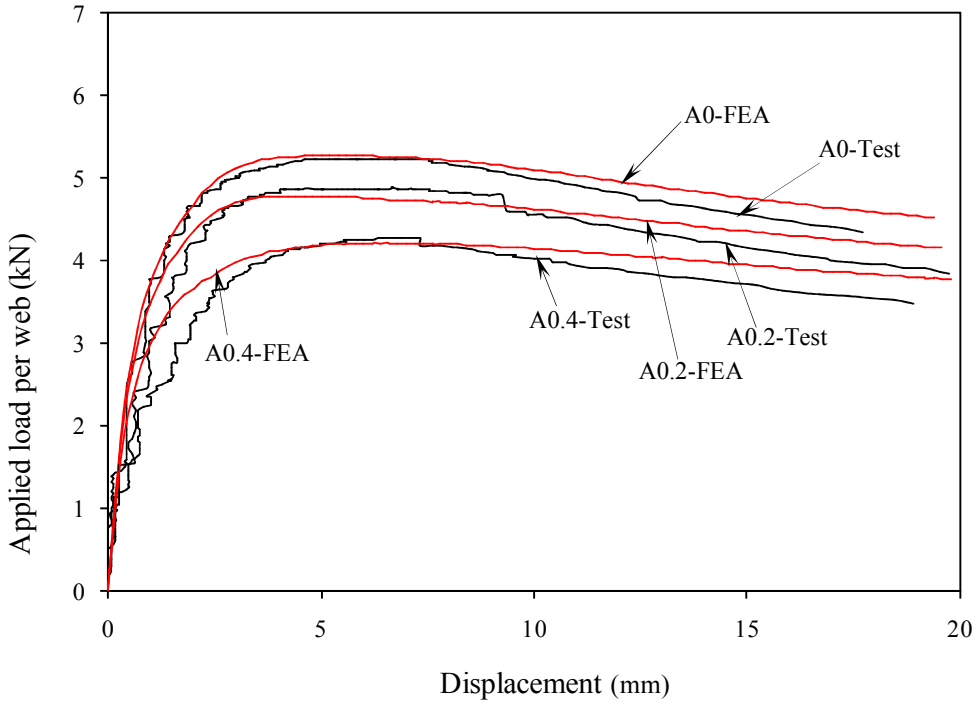

Figure B.8.4 Comparison web deformation curves for specimen ETF202×65×13-t1.4MN120FX

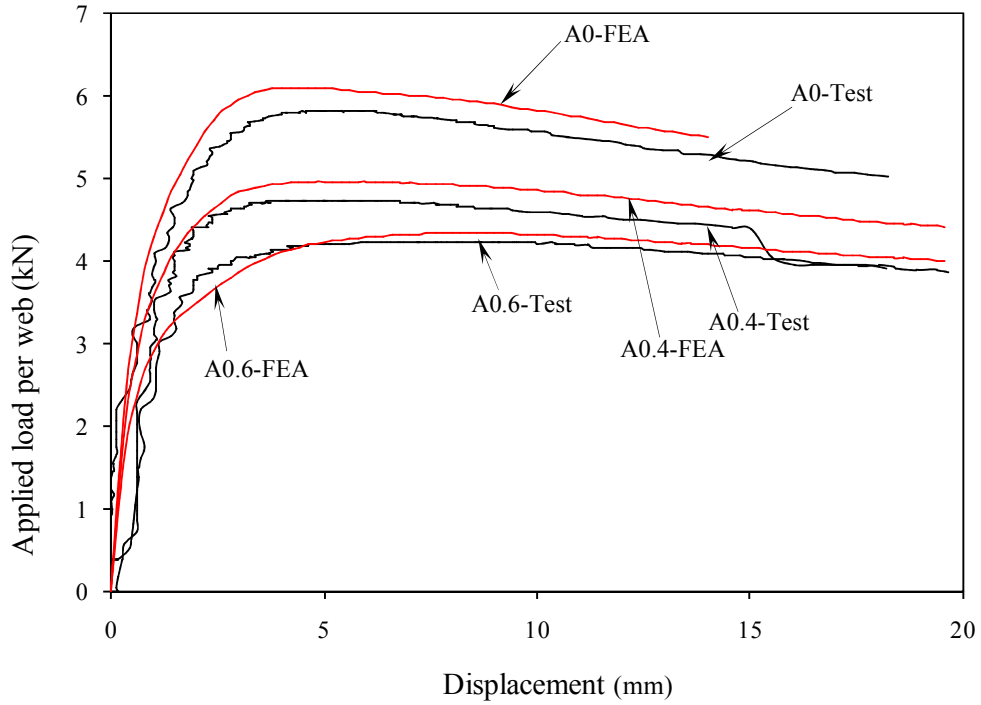

Figure B.8.5 Comparison web deformation curves for specimen 202×65×13-t1.4N150FX

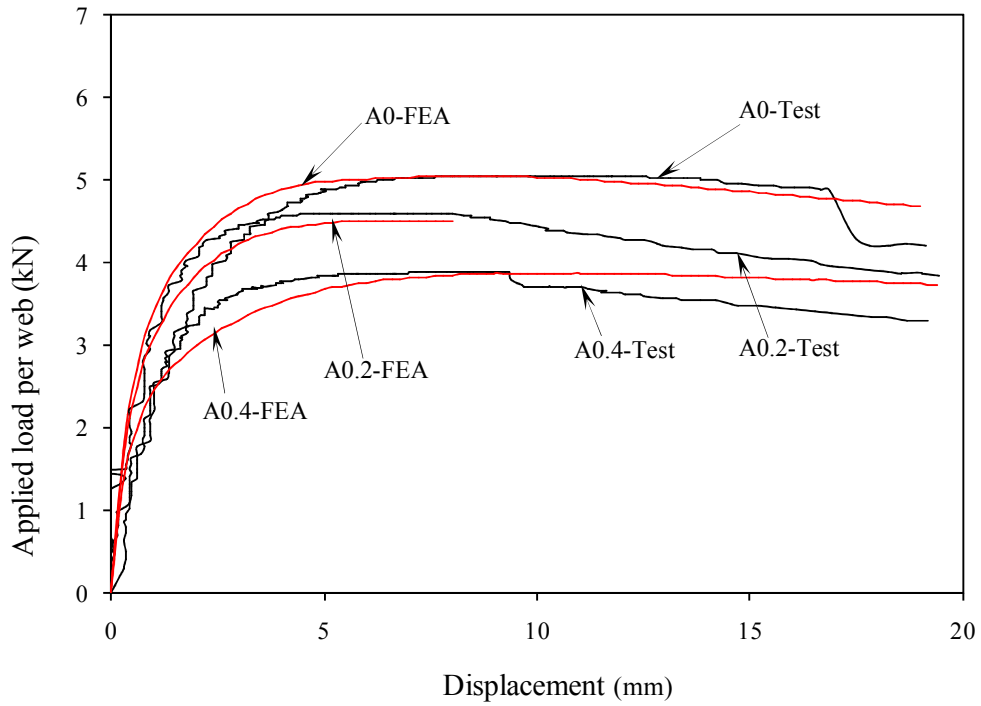

Figure B.8.6 Comparison web deformation curves for specimen ETF262×65×13-t1.6MN120FX

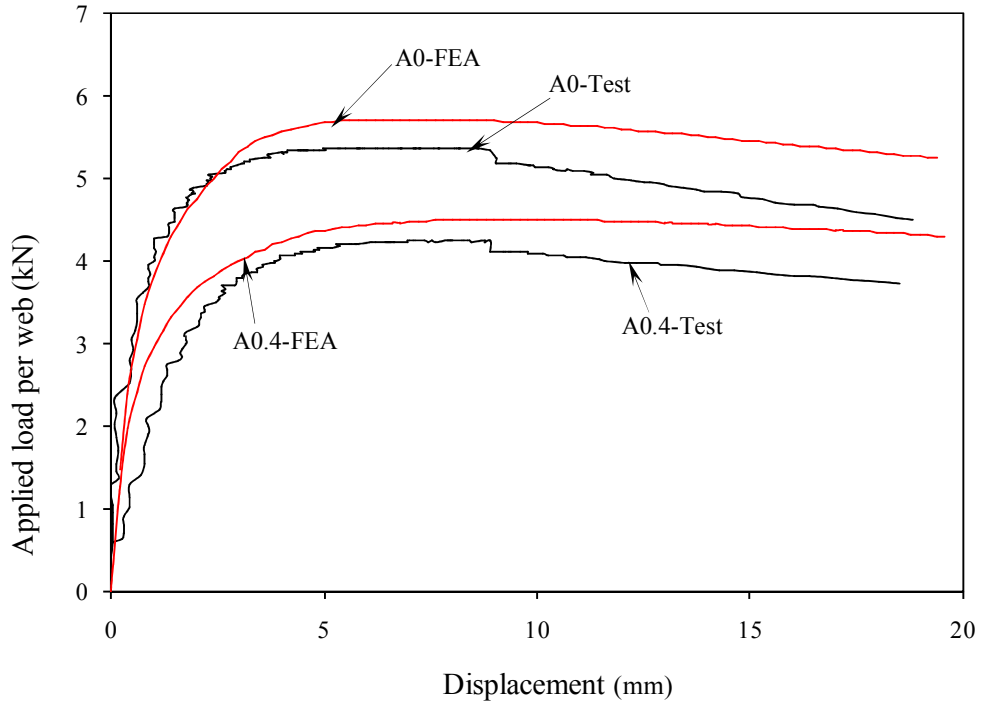

Figure B.8.7 Comparison web deformation curves for specimen ETF262×65×13-t1.6MN150FX

Appendix C :

Comparison web deformation shape predicted from the finite element analysis with the experiment tests.

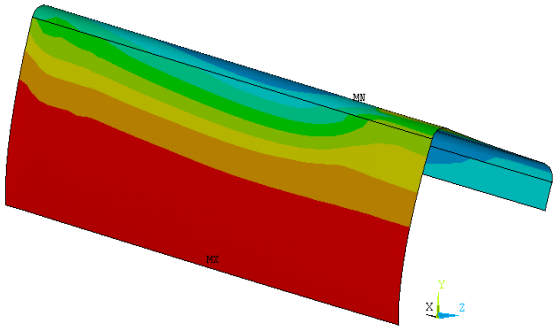


(a) Comparison deformation shape for without holes

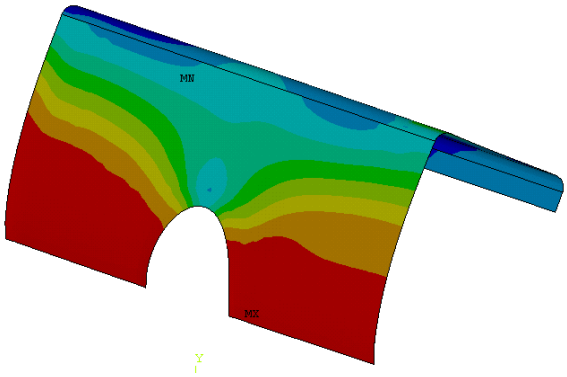


(b) Comparison deformation shape for type-1 holes

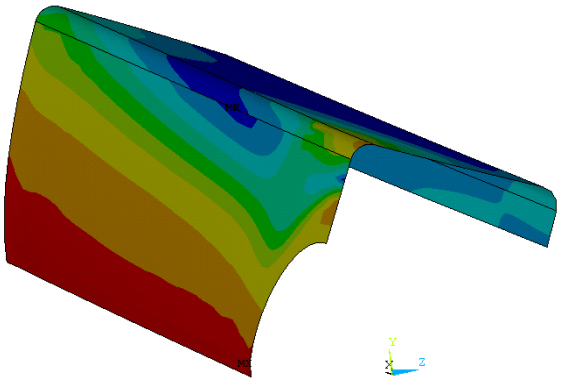
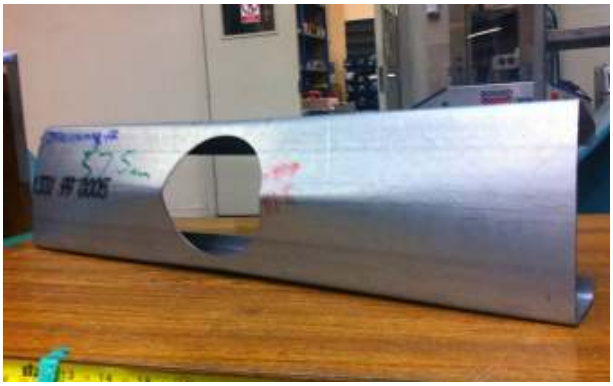

(c) Comparison deformation shape for type-2 holes

Figure C.1 Comparison web deformation shape for flanges unfastened under ITF loading condition

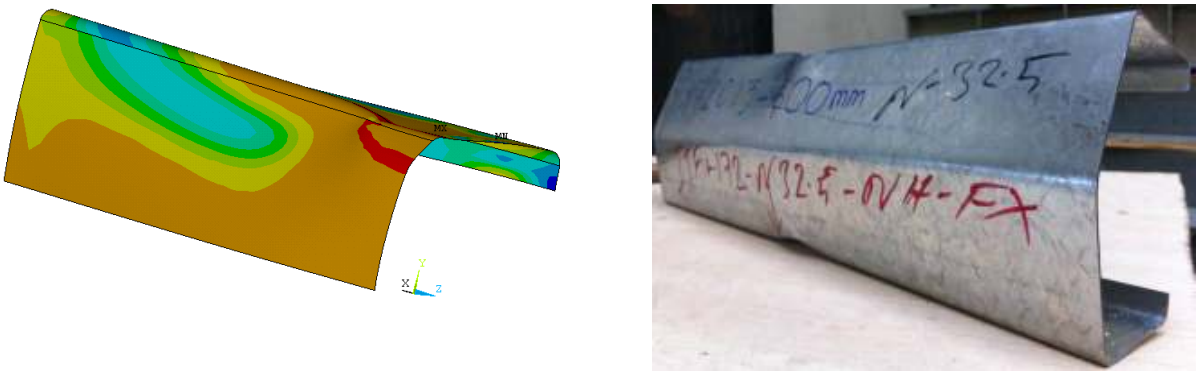

(a) Comparison deformation shape for without holes

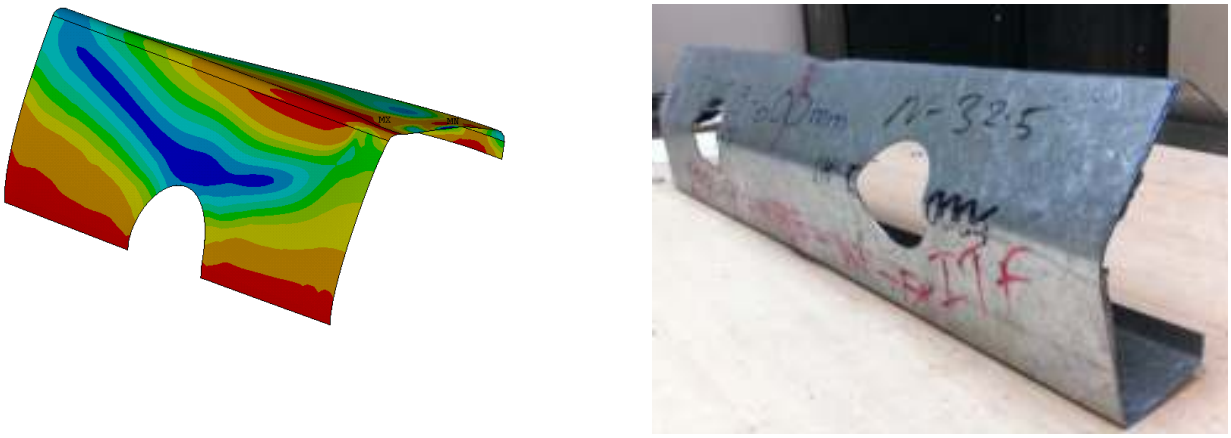

(b) Comparison deformation shape for type-1 holes

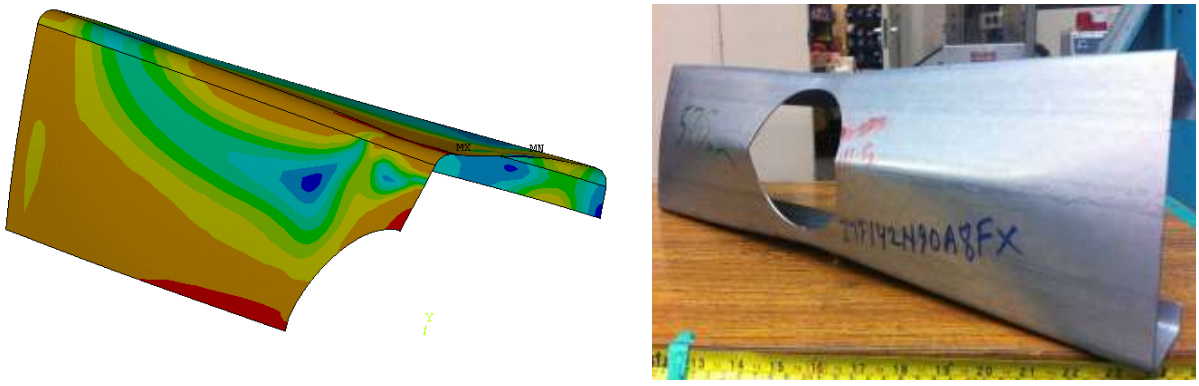

(c) Comparison deformation shape for type-2 holes

Figure C.2 Comparison web deformation shape for flanges fastened under ITF loading condition

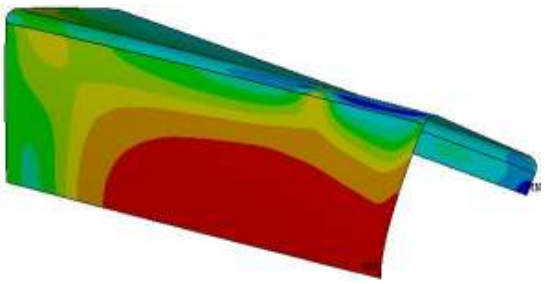

(a) Comparison deformation shape for without holes

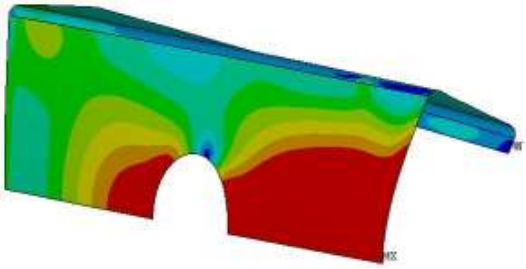

(b) Comparison deformation shape for type-1 holes

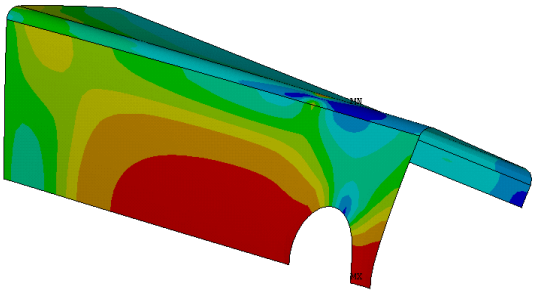

(c) Comparison deformation shape for type-2 holes

Figure C.3 Comparison web deformation shape for flanges unfastened under ETF loading condition

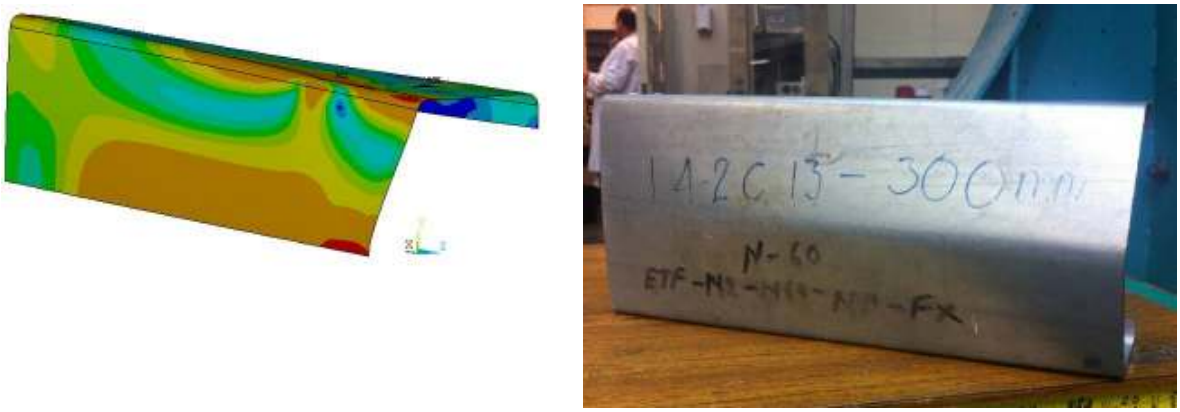

(a) Comparison deformation shape for without holes

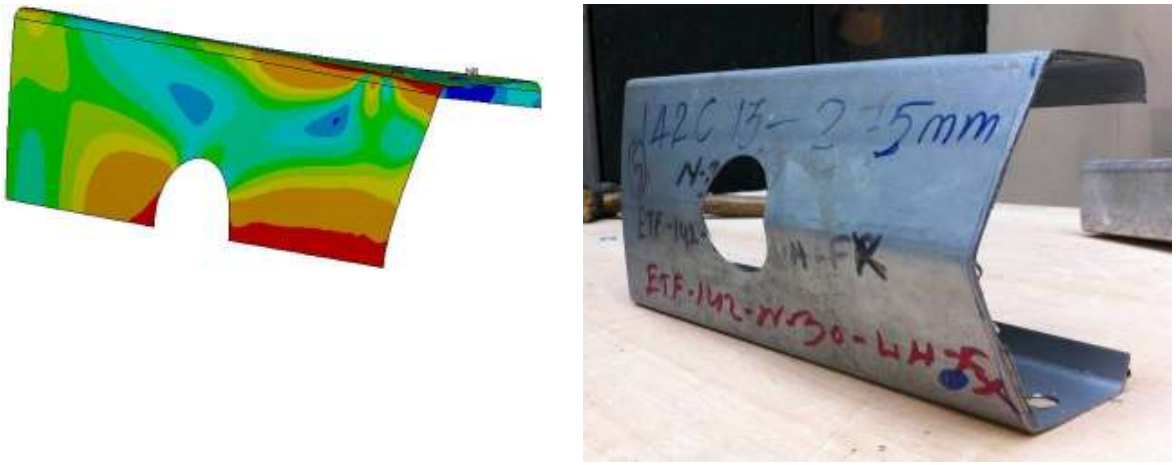

(b) Comparison deformation shape for type-1 holes

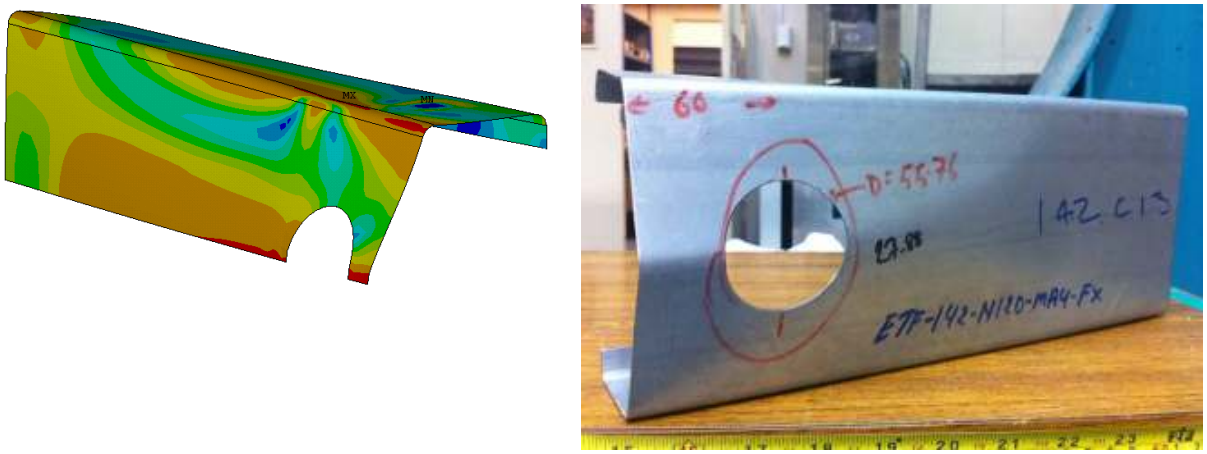

(c) Comparison deformation shape for type-2 holes

Figure C.4 Comparison web deformation shape for flanges fastened under ETF loading condition

Appendix D :

Comparison finite element analysis with the experiment tests results with proposed design equations.

D.1 Statistical analysis for the comparison of the strength reduction factor for flanges unfastened under ITF loading condition (Type 1 holes)

Specimen	Holes diameter Ratio (a/h)	Holes distance Ratio (x/h)	Failure load without holes P (kN)	Failure load with holes P(Holes) (kN)	Reduction factor R= P(Holes) / P	Proposed reduction factor Rp = 1.04-0.68 (a/h)+0.023 (x/h)	Comparison with proposed reduction factor R/Rp
ITF202x65x13-t1.4N32.5A0.2FR	0.20	0.85	6.90	6.32	0.92	0.92	0.99
ITF202x65x13-t1.4N32.5A0.4FR	0.40	0.85	6.90	5.45	0.79	0.79	1.00
ITF202x65x13-t1.4N32.5A0.6FR	0.60	0.85	6.90	4.55	0.66	0.65	1.01
ITF202x65x13-t1.4N32.5A0.8FR	0.80	0.85	6.90	3.55	0.52	0.52	1.00
ITF202x65x13-t2.0N32.5A0.2FR	0.20	0.85	17.81	15.90	0.89	0.92	0.97
ITF202x65x13-t2.0N32.5A0.4FR	0.40	0.85	17.81	13.54	0.76	0.79	0.97
ITF202x65x13-t2.0N32.5A0.6FR	0.60	0.85	17.81	11.07	0.62	0.65	0.96
ITF202x65x13-t2.0N32.5A0.8FR	0.80	0.85	17.81	8.41	0.47	0.51	0.92
ITF202x65x13-t2.5N32.5A0.2FR	0.20	0.86	30.61	27.25	0.89	0.92	0.97
ITF202x65x13-t2.5N32.5A0.4FR	0.40	0.86	30.61	22.79	0.74	0.78	0.95
ITF202x65x13-t2.5N32.5A0.6FR	0.61	0.86	30.61	18.41	0.60	0.65	0.93
ITF202x65x13-t2.5N32.5A0.8FR	0.81	0.86	30.61	14.10	0.46	0.51	0.90
ITF202x65x13-t3.0N32.5A0.2FR	0.20	0.86	43.82	41.39	0.94	0.92	1.02
ITF202x65x13-t3.0N32.5A0.4FR	0.41	0.86	43.82	34.06	0.78	0.78	0.99
ITF202x65x13-t3.0N32.5A0.6FR	0.61	0.86	43.82	27.49	0.63	0.65	0.97
ITF202x65x13-t3.0N32.5A0.8FR	0.81	0.86	43.82	21.24	0.48	0.51	0.96
ITF202x65x13-t4.0N32.5A0.2FR	0.21	0.87	86.63	74.24	0.86	0.92	0.93
ITF202x65x13-t4.0N32.5A0.4FR	0.41	0.87	86.63	61.85	0.71	0.78	0.91
ITF202x65x13-t4.0N32.5A0.6FR	0.62	0.87	86.63	49.66	0.57	0.64	0.89
ITF202x65x13-t4.0N32.5A0.8FR	0.82	0.87	86.63	38.58	0.45	0.50	0.89
ITF202x65x13-t5.0N32.5A0.2FR	0.21	0.88	129.05	112.71	0.87	0.92	0.95
ITF202x65x13-t5.0N32.5A0.4FR	0.41	0.88	129.05	96.37	0.75	0.78	0.96
ITF202x65x13-t5.0N32.5A0.6FR	0.62	0.88	129.05	76.52	0.59	0.64	0.93
ITF202x65x13-t5.0N32.5A0.8FR	0.83	0.88	129.05	59.33	0.46	0.50	0.93
ITF202x65x13-t6.0N32.5A0.2FR	0.21	0.89	185.45	161.50	0.87	0.92	0.95
ITF202x65x13-t6.0N32.5A0.4FR	0.42	0.89	185.45	137.55	0.74	0.78	0.96
ITF202x65x13-t6.0N32.5A0.6FR	0.63	0.89	185.45	107.68	0.58	0.63	0.92
ITF202x65x13-t6.0N32.5A0.8FR	0.84	0.89	185.45	83.72	0.45	0.49	0.92
ITF202x65x13-t1.4N65A0.2FR	0.20	0.88	7.64	7.01	0.92	0.92	0.99
ITF202x65x13-t1.4N65A0.4FR	0.40	0.88	7.64	6.08	0.80	0.79	1.01
ITF202x65x13-t1.4N65A0.6FR	0.60	0.88	7.64	5.11	0.67	0.65	1.02
ITF202x65x13-t1.4N65A0.8FR	0.80	0.88	7.64	4.01	0.52	0.52	1.02
ITF202x65x13-t2.0N65A0.2FR	0.20	0.88	17.75	16.16	0.91	0.92	0.99
ITF202x65x13-t2.0N65A0.4FR	0.40	0.88	17.75	13.93	0.78	0.79	1.00
ITF202x65x13-t2.0N65A0.6FR	0.60	0.88	17.75	11.49	0.65	0.65	1.00
ITF202x65x13-t2.0N65A0.8FR	0.80	0.88	17.75	8.85	0.50	0.51	0.97
ITF202x65x13-t2.5N65A0.2FR	0.20	0.89	30.02	27.21	0.91	0.92	0.98
ITF202x65x13-t2.5N65A0.4FR	0.40	0.89	30.02	23.39	0.78	0.79	0.99
ITF202x65x13-t2.5N65A0.6FR	0.61	0.89	30.02	19.19	0.64	0.65	0.99
ITF202x65x13-t2.5N65A0.8FR	0.81	0.89	30.02	14.93	0.50	0.51	0.97
ITF202x65x13-t3.0N65A0.2FR	0.20	0.89	44.60	40.25	0.90	0.92	0.98
ITF202x65x13-t3.0N65A0.4FR	0.41	0.89	44.60	34.54	0.77	0.78	0.99
ITF202x65x13-t3.0N65A0.6FR	0.61	0.89	44.60	28.41	0.64	0.65	0.99
ITF202x65x13-t3.0N65A0.8FR	0.81	0.89	44.60	22.26	0.50	0.51	0.98
ITF202x65x13-t4.0N65A0.2FR	0.21	0.90	80.36	72.39	0.90	0.92	0.98
ITF202x65x13-t4.0N65A0.4FR	0.41	0.90	80.36	62.09	0.77	0.78	0.99
ITF202x65x13-t4.0N65A0.6FR	0.62	0.90	80.36	51.66	0.64	0.64	1.00
ITF202x65x13-t4.0N65A0.8FR	0.82	0.90	80.36	40.99	0.51	0.50	1.02
ITF202x65x13-t5.0N65A0.2FR	0.21	0.91	124.83	111.78	0.90	0.92	0.97
ITF202x65x13-t5.0N65A0.4FR	0.41	0.91	124.83	95.67	0.77	0.78	0.98
ITF202x65x13-t5.0N65A0.6FR	0.62	0.91	124.83	79.74	0.64	0.64	1.00
ITF202x65x13-t5.0N65A0.8FR	0.83	0.91	124.83	63.84	0.51	0.50	1.03
ITF202x65x13-t6.0N65A0.2FR	0.21	0.92	176.19	158.64	0.90	0.92	0.98
ITF202x65x13-t6.0N65A0.4FR	0.42	0.92	176.19	135.00	0.77	0.78	0.99

Continue-

Specimen	Holes diameter Ratio (a/h)	Holes distance Ratio (x/h)	Failure load without holes P (kN)	Failure load with holes P(Holes) (kN)	Reduction factor R= P(Holes) / P	Proposed reduction factor Rp = 1.04-0.68 (a/h)+0.023 (x/h)	Comparison with proposed reduction factor R/Rp
ITF202x65x13-t6.0N65A0.6FR	0.63	0.92	176.19	112.78	0.64	0.63	1.01
ITF202x65x13-t6.0N65A0.8FR	0.84	0.92	176.19	89.80	0.51	0.49	1.04
ITF302x90x18-t2N44A0.2FR	0.20	0.83	12.39	11.43	0.92	0.92	1.00
ITF302x90x18-t2N44A0.4FR	0.40	0.83	12.39	9.84	0.79	0.79	1.01
ITF302x90x18-t2N44A0.6FR	0.60	0.83	12.39	8.17	0.66	0.65	1.01
ITF302x90x18-t2N44A0.8FR	0.80	0.83	12.39	6.37	0.51	0.52	1.00
ITF302x90x18-t2.5N44A0.2FR	0.20	0.84	24.93	22.73	0.91	0.92	0.99
ITF302x90x18-t2.5N44A0.4FR	0.40	0.84	24.93	19.47	0.78	0.79	0.99
ITF302x90x18-t2.5N44A0.6FR	0.60	0.84	24.93	15.97	0.64	0.65	0.99
ITF302x90x18-t2.5N44A0.8FR	0.80	0.84	24.93	12.06	0.48	0.51	0.94
ITF302x90x18-t3.0N44A0.2FR	0.20	0.84	39.89	35.96	0.90	0.92	0.98
ITF302x90x18-t3.0N44A0.4FR	0.40	0.84	39.89	30.54	0.77	0.79	0.98
ITF302x90x18-t3.0N44A0.6FR	0.60	0.84	39.89	24.74	0.62	0.65	0.96
ITF302x90x18-t3.0N44A0.8FR	0.81	0.84	39.89	18.64	0.47	0.51	0.91
ITF302x90x18-t4.0N44A0.2FR	0.20	0.84	74.49	70.39	0.94	0.92	1.03
ITF302x90x18-t4.0N44A0.4FR	0.41	0.84	74.49	59.05	0.79	0.78	1.01
ITF302x90x18-t4.0N44A0.6FR	0.61	0.84	74.49	47.49	0.64	0.65	0.99
ITF302x90x18-t4.0N44A0.8FR	0.81	0.84	74.49	36.24	0.49	0.51	0.96
ITF302x90x18-t5.0N44A0.2FR	0.20	0.85	115.07	112.87	0.98	0.92	1.07
ITF302x90x18-t5.0N44A0.4FR	0.41	0.85	115.07	94.77	0.82	0.78	1.05
ITF302x90x18-t5.0N44A0.6FR	0.61	0.85	115.07	76.25	0.66	0.64	1.03
ITF302x90x18-t5.0N44A0.8FR	0.82	0.85	115.07	58.66	0.51	0.50	1.01
ITF302x90x18-t6.0N44A0.2FR	0.21	0.86	160.08	158.53	0.99	0.92	1.08
ITF302x90x18-t6.0N44A0.4FR	0.41	0.86	160.08	137.45	0.86	0.78	1.10
ITF302x90x18-t6.0N44A0.6FR	0.62	0.86	160.08	109.76	0.69	0.64	1.07
ITF302x90x18-t6.0N44A0.8FR	0.82	0.86	160.08	84.76	0.53	0.50	1.06
ITF302x90x18-t2N90A0.2FR	0.20	0.88	13.55	12.52	0.92	0.92	1.00
ITF302x90x18-t2N90A0.4FR	0.40	0.88	13.55	10.87	0.80	0.79	1.02
ITF302x90x18-t2N90A0.6FR	0.60	0.88	13.55	9.13	0.67	0.65	1.03
ITF302x90x18-t2N90A0.8FR	0.80	0.88	13.55	7.19	0.53	0.52	1.03
ITF302x90x18-t2.5N90A0.2FR	0.20	0.88	25.92	23.78	0.92	0.92	0.99
ITF302x90x18-t2.5N90A0.4FR	0.40	0.88	25.92	20.56	0.79	0.79	1.01
ITF302x90x18-t2.5N90A0.6FR	0.60	0.88	25.92	17.04	0.66	0.65	1.01
ITF302x90x18-t2.5N90A0.8FR	0.80	0.88	25.92	13.07	0.50	0.51	0.98
ITF302x90x18-t3.0N90A0.2FR	0.20	0.88	40.83	37.31	0.91	0.92	0.99
ITF302x90x18-t3.0N90A0.4FR	0.40	0.88	40.83	32.18	0.79	0.79	1.00
ITF302x90x18-t3.0N90A0.6FR	0.60	0.88	40.83	26.41	0.65	0.65	1.00
ITF302x90x18-t3.0N90A0.8FR	0.81	0.88	40.83	20.28	0.50	0.51	0.97
ITF302x90x18-t4.0N90A0.2FR	0.20	0.89	78.47	71.41	0.91	0.92	0.99
ITF302x90x18-t4.0N90A0.4FR	0.41	0.89	78.47	61.46	0.78	0.78	1.00
ITF302x90x18-t4.0N90A0.6FR	0.61	0.89	78.47	50.57	0.64	0.65	1.00
ITF302x90x18-t4.0N90A0.8FR	0.81	0.89	78.47	39.42	0.50	0.51	0.99
ITF302x90x18-t5.0N90A0.2FR	0.20	0.90	124.95	113.71	0.91	0.92	0.99
ITF302x90x18-t5.0N90A0.4FR	0.41	0.90	124.95	97.80	0.78	0.78	1.00
ITF302x90x18-t5.0N90A0.6FR	0.61	0.90	124.95	81.17	0.65	0.64	1.01
ITF302x90x18-t5.0N90A0.8FR	0.82	0.90	124.95	64.21	0.51	0.50	1.02
ITF302x90x18-t6.0N90A0.2FR	0.21	0.90	179.97	163.33	0.91	0.92	0.99
ITF302x90x18-t6.0N90A0.4FR	0.41	0.90	179.97	140.56	0.78	0.78	1.00
ITF302x90x18-t6.0N90A0.6FR	0.62	0.90	179.97	117.28	0.65	0.64	1.02

Continue-

Specimen	Holes diameter Ratio (a/h)	Holes distance Ratio (x/h)	Failure load without holes P (kN)	Failure load with holes P(Holes) (kN)	Reduction factor R= P(Holes) / P	Proposed reduction factor Rp = 1.04-0.68 (a/h)+0.023 (x/h)	Comparison with proposed reduction factor R/Rp
ITF302x90x18-t6.0N90A0.8FR	0.82	0.90	179.97	93.35	0.52	0.50	1.03
ITF202x65x13-t1.4N32.5A0.2X0FR	0.20	0.00	6.90	6.29	0.91	0.90	1.01
ITF202x65x13-t1.4N32.5A0.2X0.1FR	0.20	0.10	6.90	6.32	0.92	0.91	1.01
ITF202x65x13-t1.4N32.5A0.2X0.2FR	0.20	0.20	6.90	6.32	0.92	0.91	1.01
ITF202x65x13-t1.4N32.5A0.2X0.4FR	0.20	0.40	6.90	6.31	0.92	0.91	1.00
ITF202x65x13-t1.4N32.5A0.2X0.6FR	0.20	0.60	6.90	6.32	0.92	0.92	1.00
ITF202x65x13-t1.4N32.5A0.4X0FR	0.40	0.00	6.90	5.31	0.77	0.77	1.00
ITF202x65x13-t1.4N32.5A0.4X0.1FR	0.40	0.10	6.90	5.35	0.78	0.77	1.01
ITF202x65x13-t1.4N32.5A0.4X0.2FR	0.40	0.20	6.90	5.38	0.78	0.77	1.01
ITF202x65x13-t1.4N32.5A0.4X0.4FR	0.40	0.40	6.90	5.42	0.79	0.78	1.01
ITF202x65x13-t1.4N32.5A0.4X0.6FR	0.40	0.60	6.90	5.46	0.79	0.78	1.01
ITF202x65x13-t1.4N32.5A0.6X0FR	0.60	0.00	6.90	4.27	0.62	0.63	0.98
ITF202x65x13-t1.4N32.5A0.6X0.1FR	0.60	0.10	6.90	4.32	0.63	0.63	0.99
ITF202x65x13-t1.4N32.5A0.6X0.2FR	0.60	0.20	6.90	4.39	0.64	0.64	1.00
ITF202x65x13-t1.4N32.5A0.6X0.4FR	0.60	0.40	6.90	4.52	0.66	0.64	1.02
ITF202x65x13-t1.4N32.5A0.6X0.6FR	0.60	0.60	6.90	4.59	0.67	0.65	1.03
ITF202x65x13-t1.4N32.5A0.8X0FR	0.80	0.00	6.90	3.05	0.44	0.50	0.89
ITF202x65x13-t1.4N32.5A0.8X0.1FR	0.80	0.10	6.90	3.16	0.46	0.50	0.92
ITF202x65x13-t1.4N32.5A0.8X0.2FR	0.80	0.20	6.90	3.29	0.48	0.50	0.95
ITF202x65x13-t1.4N32.5A0.8X0.4FR	0.80	0.40	6.90	3.59	0.52	0.51	1.03
ITF202x65x13-t1.4N32.5A0.8X0.6FR	0.80	0.60	6.90	3.73	0.54	0.51	1.06
ITF202x65x13-t1.4N65A0.2X0FR	0.20	0.00	7.64	6.98	0.91	0.90	1.01
ITF202x65x13-t1.4N65A0.2X0.1FR	0.20	0.10	7.64	7.00	0.92	0.91	1.01
ITF202x65x13-t1.4N65A0.2X0.2FR	0.20	0.20	7.64	6.99	0.92	0.91	1.01
ITF202x65x13-t1.4N65A0.2X0.4FR	0.20	0.40	7.64	6.99	0.91	0.91	1.00
ITF202x65x13-t1.4N65A0.2X0.6FR	0.20	0.60	7.64	7.01	0.92	0.92	1.00
ITF202x65x13-t1.4N65A0.4X0FR	0.40	0.00	7.64	5.92	0.77	0.77	1.01
ITF202x65x13-t1.4N65A0.4X0.1FR	0.40	0.10	7.64	5.97	0.78	0.77	1.01
ITF202x65x13-t1.4N65A0.4X0.2FR	0.40	0.20	7.64	6.00	0.79	0.77	1.02
ITF202x65x13-t1.4N65A0.4X0.4FR	0.40	0.40	7.64	6.05	0.79	0.78	1.02
ITF202x65x13-t1.4N65A0.4X0.6FR	0.40	0.60	7.64	6.10	0.80	0.78	1.02
ITF202x65x13-t1.4N65A0.6X0FR	0.60	0.00	7.64	4.79	0.63	0.63	0.99
ITF202x65x13-t1.4N65A0.6X0.1FR	0.60	0.10	7.64	4.87	0.64	0.63	1.00
ITF202x65x13-t1.4N65A0.6X0.2FR	0.60	0.20	7.64	4.96	0.65	0.64	1.02
ITF202x65x13-t1.4N65A0.6X0.4FR	0.60	0.40	7.64	5.10	0.67	0.64	1.04
ITF202x65x13-t1.4N65A0.6X0.6FR	0.60	0.60	7.64	5.19	0.68	0.65	1.05
ITF202x65x13-t1.4N65A0.8X0FR	0.80	0.00	7.64	3.49	0.46	0.50	0.92
ITF202x65x13-t1.4N65A0.8X0.1FR	0.80	0.10	7.64	3.63	0.47	0.50	0.95
ITF202x65x13-t1.4N65A0.8X0.2FR	0.80	0.20	7.64	3.81	0.50	0.50	0.99
ITF202x65x13-t1.4N65A0.8X0.4FR	0.80	0.40	7.64	4.12	0.54	0.51	1.07
ITF202x65x13-t1.4N65A0.8X0.6FR	0.80	0.60	7.64	4.27	0.56	0.51	1.10
ITF302x90x18-t2N44A0.2X0FR	0.20	0.00	12.39	11.37	0.92	0.90	1.02
ITF302x90x18-t2N44A0.2X0.1FR	0.20	0.10	12.39	11.43	0.92	0.91	1.02
ITF302x90x18-t2N44A0.2X0.2FR	0.20	0.20	12.39	11.43	0.92	0.91	1.02
ITF302x90x18-t2N44A0.2X0.4FR	0.20	0.40	12.39	11.41	0.92	0.91	1.01
ITF302x90x18-t2N44A0.2X0.6FR	0.20	0.60	12.39	11.42	0.92	0.92	1.00
ITF302x90x18-t2N44A0.4X0FR	0.40	0.00	12.39	9.59	0.77	0.77	1.01
ITF302x90x18-t2N44A0.4X0.1FR	0.40	0.10	12.39	9.67	0.78	0.77	1.01
ITF302x90x18-t2N44A0.4X0.2FR	0.40	0.20	12.39	9.73	0.79	0.77	1.02
ITF302x90x18-t2N44A0.4X0.4FR	0.40	0.40	12.39	9.78	0.79	0.78	1.02
ITF302x90x18-t2N44A0.4X0.6FR	0.40	0.60	12.39	9.85	0.80	0.78	1.02
ITF302x90x18-t2N44A0.6X0FR	0.60	0.00	12.39	7.70	0.62	0.63	0.98
ITF302x90x18-t2N44A0.6X0.1FR	0.60	0.10	12.39	7.79	0.63	0.63	0.99

Continue

Specimen	Holes diameter Ratio (a/h)	Holes distance Ratio (x/h)	Failure load without holes P (kN)	Failure load with holes P(Holes) (kN)	Reduction factor R= P(Holes) / P	Proposed reduction factor Rp = 1.04-0.68 (a/h)+0.023 (x/h)	Comparison with proposed reduction factor R/Rp
ITF302x90x18-t2N44A0.6X0.2FR	0.60	0.20	12.39	7.94	0.64	0.64	1.01
ITF302x90x18-t2N44A0.6X0.4FR	0.60	0.40	12.39	8.13	0.66	0.64	1.02
ITF302x90x18-t2N44A0.6X0.6FR	0.60	0.60	12.39	8.25	0.67	0.65	1.03
ITF302x90x18-t2N44A0.8X0FR	0.80	0.00	12.39	5.46	0.44	0.50	0.89
ITF302x90x18-t2N44A0.8X0.1FR	0.80	0.10	12.39	5.66	0.46	0.50	0.92
ITF302x90x18-t2N44A0.8X0.2FR	0.80	0.20	12.39	5.91	0.48	0.50	0.95
ITF302x90x18-t2N44A0.8X0.4FR	0.80	0.40	12.39	6.44	0.52	0.51	1.03
ITF302x90x18-t2N44A0.8X0.6FR	0.80	0.60	12.39	6.66	0.54	0.51	1.05
ITF302x90x18-t2N90A0.2X0FR	0.20	0.00	13.55	12.49	0.92	0.90	1.02
ITF302x90x18-t2N90A0.2X0.1FR	0.20	0.10	13.55	12.51	0.92	0.91	1.02
ITF302x90x18-t2N90A0.2X0.2FR	0.20	0.20	13.55	12.50	0.92	0.91	1.02
ITF302x90x18-t2N90A0.2X0.4FR	0.20	0.40	13.55	12.49	0.92	0.91	1.01
ITF302x90x18-t2N90A0.2X0.6FR	0.20	0.60	13.55	12.52	0.92	0.92	1.01
ITF302x90x18-t2N90A0.4X0FR	0.40	0.00	13.55	10.60	0.78	0.77	1.02
ITF302x90x18-t2N90A0.4X0.1FR	0.40	0.10	13.55	10.69	0.79	0.77	1.02
ITF302x90x18-t2N90A0.4X0.2FR	0.40	0.20	13.55	10.73	0.79	0.77	1.03
ITF302x90x18-t2N90A0.4X0.4FR	0.40	0.40	13.55	10.81	0.80	0.78	1.03
ITF302x90x18-t2N90A0.4X0.6FR	0.40	0.60	13.55	10.90	0.80	0.78	1.03
ITF302x90x18-t2N90A0.6X0FR	0.60	0.00	13.55	8.57	0.63	0.63	1.00
ITF302x90x18-t2N90A0.6X0.1FR	0.60	0.10	13.55	8.72	0.64	0.63	1.01
ITF302x90x18-t2N90A0.6X0.2FR	0.60	0.20	13.55	8.90	0.66	0.64	1.03
ITF302x90x18-t2N90A0.6X0.4FR	0.60	0.40	13.55	9.11	0.67	0.64	1.05
ITF302x90x18-t2N90A0.6X0.6FR	0.60	0.60	13.55	9.26	0.68	0.65	1.06
ITF302x90x18-t2N90A0.8X0FR	0.80	0.00	13.55	6.19	0.46	0.50	0.92
ITF302x90x18-t2N90A0.8X0.1FR	0.80	0.10	13.55	6.45	0.48	0.50	0.96
ITF302x90x18-t2N90A0.8X0.2FR	0.80	0.20	13.55	6.79	0.50	0.50	1.00
ITF302x90x18-t2N90A0.8X0.4FR	0.80	0.40	13.55	7.36	0.54	0.50	1.08
ITF302x90x18-t2N90A0.8X0.6FR	0.80	0.60	13.55	7.63	0.56	0.51	1.10
ITF142x60x13t1.3N30A0.4X0.4FR	0.39	0.88	5.62	4.46	0.79	0.80	1.00
ITF142x60x13-t1.3N60A0.4X0.4FR	0.39	0.98	6.01	4.91	0.82	0.80	1.03
ITF172x65x13-t1.3N32.5A0.4X0.4FR	0.39	0.89	5.70	4.56	0.80	0.79	1.01
ITF172x65x13-t1.3N65A0.4X0.4FR	0.39	0.95	6.29	5.15	0.82	0.79	1.03
ITF202x65x13-t1.4N32.5A0.4X0.4FR	0.40	0.85	6.82	5.62	0.82	0.79	1.04
ITF202x65x13-t1.4N65A0.4X0.4FR	0.40	0.88	7.37	5.76	0.78	0.79	0.99
ITF262x65x13-t1.6N32.5A0.4X0.4FR	0.39	0.80	6.60	5.26	0.80	0.79	1.01
ITF262x65x13-t1.6N65A0.4X0.4FR	0.39	0.86	7.66	5.53	0.72	0.79	0.91
ITF302x90x18-t2N90A0.4X0.4FR	0.39	0.88	14.08	11.29	0.80	0.79	1.01
Mean, Pm							1.00
STD							0.04
COV, Vp							0.04
Reliability index, β							2.83
Resistance factor, φ							0.85

D.2 Statistical analysis for the comparison of the strength reduction factor for flanges unfastened under ITF loading condition (Type 2 holes)

Specimen	Holes diameter ratio	Bearing ratio	Failure load without holes	Failure load with holes	Reduction factor	Proposed reduction factor	Comparison with proposed reduction factor
	a/h	*N/h*	*P*	*P(Holes)*	*R*= P(Holes) / P(A0)	*Rp* = 1.05-0.54 *(a/h)*+0.01 *(N/h)*	*R/Rp*
			(kN)	(kN)			
ITF202x65x13-t1.4N100MA0.2FR	0.20	0.50	18.37	17.41	0.95	0.95	1.00
ITF202x65x13-t1.4N100MA0.4FR	0.40	0.50	18.37	15.67	0.85	0.84	1.02
ITF202x65x13-t4N100MA0.2FR	0.21	0.51	81.81	76.02	0.93	0.94	0.98
ITF202x65x13-t4N100MA0.4FR	0.41	0.51	81.81	66.20	0.81	0.83	0.97
ITF202x65x13-t6N100MA0.2FR	0.21	0.53	176.27	162.96	0.92	0.94	0.98
ITF202x65x13-t6N100MA0.4FR	0.42	0.53	176.27	142.01	0.81	0.83	0.97
ITF202x65x13-t1.4N150MA0.2FR	0.20	0.75	19.27	18.23	0.95	0.95	1.00
ITF202x65x13-t1.4N150MA0.4FR	0.40	0.75	19.27	16.53	0.86	0.84	1.02
ITF202x65x13-t1.4N150MA0.6FR	0.60	0.75	19.27	14.19	0.74	0.73	1.00
ITF202x65x13-t4N150MA0.2FR	0.21	0.77	84.42	78.86	0.93	0.95	0.99
ITF202x65x13-t4N150MA0.4FR	0.41	0.77	84.42	69.76	0.83	0.84	0.99
ITF202x65x13-t4N150MA0.6FR	0.62	0.77	84.42	58.94	0.70	0.73	0.96
ITF202x65x13-t6N150MA0.2FR	0.21	0.79	183.01	170.62	0.93	0.94	0.99
ITF202x65x13-t6N150MA0.4FR	0.42	0.79	183.01	151.04	0.83	0.83	0.99
ITF202x65x13-t6N150MA0.6FR	0.63	0.79	183.01	129.18	0.71	0.72	0.98
ITF202x65x13-t1.4N200MA0.2FR	0.20	1.00	20.18	19.10	0.95	0.95	0.99
ITF202x65x13-t1.4N200MA0.4FR	0.40	1.00	20.18	17.48	0.87	0.84	1.03
ITF202x65x13-t1.4N200MA0.6FR	0.60	1.00	20.18	15.28	0.76	0.74	1.03
ITF202x65x13-t1.4N200MA0.8FR	0.80	1.00	20.18	12.25	0.61	0.63	0.97
ITF202x65x13-t4N200MA0.2FR	0.21	1.03	87.50	82.06	0.94	0.95	0.99
ITF202x65x13-t4N200MA0.4FR	0.41	1.03	87.50	73.85	0.84	0.84	1.01
ITF202x65x13-t4N200MA0.6FR	0.62	1.03	87.50	63.82	0.73	0.73	1.00
ITF202x65x13-t4N200MA0.8FR	0.82	1.03	87.50	54.08	0.62	0.62	1.00
ITF202x65x13-t6N200MA0.2FR	0.21	1.05	189.99	178.03	0.94	0.95	0.99
ITF202x65x13-t6N200MA0.4FR	0.42	1.05	189.99	160.17	0.84	0.83	1.01
ITF202x65x13-t6N200MA0.6FR	0.63	1.05	189.99	139.22	0.73	0.72	1.02
ITF202x65x13-t6N200MA0.8FR	0.84	1.05	189.99	120.38	0.63	0.61	1.04
ITF302x90x18-t2N150MA0.2FR	0.20	0.50	15.05	14.50	0.96	0.95	1.02
ITF302x90x18-t2N150MA0.4FR	0.40	0.50	15.05	13.43	0.89	0.84	1.06
ITF302x90x18-t4N150MA0.2FR	0.20	0.51	80.49	75.11	0.93	0.95	0.99
ITF302x90x18-t4N150MA0.4FR	0.41	0.51	80.49	65.64	0.82	0.84	0.98
ITF302x90x18-t6N150MA0.2FR	0.21	0.51	184.28	170.59	0.93	0.94	0.98
ITF302x90x18-t6N150MA0.4FR	0.41	0.51	184.28	147.85	0.80	0.83	0.96
ITF302x90x18-t2N220MA0.2FR	0.20	0.73	15.93	15.32	0.96	0.95	1.01
ITF302x90x18-t2N220MA0.4FR	0.40	0.73	15.93	14.22	0.89	0.84	1.06
ITF302x90x18-t2N220MA0.6FR	0.60	0.73	15.93	12.79	0.80	0.73	1.09
ITF302x90x18-t4N220MA0.2FR	0.20	0.74	83.18	77.79	0.94	0.95	0.99
ITF302x90x18-t4N220MA0.4FR	0.41	0.74	83.18	68.82	0.83	0.84	0.99
ITF302x90x18-t4N220MA0.6FR	0.61	0.74	83.18	57.45	0.69	0.73	0.95
ITF302x90x18-t6N220MA0.2FR	0.21	0.75	189.96	176.89	0.93	0.95	0.98
ITF302x90x18-t6N220MA0.4FR	0.41	0.75	189.96	155.57	0.82	0.84	0.98
ITF302x90x18-t6N220MA0.6FR	0.62	0.75	189.96	130.34	0.69	0.72	0.95
ITF302x90x18-t2N300MA0.2FR	0.20	1.00	16.93	16.27	0.96	0.95	1.01
ITF302x90x18-t2N300MA0.4FR	0.40	1.00	16.93	15.17	0.90	0.84	1.06
ITF302x90x18-t2N300MA0.6FR	0.60	1.00	16.93	13.74	0.81	0.74	1.10
ITF302x90x18-t2N300MA0.8FR	0.80	1.00	16.93	10.85	0.64	0.63	1.02
ITF302x90x18-t4N300MA0.2FR	0.20	1.01	86.55	81.17	0.94	0.95	0.99
ITF302x90x18-t4N300MA0.4FR	0.41	1.01	86.55	73.00	0.84	0.84	1.00
ITF302x90x18-t4N300MA0.6FR	0.61	1.01	86.55	62.79	0.73	0.73	0.99
ITF302x90x18-t4N300MA0.8FR	0.81	1.01	86.55	51.44	0.59	0.62	0.96
ITF302x90x18-t6N300MA0.2FR	0.21	1.03	197.73	184.73	0.93	0.95	0.98

Continue

Specimen	Holes diameter ratio	Bearing ratio	Failure load without holes	Failure load with holes	Reduction factor	Proposed reduction factor	Comparison with proposed reduction factor
	a/h	*N/h*	*P*	*P(Holes)*	*R*= P(Holes) / P(A0)	*Rp* = 1.05-0.54 *(a/h)*+0.01 *(N/h)*	*R/Rp*
			(kN)	(kN)			
ITF302x90x18-t6N300MA0.4FR	0.41	1.03	197.73	165.15	0.84	0.84	1.00
ITF302x90x18-t6N300MA0.6FR	0.62	1.03	197.73	142.10	0.72	0.73	0.99
ITF302x90x18-t6N300MA0.8FR	0.82	1.03	197.73	120.15	0.61	0.62	0.99
ITF142x60x13-t1.3N90MA0.2FR	0.20	0.64	6.03	5.96	0.99	0.95	1.04
ITF142x60x13-t1.3N90MA0.4FR	0.40	0.64	6.03	5.45	0.90	0.84	1.08
ITF142x60x13-t1.3N90MA0.6FR	0.60	0.64	6.03	4.52	0.75	0.73	1.02
ITF142x60x13-t1.3N90MA0.8FR	0.80	0.64	6.03	3.52	0.58	0.63	0.93
ITF142x60x13-t1.3N120MA0.2FR	0.20	0.86	6.32	6.05	0.96	0.95	1.01
ITF142x60x13-t1.3N120MA0.4FR	0.40	0.86	6.32	5.45	0.86	0.84	1.02
ITF142x60x13-t1.3N120MA0.6FR	0.60	0.86	6.32	4.75	0.75	0.73	1.02
ITF142x60x13-t1.3N120MA0.8FR	0.80	0.86	6.32	3.79	0.60	0.62	0.96
ITF172x65x13-t1.3N120MA0.4FR	0.40	0.71	7.05	6.20	0.88	0.84	1.04
ITF172x65x13-t1.3N120MA0.6FR	0.60	0.71	7.05	5.67	0.80	0.73	1.10
ITF202x65x13-t1.4N150MA0.4FR	0.40	0.75	8.40	7.37	0.88	0.84	1.04
ITF202x65x13-t1.4N150MA0.6FR	0.60	0.75	8.40	6.79	0.81	0.73	1.10
ITF262x65x13-t1.6N150MA0.2FR	0.20	0.58	8.19	7.88	0.96	0.95	1.01
ITF262x65x13-t1.6N150MA0.4FR	0.40	0.58	8.19	7.29	0.89	0.84	1.06
Mean	Pm						1.01
STD							0.04
COV	Vp						0.04
Reliability index	β						2.87
Resistance factor	φ						0.85

D.3 Statistical analysis for the comparison of the strength reduction factor for flanges fastened under ITF loading condition (Type 1 holes)

Specimen	Holes diameter ratio *a/h*	Bearing ratio *x/h*	Failure load without holes *P* (kN)	Failure load with holes *P(Holes)* (kN)	Reduction factor *R*= P(Holes) / P(A0)	Proposed reduction factor *Rp* = 1.00-0.45 *(a/h)*+0.09 *(x/h)*	Comparison with proposed reduction factor *R/Rp*
ITF202x65x13-t1.4N32.5A0.2FX	0.20	0.85	10.50	10.20	0.97	0.99	0.98
ITF202x65x13-t1.4N32.5A0.4FX	0.40	0.85	10.50	9.45	0.90	0.90	1.00
ITF202x65x13-t1.4N32.5A0.6FX	0.60	0.85	10.50	8.39	0.80	0.81	0.99
ITF202x65x13-t1.4N32.5A0.8FX	0.80	0.85	10.50	6.99	0.67	0.72	0.93
ITF202x65x13-t2.0N32.5A0.2FX	0.20	0.85	21.30	20.72	0.97	0.99	0.99
ITF202x65x13-t2.0N32.5A0.4FX	0.40	0.85	21.30	19.74	0.93	0.90	1.03
ITF202x65x13-t2.0N32.5A0.6FX	0.60	0.85	21.30	18.12	0.85	0.81	1.06
ITF202x65x13-t2.0N32.5A0.8FX	0.80	0.85	21.30	15.63	0.73	0.71	1.03
ITF202x65x13-t4.0N32.5A0.2FX	0.21	0.87	77.18	75.82	0.98	0.99	1.00
ITF202x65x13-t4.0N32.5A0.4FX	0.41	0.87	77.18	73.27	0.95	0.89	1.06
ITF202x65x13-t4.0N32.5A0.6FX	0.62	0.87	77.18	68.37	0.89	0.80	1.11
ITF202x65x13-t4.0N32.5A0.8FX	0.82	0.87	77.18	60.20	0.78	0.71	1.10
ITF202x65x13-t6.0N32.5A0.2FX	0.21	0.89	159.20	155.56	0.98	0.99	0.99
ITF202x65x13-t6.0N32.5A0.4FX	0.42	0.89	159.20	151.42	0.95	0.89	1.07
ITF202x65x13-t6.0N32.5A0.6FX	0.63	0.89	159.20	141.53	0.89	0.80	1.12
ITF202x65x13-t6.0N32.5A0.8FX	0.84	0.89	159.20	125.69	0.79	0.70	1.12
ITF202x65x13-t1.4N65A0.2FX	0.20	0.88	11.94	11.57	0.97	0.99	0.98
ITF202x65x13-t1.4N65A0.4FX	0.40	0.88	11.94	10.69	0.90	0.90	1.00
ITF202x65x13-t1.4N65A0.6FX	0.60	0.88	11.94	9.49	0.79	0.81	0.98
ITF202x65x13-t1.4N65A0.8FX	0.80	0.88	11.94	7.90	0.66	0.72	0.92
ITF202x65x13-t2.0N65A0.2FX	0.20	0.88	23.50	22.70	0.97	0.99	0.98
ITF202x65x13-t2.0N65A0.4FX	0.40	0.88	23.50	21.72	0.92	0.90	1.03
ITF202x65x13-t2.0N65A0.6FX	0.60	0.88	23.50	19.66	0.84	0.81	1.04
ITF202x65x13-t2.0N65A0.8FX	0.80	0.88	23.50	16.75	0.71	0.72	0.99
ITF202x65x13-t4.0N65A0.2FX	0.21	0.90	86.37	85.54	0.99	0.99	1.00
ITF202x65x13-t4.0N65A0.4FX	0.41	0.90	86.37	83.90	0.97	0.90	1.08
ITF202x65x13-t4.0N65A0.6FX	0.62	0.90	86.37	79.50	0.92	0.80	1.15
ITF202x65x13-t4.0N65A0.8FX	0.82	0.90	86.37	69.27	0.80	0.71	1.13
ITF202x65x13-t6.0N65A0.2FX	0.21	0.92	185.69	184.47	0.99	0.99	1.01
ITF202x65x13-t6.0N65A0.4FX	0.42	0.92	185.69	179.29	0.97	0.89	1.08
ITF202x65x13-t6.0N65A0.6FX	0.63	0.92	185.69	162.74	0.88	0.80	1.10
ITF202x65x13-t6.0N65A0.8FX	0.84	0.92	185.69	140.44	0.76	0.71	1.07
ITF302x90x18-t2N44A0.2FX	0.20	0.83	18.56	18.17	0.98	0.98	0.99
ITF302x90x18-t2N44A0.4FX	0.40	0.83	18.56	16.92	0.91	0.89	1.02
ITF302x90x18-t2N44A0.6FX	0.60	0.83	18.56	15.22	0.82	0.80	1.02
ITF302x90x18-t2N44A0.8FX	0.80	0.83	18.56	12.80	0.69	0.71	0.96
ITF302x90x18-t4.0N44A0.2FX	0.20	0.84	75.89	75.55	1.00	0.98	1.01
ITF302x90x18-t4.0N44A0.4FX	0.41	0.84	75.89	74.54	0.98	0.89	1.10
ITF302x90x18-t4.0N44A0.6FX	0.61	0.84	75.89	70.58	0.93	0.80	1.16
ITF302x90x18-t4.0N44A0.8FX	0.81	0.84	75.89	62.87	0.83	0.71	1.17
ITF302x90x18-t6.0N44A0.2FX	0.21	0.86	161.96	161.69	1.00	0.98	1.01
ITF302x90x18-t6.0N44A0.4FX	0.41	0.86	161.96	158.77	0.98	0.89	1.10
ITF302x90x18-t6.0N44A0.6FX	0.62	0.86	161.96	150.88	0.93	0.80	1.17
ITF302x90x18-t6.0N44A0.8FX	0.82	0.86	161.96	130.57	0.81	0.71	1.14
ITF302x90x18-t2N90A0.2FX	0.20	0.88	22.23	21.10	0.95	0.99	0.96
ITF302x90x18-t2N90A0.4FX	0.40	0.88	22.23	19.18	0.86	0.90	0.96
ITF302x90x18-t2N90A0.6FX	0.60	0.88	22.23	17.02	0.77	0.81	0.95
ITF302x90x18-t2N90A0.8FX	0.80	0.88	22.23	14.29	0.64	0.72	0.89
ITF302x90x18-t4.0N90A0.2FX	0.20	0.89	90.49	90.14	1.00	0.99	1.01
ITF302x90x18-t4.0N90A0.4FX	0.41	0.89	90.49	88.86	0.98	0.90	1.09
ITF302x90x18-t4.0N90A0.6FX	0.61	0.89	90.49	82.23	0.91	0.81	1.13

Continue

Specimen	Holes diameter ratio *a/h*	Bearing ratio *x/h*	Failure load without holes *P* (kN)	Failure load with holes *P(Holes)* (kN)	Reduction factor *R*= P(Holes) / P(A0)	Proposed reduction factor *Rp* = 1.00-0.45 *(a/h)*+0.09 *(x/h)*	Comparison with proposed reduction factor *R/Rp*
ITF302x90x18-t4.0N90A0.8FX	0.81	0.89	90.49	70.71	0.78	0.71	1.09
ITF302x90x18-t6.0N90A0.2FX	0.21	0.90	193.61	192.94	1.00	0.99	1.01
ITF302x90x18-t6.0N90A0.4FX	0.41	0.90	193.61	190.14	0.98	0.90	1.10
ITF302x90x18-t6.0N90A0.6FX	0.62	0.90	193.61	177.98	0.92	0.80	1.14
ITF302x90x18-t6.0N90A0.8FX	0.82	0.90	193.61	154.61	0.80	0.71	1.12
ITF202x65x13-t1.4N32.5A0.2X0FX	0.20	0.00	10.50	9.99	0.95	0.91	1.05
ITF202x65x13-t1.4N32.5A0.2X0.2FX	0.20	0.20	10.50	9.96	0.95	0.93	1.02
ITF202x65x13-t1.4N32.5A0.2X0.4FX	0.20	0.40	10.50	10.04	0.96	0.95	1.01
ITF202x65x13-t1.4N32.5A0.2X0.6FX	0.20	0.60	10.50	10.16	0.97	0.96	1.00
ITF202x65x13-t1.4N32.5A0.4X0FX	0.40	0.00	10.50	8.62	0.82	0.82	1.00
ITF202x65x13-t1.4N32.5A0.4X0.2FX	0.40	0.20	10.50	8.95	0.85	0.84	1.02
ITF202x65x13-t1.4N32.5A0.4X0.4FX	0.40	0.40	10.50	9.22	0.88	0.86	1.03
ITF202x65x13-t1.4N32.5A0.4X0.6FX	0.40	0.60	10.50	9.50	0.90	0.87	1.03
ITF202x65x13-t1.4N32.5A0.6X0FX	0.60	0.00	10.50	7.10	0.68	0.73	0.93
ITF202x65x13-t1.4N32.5A0.6X0.2FX	0.60	0.20	10.50	7.74	0.74	0.75	0.98
ITF202x65x13-t1.4N32.5A0.6X0.4FX	0.60	0.40	10.50	8.23	0.78	0.77	1.02
ITF202x65x13-t1.4N32.5A0.6X0.6FX	0.60	0.60	10.50	8.70	0.83	0.78	1.06
ITF202x65x13-t1.4N32.5A0.8X0FX	0.80	0.00	10.50	5.11	0.49	0.64	0.76
ITF202x65x13-t1.4N32.5A0.8X0.2FX	0.80	0.20	10.50	6.25	0.60	0.66	0.90
ITF202x65x13-t1.4N32.5A0.8X0.4FX	0.80	0.40	10.50	7.12	0.68	0.68	1.00
ITF202x65x13-t1.4N32.5A0.8X0.6FX	0.80	0.60	10.50	7.88	0.75	0.69	1.08
ITF202x65x13-t1.4N65A0.2X0FX	0.20	0.00	11.94	11.45	0.96	0.91	1.05
ITF202x65x13-t1.4N65A0.2X0.2FX	0.20	0.20	11.94	11.39	0.95	0.93	1.03
ITF202x65x13-t1.4N65A0.2X0.4FX	0.20	0.40	11.94	11.45	0.96	0.95	1.01
ITF202x65x13-t1.4N65A0.2X0.6FX	0.20	0.60	11.94	11.56	0.97	0.96	1.01
ITF202x65x13-t1.4N65A0.4X0FX	0.40	0.00	11.94	10.00	0.84	0.82	1.02
ITF202x65x13-t1.4N65A0.4X0.2FX	0.40	0.20	11.94	10.28	0.86	0.84	1.03
ITF202x65x13-t1.4N65A0.4X0.4FX	0.40	0.40	11.94	10.53	0.88	0.86	1.03
ITF202x65x13-t1.4N65A0.4X0.6FX	0.40	0.60	11.94	10.81	0.91	0.87	1.04
ITF202x65x13-t1.4N65A0.6X0FX	0.60	0.00	11.94	8.20	0.69	0.73	0.94
ITF202x65x13-t1.4N65A0.6X0.2FX	0.60	0.20	11.94	8.91	0.75	0.75	1.00
ITF202x65x13-t1.4N65A0.6X0.4FX	0.60	0.40	11.94	9.45	0.79	0.77	1.03
ITF202x65x13-t1.4N65A0.6X0.6FX	0.60	0.60	11.94	9.96	0.83	0.78	1.06
ITF202x65x13-t1.4N65A0.8X0FX	0.80	0.00	11.94	6.18	0.52	0.64	0.81
ITF202x65x13-t1.4N65A0.8X0.2FX	0.80	0.20	11.94	7.36	0.62	0.66	0.94
ITF202x65x13-t1.4N65A0.8X0.4FX	0.80	0.40	11.94	8.29	0.69	0.68	1.03
ITF202x65x13-t1.4N65A0.8X0.6FX	0.80	0.60	11.94	9.12	0.76	0.69	1.10
ITF302x90x18-t2N44A0.2X0FX	0.20	0.00	18.56	17.83	0.96	0.91	1.06
ITF302x90x18-t2N44A0.2X0.2FX	0.20	0.20	18.56	17.78	0.96	0.93	1.03
ITF302x90x18-t2N44A0.2X0.4FX	0.20	0.40	18.56	17.93	0.97	0.95	1.02
ITF302x90x18-t2N44A0.2X0.6FX	0.20	0.60	18.56	18.12	0.98	0.96	1.01
ITF302x90x18-t2N44A0.4X0FX	0.40	0.00	18.56	15.58	0.84	0.82	1.02
ITF302x90x18-t2N44A0.4X0.2FX	0.40	0.20	18.56	16.10	0.87	0.84	1.04
ITF302x90x18-t2N44A0.4X0.4FX	0.40	0.40	18.56	16.52	0.89	0.86	1.04
ITF302x90x18-t2N44A0.4X0.6FX	0.40	0.60	18.56	17.02	0.92	0.87	1.05

Continue

Specimen	Holes diameter ratio	Bearing ratio	Failure load without holes	Failure load with holes	Reduction factor	Proposed reduction factor	Comparison with proposed reduction factor
	a/h	*x/h*	*P*	*P(Holes)*	*R*= P(Holes) / P(A0)	*Rp* = 1.00-0.45 *(a/h)*+0.09 *(x/h)*	*R/Rp*
			(kN)	(kN)			
ITF302x90x18-t2N44A0.6X0FX	0.60	0.00	18.56	12.87	0.69	0.73	0.95
ITF302x90x18-t2N44A0.6X0.2FX	0.60	0.20	18.56	14.11	0.76	0.75	1.02
ITF302x90x18-t2N44A0.6X0.4FX	0.60	0.40	18.56	14.98	0.81	0.77	1.05
ITF302x90x18-t2N44A0.6X0.6FX	0.60	0.60	18.56	15.77	0.85	0.78	1.08
ITF302x90x18-t2N44A0.8X0FX	0.80	0.00	18.56	9.03	0.49	0.64	0.76
ITF302x90x18-t2N44A0.8X0.2FX	0.80	0.20	18.56	11.46	0.62	0.66	0.94
ITF302x90x18-t2N44A0.8X0.4FX	0.80	0.40	18.56	13.11	0.71	0.68	1.05
ITF302x90x18-t2N44A0.8X0.6FX	0.80	0.60	18.56	14.45	0.78	0.69	1.12
ITF302x90x18-t2N90A0.2X0FX	0.20	0.00	22.23	20.69	0.93	0.91	1.02
ITF302x90x18-t2N90A0.2X0.2FX	0.20	0.20	22.23	20.66	0.93	0.93	1.00
ITF302x90x18-t2N90A0.2X0.4FX	0.20	0.40	22.23	20.80	0.94	0.95	0.99
ITF302x90x18-t2N90A0.2X0.6FX	0.20	0.60	22.23	21.06	0.95	0.96	0.98
ITF302x90x18-t2N90A0.4X0FX	0.40	0.00	22.23	17.78	0.80	0.82	0.98
ITF302x90x18-t2N90A0.4X0.2FX	0.40	0.20	22.23	18.35	0.83	0.84	0.98
ITF302x90x18-t2N90A0.4X0.4FX	0.40	0.40	22.23	18.83	0.85	0.86	0.99
ITF302x90x18-t2N90A0.4X0.6FX	0.40	0.60	22.23	19.38	0.87	0.87	1.00
ITF302x90x18-t2N90A0.6X0FX	0.60	0.00	22.23	14.48	0.65	0.73	0.89
ITF302x90x18-t2N90A0.6X0.2FX	0.60	0.20	22.23	15.90	0.72	0.75	0.96
ITF302x90x18-t2N90A0.6X0.4FX	0.60	0.40	22.23	16.89	0.76	0.77	0.99
ITF302x90x18-t2N90A0.6X0.6FX	0.60	0.60	22.23	17.83	0.80	0.78	1.02
ITF302x90x18-t2N90A0.8X0FX	0.80	0.00	22.23	10.86	0.49	0.64	0.76
ITF302x90x18-t2N90A0.8X0.2FX	0.80	0.20	22.23	13.19	0.59	0.66	0.90
ITF302x90x18-t2N90A0.8X0.4FX	0.80	0.40	22.23	14.91	0.67	0.68	0.99
ITF302x90x18-t2N90A0.8X0.6FX	0.80	0.60	22.23	16.35	0.74	0.69	1.06
ITF142x60x13t1.3N30A0.4FX	0.40	0.90	7.48	6.95	0.93	0.90	1.03
ITF142x60x13-t1.3N60A0.4FX	0.40	0.98	8.14	7.29	0.90	0.91	0.98
ITF172x65x13-t1.3N32.5A0.4FX	0.40	0.89	8.92	7.68	0.86	0.90	0.96
ITF172x65x13-t1.3N65A0.4FX	0.40	0.95	9.48	8.46	0.89	0.91	0.98
ITF202x65x13-t1.4N32.5A0.4FX	0.40	0.85	11.46	9.59	0.84	0.90	0.93
ITF202x65x13-t1.4N65A0.4FX	0.40	0.88	11.65	10.25	0.88	0.90	0.98
ITF262x65x13-t1.6N32.5A0.4FX	0.40	0.80	11.46	9.64	0.84	0.89	0.94
ITF302x90x18-t2N90A0.4FX	0.40	0.88	22.31	19.35	0.87	0.90	0.96
Mean, Pm							1.02
STD							0.07
COV, Vp							0.07
Reliability index, β							2.81
Resistance factor, φ							0.85

D.4 Statistical analysis for the comparison of the strength reduction factor for flanges fastened under ITF loading condition (Type 2 holes)

Specimen	Holes diameter ratio	Bearing ratio	Failure load without holes	Failure load with holes	Reduction factor	Proposed reduction factor	Comparison with proposed reduction factor
	a/h	*N/h*	*P*	*P(Holes)*	*R*= P(Holes) / P(A0)	*Rp* = 1.01-0.51 *(a/h)*+0.06 *(N/h)*	*R/Rp*
			(kN)	(kN)			
ITF202x65x13-t1.4N100MA0.2FX	0.20	0.50	26.72	25.96	0.97	0.94	1.04
ITF202x65x13-t1.4N100MA0.4FX	0.40	0.50	26.72	22.90	0.86	0.84	1.03
ITF202x65x13-t4N100MA0.2FX	0.21	0.51	99.61	97.62	0.98	0.94	1.05
ITF202x65x13-t4N100MA0.4FX	0.41	0.51	99.61	88.48	0.89	0.83	1.07
ITF202x65x13-t6N100MA0.2FX	0.21	0.53	207.70	206.00	0.99	0.93	1.06
ITF202x65x13-t6N100MA0.4FX	0.42	0.53	207.70	178.31	0.86	0.83	1.04
ITF202x65x13-t1.4N150MA0.2FX	0.20	0.75	28.35	27.01	0.95	0.95	1.00
ITF202x65x13-t1.4N150MA0.4FX	0.40	0.75	28.35	24.18	0.85	0.85	1.00
ITF202x65x13-t1.4N150MA0.6FX	0.60	0.75	28.35	20.65	0.73	0.75	0.97
ITF202x65x13-t4N150MA0.2FX	0.21	0.77	114.05	107.20	0.94	0.95	0.99
ITF202x65x13-t4N150MA0.4FX	0.41	0.77	114.05	94.98	0.83	0.85	0.98
ITF202x65x13-t4N150MA0.6FX	0.62	0.77	114.05	81.99	0.72	0.74	0.97
ITF202x65x13-t6N150MA0.2FX	0.21	0.79	232.20	218.74	0.94	0.95	0.99
ITF202x65x13-t6N150MA0.4FX	0.42	0.79	232.20	195.26	0.84	0.84	1.00
ITF202x65x13-t6N150MA0.6FX	0.63	0.79	232.20	170.66	0.73	0.74	1.00
ITF202x65x13-t1.4N200MA0.2FX	0.20	1.00	29.58	28.14	0.95	0.97	0.98
ITF202x65x13-t1.4N200MA0.4FX	0.40	1.00	29.58	25.57	0.86	0.87	1.00
ITF202x65x13-t1.4N200MA0.6FX	0.60	1.00	29.58	22.40	0.76	0.76	0.99
ITF202x65x13-t1.4N200MA0.8FX	0.80	1.00	29.58	19.04	0.64	0.66	0.97
ITF202x65x13-t4N200MA0.2FX	0.21	1.03	119.25	112.69	0.94	0.97	0.98
ITF202x65x13-t4N200MA0.4FX	0.41	1.03	119.25	101.95	0.85	0.86	0.99
ITF202x65x13-t4N200MA0.6FX	0.62	1.03	119.25	89.73	0.75	0.76	0.99
ITF202x65x13-t4N200MA0.8FX	0.82	1.03	119.25	78.07	0.65	0.65	1.00
ITF202x65x13-t6N200MA0.2FX	0.21	1.05	245.92	232.91	0.95	0.97	0.98
ITF202x65x13-t6N200MA0.4FX	0.42	1.05	245.92	212.24	0.86	0.86	1.00
ITF202x65x13-t6N200MA0.6FX	0.63	1.05	245.92	189.58	0.77	0.75	1.02
ITF202x65x13-t6N200MA0.8FX	0.84	1.05	245.92	167.38	0.68	0.65	1.05
ITF302x90x18-t2N150MA0.2FX	0.20	0.50	24.53	23.68	0.97	0.94	1.03
ITF302x90x18-t2N150MA0.4FX	0.40	0.50	24.53	21.28	0.87	0.84	1.04
ITF302x90x18-t4N150MA0.2FX	0.20	0.51	111.08	104.69	0.94	0.94	1.01
ITF302x90x18-t4N150MA0.4FX	0.41	0.51	111.08	91.12	0.82	0.83	0.98
ITF302x90x18-t6N150MA0.2FX	0.21	0.51	233.71	225.12	0.96	0.94	1.03
ITF302x90x18-t6N150MA0.4FX	0.41	0.51	233.71	194.96	0.83	0.83	1.00
ITF302x90x18-t2N220MA0.2FX	0.20	0.73	25.56	24.51	0.96	0.95	1.01
ITF302x90x18-t2N220MA0.4FX	0.40	0.73	25.56	22.21	0.87	0.85	1.02
ITF302x90x18-t2N220MA0.6FX	0.60	0.73	25.56	18.86	0.74	0.75	0.99
ITF302x90x18-t4N220MA0.2FX	0.20	0.74	115.48	108.53	0.94	0.95	0.99
ITF302x90x18-t4N220MA0.4FX	0.41	0.74	115.48	96.11	0.83	0.85	0.98
ITF302x90x18-t4N220MA0.6FX	0.61	0.74	115.48	81.90	0.71	0.74	0.95
ITF302x90x18-t6N220MA0.2FX	0.21	0.75	250.76	234.77	0.94	0.95	0.99
ITF302x90x18-t6N220MA0.4FX	0.41	0.75	250.76	207.84	0.83	0.85	0.98
ITF302x90x18-t6N220MA0.6FX	0.62	0.75	250.76	178.97	0.71	0.74	0.96
ITF302x90x18-t2N300MA0.2FX	0.20	1.00	26.75	25.54	0.95	0.97	0.99
ITF302x90x18-t2N300MA0.4FX	0.40	1.00	26.75	23.45	0.88	0.87	1.01
ITF302x90x18-t2N300MA0.6FX	0.60	1.00	26.75	20.65	0.77	0.76	1.01
ITF302x90x18-t2N300MA0.8FX	0.80	1.00	26.75	17.58	0.66	0.66	0.99
ITF302x90x18-t4N300MA0.2FX	0.20	1.01	120.92	113.82	0.94	0.97	0.97
ITF302x90x18-t4N300MA0.4FX	0.41	1.01	120.92	102.81	0.85	0.86	0.98
ITF302x90x18-t4N300MA0.6FX	0.61	1.01	120.92	89.82	0.74	0.76	0.98

Continue

Specimen	Holes diameter ratio	Bearing ratio	Failure load without holes	Failure load with holes	Reduction factor	Proposed reduction factor	Comparison with proposed reduction factor
	a/h	*N/h*	*P*	*P(Holes)*	*R*= P(Holes) / P(A0)	*Rp* = 1.01-0.51 *(a/h)*+0.06 *(N/h)*	*R/Rp*
			(kN)	(kN)			
ITF302x90x18-t4N300MA0.8FX	0.81	1.01	120.92	76.48	0.63	0.66	0.96
ITF302x90x18-t6N300MA0.2FX	0.21	1.03	264.32	248.27	0.94	0.97	0.97
ITF302x90x18-t6N300MA0.4FX	0.41	1.03	264.32	224.47	0.85	0.86	0.99
ITF302x90x18-t6N300MA0.6FX	0.62	1.03	264.32	197.37	0.75	0.76	0.99
ITF302x90x18-t6N300MA0.8FX	0.82	1.03	264.32	170.61	0.65	0.65	0.99
ITF142x60x13-t1.3N90MA0.2FX	0.20	0.64	8.97	8.92	0.99	0.95	1.05
ITF142x60x13-t1.3N90MA0.4FX	0.40	0.64	8.97	7.75	0.86	0.84	1.02
ITF142x60x13-t1.3N90MA0.6FX	0.60	0.64	8.97	6.64	0.74	0.74	1.00
ITF142x60x13-t1.3N90MA0.8FX	0.80	0.64	8.97	5.55	0.62	0.64	0.96
ITF142x60x13-t1.3N120MA0.2FX	0.20	0.86	9.44	9.26	0.98	0.96	1.02
ITF142x60x13-t1.3N120MA0.4FX	0.40	0.86	9.44	8.19	0.87	0.86	1.01
ITF142x60x13-t1.3N120MA0.6FX	0.60	0.86	9.44	7.06	0.75	0.75	0.99
ITF142x60x13-t1.3N120MA0.8FX	0.80	0.86	9.44	5.94	0.63	0.65	0.96
ITF172x65x13-t1.3N120MA0.4FX	0.40	0.71	10.72	9.31	0.87	0.85	1.02
ITF172x65x13-t1.3N120MA0.6FX	0.60	0.71	10.72	7.87	0.73	0.75	0.98
ITF202x65x13-t1.4N150MA0.4FX	0.40	0.75	13.51	11.42	0.85	0.85	0.99
ITF202x65x13-t1.4N150MA0.6FX	0.60	0.75	13.51	10.10	0.75	0.75	1.00
ITF262x65x13-t1.6N150MA0.2FX	0.20	0.58	12.78	12.41	0.97	0.94	1.03
ITF262x65x13-t1.6N150MA0.4FX	0.40	0.58	12.78	11.31	0.88	0.84	1.05
Mean	Pm						1.00
STD							0.03
COV	Vp						0.03
Reliability index	β						2.86
Resistance factor	φ						0.85

D.5 Statistical analysis for the comparison of the strength reduction factor for flanges unfastened under ETF loading condition (Type 1 holes)

Specimen	Holes diameter ratio	Bearing ratio	Failure load without holes	Failure load with holes	Reduction factor	Proposed reduction factor	Comparison with proposed reduction factor
	a/h	*x/h*	*P* (kN)	*P(Holes)* (kN)	*R*= P(Holes) / P(A0)	*Rp* = 0.95-0.49 *(a/h)*+0.17 *(x/h)*	*R/Rp*
ETF202x65x13-t1.4N32.5A0.2FR	0.20	0.78	1.89	1.80	0.95	0.98	0.97
ETF202x65x13-t1.4N32.5A0.4FR	0.40	0.78	1.89	1.62	0.86	0.89	0.97
ETF202x65x13-t1.4N32.5A0.6FR	0.60	0.78	1.89	1.43	0.76	0.79	0.96
ETF202x65x13-t1.4N32.5A0.8FR	0.80	0.78	1.89	1.21	0.64	0.69	0.93
ETF202x65x13-t2.0N32.5A0.2FR	0.20	0.78	5.46	5.18	0.95	0.98	0.96
ETF202x65x13-t2.0N32.5A0.4FR	0.40	0.78	5.46	4.68	0.86	0.89	0.97
ETF202x65x13-t2.0N32.5A0.6FR	0.60	0.78	5.46	4.08	0.75	0.79	0.95
ETF202x65x13-t2.0N32.5A0.8FR	0.80	0.78	5.46	3.43	0.63	0.69	0.91
ETF202x65x13-t4.0N32.5A0.2FR	0.21	0.80	26.92	25.80	0.96	0.99	0.97
ETF202x65x13-t4.0N32.5A0.4FR	0.41	0.80	26.92	23.33	0.87	0.88	0.98
ETF202x65x13-t4.0N32.5A0.6FR	0.62	0.80	26.92	20.46	0.76	0.78	0.97
ETF202x65x13-t4.0N32.5A0.8FR	0.82	0.80	26.92	17.44	0.65	0.68	0.95
ETF202x65x13-t6.0N32.5A0.2FR	0.21	0.82	62.16	60.39	0.97	0.99	0.99
ETF202x65x13-t6.0N32.5A0.4FR	0.42	0.82	62.16	54.94	0.88	0.88	1.00
ETF202x65x13-t6.0N32.5A0.6FR	0.63	0.82	62.16	48.22	0.78	0.78	0.99
ETF202x65x13-t6.0N32.5A0.8FR	0.84	0.82	62.16	41.05	0.66	0.68	0.97
ETF202x65x13-t1.4N65A0.2FR	0.20	0.68	2.50	2.38	0.95	0.97	0.98
ETF202x65x13-t1.4N65A0.4FR	0.40	0.68	2.50	2.16	0.86	0.87	0.99
ETF202x65x13-t1.4N65A0.6FR	0.60	0.68	2.50	1.92	0.77	0.77	1.00
ETF202x65x13-t1.4N65A0.8FR	0.80	0.68	2.50	1.65	0.66	0.67	0.98
ETF202x65x13-t2.0N65A0.2FR	0.20	0.68	6.30	6.01	0.95	0.97	0.99
ETF202x65x13-t2.0N65A0.4FR	0.40	0.68	6.30	5.46	0.87	0.87	1.00
ETF202x65x13-t2.0N65A0.6FR	0.60	0.68	6.30	4.82	0.77	0.77	0.99
ETF202x65x13-t2.0N65A0.8FR	0.80	0.68	6.30	4.16	0.66	0.67	0.98
ETF202x65x13-t4.0N65A0.2FR	0.21	0.70	30.39	29.22	0.96	0.97	0.99
ETF202x65x13-t4.0N65A0.4FR	0.41	0.70	30.39	26.69	0.88	0.87	1.01
ETF202x65x13-t4.0N65A0.6FR	0.62	0.70	30.39	23.71	0.78	0.77	1.02
ETF202x65x13-t4.0N65A0.8FR	0.82	0.70	30.39	20.59	0.68	0.67	1.02
ETF202x65x13-t6.0N65A0.2FR	0.21	0.71	70.17	68.11	0.97	0.97	1.00
ETF202x65x13-t6.0N65A0.4FR	0.42	0.71	70.17	62.59	0.89	0.87	1.03
ETF202x65x13-t6.0N65A0.6FR	0.63	0.71	70.17	55.55	0.79	0.76	1.04
ETF202x65x13-t6.0N65A0.8FR	0.84	0.71	70.17	48.03	0.68	0.66	1.04
ETF302x90x18-t2N44A0.2FR	0.20	0.76	3.71	3.51	0.95	0.98	0.96
ETF302x90x18-t2N44A0.4FR	0.40	0.76	3.71	3.16	0.85	0.88	0.96
ETF302x90x18-t2N44A0.6FR	0.60	0.76	3.71	2.77	0.75	0.79	0.95
ETF302x90x18-t2N44A0.8FR	0.80	0.76	3.71	2.33	0.63	0.69	0.91
ETF302x90x18-t4.0N44A0.2FR	0.20	0.77	23.95	22.79	0.95	0.98	0.97
ETF302x90x18-t4.0N44A0.4FR	0.41	0.77	23.95	20.48	0.86	0.88	0.97
ETF302x90x18-t4.0N44A0.6FR	0.61	0.77	23.95	17.79	0.74	0.78	0.95
ETF302x90x18-t4.0N44A0.8FR	0.81	0.77	23.95	14.95	0.62	0.68	0.91
ETF302x90x18-t6.0N44A0.2FR	0.21	0.78	59.06	56.73	0.96	0.98	0.98
ETF302x90x18-t6.0N44A0.4FR	0.41	0.78	59.06	51.20	0.87	0.88	0.98
ETF302x90x18-t6.0N44A0.6FR	0.62	0.78	59.06	44.69	0.76	0.78	0.97
ETF302x90x18-t6.0N44A0.8FR	0.82	0.78	59.06	37.79	0.64	0.68	0.94
ETF302x90x18-t2N90A0.2FR	0.20	0.70	4.26	4.07	0.96	0.97	0.98
ETF302x90x18-t2N90A0.4FR	0.40	0.70	4.26	3.70	0.87	0.87	0.99
ETF302x90x18-t2N90A0.6FR	0.60	0.70	4.26	3.29	0.77	0.78	1.00
ETF302x90x18-t2N90A0.8FR	0.80	0.70	4.26	2.84	0.67	0.68	0.98
ETF302x90x18-t4.0N90A0.2FR	0.20	0.71	27.72	26.55	0.96	0.97	0.99
ETF302x90x18-t4.0N90A0.4FR	0.41	0.71	27.72	24.22	0.87	0.87	1.00
ETF302x90x18-t4.0N90A0.6FR	0.61	0.71	27.72	21.50	0.78	0.77	1.00
ETF302x90x18-t4.0N90A0.8FR	0.81	0.71	27.72	18.65	0.67	0.67	1.00
ETF302x90x18-t6.0N90A0.2FR	0.21	0.72	66.98	64.30	0.96	0.97	0.99

Continue

Specimen	Holes diameter ratio *a/h*	Bearing ratio *x/h*	Failure load without holes *P* (kN)	Failure load with holes *P(Holes)* (kN)	Reduction factor *R*= P(Holes) / P(A0)	Proposed reduction factor *Rp = 0*.95-0.49 *(a/h)*+0.17 *(x/h)*	Comparison with proposed reduction factor *R/Rp*
ETF302x90x18-t6.0N90A0.4FR	0.41	0.72	66.98	59.75	0.89	0.87	1.02
ETF302x90x18-t6.0N90A0.6FR	0.62	0.72	66.98	53.41	0.80	0.77	1.03
ETF302x90x18-t6.0N90A0.8FR	0.82	0.72	66.98	46.55	0.69	0.67	1.04
ETF202x65x13-t1.4N32.5A0.2X0FR	0.20	0.00	1.89	1.64	0.87	0.85	1.02
ETF202x65x13-t1.4N32.5A0.2X0.2FR	0.20	0.20	1.89	1.70	0.90	0.89	1.02
ETF202x65x13-t1.4N32.5A0.2X0.4FR	0.20	0.40	1.89	1.75	0.93	0.92	1.01
ETF202x65x13-t1.4N32.5A0.2X0.6FR	0.20	0.60	1.89	1.79	0.94	0.95	0.99
ETF202x65x13-t1.4N32.5A0.4X0FR	0.40	0.00	1.89	1.35	0.72	0.75	0.95
ETF202x65x13-t1.4N32.5A0.4X0.2FR	0.40	0.20	1.89	1.45	0.77	0.79	0.98
ETF202x65x13-t1.4N32.5A0.4X0.4FR	0.40	0.40	1.89	1.55	0.82	0.82	1.00
ETF202x65x13-t1.4N32.5A0.4X0.6FR	0.40	0.60	1.89	1.63	0.86	0.86	1.01
ETF202x65x13-t1.4N32.5A0.6X0FR	0.60	0.00	1.89	1.10	0.58	0.66	0.89
ETF202x65x13-t1.4N32.5A0.6X0.2FR	0.60	0.20	1.89	1.24	0.65	0.69	0.95
ETF202x65x13-t1.4N32.5A0.6X0.4FR	0.60	0.40	1.89	1.38	0.73	0.72	1.01
ETF202x65x13-t1.4N32.5A0.6X0.6FR	0.60	0.60	1.89	1.50	0.79	0.76	1.05
ETF202x65x13-t1.4N32.5A0.8X0FR	0.80	0.00	1.89	0.87	0.46	0.56	0.83
ETF202x65x13-t1.4N32.5A0.8X0.2FR	0.80	0.20	1.89	1.05	0.55	0.59	0.94
ETF202x65x13-t1.4N32.5A0.8X0.4FR	0.80	0.40	1.89	1.23	0.65	0.63	1.04
ETF202x65x13-t1.4N32.5A0.8X0.6FR	0.80	0.60	1.89	1.38	0.73	0.66	1.11
ETF202x65x13-t1.4N65A0.2X0FR	0.20	0.00	2.50	2.23	0.89	0.85	1.04
ETF202x65x13-t1.4N65A0.2X0.2FR	0.20	0.20	2.50	2.30	0.92	0.89	1.04
ETF202x65x13-t1.4N65A0.2X0.4FR	0.20	0.40	2.50	2.35	0.94	0.92	1.02
ETF202x65x13-t1.4N65A0.2X0.6FR	0.20	0.60	2.50	2.38	0.95	0.95	1.00
ETF202x65x13-t1.4N65A0.4X0FR	0.40	0.00	2.50	1.89	0.76	0.75	1.00
ETF202x65x13-t1.4N65A0.4X0.2FR	0.40	0.20	2.50	2.02	0.81	0.79	1.03
ETF202x65x13-t1.4N65A0.4X0.4FR	0.40	0.40	2.50	2.13	0.85	0.82	1.03
ETF202x65x13-t1.4N65A0.4X0.6FR	0.40	0.60	2.50	2.21	0.89	0.86	1.03
ETF202x65x13-t1.4N65A0.6X0FR	0.60	0.00	2.50	1.60	0.64	0.66	0.97
ETF202x65x13-t1.4N65A0.6X0.2FR	0.60	0.20	2.50	1.78	0.71	0.69	1.03
ETF202x65x13-t1.4N65A0.6X0.4FR	0.60	0.40	2.50	1.93	0.77	0.72	1.07
ETF202x65x13-t1.4N65A0.6X0.6FR	0.60	0.60	2.50	2.07	0.83	0.76	1.09
ETF202x65x13-t1.4N65A0.8X0FR	0.80	0.00	2.50	1.35	0.54	0.56	0.97
ETF202x65x13-t1.4N65A0.8X0.2FR	0.80	0.20	2.50	1.57	0.63	0.59	1.06
ETF202x65x13-t1.4N65A0.8X0.4FR	0.80	0.40	2.50	1.77	0.71	0.63	1.13
ETF202x65x13-t1.4N65A0.8X0.6FR	0.80	0.60	2.50	1.94	0.78	0.66	1.17
ETF302x90x18-t2N44A0.2X0FR	0.20	0.00	3.71	3.21	0.87	0.85	1.02
ETF302x90x18-t2N44A0.2X0.2FR	0.20	0.20	3.71	3.34	0.90	0.89	1.02
ETF302x90x18-t2N44A0.2X0.4FR	0.20	0.40	3.71	3.43	0.92	0.92	1.01
ETF302x90x18-t2N44A0.2X0.6FR	0.20	0.60	3.71	3.50	0.94	0.95	0.99
ETF302x90x18-t2N44A0.4X0FR	0.40	0.00	3.71	2.62	0.71	0.75	0.94
ETF302x90x18-t2N44A0.4X0.2FR	0.40	0.20	3.71	2.84	0.77	0.79	0.97
ETF302x90x18-t2N44A0.4X0.4FR	0.40	0.40	3.71	3.04	0.82	0.82	1.00
ETF302x90x18-t2N44A0.4X0.6FR	0.40	0.60	3.71	3.19	0.86	0.86	1.01
ETF302x90x18-t2N44A0.6X0FR	0.60	0.00	3.71	2.11	0.57	0.66	0.87
ETF302x90x18-t2N44A0.6X0.2FR	0.60	0.20	3.71	2.41	0.65	0.69	0.94
ETF302x90x18-t2N44A0.6X0.4FR	0.60	0.40	3.71	2.69	0.73	0.72	1.00
ETF302x90x18-t2N44A0.6X0.6FR	0.60	0.60	3.71	2.93	0.79	0.76	1.04
ETF302x90x18-t2N44A0.8X0FR	0.80	0.00	3.71	1.65	0.45	0.56	0.80
ETF302x90x18-t2N44A0.8X0.2FR	0.80	0.20	3.71	2.04	0.55	0.59	0.93
ETF302x90x18-t2N44A0.8X0.4FR	0.80	0.40	3.71	2.40	0.65	0.63	1.03
ETF302x90x18-t2N44A0.8X0.6FR	0.80	0.60	3.71	2.71	0.73	0.66	1.11
ETF302x90x18-t2N90A0.2X0FR	0.20	0.00	4.26	3.81	0.90	0.85	1.05
ETF302x90x18-t2N90A0.2X0.2FR	0.20	0.20	4.26	3.93	0.92	0.89	1.04

Continue

Specimen	Holes diameter ratio *a/h*	Bearing ratio *x/h*	Failure load without holes *P* (kN)	Failure load with holes *P(Holes)* (kN)	Reduction factor *R*= P(Holes) / P(A0)	Proposed reduction factor *Rp = 0.*95-0.49 *(a/h)*+0.17 *(x/h)*	Comparison with proposed reduction factor *R/Rp*
ETF302x90x18-t2N90A0.2X0.4FR	0.20	0.40	4.26	4.01	0.94	0.92	1.02
ETF302x90x18-t2N90A0.2X0.6FR	0.20	0.60	4.26	4.06	0.95	0.95	1.00
ETF302x90x18-t2N90A0.4X0FR	0.40	0.00	4.26	3.24	0.76	0.75	1.01
ETF302x90x18-t2N90A0.4X0.2FR	0.40	0.20	4.26	3.45	0.81	0.79	1.03
ETF302x90x18-t2N90A0.4X0.4FR	0.40	0.40	4.26	3.62	0.85	0.82	1.04
ETF302x90x18-t2N90A0.4X0.6FR	0.40	0.60	4.26	3.77	0.88	0.86	1.03
ETF302x90x18-t2N90A0.6X0FR	0.60	0.00	4.26	2.72	0.64	0.66	0.97
ETF302x90x18-t2N90A0.6X0.2FR	0.60	0.20	4.26	3.03	0.71	0.69	1.03
ETF302x90x18-t2N90A0.6X0.4FR	0.60	0.40	4.26	3.28	0.77	0.72	1.07
ETF302x90x18-t2N90A0.6X0.6FR	0.60	0.60	4.26	3.51	0.82	0.76	1.09
ETF302x90x18-t2N90A0.8X0FR	0.80	0.00	4.26	2.28	0.53	0.56	0.96
ETF302x90x18-t2N90A0.8X0.2FR	0.80	0.20	4.26	2.66	0.63	0.59	1.06
ETF302x90x18-t2N90A0.8X0.4FR	0.80	0.40	4.26	3.00	0.70	0.63	1.12
ETF302x90x18-t2N90A0.8X0.6FR	0.80	0.60	4.26	3.29	0.77	0.66	1.17
ETF142x60x13t1.3N30A0.4X0.2FR	0.20	0.76	1.68	1.62	0.96	0.98	0.98
ETF142x60x13t1.3N30A0.4X0.4FR	0.39	0.76	1.68	1.44	0.86	0.89	0.97
ETF142x60x13t1.3N30A0.4X0.6FR	0.59	0.76	1.68	1.30	0.77	0.79	0.98
ETF142x60x13t1.3N30A0.4X0.8FR	0.78	0.76	1.68	1.08	0.64	0.69	0.93
ETF142x60x13-t1.3N60A0.4X0.4FR	0.40	0.65	1.95	1.64	0.84	0.87	0.97
ETF142x60x13-t1.3N60A0.4X0.6FR	0.60	0.65	1.95	1.53	0.78	0.77	1.02
ETF172x65x13-t1.3N32.5A0.4X0.4FR	0.40	0.77	1.70	1.55	0.91	0.89	1.03
ETF172x65x13-t1.3N65A0.4X0.4FR	0.40	0.58	1.88	1.64	0.87	0.85	1.02
ETF202x65x13-t1.4N32.5A0.4X0.4FR	0.40	0.78	1.98	1.82	0.92	0.89	1.04
ETF202x65x13-t1.4N65A0.4X0.4FR	0.40	0.68	2.39	1.98	0.83	0.87	0.95
ETF262x65x13-t1.6N32.5A0.4X0.4FR	0.40	0.74	2.04	1.82	0.89	0.88	1.01
ETF262x65x13-t1.6N65A0.4X0.4FR	0.40	0.71	2.19	2.00	0.91	0.88	1.04
ETF302x90x18-t2N44A0.4X0.4FR	0.40	0.86	3.96	3.35	0.85	0.90	0.94
Mean, Pm							1.00
STD							0.05
COV, Vp							0.05
Reliability index, β							2.80
Resistance factor, φ							0.85

D.6 Statistical analysis for the comparison of the strength reduction factor for flanges unfastened under ETF loading condition (Type 2 holes)

Specimen	Holes diameter ratio	Bearing ratio	Failure load without holes	Failure load with holes	Reduction factor	Proposed reduction factor	Comparison with proposed reduction factor
	a/h	*x/h*	*P*	*P(Holes)*	*R*= P(Holes) / P(A0)	*Rp = 0*.90-0.60 *(a/h)*+0.12 *(N/h)*	*R/Rp*
			(kN)	(kN)			
ETF202x65x13-t1.4N100A0.2FR	0.20	0.50	2.93	2.54	0.87	0.84	1.03
ETF202x65x13-t1.4N100A0.4FR	0.40	0.50	2.93	2.08	0.71	0.72	0.99
ETF202x65x13-t4N100A0.2FR	0.21	0.51	35.20	30.03	0.85	0.84	1.02
ETF202x65x13-t4N100A0.4FR	0.41	0.51	35.20	25.22	0.72	0.72	1.00
ETF202x65x13-t6N100A0.2FR	0.21	0.53	80.07	67.81	0.85	0.84	1.01
ETF202x65x13-t6N100A0.4FR	0.42	0.53	80.07	57.32	0.72	0.71	1.01
ETF202x65x13-t1.4N150A0.2FR	0.20	0.75	3.19	2.82	0.88	0.87	1.02
ETF202x65x13-t1.4N150A0.4FR	0.40	0.75	3.19	2.37	0.74	0.75	0.99
ETF202x65x13-t1.4N150A0.6FR	0.60	0.75	3.19	1.95	0.61	0.63	0.97
ETF202x65x13-t4N150A0.2FR	0.21	0.77	43.03	37.39	0.87	0.87	1.00
ETF202x65x13-t4N150A0.4FR	0.41	0.77	43.03	31.94	0.74	0.75	0.99
ETF202x65x13-t4N150A0.6FR	0.62	0.77	43.03	26.84	0.62	0.62	1.00
ETF202x65x13-t6N150A0.2FR	0.21	0.79	95.84	83.51	0.87	0.87	1.00
ETF202x65x13-t6N150A0.4FR	0.42	0.79	95.84	72.21	0.75	0.74	1.01
ETF202x65x13-t6N150A0.6FR	0.63	0.79	95.84	61.28	0.64	0.62	1.04
ETF202x65x13-t1.4N200A0.2FR	0.20	1.00	3.88	3.49	0.90	0.90	1.00
ETF202x65x13-t1.4N200A0.4FR	0.40	1.00	3.88	3.02	0.78	0.78	1.00
ETF202x65x13-t1.4N200A0.6FR	0.60	1.00	3.88	2.59	0.67	0.66	1.01
ETF202x65x13-t1.4N200A0.8FR	0.80	1.00	3.88	2.21	0.57	0.54	1.06
ETF202x65x13-t4N200A0.2FR	0.21	1.03	50.90	45.17	0.89	0.90	0.99
ETF202x65x13-t4N200A0.4FR	0.41	1.03	50.90	39.50	0.78	0.78	1.00
ETF202x65x13-t4N200A0.6FR	0.62	1.03	50.90	33.88	0.67	0.65	1.02
ETF202x65x13-t4N200A0.8FR	0.82	1.03	50.90	28.36	0.56	0.53	1.05
ETF202x65x13-t6N200A0.2FR	0.21	1.05	111.90	99.13	0.89	0.90	0.98
ETF202x65x13-t6N200A0.4FR	0.42	1.05	111.90	87.35	0.78	0.77	1.01
ETF202x65x13-t6N200A0.6FR	0.63	1.05	111.90	75.85	0.68	0.65	1.05
ETF202x65x13-t6N200A0.8FR	0.84	1.05	111.90	64.34	0.57	0.52	1.10
ETF302x90x18-t2N150A0.2FR	0.20	0.50	5.13	4.47	0.87	0.84	1.04
ETF302x90x18-t2N150A0.4FR	0.40	0.50	5.13	3.64	0.71	0.72	0.99
ETF302x90x18-t4N150A0.2FR	0.20	0.51	33.18	28.19	0.85	0.84	1.01
ETF302x90x18-t4N150A0.4FR	0.41	0.51	33.18	23.38	0.70	0.72	0.98
ETF302x90x18-t6N150A0.2FR	0.21	0.51	79.55	67.39	0.85	0.84	1.01
ETF302x90x18-t6N150A0.4FR	0.41	0.51	79.55	56.30	0.71	0.71	0.99
ETF302x90x18-t2N220A0.2FR	0.20	0.73	6.37	5.64	0.89	0.87	1.02
ETF302x90x18-t2N220A0.4FR	0.40	0.73	6.37	4.70	0.74	0.75	0.99
ETF302x90x18-t2N220A0.6FR	0.60	0.73	6.37	3.80	0.60	0.63	0.95
ETF302x90x18-t4N220A0.2FR	0.20	0.74	39.96	34.51	0.86	0.87	1.00
ETF302x90x18-t4N220A0.4FR	0.41	0.74	39.96	29.00	0.73	0.75	0.97
ETF302x90x18-t4N220A0.6FR	0.61	0.74	39.96	23.98	0.60	0.62	0.96
ETF302x90x18-t6N220A0.2FR	0.21	0.75	94.77	81.83	0.86	0.87	1.00
ETF302x90x18-t6N220A0.4FR	0.41	0.75	94.77	69.40	0.73	0.74	0.98
ETF302x90x18-t6N220A0.6FR	0.62	0.75	94.77	56.86	0.60	0.62	0.97
ETF302x90x18-t2N300A0.2FR	0.20	1.00	7.85	7.09	0.90	0.90	1.00
ETF302x90x18-t2N300A0.4FR	0.40	1.00	7.85	6.06	0.77	0.78	0.99
ETF302x90x18-t2N300A0.6FR	0.60	1.00	7.85	5.05	0.64	0.66	0.98
ETF302x90x18-t2N300A0.8FR	0.80	1.00	7.85	4.10	0.52	0.54	0.97
ETF302x90x18-t4N300A0.2FR	0.20	1.01	48.25	42.70	0.88	0.90	0.98
ETF302x90x18-t4N300A0.4FR	0.41	1.01	48.25	36.93	0.77	0.78	0.98
ETF302x90x18-t4N300A0.6FR	0.61	1.01	48.25	31.24	0.65	0.66	0.99
ETF302x90x18-t4N300A0.8FR	0.81	1.01	48.25	25.77	0.53	0.53	1.00
ETF302x90x18-t6N300A0.2FR	0.21	1.03	112.50	99.34	0.88	0.90	0.98

Continue

Specimen	Holes diameter ratio *a/h*	Bearing ratio *x/h*	Failure load without holes *P* (kN)	Failure load with holes *P(Holes)* (kN)	Reduction factor *R*= P(Holes) / P(A0)	Proposed reduction factor *Rp = 0*.90-0.60 *(a/h)*+0.12 *(N/h)*	Comparison with proposed reduction factor *R/Rp*
ETF302x90x18-t6N300A0.4FR	0.41	1.03	112.50	86.56	0.77	0.78	0.99
ETF302x90x18-t6N300A0.6FR	0.62	1.03	112.50	74.07	0.66	0.65	1.01
ETF302x90x18-t6N300A0.8FR	0.82	1.03	112.50	61.86	0.55	0.53	1.04
ETF142x60x13-t1.3N90MA0.2FR	0.20	0.64	2.21	1.98	0.90	0.86	1.04
ETF142x60x13-t1.3N90MA0.4FR	0.40	0.64	2.21	1.62	0.73	0.74	0.99
ETF142x60x13-t1.3N90MA0.6FR	0.60	0.64	2.21	1.32	0.60	0.62	0.97
ETF142x60x13-t1.3N120MA0.2FR	0.20	0.86	2.35	1.95	0.83	0.88	0.94
ETF142x60x13-t1.3N120MA0.4FR	0.40	0.86	2.35	1.78	0.76	0.76	0.99
ETF142x60x13-t1.3N120MA0.6FR	0.60	0.86	2.35	1.49	0.63	0.64	0.99
ETF172x65x13-t1.3N120MA0.4FR	0.40	0.71	2.37	1.70	0.72	0.75	0.96
ETF172x65x13-t1.3N120MA0.6FR	0.60	0.71	2.37	1.36	0.57	0.63	0.92
ETF202x65x13-t1.4N120MA0.2FR	0.20	0.60	2.70	2.41	0.89	0.85	1.05
ETF202x65x13-t1.4N120MA0.4FR	0.40	0.60	2.70	1.88	0.70	0.73	0.95
ETF202x65x13-t1.4N150MA0.4FR	0.40	0.75	2.84	2.19	0.77	0.75	1.03
ETF202x65x13-t1.4N150MA0.6FR	0.60	0.75	2.84	1.77	0.62	0.63	0.99
ETF262x65x13-t1.6N120MA0.2FR	0.20	0.46	2.55	2.29	0.90	0.84	1.07
ETF262x65x13-t1.6N120MA0.4FR	0.40	0.46	2.55	1.77	0.69	0.72	0.97
ETF262x65x13-t1.6N150MA0.4FR	0.40	0.58	2.82	2.04	0.72	0.73	0.99
Mean, Pm							1.00
STD							0.03
COV, Vp							0.03
Reliability index, β							2.85
Resistance factor, φ							0.85

D.7 Statistical analysis for the comparison of the strength reduction factor for flanges fastened under ETF loading condition (Type 1 holes)

Specimen	Holes diameter ratio	Bearing ratio	Failure load without holes	Failure load with holes	Reduction factor	Proposed reduction factor	Comparison with proposed reduction factor
	a/h	*x/h*	*P*	*P(Holes)*	*R=* P(Holes) / P(A0)	*Rp = 0.*96-0.36 *(a/h)*+0.14 *(x/h)*	*R/Rp*
			(kN)	(kN)			
ETF202x65x13-t1.4N32.5A0.2FX	0.20	0.78	3.41	3.21	0.94	1.00	0.94
ETF202x65x13-t1.4N32.5A0.4FX	0.40	0.78	3.41	3.01	0.88	0.93	0.95
ETF202x65x13-t1.4N32.5A0.6FX	0.60	0.78	3.41	2.73	0.80	0.85	0.94
ETF202x65x13-t1.4N32.5A0.8FX	0.80	0.78	3.41	2.34	0.69	0.78	0.88
ETF202x65x13-t2.0N32.5A0.2FX	0.20	0.78	8.88	8.58	0.97	1.00	0.97
ETF202x65x13-t2.0N32.5A0.4FX	0.40	0.78	8.88	7.98	0.90	0.92	0.97
ETF202x65x13-t2.0N32.5A0.6FX	0.60	0.78	8.88	7.06	0.79	0.85	0.93
ETF202x65x13-t2.0N32.5A0.8FX	0.80	0.78	8.88	6.20	0.70	0.78	0.89
ETF202x65x13-t4.0N32.5A0.2FX	0.21	0.80	36.29	35.62	0.98	1.00	0.98
ETF202x65x13-t4.0N32.5A0.4FX	0.41	0.80	36.29	33.40	0.92	0.92	1.00
ETF202x65x13-t4.0N32.5A0.6FX	0.62	0.80	36.29	30.68	0.85	0.85	0.99
ETF202x65x13-t4.0N32.5A0.8FX	0.82	0.80	36.29	27.76	0.76	0.78	0.99
ETF202x65x13-t6.0N32.5A0.2FX	0.21	0.82	75.15	74.76	0.99	1.00	1.00
ETF202x65x13-t6.0N32.5A0.4FX	0.42	0.82	75.15	71.60	0.95	0.92	1.03
ETF202x65x13-t6.0N32.5A0.6FX	0.63	0.82	75.15	66.43	0.88	0.85	1.04
ETF202x65x13-t6.0N32.5A0.8FX	0.84	0.82	75.15	60.47	0.80	0.77	1.04
ETF202x65x13-t1.4N65A0.2FX	0.20	0.68	4.51	4.37	0.97	0.98	0.99
ETF202x65x13-t1.4N65A0.4FX	0.40	0.68	4.51	4.12	0.91	0.91	1.00
ETF202x65x13-t1.4N65A0.6FX	0.60	0.68	4.51	3.81	0.85	0.84	1.01
ETF202x65x13-t1.4N65A0.8FX	0.80	0.68	4.51	3.42	0.76	0.77	0.99
ETF202x65x13-t2.0N65A0.2FX	0.20	0.68	10.48	10.18	0.97	0.98	0.99
ETF202x65x13-t2.0N65A0.4FX	0.40	0.68	10.48	9.59	0.92	0.91	1.00
ETF202x65x13-t2.0N65A0.6FX	0.60	0.68	10.48	8.79	0.84	0.84	1.00
ETF202x65x13-t2.0N65A0.8FX	0.80	0.68	10.48	8.03	0.77	0.77	1.00
ETF202x65x13-t4.0N65A0.2FX	0.21	0.70	43.10	42.53	0.99	0.98	1.00
ETF202x65x13-t4.0N65A0.4FX	0.41	0.70	43.10	40.84	0.95	0.91	1.04
ETF202x65x13-t4.0N65A0.6FX	0.62	0.70	43.10	38.53	0.89	0.84	1.07
ETF202x65x13-t4.0N65A0.8FX	0.82	0.70	43.10	36.03	0.84	0.76	1.10
ETF202x65x13-t6.0N65A0.2FX	0.21	0.71	92.01	91.20	0.99	0.98	1.01
ETF202x65x13-t6.0N65A0.4FX	0.42	0.71	92.01	88.25	0.96	0.91	1.06
ETF202x65x13-t6.0N65A0.6FX	0.63	0.71	92.01	83.56	0.91	0.83	1.09
ETF202x65x13-t6.0N65A0.8FX	0.84	0.71	92.01	77.98	0.85	0.76	1.12
ETF302x90x18-t2N44A0.2FX	0.20	0.76	6.32	6.32	1.00	0.99	1.01
ETF302x90x18-t2N44A0.4FX	0.40	0.76	6.32	5.94	0.94	0.92	1.02
ETF302x90x18-t2N44A0.6FX	0.60	0.76	6.32	5.41	0.86	0.85	1.01
ETF302x90x18-t2N44A0.8FX	0.80	0.76	6.32	4.62	0.73	0.78	0.94
ETF302x90x18-t4.0N44A0.2FX	0.20	0.77	35.30	34.40	0.97	0.99	0.98
ETF302x90x18-t4.0N44A0.4FX	0.41	0.77	35.30	32.07	0.91	0.92	0.99
ETF302x90x18-t4.0N44A0.6FX	0.61	0.77	35.30	29.17	0.83	0.85	0.97
ETF302x90x18-t4.0N44A0.8FX	0.81	0.77	35.30	26.07	0.74	0.78	0.95
ETF302x90x18-t6.0N44A0.2FX	0.21	0.78	78.08	76.89	0.98	1.00	0.99
ETF302x90x18-t6.0N44A0.4FX	0.41	0.78	78.08	72.35	0.93	0.92	1.01
ETF302x90x18-t6.0N44A0.6FX	0.62	0.78	78.08	66.34	0.85	0.85	1.00
ETF302x90x18-t6.0N44A0.8FX	0.82	0.78	78.08	59.81	0.77	0.77	0.99
ETF302x90x18-t2N90A0.2FX	0.20	0.70	7.87	7.65	0.97	0.99	0.99
ETF302x90x18-t2N90A0.4FX	0.40	0.70	7.87	7.24	0.92	0.91	1.01
ETF302x90x18-t2N90A0.6FX	0.60	0.70	7.87	6.72	0.85	0.84	1.01
ETF302x90x18-t2N90A0.8FX	0.80	0.70	7.87	6.04	0.77	0.77	1.00
ETF302x90x18-t4.0N90A0.2FX	0.20	0.71	42.45	41.65	0.98	0.99	0.99
ETF302x90x18-t4.0N90A0.4FX	0.41	0.71	42.45	39.59	0.93	0.91	1.02
ETF302x90x18-t4.0N90A0.6FX	0.61	0.71	42.45	37.10	0.87	0.84	1.04

Continue

Specimen	Holes diameter ratio	Bearing ratio	Failure load without holes	Failure load with holes	Redution factor	Proposed redution factor	Comparison with proposed redution factor
	a/h	*x/h*	*P*	*P(Holes)*	*R=* P(Holes) / P(A0)	*Rp = 0.*96-0.36 *(a/h)*+0.14 *(x/h)*	*R/Rp*
			(kN)	(kN)			
ETF302x90x18-t4.0N90A0.8FX	0.81	0.71	42.45	34.57	0.81	0.77	1.06
ETF302x90x18-t6.0N90A0.2FX	0.21	0.72	94.15	93.08	0.99	0.99	1.00
ETF302x90x18-t6.0N90A0.4FX	0.41	0.72	94.15	89.79	0.95	0.91	1.04
ETF302x90x18-t6.0N90A0.6FX	0.62	0.72	94.15	85.07	0.90	0.84	1.08
ETF302x90x18-t6.0N90A0.8FX	0.82	0.72	94.15	79.64	0.85	0.76	1.11
ETF202x65x13-t1.4N32.5A0.2X0FX	0.20	0.00	3.41	3.09	0.91	0.89	1.02
ETF202x65x13-t1.4N32.5A0.2X0.2FX	0.20	0.20	3.41	3.12	0.92	0.92	1.00
ETF202x65x13-t1.4N32.5A0.2X0.4FX	0.20	0.40	3.41	3.15	0.92	0.94	0.98
ETF202x65x13-t1.4N32.5A0.2X0.6FX	0.20	0.60	3.41	3.19	0.94	0.97	0.96
ETF202x65x13-t1.4N32.5A0.4X0FX	0.40	0.00	3.41	2.72	0.80	0.82	0.98
ETF202x65x13-t1.4N32.5A0.4X0.2FX	0.40	0.20	3.41	2.81	0.82	0.84	0.97
ETF202x65x13-t1.4N32.5A0.4X0.4FX	0.40	0.40	3.41	2.91	0.85	0.87	0.98
ETF202x65x13-t1.4N32.5A0.4X0.6FX	0.40	0.60	3.41	3.02	0.89	0.90	0.98
ETF202x65x13-t1.4N32.5A0.6X0FX	0.60	0.00	3.41	2.29	0.67	0.74	0.90
ETF202x65x13-t1.4N32.5A0.6X0.2FX	0.60	0.20	3.41	2.48	0.73	0.77	0.94
ETF202x65x13-t1.4N32.5A0.6X0.4FX	0.60	0.40	3.41	2.66	0.78	0.80	0.98
ETF202x65x13-t1.4N32.5A0.6X0.6FX	0.60	0.60	3.41	2.84	0.83	0.83	1.01
ETF202x65x13-t1.4N32.5A0.8X0FX	0.80	0.00	3.41	1.80	0.53	0.67	0.78
ETF202x65x13-t1.4N32.5A0.8X0.2FX	0.80	0.20	3.41	2.11	0.62	0.70	0.88
ETF202x65x13-t1.4N32.5A0.8X0.4FX	0.80	0.40	3.41	2.37	0.69	0.73	0.95
ETF202x65x13-t1.4N32.5A0.8X0.6FX	0.80	0.60	3.41	2.62	0.77	0.76	1.02
ETF202x65x13-t1.4N65A0.2X0FX	0.20	0.00	4.51	4.24	0.94	0.89	1.06
ETF202x65x13-t1.4N65A0.2X0.2FX	0.20	0.20	4.51	4.28	0.95	0.92	1.04
ETF202x65x13-t1.4N65A0.2X0.4FX	0.20	0.40	4.51	4.32	0.96	0.94	1.02
ETF202x65x13-t1.4N65A0.2X0.6FX	0.20	0.60	4.51	4.37	0.97	0.97	1.00
ETF202x65x13-t1.4N65A0.4X0FX	0.40	0.00	4.51	3.85	0.85	0.82	1.05
ETF202x65x13-t1.4N65A0.4X0.2FX	0.40	0.20	4.51	3.95	0.88	0.84	1.04
ETF202x65x13-t1.4N65A0.4X0.4FX	0.40	0.40	4.51	4.07	0.90	0.87	1.04
ETF202x65x13-t1.4N65A0.4X0.6FX	0.40	0.60	4.51	4.19	0.93	0.90	1.03
ETF202x65x13-t1.4N65A0.6X0FX	0.60	0.00	4.51	3.46	0.77	0.74	1.03
ETF202x65x13-t1.4N65A0.6X0.2FX	0.60	0.20	4.51	3.64	0.81	0.77	1.05
ETF202x65x13-t1.4N65A0.6X0.4FX	0.60	0.40	4.51	3.83	0.85	0.80	1.06
ETF202x65x13-t1.4N65A0.6X0.6FX	0.60	0.60	4.51	4.02	0.89	0.83	1.08
ETF202x65x13-t1.4N65A0.8X0FX	0.80	0.00	4.51	3.03	0.67	0.67	1.00
ETF202x65x13-t1.4N65A0.8X0.2FX	0.80	0.20	4.51	3.31	0.73	0.70	1.05
ETF202x65x13-t1.4N65A0.8X0.4FX	0.80	0.40	4.51	3.58	0.79	0.73	1.09
ETF202x65x13-t1.4N65A0.8X0.6FX	0.80	0.60	4.51	3.83	0.85	0.76	1.12
ETF302x90x18-t2N44A0.2X0FX	0.20	0.00	6.54	6.03	0.92	0.89	1.04
ETF302x90x18-t2N44A0.2X0.2FX	0.20	0.20	6.54	6.11	0.93	0.92	1.02
ETF302x90x18-t2N44A0.2X0.4FX	0.20	0.40	6.54	6.20	0.95	0.94	1.00
ETF302x90x18-t2N44A0.2X0.6FX	0.20	0.60	6.54	6.30	0.96	0.97	0.99
ETF302x90x18-t2N44A0.4X0FX	0.40	0.00	6.54	5.26	0.80	0.82	0.99
ETF302x90x18-t2N44A0.4X0.2FX	0.40	0.20	6.54	5.50	0.84	0.84	1.00
ETF302x90x18-t2N44A0.4X0.4FX	0.40	0.40	6.54	5.75	0.88	0.87	1.01
ETF302x90x18-t2N44A0.4X0.6FX	0.40	0.60	6.54	5.98	0.92	0.90	1.02
ETF302x90x18-t2N44A0.6X0FX	0.60	0.00	6.54	4.41	0.68	0.74	0.91
ETF302x90x18-t2N44A0.6X0.2FX	0.60	0.20	6.54	4.89	0.75	0.77	0.97
ETF302x90x18-t2N44A0.6X0.4FX	0.60	0.40	6.54	5.29	0.81	0.80	1.01
ETF302x90x18-t2N44A0.6X0.6FX	0.60	0.60	6.54	5.66	0.87	0.83	1.05
ETF302x90x18-t2N44A0.8X0FX	0.80	0.00	6.54	3.43	0.53	0.67	0.78
ETF302x90x18-t2N44A0.8X0.2FX	0.80	0.20	6.54	4.18	0.64	0.70	0.91
ETF302x90x18-t2N44A0.8X0.4FX	0.80	0.40	6.54	4.73	0.72	0.73	0.99
ETF302x90x18-t2N44A0.8X0.6FX	0.80	0.60	6.54	5.27	0.81	0.76	1.07

Continue

Specimen	Holes diameter ratio	Bearing ratio	Failure load without holes	Failure load with holes	Reduction factor	Proposed reduction factor	Comparison with proposed reduction factor
	a/h	*x/h*	*P*	*P(Holes)*	*R=* P(Holes) / P(A0)	*Rp = 0.*96-0.36 *(a/h)*+0.14 *(x/h)*	*R/Rp*
			(kN)	(kN)			
ETF302x90x18-t2N90A0.2X0FX	0.20	0.00	7.87	7.39	0.94	0.89	1.06
ETF302x90x18-t2N90A0.2X0.2FX	0.20	0.20	7.87	7.46	0.95	0.92	1.04
ETF302x90x18-t2N90A0.2X0.4FX	0.20	0.40	7.87	7.55	0.96	0.94	1.02
ETF302x90x18-t2N90A0.2X0.6FX	0.20	0.60	7.87	7.65	0.97	0.97	1.00
ETF302x90x18-t2N90A0.4X0FX	0.40	0.00	7.87	6.69	0.85	0.82	1.04
ETF302x90x18-t2N90A0.4X0.2FX	0.40	0.20	7.87	6.89	0.88	0.84	1.04
ETF302x90x18-t2N90A0.4X0.4FX	0.40	0.40	7.87	7.12	0.91	0.87	1.04
ETF302x90x18-t2N90A0.4X0.6FX	0.40	0.60	7.87	7.34	0.93	0.90	1.04
ETF302x90x18-t2N90A0.6X0FX	0.60	0.00	7.87	6.01	0.76	0.74	1.03
ETF302x90x18-t2N90A0.6X0.2FX	0.60	0.20	7.87	6.36	0.81	0.77	1.05
ETF302x90x18-t2N90A0.6X0.4FX	0.60	0.40	7.87	6.71	0.85	0.80	1.07
ETF302x90x18-t2N90A0.6X0.6FX	0.60	0.60	7.87	7.03	0.89	0.83	1.08
ETF302x90x18-t2N90A0.8X0FX	0.80	0.00	7.87	5.26	0.67	0.67	0.99
ETF302x90x18-t2N90A0.8X0.2FX	0.80	0.20	7.87	5.79	0.74	0.70	1.05
ETF302x90x18-t2N90A0.8X0.4FX	0.80	0.40	7.87	6.27	0.80	0.73	1.09
ETF302x90x18-t2N90A0.8X0.6FX	0.80	0.60	7.87	6.70	0.85	0.76	1.13
ETF142x60x13t1.3N30A0.4X0.2FX	0.20	0.76	2.96	2.80	0.95	1.00	0.95
ETF142x60x13t1.3N30A0.4X0.4FX	0.39	0.76	2.96	2.53	0.85	0.92	0.92
ETF142x60x13t1.3N30A0.4X0.6FX	0.59	0.76	2.96	2.27	0.77	0.85	0.90
ETF142x60x13t1.3N30A0.4X0.8FX	0.78	0.76	2.96	1.93	0.65	0.78	0.83
ETF142x60x13-t1.3N60A0.4X0.2FX	0.20	0.64	3.32	3.23	0.97	0.98	0.99
ETF142x60x13-t1.3N60A0.4X0.4FX	0.39	0.64	3.32	2.70	0.81	0.91	0.90
ETF142x60x13-t1.3N60A0.4X0.6FX	0.59	0.64	3.32	2.64	0.80	0.84	0.95
ETF142x60x13-t1.3N60A0.4X0.8FX	0.78	0.64	3.32	2.47	0.74	0.77	0.97
ETF172x65x13-t1.3N32.5A0.4X0.4FX	0.40	0.77	2.88	2.71	0.94	0.92	1.02
ETF172x65x13-t1.3N65A0.4X0.4FX	0.40	0.58	3.31	3.03	0.92	0.90	1.02
ETF202x65x13-t1.4N65A0.4X0.4FX	0.40	0.68	4.37	3.80	0.87	0.91	0.95
ETF262x65x13-t1.6N32.5A0.4X0.4FX	0.40	0.74	3.63	3.16	0.87	0.92	0.95
ETF262x65x13-t1.6N65A0.4X0.4FX	0.40	0.71	3.94	3.68	0.93	0.92	1.02
ETF302x90x18-t2N44A0.4X0.4FX	0.40	0.86	6.95	6.03	0.87	0.93	0.93
Mean, Pm							1.00
STD							0.06
COV, Vp							0.06
Reliability index, β							2.80
Resistance factor, φ							0.85

D.8 Statistical analysis for the comparison of the strength reduction factor for flanges fastened under ETF loading condition (Type 2 holes)

Specimen	Holes diameter ratio	Bearing ratio	Failure load without holes	Failure load with holes	Reduction factor	Proposed reduction factor	Comparison with proposed reduction factor
	a/h	*x/h*	*P*	*P(Holes)*	*R*= P(Holes) / P(A0)	*Rp = 0.*95-0.50 *(a/h)*+0.08 *(N/h)*	*R/Rp*
			(kN)	(kN)			
ETF202x65x13-t1.4N100A0.2FX	0.20	0.50	5.40	4.93	0.91	0.89	1.03
ETF202x65x13-t1.4N100A0.4FX	0.40	0.50	5.40	4.33	0.80	0.79	1.01
ETF202x65x13-t4N100A0.2FX	0.21	0.51	52.39	46.56	0.89	0.89	1.00
ETF202x65x13-t4N100A0.4FX	0.41	0.51	52.39	41.18	0.79	0.79	1.00
ETF202x65x13-t6N100A0.2FX	0.21	0.53	112.27	98.54	0.88	0.89	0.99
ETF202x65x13-t6N100A0.4FX	0.42	0.53	112.27	86.73	0.77	0.78	0.99
ETF202x65x13-t1.4N150A0.2FX	0.20	0.75	6.00	5.56	0.93	0.91	1.02
ETF202x65x13-t1.4N150A0.4FX	0.40	0.75	6.00	4.99	0.83	0.81	1.03
ETF202x65x13-t1.4N150A0.6FX	0.60	0.75	6.00	4.37	0.73	0.71	1.03
ETF202x65x13-t4N150A0.2FX	0.21	0.77	67.11	60.36	0.90	0.91	0.99
ETF202x65x13-t4N150A0.4FX	0.41	0.77	67.11	54.06	0.81	0.81	1.00
ETF202x65x13-t4N150A0.6FX	0.62	0.77	67.11	47.91	0.71	0.70	1.01
ETF202x65x13-t6N150A0.2FX	0.21	0.79	143.95	128.67	0.89	0.91	0.98
ETF202x65x13-t6N150A0.4FX	0.42	0.79	143.95	114.93	0.80	0.80	0.99
ETF202x65x13-t6N150A0.6FX	0.63	0.79	143.95	102.23	0.71	0.70	1.02
ETF202x65x13-t1.4N200A0.2FX	0.20	1.00	7.19	6.75	0.94	0.93	1.01
ETF202x65x13-t1.4N200A0.4FX	0.40	1.00	7.19	6.15	0.86	0.83	1.03
ETF202x65x13-t1.4N200A0.6FX	0.60	1.00	7.19	5.48	0.76	0.73	1.04
ETF202x65x13-t1.4N200A0.8FX	0.80	1.00	7.19	4.56	0.63	0.63	1.01
ETF202x65x13-t4N200A0.2FX	0.21	1.03	82.01	75.43	0.92	0.93	0.99
ETF202x65x13-t4N200A0.4FX	0.41	1.03	82.01	67.90	0.83	0.83	1.00
ETF202x65x13-t4N200A0.6FX	0.62	1.03	82.01	60.32	0.74	0.72	1.02
ETF202x65x13-t4N200A0.8FX	0.82	1.03	82.01	50.79	0.62	0.62	1.00
ETF202x65x13-t6N200A0.2FX	0.21	1.05	175.59	159.72	0.91	0.93	0.98
ETF202x65x13-t6N200A0.4FX	0.42	1.05	175.59	144.40	0.82	0.82	1.00
ETF202x65x13-t6N200A0.6FX	0.63	1.05	175.59	129.06	0.74	0.72	1.02
ETF202x65x13-t6N200A0.8FX	0.84	1.05	175.59	109.00	0.62	0.61	1.01
ETF302x90x18-t2N150A0.2FX	0.20	0.50	9.78	8.93	0.91	0.89	1.03
ETF302x90x18-t2N150A0.4FX	0.40	0.50	9.78	7.75	0.79	0.79	1.00
ETF302x90x18-t4N150A0.2FX	0.20	0.51	53.00	47.09	0.89	0.89	1.00
ETF302x90x18-t4N150A0.4FX	0.41	0.51	53.00	41.33	0.78	0.79	0.99
ETF302x90x18-t6N150A0.2FX	0.21	0.51	119.12	104.62	0.88	0.89	0.99
ETF302x90x18-t6N150A0.4FX	0.41	0.51	119.12	91.81	0.77	0.79	0.98
ETF302x90x18-t2N220A0.2FX	0.20	0.73	12.27	11.33	0.92	0.91	1.02
ETF302x90x18-t2N220A0.4FX	0.40	0.73	12.27	10.04	0.82	0.81	1.01
ETF302x90x18-t2N220A0.6FX	0.60	0.73	12.27	8.64	0.70	0.71	0.99
ETF302x90x18-t4N220A0.2FX	0.20	0.74	65.74	59.49	0.90	0.91	1.00
ETF302x90x18-t4N220A0.4FX	0.41	0.74	65.74	52.75	0.80	0.81	0.99
ETF302x90x18-t4N220A0.6FX	0.61	0.74	65.74	46.14	0.70	0.71	1.00
ETF302x90x18-t6N220A0.2FX	0.21	0.75	148.86	133.16	0.89	0.91	0.99
ETF302x90x18-t6N220A0.4FX	0.41	0.75	148.86	117.64	0.79	0.80	0.98
ETF302x90x18-t6N220A0.6FX	0.62	0.75	148.86	103.49	0.70	0.70	0.99
ETF302x90x18-t2N300A0.2FX	0.20	1.00	14.91	13.94	0.93	0.93	1.01
ETF302x90x18-t2N300A0.4FX	0.40	1.00	14.91	12.63	0.85	0.83	1.02
ETF302x90x18-t2N300A0.6FX	0.60	1.00	14.91	11.17	0.75	0.73	1.03
ETF302x90x18-t2N300A0.8FX	0.80	1.00	14.91	9.19	0.62	0.63	0.98
ETF302x90x18-t4N300A0.2FX	0.20	1.01	80.97	74.88	0.92	0.93	0.99
ETF302x90x18-t4N300A0.4FX	0.41	1.01	80.97	67.31	0.83	0.83	1.00
ETF302x90x18-t4N300A0.6FX	0.61	1.01	80.97	58.92	0.73	0.73	1.00

Continue

Specimen	Holes diameter ratio	Bearing ratio	Failure load without holes	Failure load with holes	Reduction factor	Proposed reduction factor	Comparison with proposed reduction factor
	a/h	*x/h*	*P*	*P(Holes)*	*R*= P(Holes) / P(A0)	*Rp = 0*.95-0.50 *(a/h)*+0.08 *(N/h)*	*R/Rp*
			(kN)	(kN)			
ETF302x90x18-t4N300A0.8FX	0.81	1.01	80.97	47.67	0.59	0.63	0.94
ETF302x90x18-t6N300A0.2FX	0.21	1.03	183.43	167.48	0.91	0.93	0.98
ETF302x90x18-t6N300A0.4FX	0.41	1.03	183.43	150.08	0.82	0.83	0.99
ETF302x90x18-t6N300A0.6FX	0.62	1.03	183.43	132.54	0.72	0.72	1.00
ETF302x90x18-t6N300A0.8FX	0.82	1.03	183.43	109.52	0.60	0.62	0.96
ETF142x60x13-t1.3N90MA0.2FX	0.20	0.64	3.75	3.16	0.84	0.90	0.93
ETF142x60x13-t1.3N90MA0.4FX	0.40	0.64	3.75	2.79	0.74	0.80	0.93
ETF142x60x13-t1.3N90MA0.6FX	0.60	0.64	3.75	2.55	0.68	0.70	0.97
ETF142x60x13-t1.3N120MA0.2FX	0.20	0.86	4.06	3.58	0.88	0.92	0.96
ETF142x60x13-t1.3N120MA0.4FX	0.40	0.86	4.06	3.44	0.85	0.82	1.04
ETF142x60x13-t1.3N120MA0.6FX	0.60	0.86	4.06	2.94	0.72	0.72	1.01
ETF172x65x13-t1.3N120MA0.4FX	0.40	0.71	4.16	3.48	0.84	0.81	1.04
ETF172x65x13-t1.3N120MA0.6FX	0.60	0.71	4.16	3.00	0.72	0.71	1.02
ETF202x65x13-t1.4N120MA0.2FX	0.20	0.60	5.24	4.88	0.93	0.90	1.04
ETF202x65x13-t1.4N120MA0.4FX	0.40	0.60	5.24	4.27	0.81	0.80	1.02
ETF202x65x13-t1.4N150MA0.4FX	0.40	0.75	5.82	4.73	0.81	0.81	1.00
ETF202x65x13-t1.4N150MA0.6FX	0.60	0.75	5.82	4.24	0.73	0.71	1.03
ETF262x65x13-t1.6N120MA0.2FX	0.20	0.46	5.06	4.60	0.91	0.89	1.02
ETF262x65x13-t1.6N120MA0.4FX	0.40	0.46	5.06	3.89	0.77	0.79	0.98
ETF262x65x13-t1.6N150MA0.4FX	0.40	0.58	5.37	4.25	0.79	0.80	0.99
Mean, Pm							1.00
STD							0.02
COV, Vp							0.02
Reliability index, β							2.86
Resistance factor, φ							0.85